NTNU
Norwegian University of
Science and Technology

Synthesis of Selectively Fully Protected Glucose Derivatives via a Furanose-to-Pyranose Rearrangement Method

Nicolai Etwin Alsaker

Chemistry
Submission date: May 2018
Supervisor: Nebojsa Simic, IKJ
Co-supervisor: Sondre Nervik, IKJ

Norwegian University of Science and Technology
Department of Chemistry

Declaration

I hereby declare the presented Master's thesis as an independent work in accordance with the rules and regulations of the Norwegian University of Science and Technology.

Trondheim, 25 May 2018

_____

Nicolai Etwin Alsaker

Preface

The presented work in this Master's thesis was conducted during the period between August 2016 and May 2018 as part of the study programme "Master in Organic Chemistry" at the Department of Chemistry at the Norwegian University of Science and Technology.

For the opportunity to partake in the present work, I want to thank my supervisor, Associate Professor Nebojša Simić, whose support and faith has been insightful and invigorating. I also want to extend my appreciation to my co-supervisor PhD student Sondre Nervik for unconditional guidance, patience and conversation. To both, I am forever grateful.

Furthermore, I wish to thank Roger Aarvik, Jon Erik Aaseng, Julie Asmussen, Susanna Gonzales and Torunn Melø for their technical support these past two years. To my fellow students in the lab, I am thankful for company we shared.

Lastly, my deepest gratitude goes to Elena G. Austlid for being my rock in this weary land.

Abstract

Towards the total synthesis of the natural anti-inflammatory compound **1**, present in the plant *Sclerochloa dura*, three full protection strategies were developed for selectively full protected glucose derivatives, available for subsequent 1,3,6- functionalization.

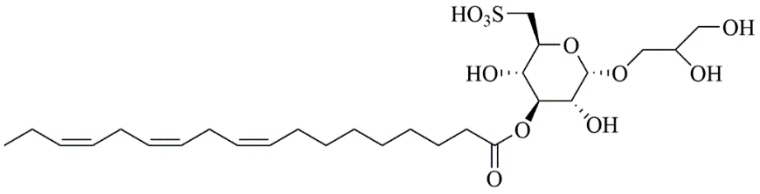

1

The current strategies are based on a furanose to pyranose rearrangement for regioselective protection of 3-OH, meanwhile protecting 1-OH in a Fischer type glycosidation. Optimization of anomerization was attempted in respect to **4a**, but composition did not exceed α:β = 73:27. The common intermediate allyl 3-*O*-benzyl-D-glucopyranoside afforded anomeric mixtures of the fully protected species **6** and **9**. Allyl 3-*O*-benzyl-4,6-*O*-di-*tert*-butylsilylene-2-*O*-tert-butyldimethylsilyl-α/β-D-glucopyranoside (**8a**/**8b**) were obtained as isolated anomers, for which the preceding substrate (**7a**/**7b**) anomers were separated. All present compounds and two by-products were spectroscopically characterized, including shift assignment.

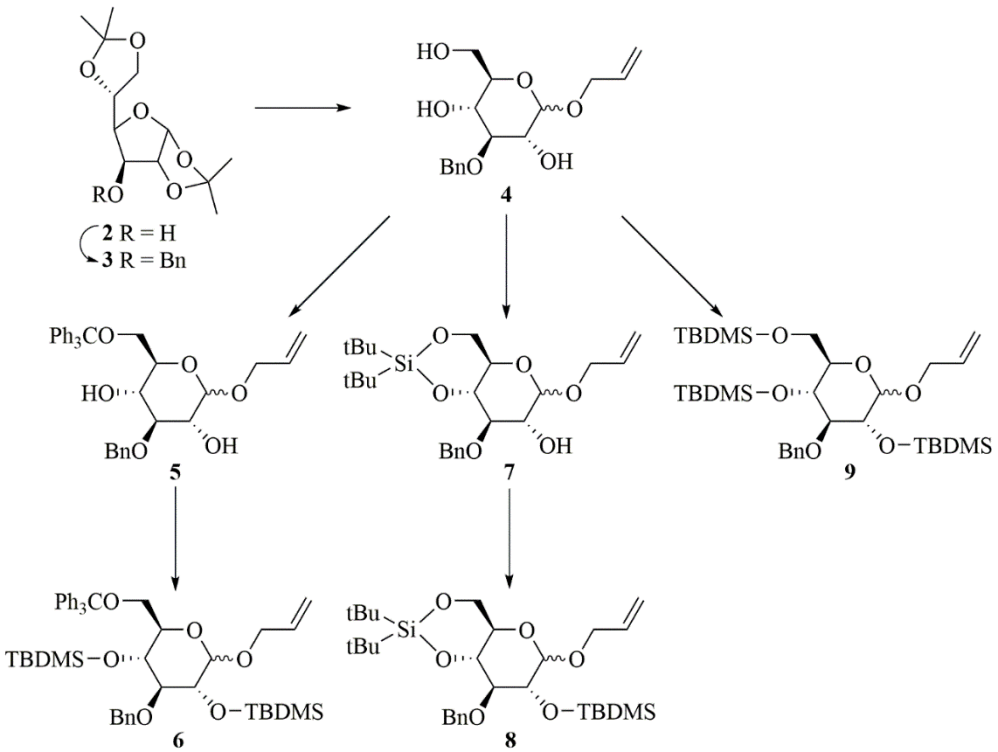

Sammendrag

Som en del av et større prosjekt hvis mål er å syntetisere den anti-inflammatoriske forbindelsen **1**, ble det utviklet tre selektive fullbeskyttelsesmønstre av glukose hensiktsmessig for fremtidig funksjonalisering av posisjon 1, 3 og 6.

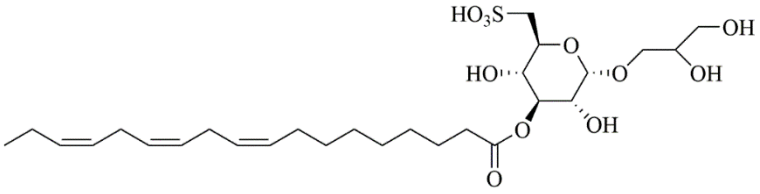

1

De benyttede strategiene er basert på en omleiringsreaksjon fra furanose til pyranose for regioselektiv beskyttelse av 3-OH, samtidig som en allyl gruppe installeres på C-1 via Fischer type glycosidering. Omleiringen ble forsøkt optimalisert med hensyn på **4a**, der et *α*:*β*-forhold på høyst 73:27 ble oppnådd. Følgelig ga mellomproduktet allyl 3-*O*-bensyl-D-glukopyranosid anomer blanding av de fullbeskytede derivatene **6** og **9**. Allyl 3-*O*-bensyl-4,6-*O*-di-*tert*-butylsilylene-2-*O*-*tert*-butyldimetylsilyl-*α*/*β*-D-glukopyranosid (**8a**/**8b**) ble oppnådd som individuelle anomerer, ettersom de foregående substratene (**7a**/**7b**) var mulig å separere. Aktuelle syntetiske forbindelser, samt to biprodukter, har blitt spektroskopisk karakterisert.

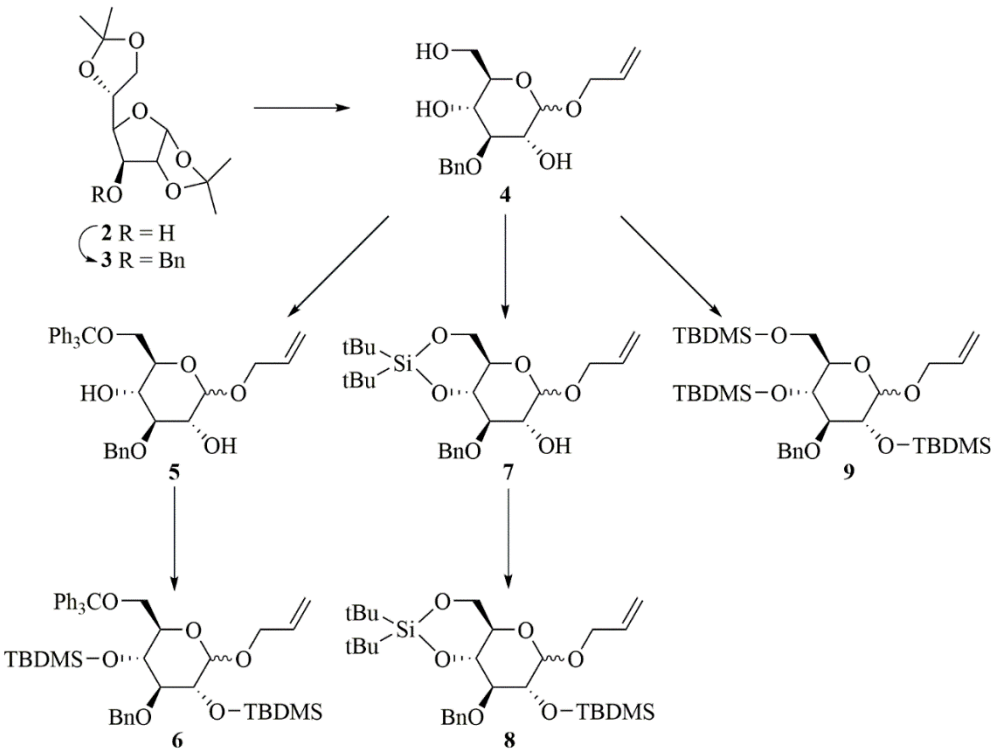

Contents

Symbols and abbreviations

1D	One dimensional
ACN	Acetonitrile
ASAP	Atmospheric solid analysis probe
b	Broad
Calcd.	Calculated
COSY	^{1}H-^{1}H Correlation spectroscopy
d	Doublet
DAD	Diode array detector
DCM	Dichloromethane
dd	Doublet of doublets
ddd	Doublet of doublet of doublets
ddt	Doublet of doublet of triplets
dddd	Doublet of doublet of doublet of doublet
DMAP	4-Dimethylaminopyridine
DMF	N,N-Dimethylformamide
eq.	Equivalent
ESI	Electron spray ionization
HMBC	Heteronuclear (^{1}H-^{13}C) multiple bond coherence
HPLC	High performance liquid chromatography
HRMS	High resolution mass spectroscopy
HSQC	Heteronuclear (^{1}H-^{13}C) single quantum coherence
IR	Infrared spectroscopy
J	Coupling constant
JRES	*J*-resolved spectroscopy
LG	Leaving group
m	Multiplet, medium
M	Molecular ion
mp.	Melting point
MS	Mass spectroscopy
m/z	Mass over charge ratio
n/a	Not applicable
NMR	Nuclear magnetic resonance spectroscopy
NOESY	Nuclear Overhauser effect spectroscopy
nr.	Number
NR	Not resolved
PG	Protecting group
PMB	*para*-Methoxybenzene
ppm	Parts per million
prep.	Preparative
q	Quartet
rt.	Room temperature
R_f	Retention factor
s	Singlet, strong
t	Triplet
TBDMS	*tert*-butyldimethylsilyl

TBDPS	*tert*-butyldiphenylsilyl
td	Triplet of doublets
TEA	Triethylamine
TES	Trethylsilyl
THF	Tetrahydrofuran
TLC	Thin layer chromatography
TMS	Trimethylsilyl, tetramethylsilane
TOCSY	Total correlation spectroscopy
t_R	Time of retention
UR	Undesired reaction
UV	Ultraviolet
w	Weak
w/v	Weight per volume
δ	Chemical shift

List of compounds

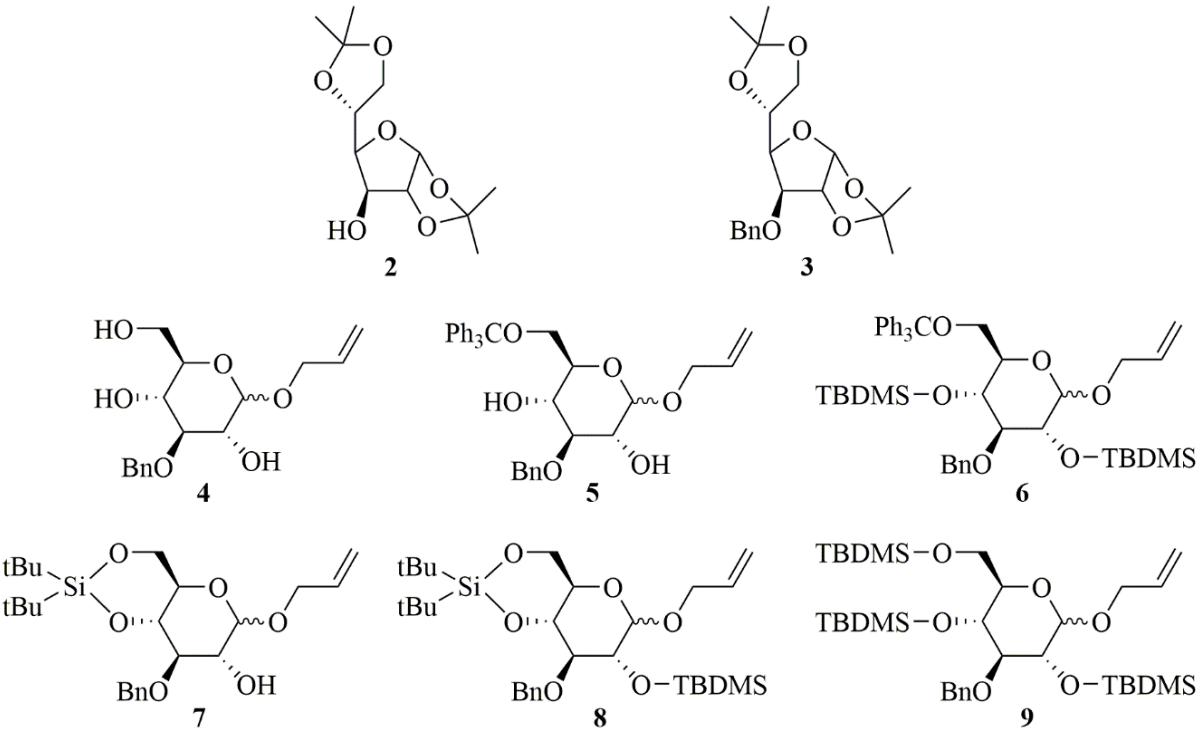

1 Introduction

The plant *Sclerochloa dura* has been reported to have anti-inflammatory properties by Bukhari *et al.*[1] Investigations of plant extracts revealed several anti-inflammatory compounds, of which **1** (figure 1.1) was found to be a novel structure.[2] Due to very low isolable yields,[2] material has been scant for further investigation into drug development aspects, such as mode of action, potency and toxicity. The research group of Nebojša Simić is currently working on a total synthesis of **1**. As part of the project, the present work aims to create a reliable synthetic route towards a fully protected glucose intermediate, suitable for selective insertion of desired substituents on positions 1, 3 and 6.

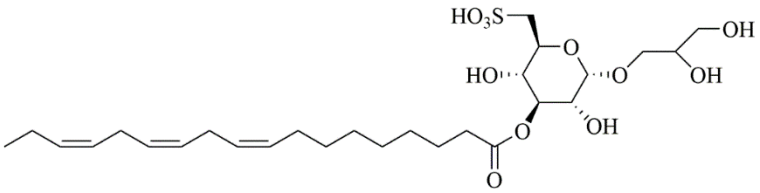

1

Figure 1.1: The anti-inflammatory compound isolated from *Sclerochloa dura* by Bukhari *et al.*[1-2]

Towards suitably fully protected glucose for selective functionalization at the desired positions, a furanose to pyranose rearrangement method has been previously employed in order to combat troublesome indiscrimination of secondary carbohydrate hydroxyls.[3] From a common intermediate **4**, three selective full protection methods were imagined, and explored according to scheme 1.1. The three routes present options applicable in the total synthesis of **1**. To the best of our knowledge, four new compounds were produced, which have been characterized by spectroscopic and chromatographic techniques. Additionally, two fully protected glucose derivative by-products were isolated and characterized.

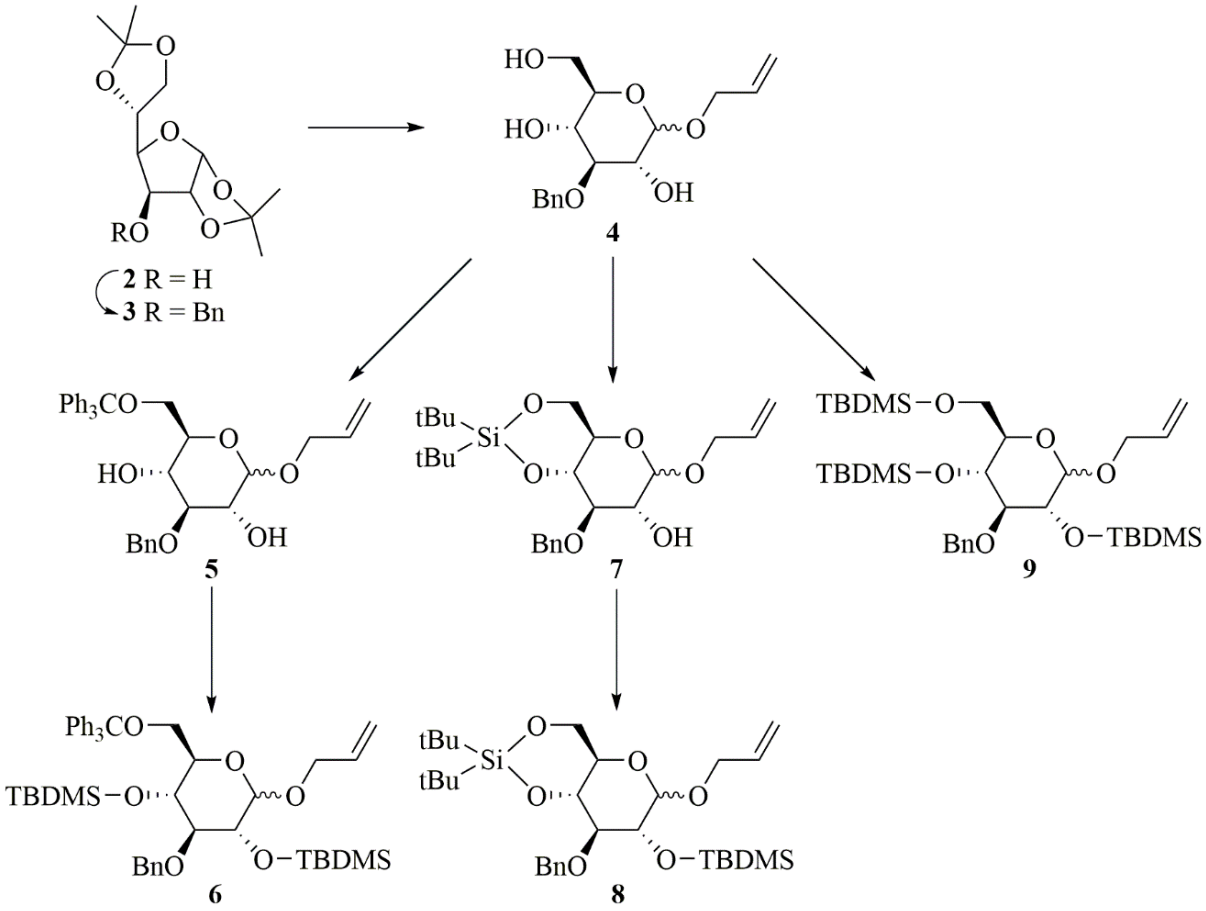

Scheme 1.1: Present protection strategies for selective full protected glucose available for functionalization at positions 1, 3 and 6.

2 Theory

2.1 Concerns in carbohydrate chemistry

Bioactive carbohydrates are often isolated from natural sources in small quantities, scant for structural and biological analysis.[4-5] Synthetic development presents an alternative for obtaining material for these purposes, albeit often difficult. The synthesis of carbohydrate-based drugs can prove a formidable task involving much experimental work and can be expensive.[6-7] This chapter covers some of the challenges the organic chemist faces as a consequence of the nature of carbohydrates, focusing on the saccharide of relevance: glucose. Aspects of polymerizations have not been considered, as it does not pertain to the research topic.

2.1.1 Isomerism

Compared to the two other major biomolecule polymers, peptides and nucleic acids, carbohydrates elicit an exponential increase in complexity.[5, 8] This is due to individual saccharides having several stereocenters and isomeric forms. An unfortunate reality when dealing with carbohydrates is the occurrence of isomeric mixtures, inferring analytical complexity and increased likelihood of errors.

Free glucose undergoes cyclization between the carbonyl functionality and the 4- or 5-hydroxyl, forming five-membered furanose, or six-membered pyranose, respectively (see scheme 2.1). Sugars greatly prefer the cyclic structures,[9] with the acyclic form being present in minor amounts in solution. Furthermore, the pyranose ring is typically more stable than furanose, because of less ring strain. During the cyclization, attack on the prochiral aldehyde produces a new stereocenter at the hemiacetal position, also known as the anomeric position. The resulting diastereomeric saccharides are called anomers and differ in orientation of the hemiacetal hydroxyl, affixed α or β depending upon their relative configuration of 1-OH.

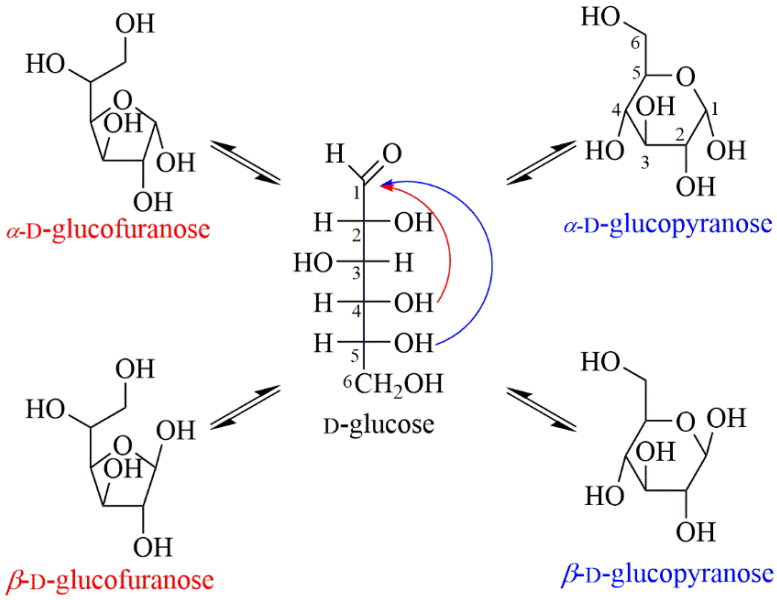

Scheme 2.1: Tautomeric equilibrium between furanose and pyranose forms of D-glucose.

Both furanose-pyranose equilibrium and anomerization occur simultaneously in solution, but tautomeric composition vary for individual monosaccharides.[10] For a certain species, the equilibria are influenced by several factors, including temperature, solvent, ring substituents, steric interaction, and sugar concentration, among others.[10-16] In addition, the use of promoters is influential, such as enzymes or acids.[17] Observed isomeric compositions of basic carbohydrates provide a basis for predicting composition of derivatives.

Anomeric composition of the most basic carbohydrates and common derivatives is frequently reported in literature.[7, 9-10, 14, 18] In solution, unsubstituted glucose exists in anomeric α:β ratio of 36:64, despite a predicted 11:89 based on steric interaction alone.[10] For heterocycles, such as pyranose, substituents adjacent heteroatoms (O for sugars) tend to occupy axial orientation, despite steric interactions being less favourable. This preference was dubbed "the anomeric effect",[19] after the discovery of the anomeric equilibrium of α- and β-glycosides.[20] The effect was traditionally explained through repulsive electrostatic dipole forces, but stereoelectronic orbital interactions have been proposed as origin of the effect.[18] An "exoanomeric" effect is also present for heteroatomic bound substituents (e.g. alkoxy).[7, 10, 14, 18] Although similarly explained, stabilizing contributions are present for both anomeric configurations.[10]

According to the anomeric effect, an electron-withdrawing inductive group substituted at the anomeric position enhances the effect. For example, methyl glucopyranoside has a dramatically different α:β ratio compared to glucose, at 77:23.[21] Less polar solvent also contributes towards

increased anomeric effect.[22] Interestingly, the steric bulk of the substituent has little effect on the anomeric preference.[23]

Derivatization of other hydroxyl groups is also influential on degree of saccharide anomerization. The anomeric compositions of unsubstituted glucopyranose and methyl glucopyranoside have been quantified for different 2-, 3- and 6-substituents, and combinatory patterns of these.[21] Increased proportion of the α-anomer was reported for unsubstituted glucose for all substitution patterns. However, the same observations were inconclusive for methyl glucopyranoside. Although the α:β ratio appears most influenced by the C-1 substituent, the influence of other substituents should not be disregarded.

2.1.2 Identification and separation

The importance of separate species is unambiguous in biological analysis, as isomers can exhibit different effects.[24-25] Separation of carbohydrate saccharides was, historically, hard-won and applied to different sugars.[26] Advances and development within chromatography and mass spectroscopy now allow for simultaneous separation of several genuine (i.e. not derivatized) isomers, enantiomers and even anomers.[22, 27-29]

In the advent of unsuccessful separation of carbohydrates, structural elucidation by NMR represents a tedious and complex exercise, even for mixtures of only two isomers.[5, 11] Generally, only the two pyranose forms of glucose are detectable by NMR. Identification of pyranosidic anomers is possible, despite overlapping ^{1}H-NMR signals at δ = 3-4 ppm stemming from the ring protons ("sugar region", common for carbohydrates).[30] The anomeric protons occupy a different chemical environment as hemiacetal, than do the other ring protons. As a result, both anomeric protons have much higher shifts, and are well separated from the sugar region. Relative configurations give α- and β-protons noticeably different shifts as well, α often higher than β, shown in figure 2.1a for D-glucose.[30] Attributing signals to the respective anomeric protons is possible, based on inherent difference in magnitude of vicinal coupling to the neighbouring H-2. Characteristic interactions between axial (a) and equatorial (e) is shown in figure 2.1b, specifically coupling constants J_{aa} = 7-9 Hz and $J_{ae} \approx J_{ee}$ = 2-5 Hz.[31] Thus, anomeric identification and quantification is possible for sufficiently spaced anomeric signals.

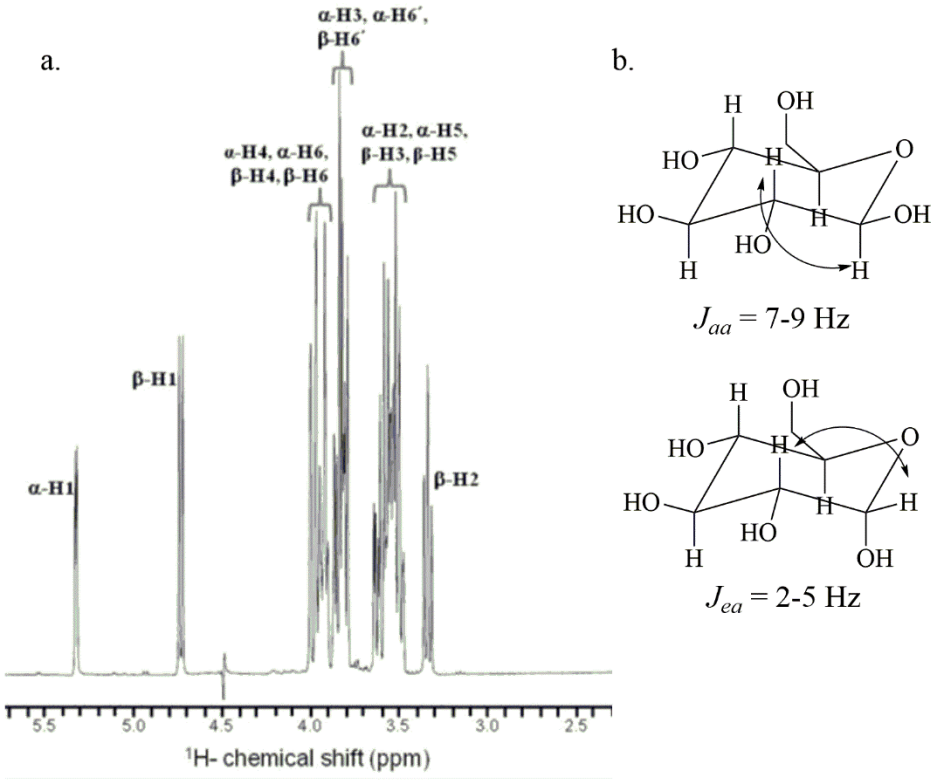

Figure 2.1: a. ^{1}H-NMR spectrum of anomerically mixed D-glucose for the sugar region, attributed "*Glycosidation. Chapter 4: Unravelling Glycobiology by NMR spectroscopy"*, re-used and adapted according to open access CC-BY license.[30] b. Characteristic proton spin-spin couplings for *α*- and *β*-glucopyranose.

2.1.3 Selectivity

The polyhydroxyl nature of carbohydrates is responsible for difficulty in achieving selective functionalization. Similar behaviour of the hydroxyl groups gives rise to an array of challenges for the organic chemist, notably, troublesome regio – and stereoselective control[7, 9] and anomalous reactivities and properties.[32]

Aldohexose carbohydrates and derivatives have up to five chemically inequivalent hydroxyls. The 1-OH and 6-OH have behaviour similar to hemiacetal (as discussed before) and primary alcohol, respectively, and are more easily distinguishable from 2-, 3- and 4-hydroxyls. A study performed by Yoshida *et al.*[33] on the selective acetylation of pyranoside hydroxyl groups revealed a preference for 3-OH and 4-OH, regardless of anomeric configuration. An intramolecular H-bonding network of glucopyranoside was proposed, illustrated in figure 2.2. Meanwhile, a substantially larger proportion of 4-acetylated product was observed for the *α*-anomer, indicating weaker 2-OH to O-1 coordination for the axial orientation. The presence of

a H-bond network is supported by substantially higher acidities of vicinal glycopyranoside hydroxyls compared to non-vicinal, due to being able to better delocalize charge.[32]

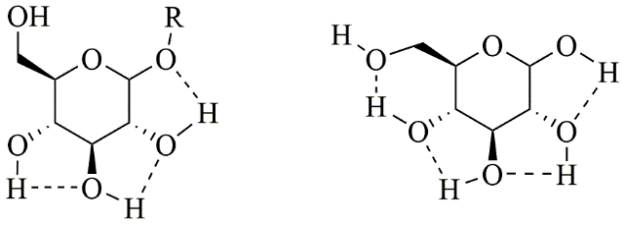

Figure 2.2: Intramolecular H-bonding network in glucose as proposed by Yoshida *et al.*[33] and Davies *et al.*,[34] respectively.

Relative hydroxyl acidities can give an indication towards relative reactivities. A recent acidity study of partially protected glycosides reported ascending order of acidity for isolated methyl glucopyranoside hydroxyls: 4-OH < 3-OH < 2-OH < 6-OH.[32] The reported order of acidity coincide with previously reported relative methylation rate constants on methyl glucopyranosides.[35-36] However, sequences where 6-OH < 2-OH have also been reported.[37] Specific sequence of reactivity depends upon reaction conditions and structural variation,[33] but there seems to be a consensus on lower reactivity of 4-OH and 3-OH compared to 6-OH and 2-OH for glucopyranosides.[29, 38]

Stereoelectonic or steric interactions of neighbouring substituents can have pronounced effects on the reactivity of a given hydroxyl.[38] Although the effect of the former can be difficult to predict, the steric effect of large substituents (e.g. bulky protection groups) is more obvious. In order to predict such interactions, the basic carbohydrate structure(s) must be known. Multiple models have been formulated to illustrate carbohydrates, some of which are shown in figure 2.3a-c for β-D-glucopyranose. Realistic spatial configuration is best represented by the Reeves projection (c). In addition, the presence of numerous conformers needs to be taken into account. Fortunately, they equilibriate rapidly, often having one or a few predominant conformations.[10] For glucose, the chair conformation is by far the most occupied. Specifically, the $^4C_1$ chair is greatly preferred over the $^1C_4$ chair (figure 2.3d), due to unfavourable steric interactions between the anomeric hydroxyl and hydroxymethyl group.[7, 10] In general, the effective size of substituents lead to a higher degree of steric obstruction. The size of neighbouring substituents provides a basis for predicting hydroxyl reactivities in carbohydrates. Software modelling is a viable tool for more representative predictions through finding preferred conformations.

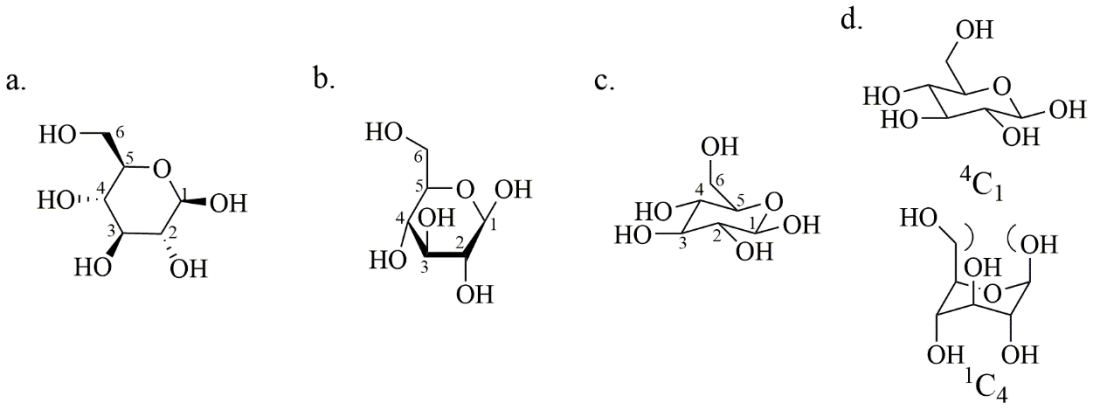

Figure 2.3: a. Mills- ; b. Haworth- ; c. Reeves projection[7] of *β*-D-glucopyranose; d. Different chair conformations of *β*-D-glucopyranose.

2.2 Protection chemistry of carbohydrates

The business of protection chemistry as a concept is elegant, but lengthens the synthetic route by two steps. Reduction to yields, as well as increase in costs, is inevitable.[39] However, avoiding their use is near impossible in carbohydrate-based synthesis at the current maturation of the field.

Difficulty of selective functionalization of carbohydrates arise from their polyhydroxyl nature, overcome through implementation of protection strategies or enzymatic use (or other catalytic methods). Unlike enzymes, protection chemistry seldom apply substrate restrictions, but involve multistep synthesis for the activation of one particular hydroxyl group.[32, 40] New challenges are presented with the use of protection chemistry, but fortunately the field has rich roots within carbohydrate chemistry, and there exists authoritative literature on the subject.[7, 9-10, 40] Still, the need for developing new techniques and tailoring strategies arise frequently, especially in total synthesis of complex derivatives.[41] This chapter details characteristics of carbohydrate protection chemistry and common carbohydrate protection groups, surveying their implementation towards protection at various positions.

2.2.1 Protection group characteristics

Protection strategy can be decisive for successful syntheses of complex carbohydrate derivatives. Some factors needs consideration when planning a protection pattern. In general, protection groups should be stable under conditions during all subsequent steps, compatible with other functionalities in the compound (including other protecting groups), and be capable of highly selective cleavage under mild conditions.[10, 39] Furthermore, in order to ensure selective chemical manipulations during a synthetic sequence, protecting groups are required to be *orthogonal*. Orthogonal protection groups are capable of being selectively liberated without interfering with other protecting groups present. Maintaining functional group blockage in order to avoid unwanted reactions is required for regioselective functionalization.

Protection groups are considered temporary or permanent, depending on the stage they are planned for removal during a synthesis. Permanent protection groups are usually more robust, a required trait for withstanding subsequent reaction conditions. The distinction is useful when planning a protection pattern, where multiple derivatizations are to be performed. It is important to keep in mind that protection groups can influence the compounds reactivity and give rise to

unpredictable behaviour for elaborate protection patterns.[7, 9-10] Adjacent positions are most susceptible to stereoelectronic and steric effects of protection groups (see section 2.1.3).

Hydroxyl protection groups are by far the most important protecting group in carbohydrate chemistry, which are commonly protected as ethers, esters and acetals/ketals.[7, 9-10] Mechanisms vary and depend upon employed protecting group and conditions. However, generalizations can be made: sugar hydroxyls are often nucleophilic, while protecting reagents are electrophilic and bear a leaving group or leaving group precursor, as shown in scheme 2.2.

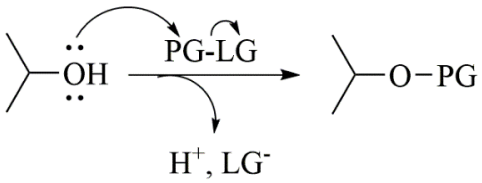

Scheme 2.2: Generalized protection of sugar hydroxyl. PG = protection group; LG = leaving group.

Benzylic and allylic ethers

Benzyl ether (Bn) is one of few protection groups simultaneously having stability and efficiency of introduction to satisfy the criteria of permanent protection groups.[7, 9-10] High stability make them able to withstand strongly acidic and basic conditions. Introduction is commonly done with benzyl bromide and sodium hydride in polar aprotic solvents (usually DMF), although alternative conditions can be used to accommodate more labile functionalities.[7, 10] Catalytic Pd/Pb hydrogenation, essentially neutral conditions, is generally employed for deprotection.[7, 10]

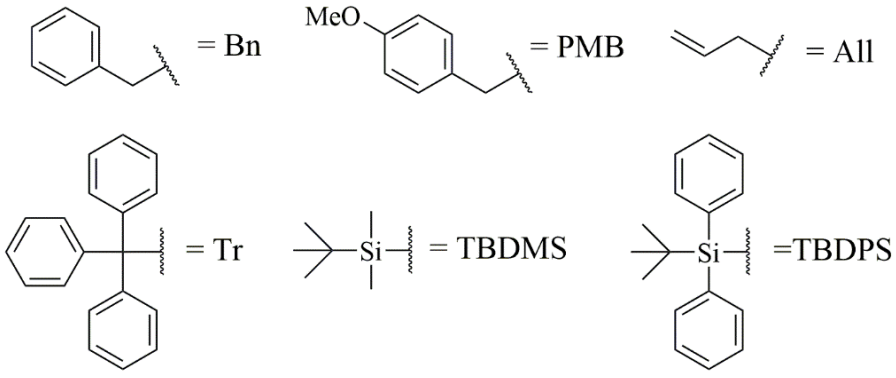

Figure 2.4: Common carbohydrate protection groups.

p-Methoxybenzyl ether (PMB) is another common benzylic ether, but more electron-rich than regular benzyl ethers, making them more labile towards acidic conditions. Thus, they are

potentially troublesome under acid catalysed glycosidation.[7] While introduced in the same manner as benzyl ethers, dissociation is more readily accomplished.

Allyl ethers (All) are stable towards moderately acidic and basic conditions, but vulnerable towards strong electrophiles.[10] Introduction is done similarly to benzyl ethers: reaction between allyl bromide and the carbohydrate alkoxide.[7, 10] Cleavage is done through catalytic Hg/Pd/Pb hydrogenation.[7, 10] Nonaromatic alcohols are in general applicable for the protection of the anomeric (hemiacetal) hydroxyl (see section 2.2.2).

Trityl ethers

The triphenylmethyl/trityl ether (Tr) is a sterically bulky protection group, often applied for regioselective protection of the primary 6-OH.[7, 9-10] A common protection procedure involve treating the carbohydrate with trityl chloride in pyridine, with 4-dimethylaminopyridine (DMAP) as accelerant.[7, 10] The trityl ether is labile in mild protic acid and Lewis acids due to having a relatively stable carbocation, also dissociating under catalytic hydrogenation conditions.[7, 10] The trityl group greatly affect the polarity of monosaccharides, reducing solubility in polar protic solvents through its hydrophobic property.[39]

Silyl ethers

There are several silyl protection groups, but the most frequent by far are *tert*-butyldimethylsilyl ($tBuMe_2Si$ or TBDMS) and *tert*-butyldiphenylsilyl (TBDPS) groups.[7, 9-10] Substituents on Si can be varied for tuning stability, but usually the aforementioned groups are of satisfactory stability.[10] Silyl ethers are normally introduced by treatment with the respective silyl chlorides in a polar aprotic solvent in presence of an amine base, such as imidazole, DMAP/pyridine, triethylamine or 2,6-lutidine.[7, 10, 39] More powerful silylating reagents, such as triflates, have successfully been employed for protection of sterically hindered sugar hydroxyls.[42-45] Silyl ethers are cleaved by nucleophilic attack of fluoride ions, under basic, neutral or acidic conditions, depending on specific group. TBDMS is less stable towards acid than TBDPS.

Less bulky protection groups such as trimethylsilyl (TMS) and triethylsilyl (TES) ethers are relatively labile. TES cleaves under mild conditions, and can be used where other sensitive functionalities are present. TMS ethers of primary and secondary alcohols do not survive the simplest of chemical manipulations, labile even to column chromatography.[9, 39] Their use is therefore limited.

2.2.2 Hemiacetal (anomeric) protection

The first reported synthetic glycosidation was performed by Emil Fischer on glucopyranose, via acid catalysed solvolysis in alcohol.[46] The method, what has come to be known as Fischer glycosidation, has since been extensively developed. The use of external promoters, such as various acids or enzymes, allows for installation of more complex alcohols.[9, 17, 47] Mild and effective conditions have been achieved using catalysts such as sulfamic acid, TfOH[47] and TMSCl.[48] Mechanisms for glycosidation of glucopyranose via the Fischer method have been proposed,[49-50] which is illustrated in scheme 2.3. The boat conformation intermediate is also in equilibrium with α- and β-glucofuranoside, but was omitted due to relevance.

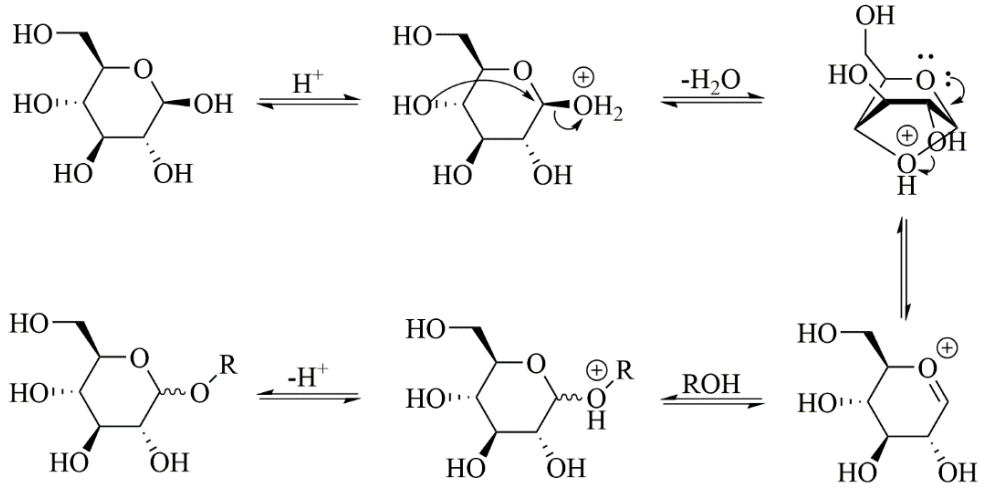

Scheme 2.3: Fischer glycosidation mechanism as proposed by Mowery *et al.*,[49] where β-D-glucopyranose is the reacting species.

Fischer glycosidation is the general method employed for the protection of the anomeric position.[7, 9-10] Common protection groups include alkyl, allyl and benzyl, prepared through solvolysis with the respective alcohol. Allyl and benzyl glycosides are liberated via the same procedure as mentioned in section 2.2.1. As can be seen in scheme 2.3, the glycosidation affords pyranoside anomeric mixtures. In some cases, crystallization can be used for separation,[10] otherwise, chromatographic techniques must be explored.

3 Current status of knowledge

3.1 Carbohydrates in drugs

Carbohydrates are the most widely distributed and diverse biomolecules found on the planet, and are of great importance in a vast array of biological processes. Historically, natural compounds has served as guides for development of new pharmaceuticals. Due to the structural diversity of carbohydrates (among other things), the most potential library for discovery of bioactive carbohydrates derivatives is established by the naturally occurring compounds.[51-52] Despite their abundance in nature, there are relatively few commercial carbohydrate – and carbohydrate derivative based drugs.[53]

Drugs of this class have often been associated with poor pharmacokinetic properties (poor intestinal absorption), a consequence of their inherently high polarities.[54] Together with a time-long underestimation of their importance in biological functions, previous reluctance towards sugar chemistry by pharmaceutical and academic instances is understandable.[4, 8, 40, 55] However, advances in spectroscopy and chromatography allow for more routinely analysis, which has founded a resurgence into the field.[4-5, 9, 22, 56]

3.2 Other work by the research group

Development of a synthetic route for the synthesis of compound **1** based on the glucose skeleton has hitherto been the focus of the research group. Selective functionalization at positions 1, 3 and 6 was deemed best manageable by implementation of protection chemistry. The initially investigated strategy was based around the selective protection of 2-OH on allyl 4,6-*O*-benzylidene-D-glucopyranoside as shown in scheme 3.1.[57] The observed regioselectivity was inconsistent with previous reports,[58] founding investigation of alternative synthetic routes.

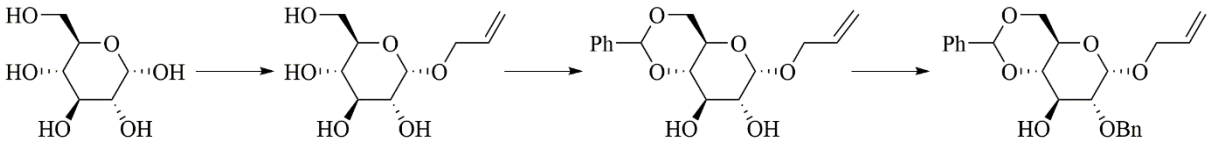

Scheme 3.1: Selective protection strategy initially explored by the research group.[57]

Exploration of functional group insertion according to the target molecule was made possible from the results of the initially investigated strategy, combined with regioselective cleavage properties of 4,6-*O*-benzylidene derivatives.[59-61] Investigations have been carried out towards sulfur functionalization on model substrates (see scheme 3.2).[62] Additionally, investigations have been launched towards esterification of O-3 as a fatty acids ester, at the time of writing.

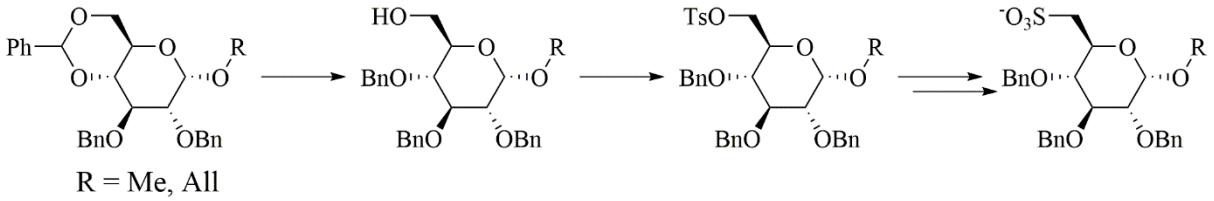

Scheme 3.2: Sulfur functional group derivatization explored by the research group.[62]

3.3 The present protection strategies

Discriminating between the secondary hydroxyls on glucose was the challenge of the initial protection strategy investigated by the research group,[57] and is generally the case with carbohydrates. The present, alternative protection strategies evolved on the premise of 3-O protected glycopyranoside via a diacetoneglucose (**2**) protection-rearrangement route, as reported by Kusumoto *et al*.[3] The pathway enable insertion of allyl as the glycosidic aglycone, which could act as a precursor to the C-1 glycerol functionality of **1** at a later stage in the synthesis, while simultaneously allowing selective protection of the desired 3-position. On the choice of protection group, withstanding the acidic conditions of the furanose-pyranose rearrangement, and presumed oxidative conditions for functionalization of C-1 and C-6, were prerequisites. Benzyl ethers are known to withstand these conditions,[7, 10] while simultaneously conferring fluorescence for convenient monitoring of reactions, and was therefore a most satisfactory choice. Although milder conditions are achievable with PMB, it does not survive the rearrangement conditions.

With allyl 3-*O*-benzyl-D-glucopyranoside (**4**) serving as a vantage, three protection patterns for selective derivatization at positions 1, 3 and 6 were devised as shown in scheme 3.3. The pathway to **5** was developed by Derrick *et al.*,[63-64] where they proceeded to protect positions 2 and 4 with PMB, achieving a 1,3,6-selective protection pattern. The same pattern is desired for the targeted synthesis of **1**, however, the use of acid labile PMB is incompatible with subsequently planned functionalization as part of the current objective. TBDMS ether was instead chosen as global protecting group, based on being able to withstand oxidative – and catalytic hydrogenation conditions, as well as acid catalysed fatty acid esterification.

Towards the functionalization at C-6, the cleavage of trityl ethers is well known, and can be performed in presence of TBDMS ethers.[7, 10] Hence, the synthetic pathway for **6** was founded (see scheme 3.3). TBDPS ether was also considered, but discarded due to steric factors.

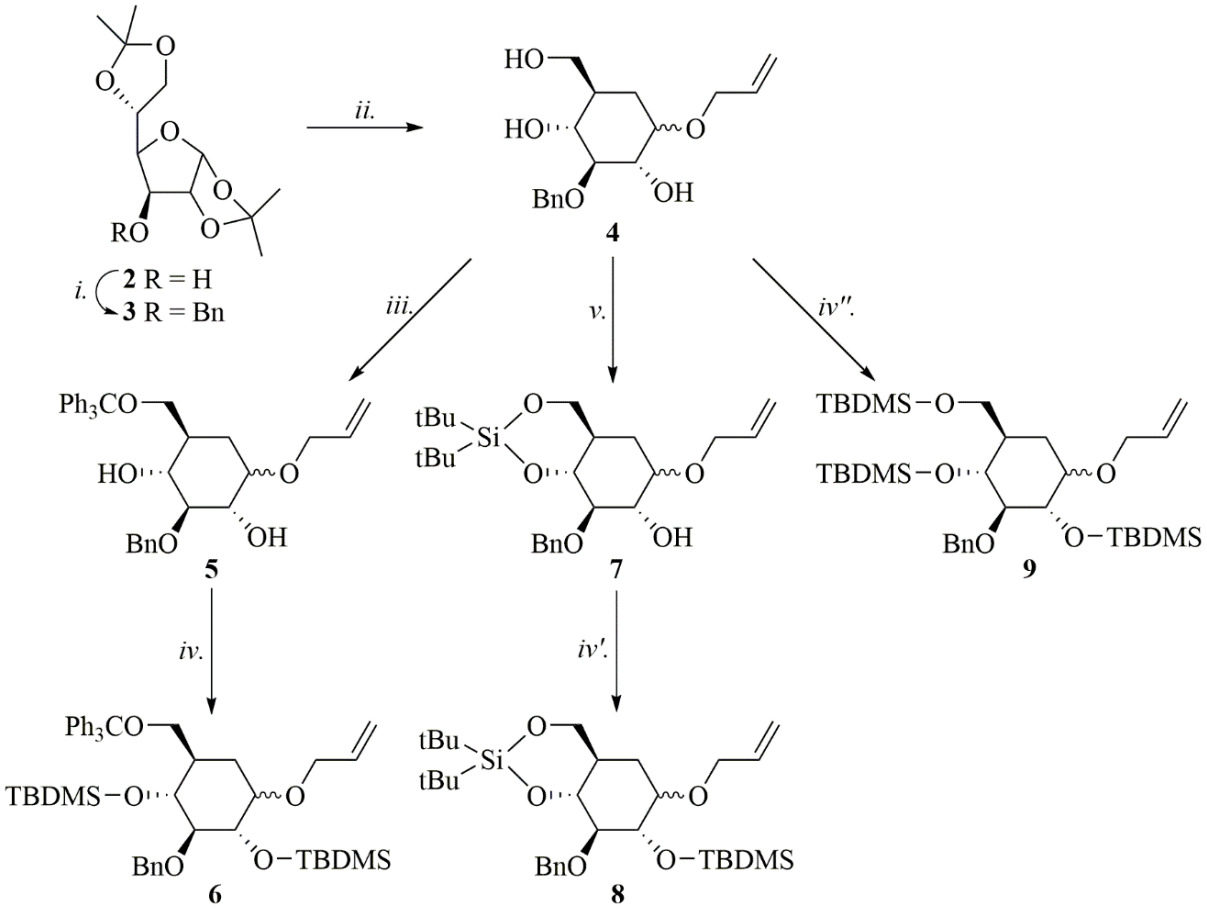

Scheme 3.3: Present protection strategies.

The direct protection of **4** with silyl ethers was inspired by authorative narratives on selective desilylation by Courch.[65-67] The silylene (silyl acetal) protection of **4** to **7**, and subsequently **8**, was envisioned as an analogous pathway to that previously investigated with benzylidene protecting the 4,6-diol.[57] Possibility of selective cleavage at O-6 is crucial for the viability of the pathway, but several methods exist as reviewed by Crouch.[66-67] Selective desilylation can be done in presence of other silyl ethers (e.g. TBDMS),[68] and is applicable to carbohydrates.[69]

Protection of **4** with three equivalents TBDMS ether toward compound **9** was alternatively imagined as a shorter route to fully protected glucose. The possibility of selective desilylation for revealing the 6-OH[65-67] carried the implication of shortening the total synthesis by at least one step. The reviews by Crouch also comprise several methods for desilylation of primary silyl ethers in the presence of secondary.[65-67] A specific method utilized CBr_4 with carbohydrates,[70] which has also been successfully applied for the removal of trityl from carbohydrate primary alcohols.[71]

Although selective deprotection of 6-OH is outside the scope of the present work, it was important when designing the protection pathways. As discussed in this chapter, selective liberation at O-6 are viable prospects for the fully protected species herein (see scheme 3.4).

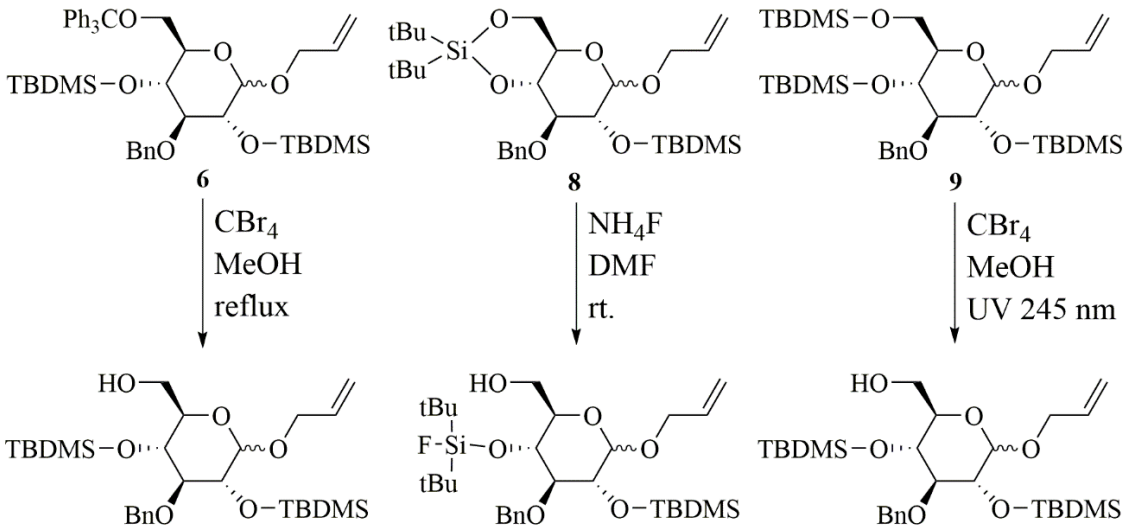

Scheme 3.4: Selective liberation at O-6 of selectively fully protected glucosepyranosides according to the present strategies. Shown conditions are that of previously reported deprotection of trityl,[71] silylene,[69] and primary TBDMS ether.[70]

4 Results and discussion

Development of fully protected glucopyranosides that are available for selective functionalization at positions 1, 3 and 6 was performed in accordance to the present strategies. Results are reported in this chapter, divided into three sections; synthesis and optimization towards the common intermediate allyl 3-*O*-benzyl glucopyranoside (**4**); synthetic development of the three selective full protection pathways; spectroscopic characterization. Pyranoside anomeric mixture following the furanose-pyranose rearrangement was substantial. Going forward, compound α- and β-anomers are suffixed **a** or **b**, respectively.

4.1 Anomeric enrichment of furanose-pyranose rearrangement to allyl 3-*O*-benzyl-D-glucopyranoside (4)

The protection of O-3 is key to the present strategies, and allyl 3-*O*-benzyl-D-glucopyranoside (**4**) serves as an intermediate to all subsequent full protection pathways. The employed method of furanose-pyranose rearrangement for producing **4** from diacetoneglucose (**2**) has previously been described by Kusumoto *et al.*[3] (see scheme 4.1), meanwhile reporting an α:β ratio of 73:27. Since the target compound **1** is strictly α-anomeric, anomeric resolution towards pure α is obviously desirable. Previous investigations by the research group found that anomers of **4** were inseparable via normal phase flash chromatography.[72] Recrystallization, trituration, LiCl extraction and freeze-drying were tried as alternative purification methods in attempts at anomeric resolution, which were all unsuccessful in this regard. Thus, exploration of ways of increasing the anomeric effect towards anomeric enrichment was founded.

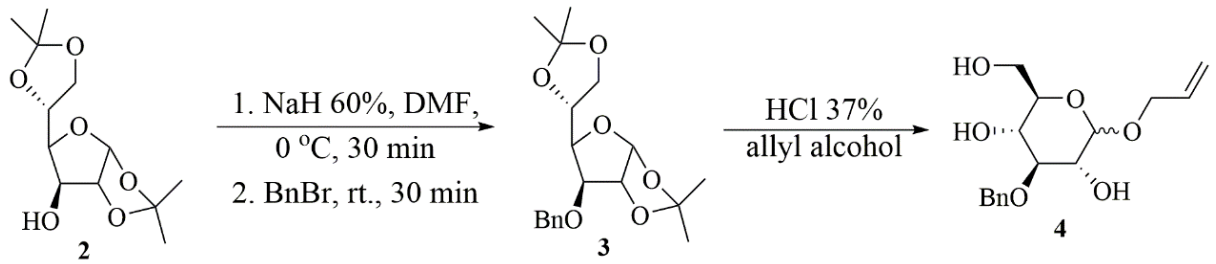

Scheme 4.1: Method employed by Kusumoto *et al.*[3] for synthesis of **4**.

4.1.1 Evaluation of anomeric composition of allyl 3-*O*-benzyl-D-glucopyranoside (4)

For the sake of efficiency, and in order to avoid tedious flash chromatography, anomeric composition was evaluated via NMR on crudes of compound **4** during the screening process. Extensive overlap of signals was evident (disregarding the sugar region), such as anomeric, benzylic and allylic signals. Consequently, no standalone characteristic pair of *α*-/*β*-signals were readily comparable. It was found that *α*:*β* ratio could be determined for integration method as shown in figure 4.1, for which signals belong to allylic[73] and anomeric[30] protons for each anomer. Using formula 1, the below example gives *α*:*β* ratio = 2.76:1 = 73:27. Although the formula is susceptible to imprecision due to overlap and inaccuracies of spectral integration,[74] its use as an indicator is acceptable at this stage.

$$\frac{\alpha H_1 + \alpha AllH}{(\beta H_1 + AllH)} = \frac{2\ \alpha - signals}{2\ \beta - signals} = \frac{\alpha}{\beta} \qquad (1)$$

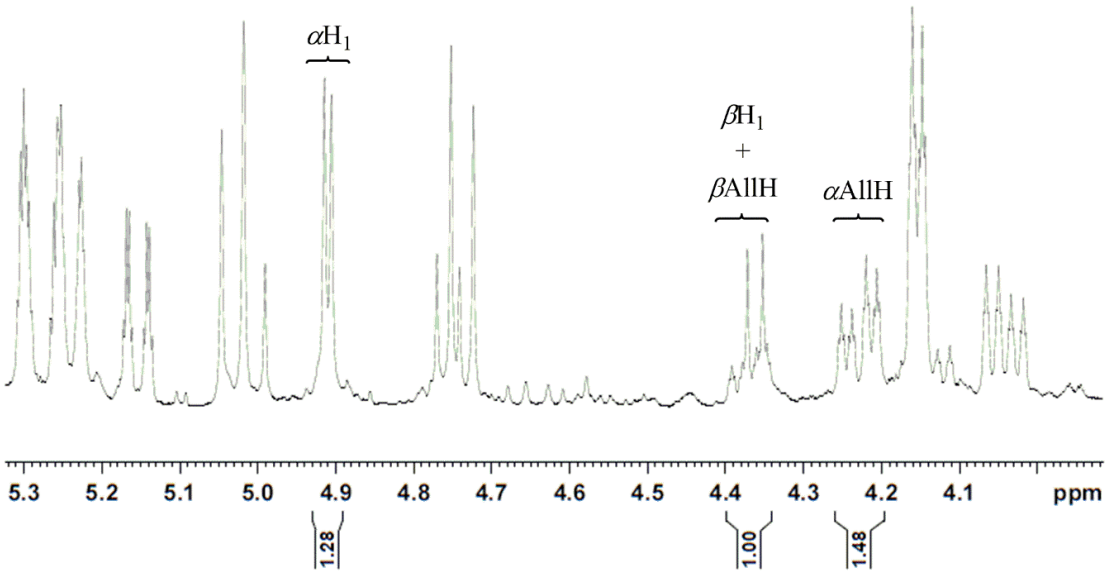

Figure 4.1: Integration method for determining *α*:*β* ratio for crude **4** in presence of allyl alcohol. Only the relevant spectral region is depicted.

The current integration method had to be representative of the anomeric composition of pure compound. In order to verify, the *α*:*β* ratio was determined for **4** (purified by flash chromatography) using ^{13}C-NMR. The same anomeric ratio was found (see appendix B), indicating that the current integration method on crude **4** can be used for estimating anomeric composition representative of that of purified compound.

4.1.2 Benzylation of diacetoneglucose (2)

Due to the simplicity of the reaction and it being relatively well established, little effort was allocated to optimization of benzylation of **2**. Following the benzylation step, ^{1}H-NMR of crude 3-*O*-benzyl-1,2:5,6-di-*O*-isopropylidine-*α*-D-glucofuranose (**3**) was found to be insignificantly different from purified **3**, as can be seen in figure 4.2. The subsequent rearrangement reaction was carried out for both crude and pure intermediate in order to confirm. The same *α*:*β* ratio (73:27) was found for **4** in both parallels, indicating purification of the intermediate **3** to be unnecessary in terms of anomeric enrichment. Moreover, reaction with crude **3** proceeded to satisfactory yields of **4**, effectively eliminating a purification step. Even on 10 g scale reaction of crude **3**, a 59% yield of **4** was achieved after flash column purification.

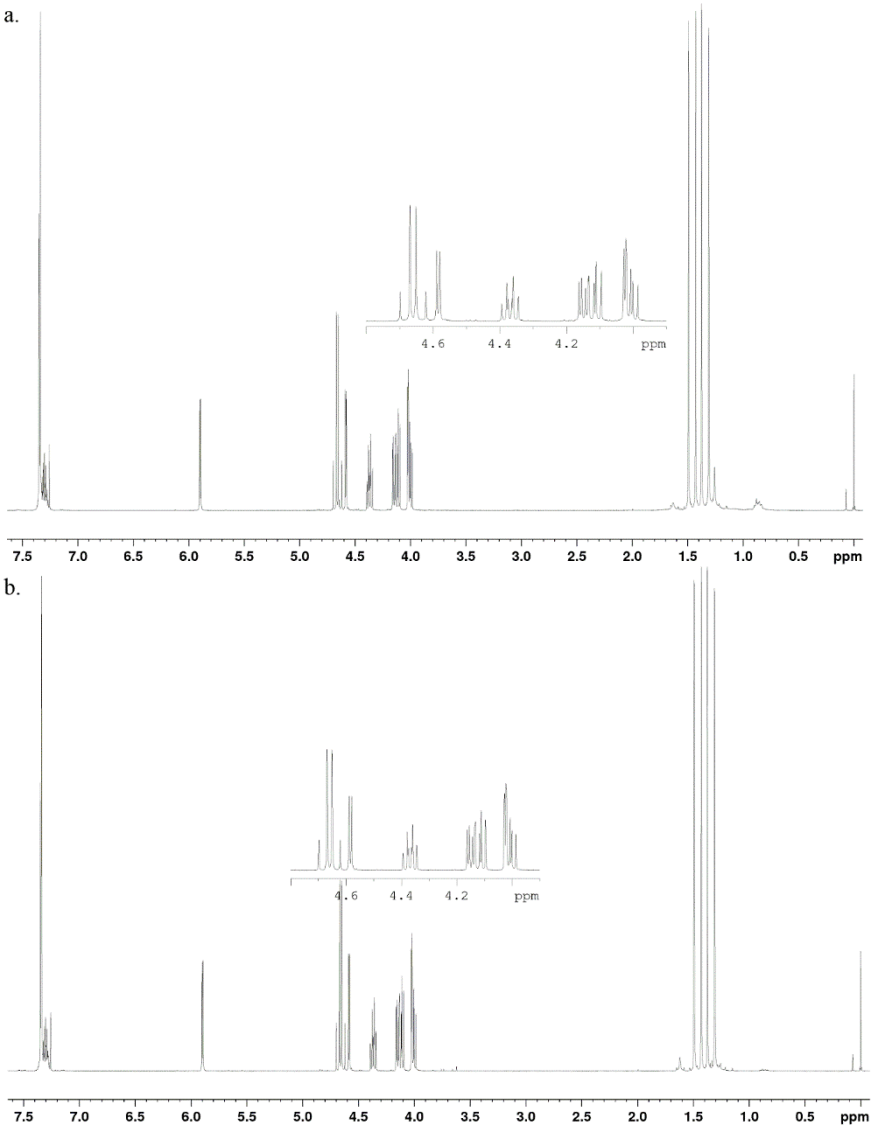

Figure 4.2: ^{1}H-NMR spectra of a. crude **3**, only preliminary purified; b. pure **3**, purified via flash chromatography (SiO_2, 3.0 x 20 cm, dichloromethane:*n*-pentane = 1:5).

4.1.3 Screening of factors for increasing anomeric effect

The reported α:β ratio of 73:27 for **4** by Kusumoto *et al.*[3] is similar to that of methyl glucopyranosides,[21] serving as a standard for comparing rearrangement reaction conditions. In attempts at influencing the anomeric compositions, experiments were carried out with varyious promoters, (co-)solvents, temperature and reaction time, which are known to influence the anomeric equilibrium.[11-13, 15-16, 22, 48] Some brief investigations of influencing factors had already been performed by the research group,[72] of which the present work expands upon. For the sake of dataset context, relevant results of the previous investigation have been recounted herein, but the original author is attributed fully the appropriate experiments. All results are summarized in table 4.1.

The effect of reaction time on anomeric composition was firstly investigated, employing the conditions of Kusumoto *et al.*[3] Similar reactions have required three days for anomerization to reach equilibrium, which have been stated to proceed more rapidly at elevated temperatures.[48] The anomeric composition of α:β = 73:27 was found of the reaction mixture after 0.5 h, 1 h, 2 h, 4 h and 20 h (entries 1-5), indicating that anomeric equilibrium instils relatively quickly. The previous experiments were reacted for 2.5 h,[72] whereas herein experiment were allowed to proceed overnight (20 h) in attempts to maximize proportion of α-anomer.

Secondly, the effect of reaction temperature was investigated for the same reaction conditions. A similar temperature study was also performed for rearrangement using TMSCl, based on successful employment in anomerization of D-glucopyranoses.[48] It was found that that HCl reached anomeric equilibrium slower at lower temperatures (entries 6-8), than TMSCl does (entries 9-11). This might be relatable to the lower equivalents used for HCl 37 % (4.25% w/v $\approx$ 1.6 eq.) compared to TMSCl. This is supported by lower proportions of α-anomer for reaction with minimal amount of TMSCl (1.1 eq.). Furthermore, the anomeric composition appears unaffected by the temperature when above 80 ^{o}C for HCl 37% (1.6 eq.), and 60 ^{o}C for TMSCl (5 eq.).

Table 4.1: Anomeric composition of crude **4** (200 mg scale) following rearrangement at different reaction times, temperatures, co-solvents and promoters. Reflux was maintained at 110-130 °C depending on solvent. UR, undesired reaction as indicated by ^{1}H-NMR.

Entry nr.	Reaction time [h]	Temperature [°C]	Co-solvent	Promoter(s) [eq.]	α:β ratio
1	0.5	reflux	-	HCl 37% (1.6)	73:27
2	1	reflux	-	HCl 37% (1.6)	73:27
3	2	reflux	-	HCl 37% (1.6)	73:27
4	4	reflux	-	HCl 37% (1.6)	73:27
5	20	reflux	-	HCl 37% (1.6)	73:27
6[a]	2.5	60	-	HCl 37% (1.6)	63:37
7[a]	2.5	80	-	HCl 37% (1.6)	73:27
8	20	reflux	-	HCl 37% (1.6)	73:27
9[a]	2.5	60	-	TMSCl (5)	74:26
10	20	80	-	TMSCl (5)	73:27
11	20	reflux	-	TMSCl (5)	73:27
12	20	reflux	Water	HCl 37% (1.6)	73:27
13	20	reflux	Toluene	HCl 37% (1.6)	72:28
14[a]	2.5	reflux	ACN	HCl 37% (1.6)	72:28
15[a]	2.5	reflux	DCM	HCl 37% (1.6)	68:32
16[a]	2.5	reflux	Butan-1-ol	HCl 37% (1.6)	UR
17[a]	2.5	reflux	THF	HCl 37% (1.6)	72:28
18	20	reflux	-	TMSCl (1.1)	70:30
19	20	reflux	-	H_2SO_4 (1.6)	UR
20	20	reflux	Water	H_3NSO_3 (1.6)	65:35
21	20	reflux	-	*p*-TsOH (1.6)	UR
22	20	reflux	-	HCl 37% (1.6) + $ZnCl_2$ (1.1)	71:29, UR
23	20	reflux	-	HCl 37% (1.6) + $SnCl_2$ (1.1)	UR
24	20	reflux	-	$ZnCl_2$ (1.1)	UR
25	20	reflux	-	$SnCl_2$ (1.1)	UR

[a] Previously performed experiment by the research group (2.5 h reaction time).[72]

Some common organic solvents were screened for influence on the anomeric effect during the rearrangement step, restricted by miscibility and possibility of undesired side reactions (particularly alcohols). Solvents are well known to influence anomeric composition, as previously stated,[11-13, 16, 22] where the anomeric effect is greater in solvents of low dielectric constant.[14, 22] Substrates were suspended in a 1:1 mix of allyl alcohol and the solvent in question. Little to no influence on the anomeric composition was observed (entries 12-17), regardless of dielectric constant of the solvent (e.g. 2.38 for toluene versus 78.54 for water[75]). It is speculated that co-solvents were administered in insufficient amounts for dictating permittivity of the mixture. The complex properties of solvent mixtures pertains to another branch of chemistry entirely, thus further attempts at explanation were not made.

Different promoters were lastly explored in attempts to increase α-anomer proportion. The choice of other acids tried for reaction was based on previous use in similar reactions.[47-48, 76] Reaction with some Lewis acids was also attempted, having been utilized in pyranose-furanose rearrangements (opposite of the currently investigated step)[77] and for carbohydrate anomerization.[78]. The majority of the catalysts were found to give undesired reactions for the employed conditions (entries 19, 21, 23-25). In the few cases the desired compound was observed, α-anomer proportion was similar to or lower than that achieved with by Kusumoto *et al.*[3] (entries 18, 20, 22). Speculation offer little insight, and further investigations would benefit the topic, in which case, use of milder conditions is recommended, be it in the form of promoter, equivalents, reaction time, or temperature.

As a summarizing remark to this chapter, no ground was gained towards anomeric resolution or enrichment of **4a** after furanose-pyranose rearrangement. The necessity of elevated reaction temperature and sufficient catalyst was solidified. However, the reaction was susceptibly fragile toward relatively harsh conditions. HCl and TMSCl seemed the most promising promoters, but further investigation is required for conclusive remarks on other catalysts tried herein. It is additionally suggested the first 30 min of the reaction be investigated, in order to monitor conversion.

4.2 Selective full protection pathways

Compounds **5**-**9** were successfully prepared in accord with the three full protection pathways as strategized in chapter 3.3. The implications of each pathway to **6**, **8** and **9** is discussed sequentially herein, and a comparison of the individual pathways is set to conclude this chapter.

4.2.1 The trityl pathway

Allyl 3-O-benzyl-6-O-trityl-D-glucopyranoside (5)

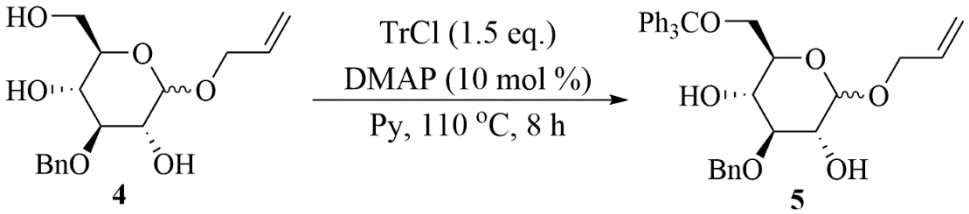

Scheme 4.2: Previously employed conditions by Derrick *et al.*[64] for the tritylation of **4** to give **5**.

Reaction conditions according to Derrick *et al.*[64] were followed for the synthesis of allyl 3-*O*-benzyl-6-*O*-trityl-D-glucopyranoside (**5**). Due to crudes being very viscous, flash chromatography was initially carried out by dry loading with Celite®, where low yield was obtained (table 4.2, entry 1). For the same reaction conditions, flash purification with minimal solvent/eluent application gave increased yield (entry 2). Crystallization was attempted as an alternative method of purification, but was unsuccessful (entry 3).

Table 4.2: Tritylation reactions of **4** (200-400 mg scale) with flash purification with/without Celite® loading, and for various temperatures and concentrations. TrCl was retrieved during flash purification.

Entry nr.	Concentration of 4 [mg/mL]	Temperature [ºC]	Celite® dry loading?	Yield [%]	Retrieved TrCl [eq.]
1	79.9	110	Yes	17	0.91
2	79.4	110	No	45	<0.5
3	77,7	110	Crystallization	-	-
4	72,8	50	No	51	0.55
5	34,3	110	No	59	0.63
6	33,6	50	No	23	0.99

For purification carried out with Celite® dry loading (entry 1), 0.9 eq. of the administered 1.5 eq. of TrCl was retrieved after flash chromatography, as opposed to <0.5 eq. for solvent application (entry 2), refuting the seemingly similar conversions observed by HPLC (figure 4.3a and c). This suggests compound **5** to be unstable towards Celite®, therefore dry loading for flash chromatography was avoided henceforth.

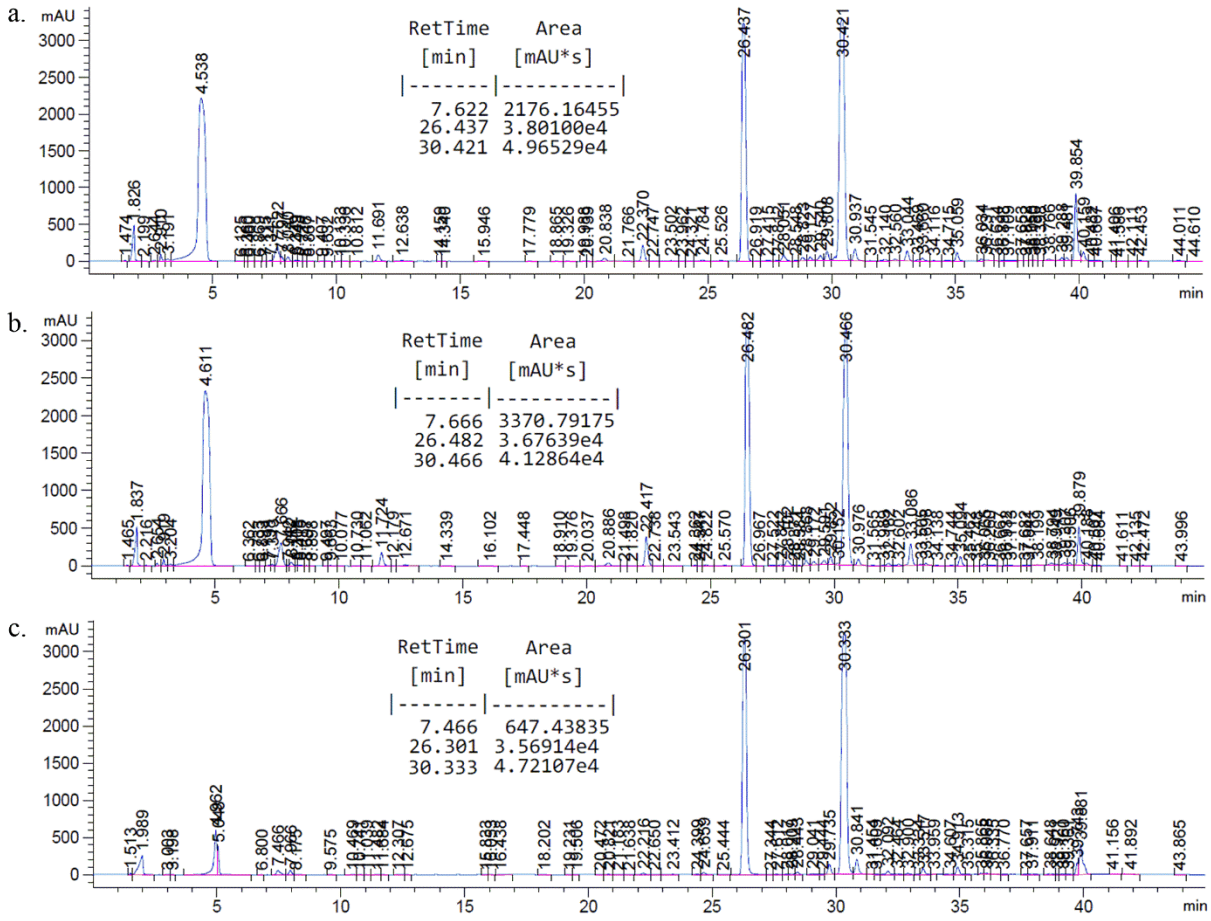

Figure 4.3: HPLC with acetonitrile:water gradient (method A) of aliquots from the tritylation step for a. entry 1 after 8 h reaction time; b. entry 1 after 24 h reaction time; c. entry 2 after 8 h reaction time. t_R (**4**) ≈ 7.5 min, t_R (TrCl) ≈ 26.4 min, t_R (**5**) ≈ 30.4 min.

Despite approximately 1 eq. of TrCl having reacted for entry 2, notably lower yield was obtained than reported by Derrick *et al.*[64] Monitoring the reaction by HPLC showed no significant difference in conversion of starting materials **4**/TrCl after 8 h or 24 h reaction time (figure 4.3a-b), indicating 8 h to be sufficient reaction time. Higher yields were achieved for reaction with decreased temperature (entry 4) and reagent concentrations (entry 5), individually. However, combination of these conditions again afforded low yield (entry 6), with substantial amount of TrCl being returned. For all experiments, lower yields were obtained than that

indicated by equivalents of TrCl retrieved/consumed, suggesting loss to be attributable the work-up procedure.

Flash chromatography purification was unsuccessful in anomeric separation of **5a** and **5b**, however, anomerically enriched fractions were collected for either anomer, indicating slight band separation. Alternative stationary phases in flash chromatography is suggested for further investigation, should anomeric resolution be desirable at the current step.

Allyl 3-O-benzyl-2,4-di-O-tert-butyldimethylsilyl-6-O-trityl-D-glucopyranoside (6)

The TBDMS protection of 2-OH/4-OH on **5** for synthesis of **6** (scheme 4.3) was inspired by reaction conditions used on similar allyl pyranoside derivatives.[43-44, 58] Silylation of 4-OH was expected to be difficult due to steric bulk of the neighbouring trityl substituent, and relatively low reactivity in terms of carbohydrate hydroxyls.[29, 38] For this reason, *tert*-butyldimethylsilyl triflate (TBDMSOTf) was used in place of the more common TBDMSCl silylation reagent, in accord with recommendations by Corey *et al.*[42] for the protection of unreactive and sterically hindered alcohols. Specifically, 1.5 equivalents TBDMSOTf and 2.0-2.5 equivalents 2,6-lutidine per alcohol functionalities present in the substrate had been suggested.

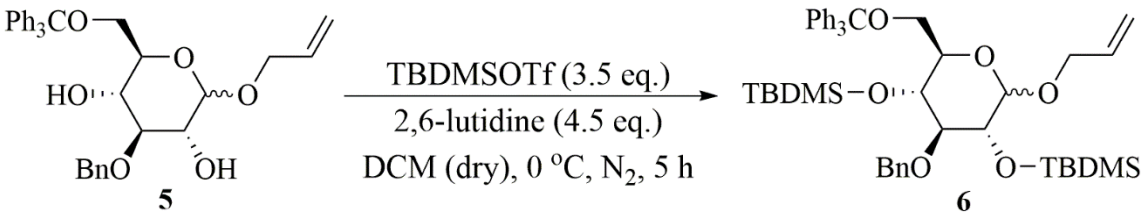

Scheme 4.3: Reaction conditions for the selectively fully protected **6** via silylation of **5**.

Silylation is regularly performed using amine bases such as 2,6-lutidine, triethylamine (TEA), imidazole or a pyridine-DMAP-system.[7, 10, 39] Reaction with 2,6-lutidine or TEA was attempted due to having the most contrasting basicities (see table 4.3), where pK_a: 2,6-lutidine ≈ imidazole < DMAP < TEA.[75] In addition, reaction was carried out with NaH as an extreme, but was discarded due to giving undesired reaction. Monitoring the reactions by HPLC indicated formation of by-products with 2,6-lutidine after just 1 h, while insufficient conversion was observed when TEA was used. The less basic 2,6-lutidine appears to be more reactive towards sugar hydroxyls than TEA. This might be related to steric availability of the respective bases towards the obstructed alcohol functionalities, or to mechanistic features. Attempts has not been made towards an explanation of either. Regardless, milder conditions are suggested for reactions using 2,6-lutidine, or alternatively employing TEA at somewhat harsher conditions

(e.g. room temperature instead of 0 ºC). It would be interesting to perform the current step using imidazole, DMAP/pyridine or other similar amine bases.

Table 4.3: Silylation of **5** (200-400 mg scale) using different bases, administered in 4.5 eq. UR, undesired reaction as indicated by ^{1}H-NMR.

Base	Yield [%]	*α*:*β* ratio	Impurities
2,6-lutidine	59	80:20	By-product[a]
TEA	86	71:29	Starting material[a]
NaH 60% + Bu_4NI (15 mol %)	UR	-	-

[a] As indicated by HPLC.

Monitoring the reaction with 2,6-lutidine by HPLC showed impurities at t_R = 52.83 min and 54.02 min, with an peak area/height ratio similar to the anomeric ratio of **6** (see figure 4.4). By-product at t_R = 52.83 min was collected during flash chromatography and isolated by preparative HPLC, found to be the benzoyl analogue of **6a** following structural elucidation (see section 4.3.2). The impurity at t_R = 54.02 min is believed to be the corresponding *β* species. This was not confirmed due to being isolated in quant amounts following preparative HPLC of the **6** product mixture, in which the by-product resided.

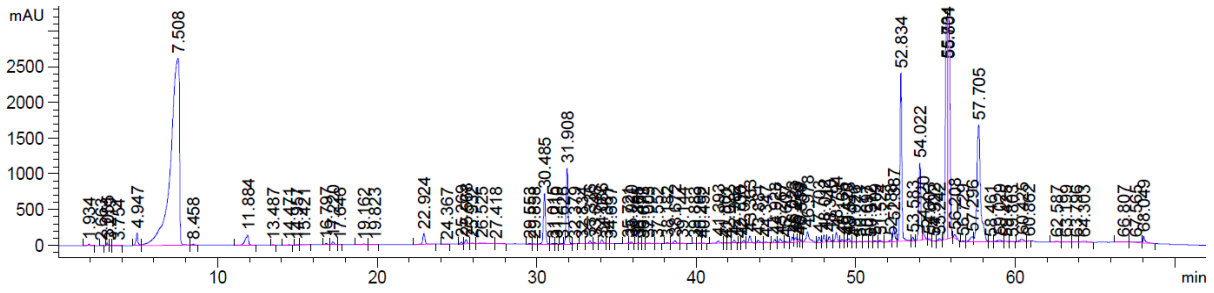

Figure 4.4: HPLC with acetonitrile:water gradient (method B) of aliquots from the silylation of **5** to **6** after 5 h. t_R (**6a**) = 55.76 min, t_R (**6b**) = 57.71 min.

4.2.2 The silylene (silyl acetal) pathway

Allyl 3-O-benzyl-4,6-O-di-tert-butylsilylene-D-glucopyranoside (7)

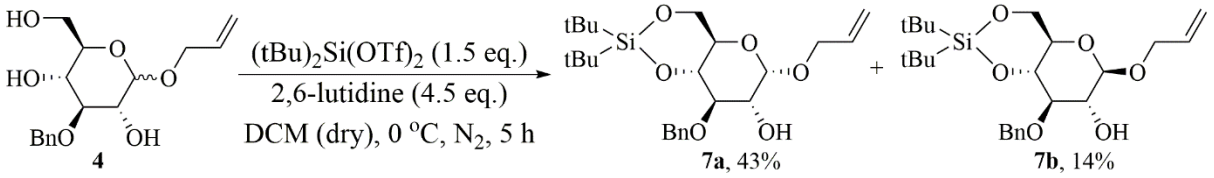

Scheme 4.4: Reaction conditions for 4,6-diol protection of **4** with silylene towards **7**.

Di-*tert*-butylsilyl bis(triflate) is an established 1,3-diol protection reagent, also used in carbohydrate chemistry.[79] For pyranosidic systems, the silylene protecting group is best utilized in systems where regioselectivity is limited, e.g. for O-3 or O-2 substituted pyranosides.[80-81] Protection of unsubstituted pyranosides is possible, although in comparatively lower yields.[45] The silylene group has only been used once before for protection of 3-substituted pyranosides,[80] and is for the first time applied to a 3-substituted glucopyranoside system in the present synthesis of allyl 3-*O*-benzyl-4,6-*O*-di-*tert*-butylsilylene-D-glucopyranoside (**7**).

Protection of the 4,6-diol **4** affording **7** was performed with $(tBu)_2Si(OTf)_2$ using 2,6-lutidine as base, due to the triflate moieties, consistent with suggestions by Corey *et al.*[42]. Potential for anomeric separation was indicated by the isolation of pure *β*-anomer on a 200 mg reaction (see table 4.4). Through increased column length and meticulous fraction collection, isolation of **7a** and **7b** was possible for increased scale of reaction (800 mg). Collection of fractions composed of both anomers indicated baseline separation to not have been achieved. This is the only time in the present work anomers were isolable in appreciable amounts. This is likely due to 2-OH being the lone hydroxyl, while simultaneously being situated near the anomeric position, thus greatly influenced by the inherent conformational differences of anomers.

Table 4.4: Yields from silylene protection of 4,6-diol **4** towards **7a**/**7b**.

Scale [mg]	Reaction time [h]	Yield [%] α	β	Total	$t_R \approx 52.8$ by-product [mg]
200	5	-	19	93	Quant
800	5	43	14	63	143.3

The occurrence of by-products was presumed less likely with a bidentate silylation reagent compared to that observed before in silylation of **5**, due to **4** having the single 1,3-diol (positions 4 and 6). For the 200 mg reaction, by-product formation was observed by HPLC at $t_R \approx 52.8$

min in minor amounts after 5 h reaction time (see figure 4.5a). However, formation of by-product can be seen as early as 1 h reaction time for the scaled-up reaction in figure 4.5b. The presence of unconverted substrate and absence of silylenation reagent indicates high reactivity of the protecting reagent. Collection of the impurity at $t_R \approx 52.8$ min during flash purification allowed for spectroscopic characterization, detailed in section 4.3.2. The by-product was found to be a fully protected glucose species, presumably having reacted with two equivalents of $(tBu)_2Si(OTf)_2$. For increasing scale of reaction, milder conditions are suggested, by decreasing temperature further or with amine base in less amounts (e.g. cat. amount) or with lower basicity.

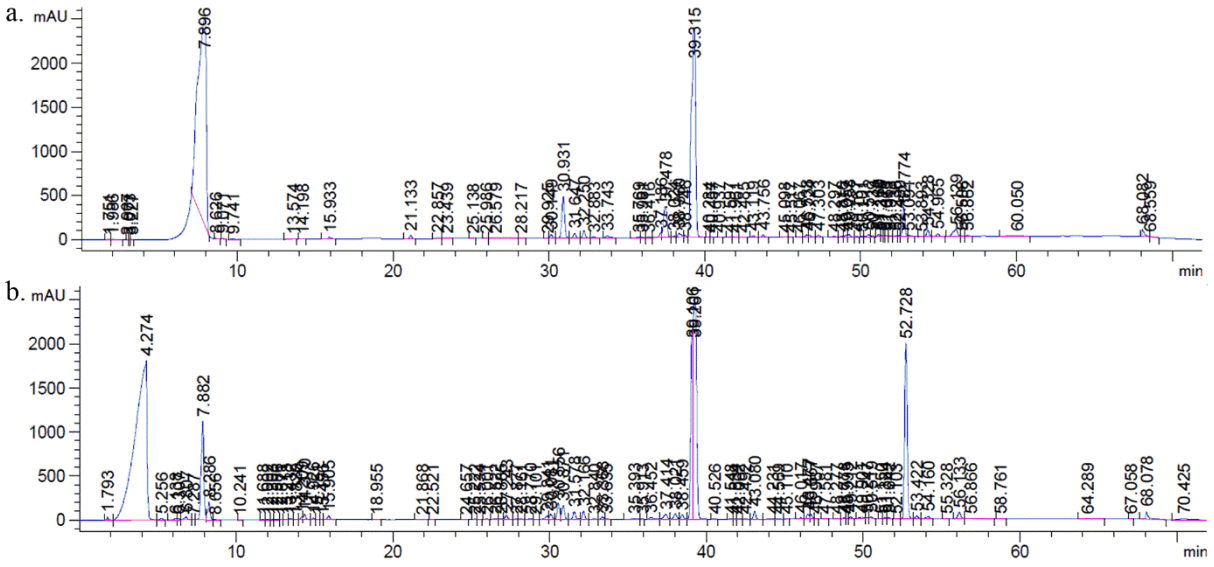

Figure 4.5: HPLC with acetonitrile:water gradient (method B) of aliquots from the silylene diol protection of **4** for a. 200 mg scale reaction after 5 h.; b. 800 mg scale reaction after 1 h. t_R (**4**) = 7.86 min; t_R (**7a**/**7b**) ≈ 39.3 min; t_R ($(tBu)_2Si(OTf)_2$) = 68.20 min.

The appearance of each anomer was different, despite identical treatment. As shown in figure 4.6, the *α*-anomer was a colourless oil, while the *β*-anomer was as a white solid. Configuration at C-1 appears to have a profound effect on the macrostructure of the compound. It is speculated that the lone equatorial 2-hydroxyl is less available to intermolecular interactions (e.g. H-bonding) for **7a** than **7b**. This is supported by lower reported relative acidity of 2-OH in selectively protected methyl glucopyranosides.[32] However, an inconsistency in this report detracts from the certainty of representativeness of the reported acidities, where 1,3,4,6-tetra-*O*-methyl-*β*-D-glucopyranoside is tabulated as galactopyranoside

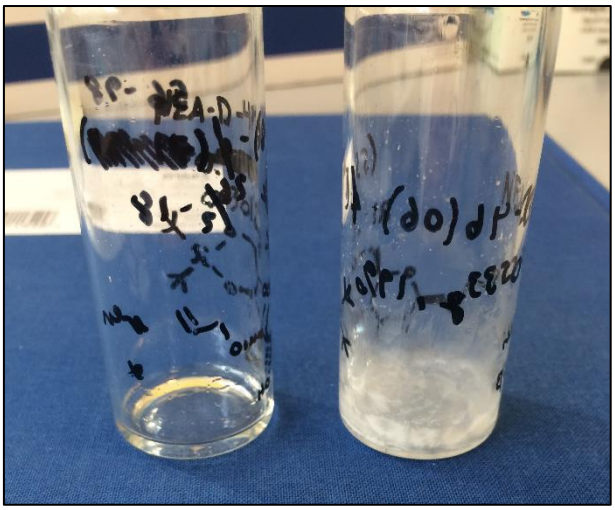

Figure 4.6: Appearance of isolated *α*-anomer (**7a**, left) and *β*-anomer (**7b**, right) allyl 3-*O*-benzyl-4,6-*O*-di-*tert*-butylsilylene-D-glucopyranoside.

Modelling of the preferred (minimized energy) conformations revealed interesting features of the compounds. The glucose ring of **7b** adapts the chair conformation, whereas **7a** adopts a distorted boat conformation (see figure 4.7). Compound **4** has been included for comparison, also preferring the chair conformation. The new ring formed by the silylene moiety likely inflicts strain on the sugar ring. By adopting the boat-like conformation, the *α*-anomeric C-1 substituent is oriented equatorial, instead of axial as in the chair conformation (as is the case for **4a**). The apparent conformational change is likely a coping mechanism for relieving strain, since axial configuration is generally less energetically favourable than equatorial for pyranoses.[7, 9-10, 14, 18]

Availability of the lone hydroxyl of **7a**/**7b** is difficult to predict, but some comments can be made based on distances to nearby alkoxy-O in the static model images. For **7b**, distance between the 2-OH proton and O-1/O-3 is 3.7 Å and 2.4 Å, respectively. Rotation about the C-O bond allows H-bonding to O-1 or O-3 according to proposed H-bond networks.[33-34] For **7a**, 2-OH and O-3 are anti-periplanar and likely have little interactions, whereas the 2-OH proton and O-1 is 2.1 Å apart. For both molecules, distances are sufficient for H-bonds to be classified as strong.[82] A shorter distance between 2-OH and adjacent alkoxy-O for **7a** than for **7b** suggests stronger H-bonding of the former anomer, and consequently, lower availability of said hydroxyl towards reactions and intramolecular interactions. It must be noted that this is speculative, and that steric effects have not been accounted for.

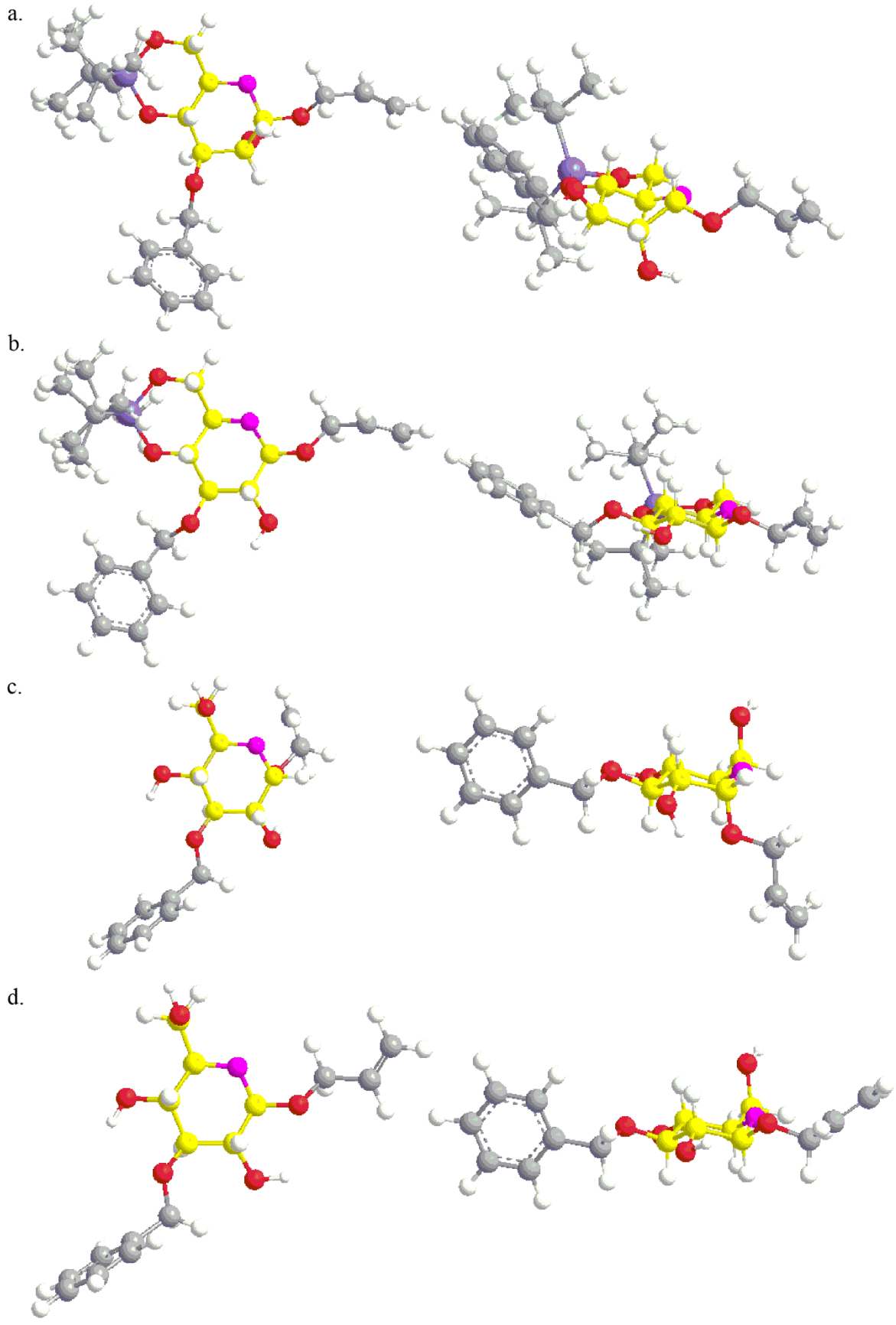

Figure 4.7: Minimized energy conformations as seen from two perspectives of a. **7a**; b. **7b**; c. **4a**; d. **4b**. The glucose moiety is highlighted for clarity (yellow, grey = C; purple, red = O; white = H).

Allyl 3-O-benzyl-4,6-O-di-tert-butylsilylene-2-O-tert-butyldimethylsilyl-D-glucopyranoside (8)

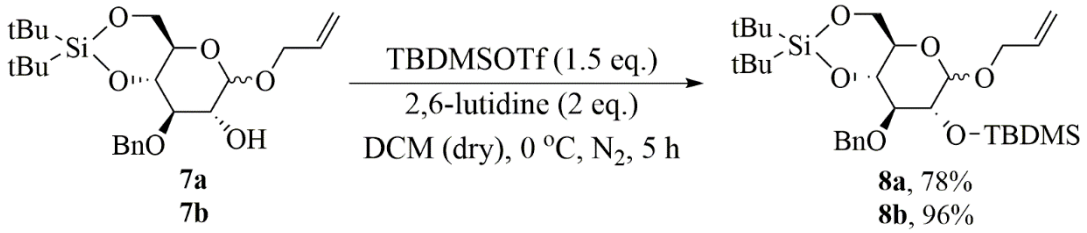

Scheme 4.5: Conditions for silylation of **7** towards selectively fully protected **8**.

Silylation of the free **7** 2-OH towards synthesis of allyl 3-*O*-benzyl-4,6-*O*-di-*tert*-butylsilylene-2-*O*-*tert*-butyldimethylsilyl-D-glucopyranoside (**8**) (scheme 4.5) was performed under conditions according to suggestions by Corey *et al.*[42] Using 2,6-lutidine, undesired reactions were presumed unlikely for the current step, due to having only one remaining available hydroxyl. The 2-OH also has relatively high reactivity in terms of carbohydrate hydroxyls.[29, 38] Reaction was carried out on anomerically pure substrate **7a**/**7b**, affording anomerically pure **8a**/**8b**. For the α-anomer, starting substrate **7a** was retrieved (0.0194 g, 0.1 eq.) after flash chromatography, indicating incomplete conversion. This was not observed for reaction with β-anomer, which proceeded to satisfactory yield, indicating the inherent differences in structure of **7a** and **7b** to be influential towards relative reactivity of each anomer. Without considering steric factors, a correlation might be made between the relative H-bond distances of the hydroxyl and relative reactivity of 2-OH (as discussed before). Regardless, the α-anomer should be allowed to react for some additional time to ensure complete conversion.

The appearances of **8a** and **8b** was different, as was the case for **7a**/**7b**, respectively being that of a colourless oil and a white solid (see figure 4.8). According to the energy minimized calculations, the chair conformation was preferred for both full protected species (figure 4.9). The boat-like conformation is not retained for the α-anomer over the reaction from **7a** to **8a**. Therefore, the difference in appearance of **7a** and **7b**, or **8a** and **8b**, cannot be attributed conformational differences of anomeric pairs, because that would imply that **8a** adopt the same conformation, which the modelled structures disputes. Intermolecular H-bonding interactions where 2-OH participates can neither be attributed as cause of the difference in appearance of the anomers, since that would imply H-bonding functionalities be present for the fully protected species, which spectroscopic evidence refutes. Cause for this observation is unclear, and would be interesting to reassess from the perspective of crystallinity, but which is outside the topic.

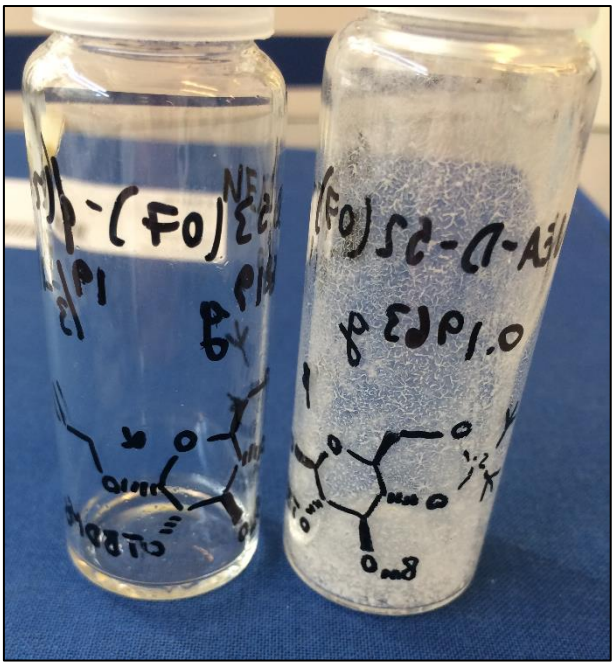

Figure 4.8: Appearance of *α*-anomer (**8a**, left) and *β*-anomer (**8b**, right) of allyl 3-*O*-benzyl-4,6-*O*-di-*tert*-butylsilylene-2-*O*-*tert*-butyldimethylsilyl-D-glucopyranoside.

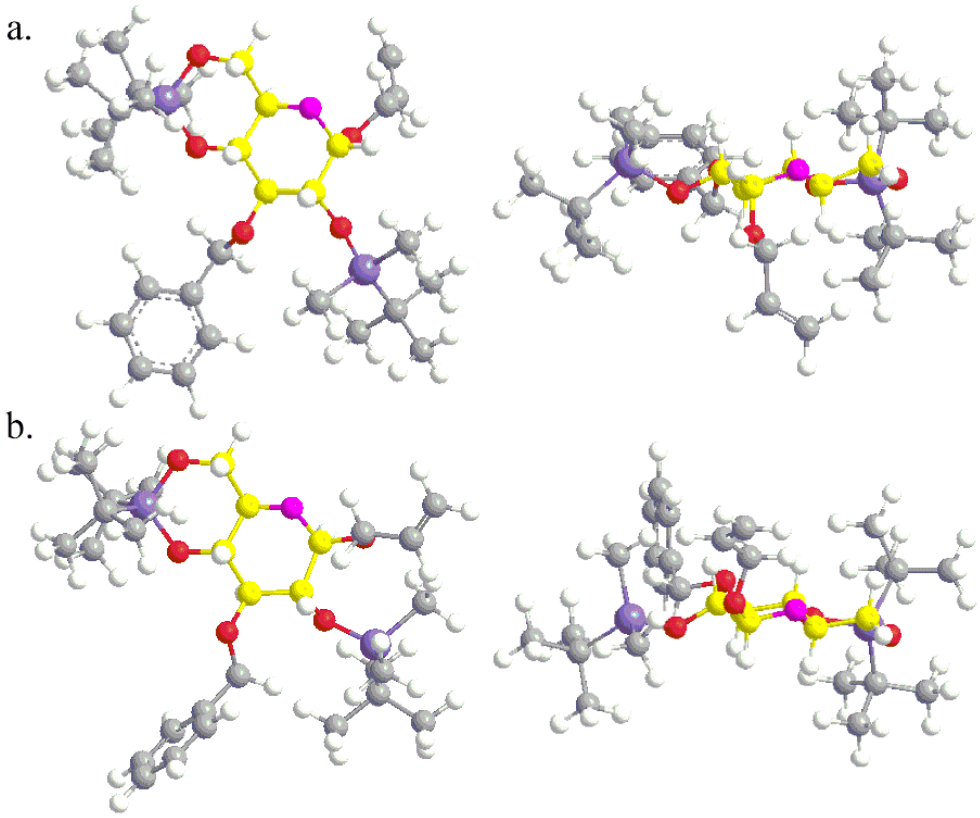

Figure 4.9: Minimized energy conformations of a. **8a**; b. **8b** as seen from two perspectives. The glucose moiety is highlighted for clarity (C = yellow, grey; O = purple, red; H = white).

4.2.3 The tri-TBDMS pathway; synthesis of allyl 3-*O*-benzyl-2,4,6-tri-*O*-*tert*-butyldimethylsilyl-D-glucopyranoside (9)

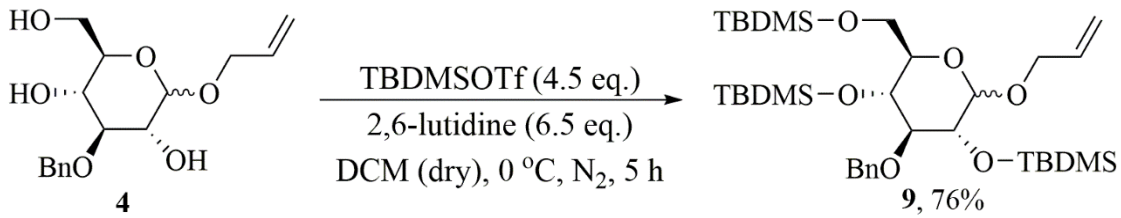

Scheme 4.6: Reaction conditions for global silylation of **4** towards fully protected **9**.

For the synthesis of allyl 3-*O*-benzyl-2,4,6-tri-*O*-*tert*-butyldimethylsilyl-D-glucopyranoside (**9**), employed conditions were that suggested by Corey *et al.*[42] Monitoring of the reaction showed little by-product, even after 24 h. No difference was apparent after 5 h or 24 h by HPLC monitoring of the reaction (see figure 4.10), thus 5 h is sufficient reaction time. The apparent splitting of signals at t_R = 57.82-58.32 min and 60.23-60.88 min into two signals of approximately 1:1 ratio is suspected to be chromatographic distortion, since it was not visible on NMR, where only **9a** and **9b** can be observed in appreciable amounts (see appendix J).

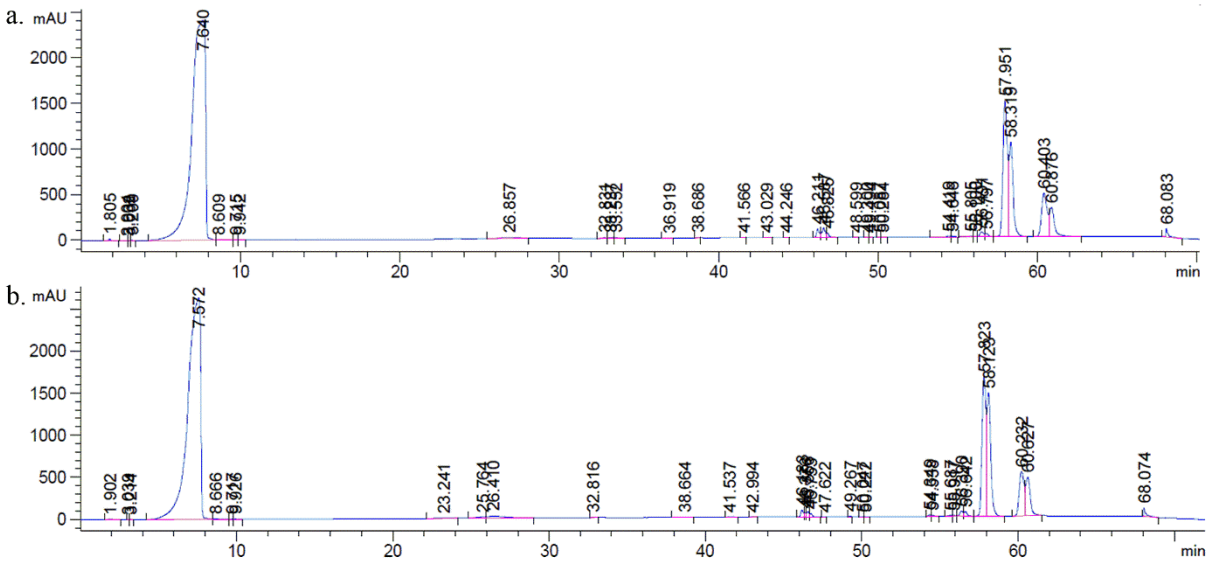

Figure 4.10: HPLC with acetonitrile:water gradient (method B) of aliquots from the silylation of **4** to **9** after a. 5 h reaction time; b. 24 h (rt. from 5 h to 24 h) reaction time. t_R (**9a**) = 57.82-58.32 min; t_R (**9b**) = 60.23-60.88 min.

Preliminary purification with subsequent flash chromatography afforded **9** as a mixture of anomers. TLC of crude **9** gave R_f (SiO_2, Et_2O:*n*-pentane = 1:50) = 0.21-0.36, whereas R_f (SiO_2, Et_2O:*n*-pentane = 1:25) = 0.60-0.77, indicating the compound to have increased retention for decreasing mobile phase polarity. However, behaviour of all fully protected silylated compounds **6**, **8** and **9** on TLC and flash silica gel has been erratically different. Regardless of observed R_f, all of the aforementioned compound were deposited in the first few fractions (depending on scale). Thus, TLC offers little insight on the success of the proposed purification method, and an attempt of the present gradient flash method is warranted. Reduction of purification steps is likely possible by using a gradient mobile phase, where only one flash column is necessary. It is recommended to try the following gradient: 100% *n*-pentane → Et_2O:*n*-pentane = 1:50 → Et_2O:*n*-pentane = 1:25.

Some separation of anomers on flash column was evident for **9**, as was also the case for the fully protected trityl species (**6**). Collection of an α-anomer enriched fraction (α:β = 83:18, 0.0323 g, 2%) indicates slight difference in silica gel affinity of anomers. Anomeric resolution for a normal phase system seems unfeasible with silica gel, and it is suggested separation be furthered attempted with reverse phase chromatography.

4.2.4 Pathway comparisons

The three investigated pathways have been evaluated and compared based on relative ease of reaction/purification and yields. Liberation of O-6 has already been proposed for the fully protected compounds **6**, **8** and **9** (see chapter 3.3), and is regarded as somewhat equal prospects.

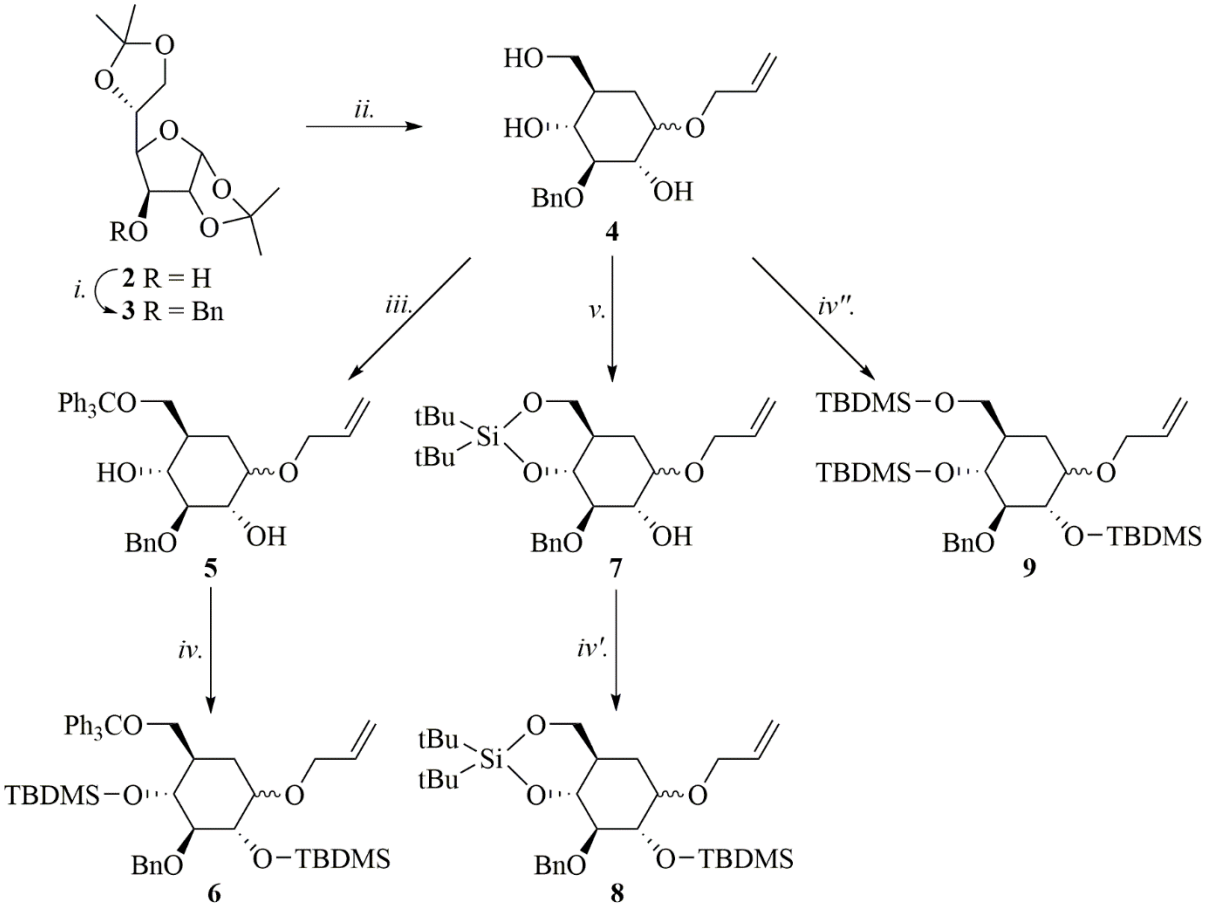

Scheme 4.7: Presently investigated selective full protection strategies of D-glucose.

Due to similarity of silyl ether protection, four out of five of the steps of the three investigated pathways involved almost identical reaction conditions. The three silylation steps (*iv*, *iv'* and *iv''*, see scheme 4.7) were efficiently scalable to appropriate equivalents based on number of alcohol functionalities present in the substrate, in accordance with Corey *et al.*[42] These conditions were also applicable for the diol protection with silylene (step v), although might require further optimization as $(tBu)_2Si(OTf)_2$ appears to be highly reactive. Depending on step and anomer, optimal reaction time with 2,6-lutidine at 0 °C is around 5 h (likely 1 h for step v), and not noticeable advantages were observed for 24 h reaction time.

By-products were observed in steps *iv* and v under these conditions, which have been characterized spectroscopically (see section 4.3.2). No by-product was observed using TEA in

place of 2,6-lutidine for step *iv*, noting lower conversion (other parameters kept identical). Further investigation of alternative amine bases for the appropriate silylation reactions is suggested

Accounting for number of steps, total yields of the respective pathways was 35% for the trityl pathway, 49% for the silylene pathway and 76% for the tri-TBDMS pathway. The tri-TBDMS pathway proceeded to highest yields, and required least steps for a fully protected allyl glucopyranoside. Despite an arguably more elaborate purification following silylation, this pathway appeared most efficient. However, premise of anomeric separation presented by the silylene presents a major advantage, depending on objective. For the future selective functionalization of positions 1, 3 and 6, regioselective liberation at O-6 requires to be proven conceptually for both the aforementioned pathways, whereas removal of trityl is well established in literature. Until deprotection of 6-OH has been assessed, all three pathways should be regarded as viable, especially considering the unexplored potential for optimization of reaction conditions.

4.3 Spectroscopic characterization

4.3.1 Spectroscopic characterization of desired synthetic compounds

Of the compounds prepared in the present work, compounds **3**, **4** and **5** have previously been synthesized, of which **3** is the only one to have been fully characterized with chemical shift assignment.[83] Only anomeric carbon shifts were reported for **4**,[3] and ^{1}H and ^{13}C resonances were unassigned for **5**.[63] Found spectral data for these compounds coincided with that previously reported, for which chemical shift assignment of **4** and **5** was completed herein. To the best of our knowledge, compounds **6**, **7**, **8** and **9** have been spectroscopically characterized for the first time. Anomers have been individually characterized for all synthetic compounds, excluding **3**. Numbering of the common backbone and protection groups is given in figure 4.11. ^{1}H and ^{13}C chemical shifts for α- and β-anomers of assigned compounds are reported in tables 4.5-4.8, with ^{1}H coupling constants reported in table 4.9.

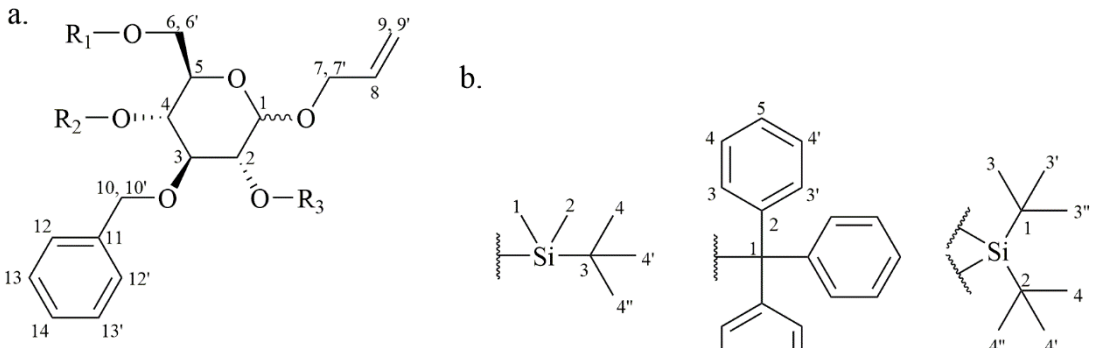

Figure 4.11: Numbering of positions for NMR shift assignment of a. common backbone; b. relevant protection groups. Chemical equivalence was assumed for each phenyl ring of the trityl moiety.

Some proton signal multiplicities and spin-spin couplings were unresolved due to overlap, but structural assignment was still unambiguous. Solvent impurities, such as water, ethyl acetate, diethyl ether, dichloromethane and *n*-pentane (to mention some),[84] are variously present in spectra included in appendices A-L. Although not detrimental to the spectral resolution, their presence should be acknowledged, as well as accounted for in respect to inaccuracies conferred upon herein reported data.

Table 4.5: ^{1}H-NMR chemical shifts (600 MHz, ppm) of α- and β-anomer of **4**, **5** and **6** in $CDCl_3$ at 25^{o}C with TMS as internal standard. Multiplicities are given in parenthesis. Presence of site without observed signal is denoted by n/a, lack of site is denoted by dash (-).

H	**4a**	**4b**	**5a**	**5b**	**6a**	**6b**
1	4.92 (d)	4.370 (d)	4.94 (d)	4.35 (d)	4.88 (d)	4.42 (d)
2	3.68 (dd)	3.55 (dd)	3.69 (m)	3.55 (dd)	3.77 (dd)	3.60 (dd)
3	3.61 (t)	3.42 (t)	3.58-3.62	3.395 (t)	3.66 (t)	3.32 (t)
4	3.56 (t)	3.59 (t)	3.58-3.62	3.65 (t)	3.27 (t)	3.37 (t)
5	3.69 (ddd)	3.37 (ddd)	3.77 (m)	3.41 (ddd)	4.01 (td)	3.57 (td)
6	3.78 (dd)	3.77 (dd)	3.32 (dd)	3.368 (dd)	3.05 (t)	3.18 (dd)
6'	3.84 (dd)	3.89 (dd)	3.373 (dd)	3.388 (dd)	3.36 (dd)	3.29 (dd)
7	4.05 (ddt)	4.14 (ddt)	4.08 (ddt)	4.17 (ddt)	4.24 (ddt)	4.27 (ddt)
7'	4.24 (ddt)	4.374 (ddt)	4.27 (ddt)	4.39 (ddt)	4.51 (ddt)	4.54 (ddt)
8	5.94 (m)	5.94 (m)	5.96 (m)	5.96 (m)	6.09 (dddd)	6.06 (dddd)
9	5.320 (d(b))	5.327 (d(b)))	5.32 (d(b)))	5.33 (d(b)))	5.44 (d(b)))	5.38 (d(b)))
9'	5.247 (d(b)))	5.240 (d(b)))	5.233 (d(b)))	5.229 (m)	5.28 (d(b)))	5.24 (d(b)))
10	4.73 (d)	4.75 (d)	4.80 (d)	4.82 (d)	4.66 (d)	4.73 (d)
10'	5.05 (d)	5.02 (d)	4.95 (d)	4.93 (d)	5.02 (d)	4.94 (d)
12, 12'	7.35-7.40	7.35-7.40	7.20-7.47	7.20-7.47	7.25-7.29	7.25-7.29
13, 13'	7.35-7.40	7.35-7.40	7.20-7.47	7.20-7.47	7.25-7.29	7.25-7.29
14	7.30 (m)	7.30 (m)	7.20-7.47	7.20-7.47	7.18 (t(b))	7.18 (t(b))
R_1	**H**	**H**	**Tr**	**Tr**	**Tr**	**Tr**
1	1.91-2.33	1.91-2.33	n/a	n/a	n/a	n/a
2	-	-	n/a	n/a	n/a	n/a
3, (3'), (3")	-	-	7.20-7.47	7.20-7.47	7.46-7.49	7.47-7.49
4, (4'), (4")	-	-	7.20-7.47	7.20-7.47	7.25-7.29	7.25-7.29
5	-	-	7.20-7.47	7.20-7.47	7.21 (t(b))	7.21 (t(b))
R_2	**H**	**H**	**H**	**H**	**TBDMS**	**TBDMS**
1	1.91-2.33	1.91-2.33	2.21-2.43	2.21-2.43	-0.44 (s)	-0.46 (s)
2	-	-	-	-	-0.26 (s)	-0.29 (s)
3, (3'), (3")	-	-	-	-	n/a	n/a
4, (4'), (4")	-	-	-	-	0.57 (s)	0.56
5	-	-	-	-	-	-
R_3	**H**	**H**	**H**	**H**	**TBDMS**	**TBDMS**
1	1-91-2.33	1-91-2.33	2.21-2.43	2.21-2.43	-0.06 (s)	-0.07 (s)
2	-	-	-	-	0.08 (s)	0.11 (s)
3, (3'), (3")	-	-	-	-	n/a	n/a
4, (4'), (4")	-	-	-	-	0.85 (s)	0.82 (s)
5	-	-	-	-	-	-

Table 4.6: ^{13}C-NMR chemical shifts (150 MHz, ppm) of α- and β-anomer of **4**, **5** and **6** in $CDCl_3$ at 25 ^{o}C with TMS as internal standard. Presence of site without observed signal is denoted by n/a, lack of site is denoted by dash (-).

C	**4a**	**4b**	**5a**	**5b**	**6a**	**6b**
1	97.7	102.0	97.4	101.7	97.3	102.3
2	72.9	74.6	72.6	74.18	74.3	75.7
3	82.9	83.6	83.0	84.0	82.6	86.5
4	70.2	70.3	71.5	71.7	71.9	71.8
5	71.2	75.2	70.4	74.26	71.8	76.4
6	62.6	62.7	63.9	64.2	64.7	64.5
7	68.7	70.6	68.4	70.1	68.1	70.1
8	133.4	133.6	133.7	133.8	134.3	134.3
9	118.2	118.2	117.99	118.05	118.0	117.8
10	75.0	74.7	75.1	74.8	74.8	74.9
11	138.6	138.5	138.68	138.61	139.3	139.1
12, 12'	127.9-128.7	127.9-128.7	127.08-128.68	127.08-128.68	126.3	126.0
13, 13'	127.9-128.7	127.9-128.7	127.08-128.68	127.08-128.68	127.8	127.75
14	127.9-128.7	127.9-128.7	127.08-128.68	127.08-128.68	126.5	126.4
R_1	**H**	**H**	**Tr**	**Tr**	**Tr**	**Tr**
1	n/a	n/a	86.91	86.95	86.5	86.3
2	-	-	143.8	143.7	144.2	144.2
3, (3'), (3'')	-	-	127.08-128.68	127.08-128.68	128.8	128.8
4, (4'), (4'')	-	-	127.08-128.68	127.08-128.68	127.8	127.79
5	-	-	127.08-128.68	127.08-128.68	126.9	126.9
R_2	**H**	**H**	**H**	**H**	**TBDMS**	**TBDMS**
1	n/a	n/a	n/a	n/a	-4.9	-4.8
2	-	-	-	-	-3.9	-3.9
3, (3'), (3'')	-	-	-	-	17.7	17.6
4, (4'), (4'')	-	-	-	-	25.75	25.7
5	-	-	-	-	-	-
R_3	**H**	**H**	**H**	**H**	**TBDMS**	**TBDMS**
1	n/a	n/a	n/a	n/a	-4.6	-4.4
2	-	-	-	-	-4.5	-3.9
3, (3'), (3'')	-	-	-	-	18.0	18.1
4, (4'), (4'')	-	-	-	-	25.80	26.0
5	-	-	-	-	-	-

Table 4.7: ^{1}H-NMR chemical shifts (600 MHz, ppm) of α- and β-anomer of **7**, **8** and **9** in $CDCl_3$ at 25 ^{o}C with TMS as internal standard. Multiplicities are given in parentheses, Presence of site without observed signal is denoted by n/a, lack of site is denoted by dash (-).

H	**7a**	**7b**	**8a**	**8b**	**9a**	**9b**
1	4.90 (d)	4.40 (d)	4.73 (d)	4.33 (d)	4.752 (d)	4.27 (d)
2	3.64 (dd)	3.49 (dd)	3.65 (dd)	3.46 (dd)	3.70 (dd)	3.53 (dd)
3	3.65 (t)	3.43 (t)	3.71 (t)	3.41 (t)	3.66 (t)	3.32 (t)
4	3.89 (t)	3.95 (t)	3.83-3.86	3.91 (t)	3.50 (t)	3.56 (t)
5	3.80 (td)	3.41 (td)	3.83-3.86	3.40 (td)	3.61 (ddd)	3.24 (ddd)
6	3.87 (t)	3.94 (t)	3.83-3.86	3.92 (t)	3.68 (dd)	3.69 (m)
6'	4.09 (dd)	4.17 (dd)	4.08-4.10	4.16 (dd)	3.855 (dd)	3.875 (dd)
7	4.07 (ddt)	4.17 (ddt)	4.05 (ddt)	4.06 (ddt)	4.00 (ddt)	4.06 (ddt)
7'	4.21 (ddt)	4.34 (ddt)	4.20 (ddt)	4.32 (ddt)	4.22 (ddt)	4.33 (ddt)
8	5.93 (dddd)	5.92 (dddd)	5.94 (dddd)	5.92 (dddd)	5.96 (dddd)	5.95 (dddd)
9	5.32 (d(b)))	5.32 (d(b)))	5.33 (d(b)))	5.28 (d(b)))	5.33 (d(b)))	5.26 (d(b)))
9'	5.23 (d(b)))	5.22 (d(b)))	5.23 (d(b)))	5.18 (d(b)))	5.21 (d(b)))	5.17 (d(b)))
10	4.80 (d)	4.81 (d)	4.76 (d)	4.75 (d)	4.68 (d)	4.747 (d)
10'	5.06 (d)	5.05 (d)	4.96 (d)	5.00 (d)	5.07 (d)	5.99 (d)
12, 12'	7.41 (dd)	7.41 (dd)	7.40 (dd)	7.41 (dd)	7.26-7.32	7.26-7.32
13, 13'	7.34 (t)	7.35 (t)	7.31 (t)	7.31 (t)	7.26-7.32	7.26-7.32
14	7.28 (tt)	7.29 (tt)	7.25 (tt)	7.26 (tt)	7.20 (t)	7.20 (t)
R_1	**bis-$(tBu)_2Si$**	**bis-$(tBu)_2Si$**	**bis-$(tBu)_2Si$**	**bis-$(tBu)_2Si$**	**TBDMS**	**TBDMS**
1	n/a	n/a	n/a	n/a	0.061-0.067	0.058 (s)
2	n/a	n/a	n/a	n/a	0.061-0.067	0.070 (s)
3, (3'), (3'')	1.02 (s)	1.02 (s)	0.99 (s)	1.00 (s)	n/a	n/a
4, (4'), (4'')	1.08 (s)	1.08 (s)	1.06 (s)	1.05 (s)	0.904 (s)	0.899 (s)
5	-	-	-	-	-	-
R_2	**bis-$(tBu)_2Si$**	**bis-$(tBu)_2Si$**	**bis-$(tBu)_2Si$**	**bis-$(tBu)_2Si$**	**TBDMS**	**TBDMS**
1	n/a	n/a	n/a	n/a	-0.11 (s)	-0.14 (s)
2	n/a	n/a	n/a	n/a	0.037-0.051	0.037-0.051
3, (3'), (3'')	1.02 (s)	1.02 (s)	0.99 (s)	1.00 (s)	n/a	n/a
4, (4'), (4'')	1.08 (s)	1.08 (s)	1.06 (s)	1.05 (s)	0.82-0.83	0.82-0.83
5	-	-	-	-	-	-
R_3	**H**	**H**	**TBDMS**	**TBDMS**	**TBDMS**	**TBDMS**
1	2.23	2.36	0.047 (s)	0.04 (s)	-0.07 (s)	-0.08 (s)
2	-	-	0.054 (s)	0.06 (s)	0.037-0.051	0.075 (s)
3, (3'), (3'')	-	-	n/a	n/a	n/a	n/a
4, (4'), (4'')	-	-	0.91 (s)	0.89 (s)	0.834 (s)	0.80 (s)
5	-	-	-	-	-	-

Table 4.8: ^{13}C-NMR chemical shifts (150 MHz, ppm) of α- and β-anomer of **7**, **8** and **9** in $CDCl_3$ at 25 ^{o}C with TMS as internal standard. Presence of site without observed signal is denoted by n/a, lack of site is denoted by dash (-).

C	**7a**	**7b**	**8a**	**8b**	**9a**	**9b**
1	97.6	102.0	98.3	103.1	97.6	102.1
2	71.7	73.5	72.8	74.4	74.5	75.7
3	81.9	83.5	82.1	85.2	82.3	86.3
4	78.3	77.8	78.6	78.1	70.9	70.8
5	66.7	70.7	66.4	70.3	73.1	77.3
6	66.7	66.4	66.9	66.4	62.9	62.7
7	68.6	70.3	68.7	70.7	68.1	70.0
8	133.6	133.6	133.9	133.8	134.2	134.3
9	118.0	118.1	118.3	117.8	117.8	117.6
10	75.1	74.9	75.7	75.6	74.6	74.8
11	138.9	138.7	139.2	138.8	139.4	139.1
12, 12'	128.0	128.0	128.08-128.11	128.3	126.3-127.8	126.0-127.8
13, 13'	128.4	128.5	128.08-128.11	128.2	126.3-127.8	126.0-127.8
14	127.7	127.8	127.3	127.5	126.49	126.47
R_1	**bis-$(tBu)_2Si$**	**bis-$(tBu)_2Si$**	**bis-$(tBu)_2Si$**	**bis-$(tBu)_2Si$**	**TBDMS**	**TBDMS**
1	20.0	22.0	20.0	19.9	-5.31	[-5.32]-[-5.05]
2	22.7	22.7	22.7	22.7	-5.00	[-5.32]-[-5.05]
3, (3'), (3'')	27.0	27.1	27.0	27.1	18.41	18.41
4, (4'), (4'')	27.5	27.4	27.5	27.4	25.7-26.0	25.7-26.0
5	-	-	-	-	-	-
R_2	**bis-$(tBu)_2Si$**	**bis-$(tBu)_2Si$**	**bis-$(tBu)_2Si$**	**bis-$(tBu)_2Si$**	**TBDMS**	**TBDMS**
1	20.0	22.0	20.0	19.9	-3.92	[-3.94]-[-3.93]
2	22.7	22.7	22.7	22.7	[-4.72]-[-4.54]	-4.70
3, (3'), (3'')	27.0	27.1	27.0	27.1	18.07	18.02
4, (4'), (4'')	27.5	27.4	27.5	27.4	25.7-26.0	25.7-26.0
5	-	-	-	-	-	-
R_3	**H**	**H**	**TBDMS**	**TBDMS**	**TBDMS**	**TBDMS**
1	n/a	n/a	-4.5	-4.3	[-4.72]-[-4.54]	-4.37
2		-	-4.8	-4.4	[-4.72]-[-4.54]	[-3.94]-[-3.93]
3, (3'), (3'')		-	18.1	18.2	18.00	18.13
4, (4'), (4'')		-	25.8	25.9	25.7-26.0	25.7-26.0
5		-	-	-	-	-

Table 4.9: ^{1}H coupling constants (Hz) resolved for both anomers of **4-9** in $CDCl_3$ at 25 °C with TMS as internal standard. NR, not resolved due to overlap.

	4a	**4b**	**5a**	**5b**	**6a**	**6b**	**7a**	**7b**	**8a**	**8b**	**9a**	**9b**
H1-H2	3.9	7.5	3.8[b]	7.5[a]	3.7	7.4	3.4	7.7	3.8	7.3[a]	3.5[a]	7.3[a]
H2-H3	9.3[a]	9.3[a]	NR	9.2[a]	9.2[a]	8.8[a]	8.8[a]	9.1[a]	9.2	9.2[a]	9.0[a]	9.1[a]
H3-H4	9.2[a]	9.2[a]	NR	9.1	9.2[a]	8.8[a]	8.9[a]	9.0[a]	9.2[b]	9.1[a]	8.9[a]	9.0[a]
H4-H5	9.2	9.2	NR	9.1	9.2	8.8	9.1[b]	9.1[b]	NR	9.1[b]	9.1[a]	9.2[a]
H5-H6	4.6	5.2	5.2[b]	4.5	9.2	8.8	10.0	10.0[a]	NR	9.9[a]	6.2	5.7[b]
H5-H6'	3.6	3.5	3.8[b]	3.8	3.3	1.9	4.7	5.0	NR	5.2	2.3	2.6
H6-H6'	11.8	11.8	10.1	10.1	9.2	9.6	10.0	10.2	NR	10.2	11.1[a]	11.2[b]
H7-H7'	12.7	12.5	12.7	12.7	12.8	12.3	12.9	12.7	12.9	12.4[a]	12.8	12.2
H7-H8	6.6[b]	6.4[b]	6.5[b]	6.5[b]	6.7[a]	6.5	6.2	6.3	6.7	6.3	6.5	6.7[a]
H7'-H8	5.5[b]	5.5[b]	5.4[b]	5.4[b]	5.4	5.4	5.3	5.3	5.4	5.5[a]	5.5	5.5[a]
H8-H9	17.2[b]	17.3[b]	17.2[b]	17.3[b]	17.3	17.4	17.1	17.2	17.3	17.3	17.2	17.2
H8-H9'	10.4[b]	10.3[b]	10.4[b]	10.4[b]	10.4	10.4	10.4	10.4[a]	10.4	10.4	10.4	10.4
H9-H9'	2.0	2.1[a]	2.0	2.0[b]	2.1	2.1	2.1	2.2	2.1[a]	2.1	2.2[a]	2.1
H7/7'-H9/9'	2.0	2.0	2.0	2.0	2.1	2.2	2.0[a]	2.2	2.2	2.2[a]	2.2	2.2
H10-H10'	11.5	11.7	11.5	11.5	12.1	12.2	11.5	11.6	10.9	10.6	12.1	12.2

[a] Average taken from coupling constants of participating protons.
[b] Based on one participating proton, unresolved for the participant.

Assignment of shifts was performed using ^{1}H- and ^{13}C-NMR experiments, H,H-COSY, HSQC and HMBC for all relevant compounds. For compounds isolated as anomeric mixtures (**3**, **4** and **9**), selective 1D TOCSY experiments were run as to resolve multiplets constituted by anomeric signals. This was not necessary for **6a**/**6b**, as these were simultaneously purified and isolated on preparative HPLC. By selective irradiation of each anomeric proton, resonances not belonging to the appropriate spin systems are silenced (see figure 4.12). However, protons with similar resonance frequency are also irradiated, i.e. benzylic – or allylic protons in this case. This occurrence can be seen in figure 4.12c, where benzylic protons signals overlapping with $\delta(H_\alpha\text{-}1) = 4.94$. Fortunately, these trivial spin systems have no overlapping resonances in the region of interest.

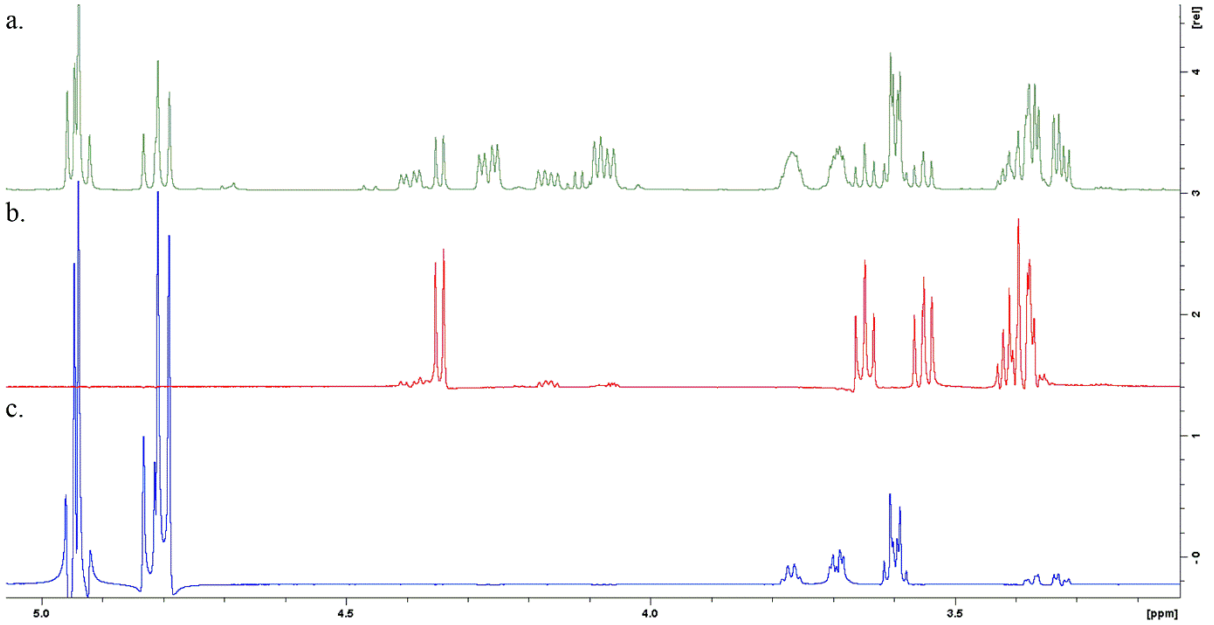

Figure 4.12: Selective 1D TOCSY experiment of anomeric mixture of **5**, irradiating each anomeric proton individually. a. sugar region of **5** in a regular ^{1}H-NMR spectrum; b. signals belonging to the *β*-anomer spin system; c. signals belonging to the *α*-anomer spin system.

JRES experiments were applied for resolving complex multiplet signals, and for deciding ambiguous coupling constants. In liaison with selective 1D TOCSY, coupling constants were simultaneously retrieved for anomeric multiplets. The olefinic CH_2 signals on the allyl group had multiplicity resembling *dq* or *ddt*. However, since the geminal coupling and ^{4}J coupling to allylic CH_2 were of similar magnitude, this cannot be decided with certainty. For this reason these signal were reported as broad doublets. Higher resolution spectra are needed.

Compounds that had more than one TBDMS substituent (i.e. **5** and **9**) required NOESY experiments to be run for correct placement of each silyl alkyl groups. Positions 2, 4 and 6 had different environments due to presence of allylic glucoside substituent and benzyl at 3-position. Benzylic proton was distinguishable using NOESY, as the silyl ethers at O-2 and O-4 coupled to one each. A similar correlation was observable for TBDMS at position 2 and 6 of **9** towards respective allylic protons, as shown in figure 4.13 for **9b**.

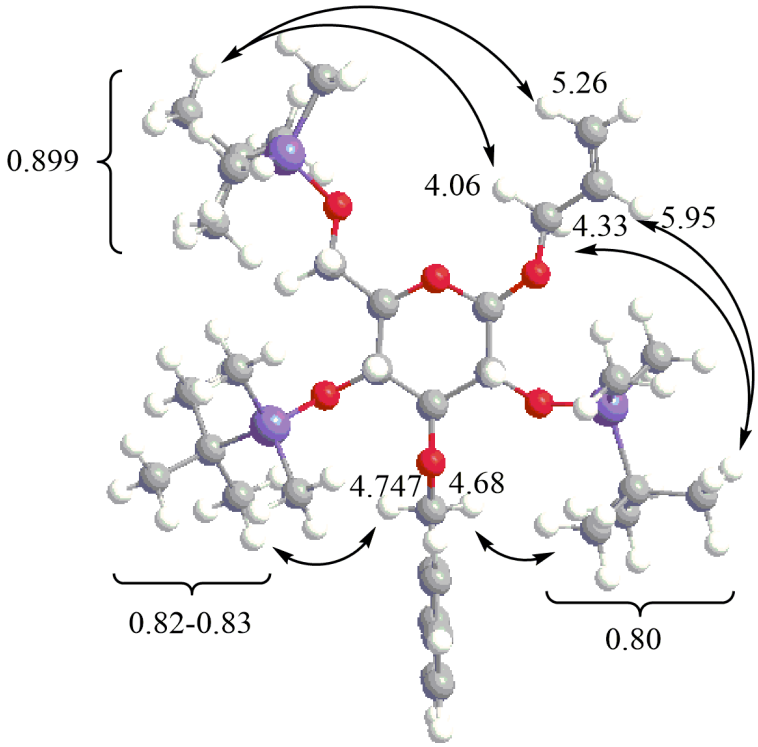

Figure 4.13: Through space interactions of TBDMS ethers with benzyl and allyl substituents of **9b**, as indicated by NOESY. Proton shifts are included for clarity where appropriate.

Assigned chemical shifts were found to be relatively consistent throughout the synthetic series, with coupling constants of magnitude to be expected for *α*-/*β*-glucose.[30-31] Arguably, the only exception are H-5 and H-6 for compounds **6**, **7** and **8**, for which the signal was that of a *td* and *t*, respectively, as opposed to *ddd* and *dd* as for preceding substrates. Accompanied differences in coupling constants were also observed. This is likely related to the steric preferences over the C5-C6 bond, induced by the protecting group(s) at O-5/O-6 for these compound. As can be seen for the modelled minimized energy conformations in figure 4.14, both H-6 protons are gauche relative to H-5 for **3a**, whereas for **8a** H-6 is anti-periplanar. The same geometry was found for model structures of **6a**/**6b**, **7a**/**7b** and **8b**. It is known that the coupling constant is dependent on the dihedral angle,[85-86] therefore change in configuration for these compounds could be accompanied by change in magnitude coupling between H-5 and H-6 to become similar to that between H-4 and H-5 (which are anti-periplanar). The result is a change in appearance of the signal due to coincidental overlap, e.g. from *dd* to *t*, as observed.

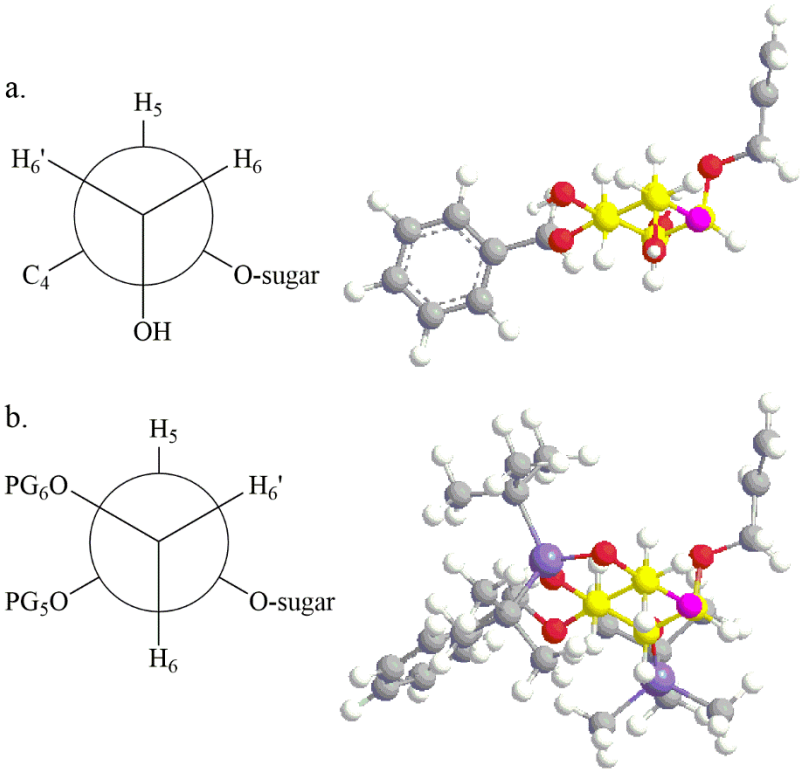

Figure 4.14: Newman projections about the C5-C6 bond with modelled minimized energy conformations of a. **3a**; b. **8a**. The glucose moiety is highlighted for clarity (yellow, grey = C; purple, red = O; white = H).

The pertinence of IR was that of monitoring presence of O-H stretching frequency at 3500-3000 cm^{-1}, specifically loss thereof, and Si-O/Si-C frequencies at 1500-1300 cm^{-1}.[87] Loss of OH signal can be seen in IR spectra of the fully protected compounds **6**, **8** and **9** (see respective appendices). Aromatic, aliphatic and ether frequencies were present for all analysed compounds. MS revealed concurring chemical formulae and specific masses with expectations for all compounds.

4.3.2 By-product characterization

Observed by-products in reactions **5** to **6** and **4** to **7** were collected during flash chromatography of their respective steps. Their evident presence signify the need for further investigation of each individual reaction, as discussed in sections 4.2.1 and 4.2.2. Spectroscopic characterization was carried out to better understand the reaction proceedings, for which HRMS (ESI) and ^{1}H-, ^{13}C-NMR, H,H-COSY, HSQC and HMBC experiments were utilized. IR was additionally performed for the latter by-product. Characterized data are reported in this chapter, as these compounds were not included in the experimental section, while spectra are included in appendices K-L. The same numbering of backbone and protection groups is used as for the desired synthetic compounds due to structural similarity. No attempts were made towards proposing mechanisms for formation of the respective by-products.

By-product from silylation of allyl 3-O-benzyl-6-O-trityl-D-glucopyranoside (6)

The by-product with t_R = 52.83 obtained during silylation of **5** was identified as the benzoyl analogue of **6**, where the benzylic position had been converted to a carbonyl functionality (see figure 4.15). Mass was confirmed by HRMS electron spray ionization in positive mode ($C_{47}H_{62}O_7Si_2Na$, 817.3943 *m/z*). Spectra indicate only presence of the α-anomer, for which ^{1}H and ^{13}C chemical shifts are reported in table 4.10. Distinguishing of the TBDMS ethers was deemed redundant. The impurity with t_R = 54.02, contained in the desired product mixture, was likely the β specie of the benzoyl analogue, as discussed previously in section 4.2.1. The amount of α-anomeric by-product, collected during flash chromatography (0.0465 g), accounts for 0.12 eq. of the administered starting material **5**. With the assumption that t_R = 54.02 is the β-anomer, another 0.05 eq. is accounted for, given an α:β-ratio identical to **5**.

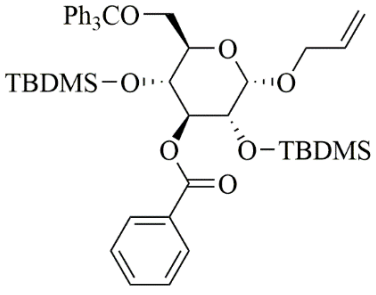

Figure 4.15: Structure of the isolated by-product from silylation reaction of **5** with TBDMSOTf and 2,6-lutidine in dry DCM, towards synthesis of **6**.

Table 4.10: ^{1}H and ^{13}C chemical shifts (400 MHz/100MHz, ppm) and ^{1}H coupling constants (Hz) of by-product isolated from silylation reaction of **5** to **6** in $CDCl_3$ at 25 °C with TMS as internal standard. NR, not resolved due to overlap.

Position	^{1}H [ppm]	J [Hz]	^{13}C [ppm]
1	4.93 (d)	3.8	97.1
2	3.80 (dd)	3.8, 9.6	72.0
3	5.59 (t)	9.3	76.3
4	3.53 (t)	9.3	3.53
5	4.12 (td)	1.8, 9.0	71.6
6	3.11 (t)	9.0	64.4
6'	3.41 (dd)	1.8, 9.5	64.4
7	4.23 (ddt)	6.5, 12.9	68.2
7'	4.51 (ddt)	5.1, 12.9	68.2
8	6.07 (dddd)	5.2, 6.4, 10.6, 17.2	134.1
9	5.44 (d(b))	17.2	117.8
9'	5.27 (d(b))	10.4	117.8
10, 10'	n/a	n/a	165.2
11	n/a	n/a	130.8
12, 12'	8.01 (d(b))	NR	129.9
13, 13'	7.40 (t(b))	7.7	128.1
14	7.52 (t(b))	7.4	132.6
R_1 = Tr			
1	n/a	n/a	86.6
2	n/a	n/a	144.2
3, 3'	7.49 (d(b))	7.5	128.8
4, 4'	7.29 (t(b))	7.6	127.8
5	7.22 (t(b))	7.4	127.0
R_2, R_3 = TBDMS			
1	-0.46 (s)/-0.21 (s)	n/a	-4.7/-5.0
2	-0.34 (s)/0.01 (s)	n/a	-4.0/-4.4
3	n/a	n/a	17.6/17.8
4, 4', 4''	0.53 (s)/0.72 (s)	n/a	25.5/25.4

The transformation from benzyl to benzoic ester on carbohydrate derivatives has been provoked using stoichiometric amounts of an oxygen source reagent.[88-91] However, no obvious oxygen donor or oxidation reagent is present for the employed conditions, and the dryness of the solvent was ensured. The oxygen atom is suspected to originate from a trifluoromethanosulfonate residue (TfO^-), where the formation of triflic anhydride (Tf_2O) could occur.[92] However, triflic anhydride has oxidative potential towards double bonds,[93] which should be noticeable in regards to loss/change of allylic signals. In addition, the discrimination between allylic and benzylic protons cannot be explained. Furthermore, none of the reagents in the mixture are sufficiently basic for deprotonation of benzylic (or allylic) protons, and triflate is a poor

nucleophile. No explanation could be made for the formation of this by-product, but use of dry solvent and N_2 atmosphere should be reassured to eliminate presence of water and O_2 in the reaction mixture.

By-product from 4,6-diol protection of allyl 3-O-benzyl-D-glucopyranoside (4)

Identification of the by-product at $t_R \approx 52.8$, isolated during flash purification of the 4,6-diol protection reaction of **4**, revealed the fully protected glucose derivative shown in figure 4.16. Mass was confirmed by HRMS electron spray ionization in positive mode ($C_{32}H_{56}O_7Si_2Na$, 631.3472 *m/z*), and IR confirmed presence of OH functionality. A similar retention time was observed for **8a**/**8b**, consolidating the evident fully protected structure. ^1H and ^{13}C chemical shifts are reported in table 4.11. Distinguishing the silyl moieties was deemed redundant. As indicated by NMR, only α-anomer was present in appreciable amounts, but some β-anomeric signals are recognizable (e.g. allylic signal). The isolated amount of the by-product during flash purification (0.1433 g) accounts for 0.09 and 0.12 eq. of starting material **4** and $(tBu)_2Si(OTf)_2$, respectively.

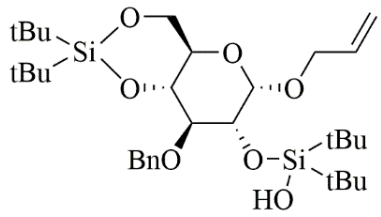

Figure 4.16: Structure of isolated by-product from the 4,6-diol protection of **4** using $(tBu)_2Si(OTf)_2$ and 2,6-lutidine in dry DCM, towards synthesis of **7**.

From the structure, it is apparent reaction of a second $(tBu)_2Si(OTf)_2$ molecule has occurred with 2-OH. The elucidated fully protected structure supports the suspected volatility/high reactivity of $(tBu)_2Si(OTf)_2$ discussed in chapter 4.2.2. Instead of the triflate moiety attached to the O-2 silicon, a hydroxyl functionality is present, as indicated by IR signal at 3500 cm^{-1} and a broad NMR signal at $\delta(H) = 3.1$, evidently originating from Si-OH.[94-95] Derivatization has likely occurred following exposure to water, occurring in both HPLC analysis and work-up, for which a possible substitution of triflate with water is expected.[96] Therefore, it is unknown if the identified compound is artificial or genuine. Previous suggestion towards using milder reaction conditions is emphasized, as discussed in chapter 4.2.2. Furthermore, a shorter reaction time (1 h) should be verified in the advent of optimization.

Table 4.11: ^{1}H and ^{13}C chemical shifts (400 MHz/100 MHz, ppm) and ^{1}H coupling constants (Hz) of by-product isolated from silylene 4,6-diol protection reaction of **4** to **7** in $CDCl_3$ at 25 °C with TMS as internal standard. NR, not resolved due to overlap.

Position	**^{1}H [ppm]**	**J [Hz]**	**^{13}C [ppm]**
1	4.85 (d)	3.7	98.3
2	3.91 (dd)	3.7, 9.4	72.0
3	3.77 (t)	8.9	81.5
4	3.96 (t)	8.9	79.4
5	3.89 (m)	NR	66.5
6	3.87 (t)	10.2	66.9
6'	4.11 (m)	NR	66.9
7	4.08 (ddt)	6.0, 13.6	68.6
7'	4.24 (ddt)	4.8, 13.6	68.6
8	5.91 (dddd)	4.8, 5.9, 10.5, 17.2	134.0
9	5.40 (d(b))	17.2	117.3
9'	5.21 (d(b))	10.4	117.3
10	4.65 (d)	10.5	75.3
10'	5.29 (d)	10.5	75.3
11	n/a	n/a	138.1
12, 12'	7.39 (d(b))	7.4	128.0
13, 13'	7.34 (t(b))	7.4	128.5
14	7.28 (t(b))	7.3	127.9
R_1, R_2 = bis-$(tBu)_2Si$			
1	n/a	n/a	20.0-22.7[b]
2	n/a	n/a	20.0-22.7[b]
3, 3', 3''	0.977-1.05[a]	n/a	27.1-27.6[c]
4, 4', 4''	0.977-1.05[a]	n/a	27.1-27.6[c]
R_3 = $(tBu)_2SiOH$			
1	n/a	n/a	20.0-22.7[b]
2	n/a	n/a	20.0-22.7[b]
3, 3', 3''	0.977-1.05[a]	n/a	27.1-27.6[c]
4, 4', 4''	0.977-1.05[a]	n/a	27.1-27.6[c]
OH	3.07 (s(b))	n/a	n/a

[a] Part of four ^{1}H singlet signals with δ = 0.977, 0.981, 1.01, 1.05.
[b] Part of four ^{13}C signals with δ = 20.0, 20.3, 20.8.
[c] Part of four ^{13}C signals with δ = 27.1, 27.4, 27.5, 27.6.

5 Conclusion and further work

The present work investigated the development of selectively fully protected glucose derivatives available for future functionalization at positions 1, 3 and 6. This was performed as part of a project aimed at synthesis of an anti-inflammatory compound isolated from the plant *Sclerochloa dura*. A furanose to pyranose rearrangement strategy was employed in order to mediate hardship associated with secondary alcohols regioselectivity. Attempts were made towards anomeric resolution/enrichment, due to formation of mixtures during the rearrangement. No success was achieved in influencing the anomeric effect through various reaction times, temperatures, (co-)solvents and catalysts. For increased proportions of the more desirable α-anomer, further investigation of the rearrangement is warranted.

Three protection pathways were explored from the common intermediate **4**, based on prospect of subsequent selective liberation at position 6, recounted in scheme 5.1. Each pathway offered individual advantages in terms of synthetic steps, ease of reaction/purification, yields, occurrence of by-products and anomeric separation. Specifically, the pathway to **9** had fewer synthetic steps, proceeded to best total yield (**6** to the lowest) and no by-products were observed. The pathway to **8** afforded lower yields, however, isolated anomers could be achieved from the preceding **7a**/**7b**, which were separable on flash column, a potentially major implication. The pathway to **6** proceeded to the least impressive yield, but should not be disregarded since it serves as a backup solution should the other pathways prove unsuccessful at deprotection at O-6, due to liberation of the trityl group being well established in literature. By-products were additionally observed and identified for the latter two pathways. The use of different bases for step *iv* was initially explored, where no by-product was observed when 2,6-lutidine was replaced by triethylamine. Optimization of reaction conditions for silylation (steps *iv*, *iv'*, *iv''*) is suggested, especially amine base used, should these pathways be desirable for future prospects.

Both anomers of the produced compounds **6**, **7**, **8** and **9** were characterized spectroscopically for the first time herein using IR, MS and ^{1}H-, ^{13}C-NMR, COSY, HSQC and HMBC. Additionally, selective 1D TOCSY, JRES and NOESY experiments were used for anomeric resolution and correctly assigning alkyl silyl ethers. Compounds **4** and **5** had previously reported chemical shifts that were unassigned, which were completed herein. Two fully protected glucose by-products were additionally isolated and characterized.

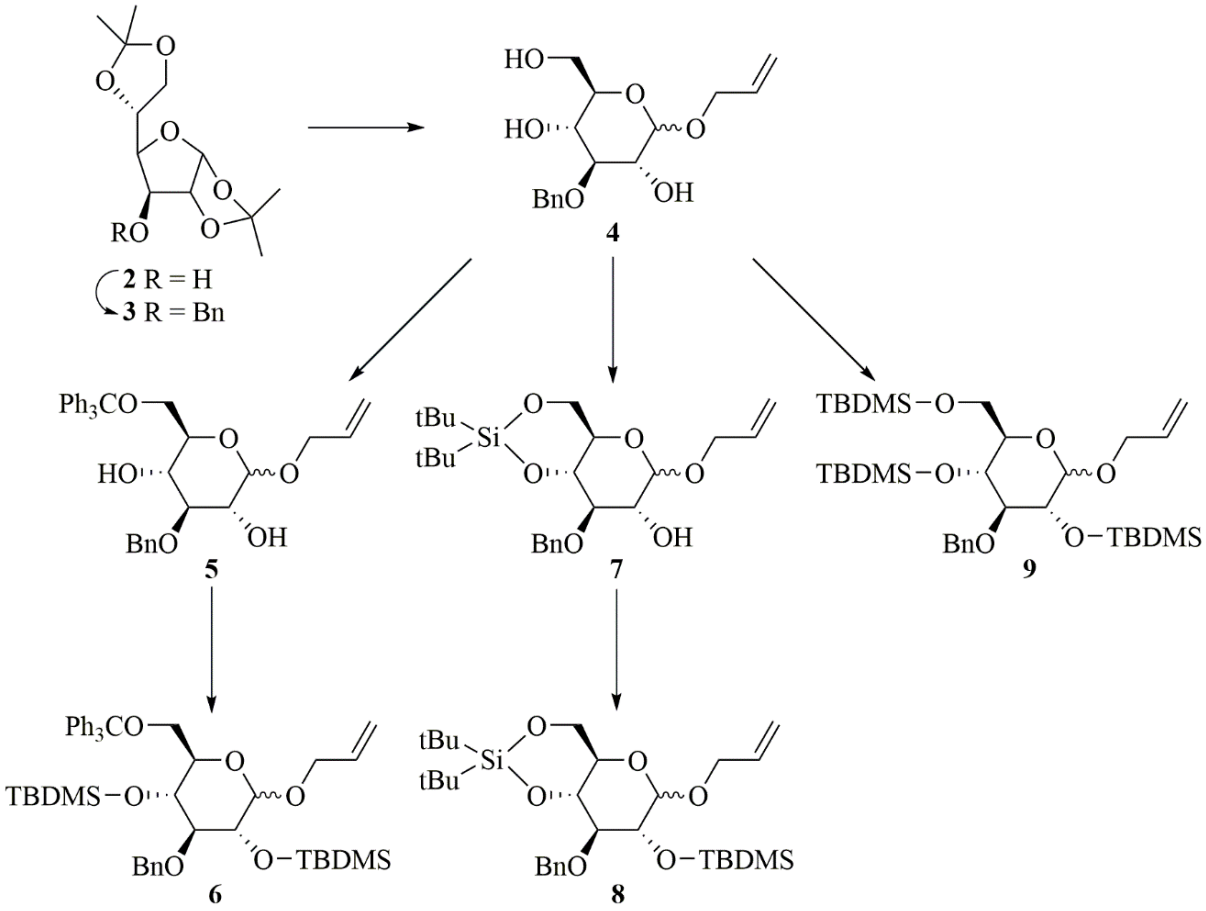

Scheme 5.1: Present selective full protection strategies.

6 Experimental

6.1 General considerations

Chemicals were purchased from Sigma Aldrich, used without prior purification. Unless otherwise stated, distilled water was used, reagents were of analytic grade and solvents of solvent grade. Dry solvents were collected from a Braun MB SPS-800 Solvent Purification System. Cryodessication was carried out on a FreeZone® 1L Benchtop freeze dry system. Stirring was done with Teflon® coated magnetic stirring bars. Temperatures above 25 ºC was regulated by silica oil immersion. Molecular modelling and conformational analyses was done using PerkinElmer Informatics Chem3D (version 16.0.1.4) plugin extension for ChemDraw. Melting points were recorded using a Stuart SMP40 automatic melting point apparatus.

6.1.1 Chromatography

Reactions were monitored by TLC with Merck Silica gel 60 F_{254} coated aluminium plates. Visualization was done by UV-254 with a CAMAG UV lamp, or with a solution of $KMnO_4$ (1%) + K_2CO_3 (10%) in water for non-UV active compounds.

Flash column chromatography was carried out with high purity grade silica gel from Sigma Aldrich, pore size 60 Å, 200-400 mesh particle size with N_2 pressurization. Celite® 545 was used for dry loading.

High-performance liquid chromatography (HPLC) separations were performed on an Agilent Technology instrument, G4220B 1290 Infinity binary pump VL, equipped with 1290 G4226A autosampler, G1316A 1260 Thermostated Column Compartment and G4212B 1260 Infinity Diode Array Detector (DAD). A Zorbax Bonus-RP 250 x 4.6 mm 5-micron column was used for separation, with a Zorbax Bonus-RP 12.5 x 4.6 mm 5-micron guard column. Agilent Technologies ChemStation for LC and CE systems (version: B.04.03.SP1[87]) software was used for automation and processing. ACN was of HPLC analytical grade, and H_2O distilled on a Milli-Q® water purification system. Two methods were used, both operating at 25 ºC and 1 mL/min flow.

- Method A: mobile phase linear gradient from 80:20 H_2O:ACN to 100 % ACN over 40 min, then kept at 100% ACN for 5 min.
- Method B: mobile phase linear gradient from 80:20 H_2O:ACN to 100% ACN over 50 min, then kept at 100% ACN for 15 min, resuming initial conditions after 5 min.

Preparative HPLC separations were performed on an Agilent Technology instrument, G1361A 1260 prep. pump, equipped with a G2260A 1260 autosampler , G1364B 1260 prep. scale fraction collector and G1315D 1260 Infinity DAD VL. An Agilent 5 Prep-C18 150 x 21.2 mm, 5-micron column was used, with an Agilent 10 Prep-C18 10 x 21.2 mm, 5-micron guard column. Isocratic 1:99 H_2O:ACN or 100% ACN mobile phase was used, at 25 ºC and 20 mL/min flow. Agilent Technologies OpenLab Chromatography Data System (version: C.01.07[27]) software was used for automation and processing. ACN was of HPLC analytical grade, and water was distilled on a Milli-Q® water purification system.

6.1.2 Spectroscopy

IR was recorded on a Bruker Alpha FRIT ECO-ATR spectrometer.

Accurate mass determination was performed on a Synapt G2-S Q-TOF instrument from Water TM. Samples were ionized in positive mode by the use of an ESI or ASAP probe. No chromatographic separation was used prior to the mass analysis. Calculated exact mass and spectral processing was done by Waters TM Software Masslynx V4.1 SCN871.

NMR full characterization spectra were recorded on a Bruker 600 MHz Avance III instrument equipped with a 5-mm cryogenic CP-TCI z-gradient probe and SampleCase, operating at 600 MHz for ^{1}H and 150 MHz for ^{13}C. For all other purposes, a Bruker 400 MHz Avance III instrument equipped with a 5-mm SmartProbe z-gradient probe and SampleCase, operating at 400 MHz for ^{1}H and 100 MHz for ^{13}C. Recording of spectra was done by Bruker automation ICON-NMR software, and spectra processing in Bruker TopSpin 4.0.3. All spectra were recorded at rt., using $CDCl_3$ as solvent with TMS as internal standard. Shifts (δ) are noted in ppm, and coupling constants (J) are reported in Hz. 1D-TOCSY experiments were run in manual mode in ICON-NMR. JRES and NOESY experiments were taken from Bruker's standard library.

6.2 Synthesis of 3-*O*-benzyl-1,2:5,6-di-*O*-isopropylidene-*α*-D-glucofuranose (3)

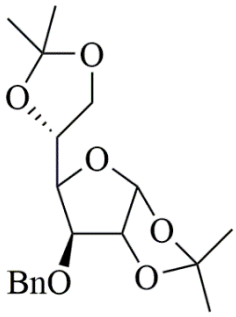

A solution of 1,2:5,6-di-*O*-isopropylidene-*α*-D-glucofuranose (**2**) (10.07 g, 38.7 mmol) in DMF (50 mL) was cooled to 0 °C before addition of 60% NaH (2.4095 g, 60.2 mmol, 1.5 eq.) and stirred for 30 min. The mixture was added benzyl bromide (5.1 mL, 42.9 mmol, 1.1 eq.), heated to rt. and stirred for another 30 min. The reaction was neutralized by addition of methanol, with subsequent concentration under reduced pressure and co-evaporated with *n*-heptane (2 x 25 mL). The resulting oil was taken up in DCM (125 mL) and water (125 mL), where the aqueous layer was extracted with DCM (50 mL). The combined organic extracts were washed with brine (3 x 125 mL), dried over $MgSO_4$ and evaporated under reduced pressure to give **3** as a yellow oil (11.27 g, 98 %). t_R (analytical HPLC, method B) = 27.41 min. IR (cm^{-1}): 3031 (w), 2986 (m), 1070 (s), 696 (s). HRMS (ESI) *m/z*: $[M+Na]^+$ Calcd. for $C_{19}H_{26}O_6Na$ 373.1627; Found 373.1630. ^{1}H-NMR (400 MHz, $CDCl_3$) δ: 1.30 (*s*, 3H, Me); 1.37 (*s*, 3H, Me); 1.42 (*s*, 3H, Me); 1.49 (*s*, 3H, Me); 4.00 (*dd*, *J* = 5.9, 8.6, H-6); 4.02 (*d*, *J* = 3.0, H-3); 4.11 (*dd*, *J* = 6.2, 8.6, H-6); 4.15 (*dd*, *J* = 3.0, 7.7, H-4); 4.37 (*dt*, *J* = 6.1, 7.7, H-5); 4.58 (*d*, *J* = 3.7, H-2); 4.63, 4.68 (*AB q*, *J* = 11.8, 2H, PhC$\underline{H}_2$); 5.89 (*d*, *J* = 3.7, H-1); 7.25-7.36 (*m*, 5H, Ph-H). ^{13}C-NMR (100 MHz, $CDCl_3$) δ: 25.5, 26.3, 26.8, 26.9 (4C, Me); 67.4 (C-6); 72.4 (Ph$\underline{C}H_2$); 72.6 (C-5); 81.3 (C-4); 81.7 (C-3); 82.7 (C-2); 105.3 (C-1); 109.0, 111.8 (2C, $\underline{C}Me_2$); 127.7, 127.9, 128.4 (5C, Ph-C); 137.7 (Ph-C_q). NMR corresponds with previously reported data.[83]

6.3 Synthesis of allyl 3-*O*-benzyl-*α* and *β*-D-glucopyranoside (4)

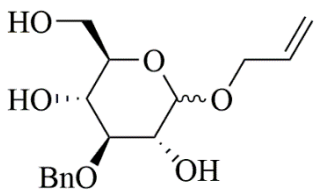

Crude 3-*O*-benzyl-1,2;5,6-di-*O*-isopropylidene-*α*-D-glucofuranose (**3**) (0.8231 g, 2.3 mmol) in allyl alcohol (10 mL) was added 37% HCl (0.32 mL, 4.25% w/v) and was refluxed at 130 ºC for 30 min. After cooling to rt, the solution was concentrated under reduced pressure and co-evaporated with toluene (3 x 15 mL). Purification of the brown residue by flash column (SiO_2, 2.5x13 cm, EtOAc:toluene = 2:1) afforded **4** as a white solid (0.5461 g, 75 %), which was a mixture of anomers (*α*:*β* = 73:27). mp. 62-69 ºC. t_R (analytical HPLC, method B) = 7.86 min. IR (cm^{-1}): 3275 (b), 2933 (w), 1082 (s), 695 (m). HRMS (ESI) *m/z*: $[M+Na]^+$ Calcd. for $C_{16}H_{22}O_6Na$ 333.1314; Found 333.1318.

6.3.1 NMR of *α*-anomer

^{1}H-NMR (600 MHz, $CDCl_3$) *δ*: 1.5-2.5 (3H, *m*(*b*), OH); 3.56 (1H, *t*, *J* = 9.2, H-4); 3.61 (1H, *t*, *J* = 9.1, H-3); 3.68 (1H, *m*, *J* = 3.9, 9.4, H-2); 3.69 (1H, *m*, *J* = 3.6, 4.6, 9.2, H-5); 3.78 (1H, *dd*, *J* = 4.6, 11.8, 1H-6); 3.84 (1H, *dd*, *J* = 3.6, 11.8, H-6); 4.05 (1H, *dd(b)*, *J* = 2.0, 6.6, 12.7, C$\underline{H}_2$-CH=CH_2); 4.24 (1H, *dd(b)*, *J* = 2.0, 5.5, 12.7, C$\underline{H}_2$-CH=CH_2); 4.73 (1H, *d*, *J* = 11.5, PhC$\underline{H}_2$); 4.92 (1H, *d*, *J* = 3.9, 1H-1); 5.05 (1H, *d*, *J* = 11.5, 1PhC$\underline{H}_2$); 5.247 (1H, *m*, *J* = 2.0, 10.4, CH_2-CH=C$\underline{H}_2$); 5.320 (1H, *m*, *J* = 2.0, 17.2, CH_2-CH=C$\underline{H}_2$); 5.94 (1H, *m*, CH_2-C$\underline{H}$=CH_2); 7.30 (1H, *m*, *J* = 8.2, *p*-Ph-H); 7.35-7.40 (4H, *m*, Ph-H). ^{13}C-NMR (150 MHz, $CDCl_3$) *δ*: 62.6 (1C, C-6); 68.7 (1C, $\underline{C}H_2$-CH=CH_2); 70.2 (1C, C-4); 71.2 (1C, C-5); 72.9 (1C, C-2); 75.0 (1C, Ph$\underline{C}H_2$); 82.9 (1C, C-3); 97.7 (1C, C-1); 118.2 (1C, CH_2-CH=$\underline{C}H_2$); 127.90-128.67 (5C, Ph-C); 133.4 (1C, CH_2-$\underline{C}$H=CH_2); 138.6 (1C, Ph-C_q).

6.3.2 NMR of *β*-anomer

^{1}H-NMR (600 MHz, $CDCl_3$) *δ*: 1.5-2.5 (3H, *m*(*b*), OH); 3.37 (1H, *ddd*, *J* = 3.5, 5.2, 9.2, H-5); 3.42 (1H, *t*, *J* = 9.1, H-3); 3.55 (1H, *dd*, *J* = 7.5, 9.4, H-2); 3.585 (1H, *m*, *J* = 9.2, H-4); 3.77 (1H, *m*, *J* = 5.2, 11.8, H-6); 3.89 (1H, *dd*, *J* = 3.5, 11.8, H-6); 4.14 (1H, *dd(b)*, *J* = 2.0, 6.4, 12.5, C$\underline{H}_2$-CH=CH_2); 4.370 (1H, *d*, *J* = 7.5, H-1); 4.374 (1H, *dd(b)*, *J* = 2.0, 5.5, 12.5, C$\underline{H}_2$-CH=CH_2); 4.75 (1H, *d*, *J* = 11.7, PhC$\underline{H}_2$); 5.02 (1H, *d*, *J* = 11.7, PhC$\underline{H}_2$); 5.240 (1H, *m*, *J* = 2.0, 10.3, CH_2-CH=C$\underline{H}_2$); 5.327 (1H, *m*, *J* = 2.1, 17.3, CH_2-CH=C$\underline{H}_2$); 5.94 (1H, *m*, CH_2-C$\underline{H}$=CH_2); 7.30 (1H, *m*, *J* = 8.2, *p*-Ph-H); 7.35-7.40 (4H, *m*, Ph-H). ^{13}C-NMR (150 MHz, $CDCl_3$) *δ*: 62.7 (1C, C-6); 70.3 (1C, C-4); 70.6 (C, $\underline{C}H_2$-CH=CH_2); 74.6 (1C, C-2); 74.7 (1C, Ph$\underline{C}H_2$); 75.2 (1C, C-5);

83.6 (1C, C-3); 102.0 (1C, C-1); 118.2 (1C, CH_2-CH=$\underline{C}H_2$); 127.90-128.67 (5C, Ph-C); 133.6 (1C, CH_2-$\underline{C}$H=CH_2); 138.5 (1C, Ph-C_q).

6.4 Synthesis of allyl 3-*O*-benzyl-6-*O*-trityl-*α*- and *β*-D-glucopyranoside (5)

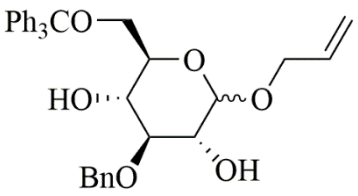

Allyl 3-*O*-benzyl-D-glucopyranoside (**4**) (0.4121 g, 1.33 mmol) was reacted with trityl chloride (0.5509 g, 1.98 mmol, 1.5 eq.) in pyridine (12 mL) with DMAP (0.0182 g, 0.15 mmol, 10 mol %) at 110 °C for 8 h under constant stirring. After cooling to rt, the mixture was concentrated in vacuo, and the residue was taken up in DCM (15 mL). The suspension was sequentially washed with cold (4 °C) HCl (0.5 M, 2 x 5mL), $NaHCO_3$ (sat., 5 mL) and brine (5 mL), then dried over $MgSO_4$ and evaporated under reduced pressure to give a brown oil (0.7853 g, >100 %). Purification of the crude by flash column (SiO_2, 2.5 x 16 cm, EtOAc:*n*-pentane = 1:4) afforded **5** as a yellow wax (0.4129 g, 59 %), which was a mixture of anomers (*α*:*β* = 73:27). t_R (analytical HPLC, method B) = 35.71 min. IR (cm^{-1}): 3481 (b), 3059 (w), 2926 (m), 1056 (s), 676 (s). HRMS (ESI) *m/z*: $[M+Na]^+$ Calcd. for $C_{35}H_{36}O_6Na$ 575.2410; Found 575.2408.

6.4.1 NMR of *α*-anomer

^{1}H-NMR (600 MHz, $CDCl_3$) *δ*: 2.1-2.7 (2H, *m*(*b*), OH); 3.32 (1H, *dd*, *J* = 5.2, 10.1, H-6); 3.373 (1H, *m*, *J* = 3.8, 10.1, H-6); 3.58-3.62 (2H, *m*, H-3, H-4); 3.69 (1H, *m*, H-2); 3.77 (1H, *m*, H-5); 4.08 (1H, *dd(b)*, *J* = 2.0, 6.5, 12.7, $C\underline{H}_2$-CH=CH_2); 4.27 (1H, *dd(b)*, *J* = 2.0, 5.4, 12.7, $C\underline{H}_2$-CH=CH_2); 4.80 (1H, *d*, *J* = 11.5, Ph$C\underline{H}_2$); 4.94 (1H, *m*, *J* = 3.8, H-1); 4.95 (1H, *d*, *J* = 11.5, Ph$C\underline{H}_2$); 5.233 (1H, *m*, *J* = 2.0, 10.4, CH_2-CH=$C\underline{H}_2$); 5.32 (1H, *m*, *J* = 2.0, 17.2, CH_2-CH=$C\underline{H}_2$); 5.96 (1H, *m*, CH_2-$C\underline{H}$=CH_2); 7.20-7.47 (20H, *m*, Ph-H). ^{13}C-NMR (150 MHz, $CDCl_3$) *δ*: 63.9 (1C, C-6); 68.4 (1C, $\underline{C}H_2$-CH=CH_2); 70.4 (1C, C-5); 71.5 (1C, C-4); 72.6 (1C, C-2); 75.1 (1C, Ph$\underline{C}H_2$); 83.0 (1C, C-3); 86.91 (1C, $\underline{C}_q(Ph)_3$); 97.4 (1C, C-1); 117.99 (1C, CH_2-CH=$\underline{C}H_2$); 127.0-128.7 (20C, Ph-C); 133.7 (1C, CH_2-$\underline{C}$H=CH_2); 138.68 (1C, Ph-C_q(Bn)); 143.8 (3C, Ph-C_q(Tr)).

6.4.2 NMR of *β*-anomer

^{1}H-NMR (600 MHz, $CDCl_3$) *δ*: 2.1-2.7 (2H, *m*(*b*), OH); 3.368 (1H, *m*, *J* = 4.5, 10.1, H-6); 3.388 (1H, *m*, *J* = 3.8, 10.1, H-6); 3.395 (1H, *m*, *J* = 9.1, H-3); 3.41 (H, *m*, *J* = 3.8, 4.5, 9.1, H-5); 3.55 (1H, *dd*, *J* = 7.4, 9.4, H-2); 3.65 (1H, *t*, *J* = 9.1, H-4); 4.17 (1H, *dd(b)*, *J* = 2.0, 6.5, 12.7, $C\underline{H}_2$-CH=CH_2); 4.35 (1H, *d*, *J* = 7.6, H-1); 4.39 (1H, *dd(b)*, *J* = 2.0, 5.4, 12.7, $C\underline{H}_2$-CH=CH_2); 4.82 (1H, *d*, *J* = 11.5, Ph$C\underline{H}_2$); 4.93 (1H, *m*, *J* = 11.5, Ph$C\underline{H}_2$); 5.229 (1H, *m*, *J* = 10.4, CH_2-

CH=C$\underline{H}_2$); 5.33 (1H, *m*, *J* = 2.0, 17.3, CH_2-CH=C$\underline{H}_2$); 5.96 (1H, *m*, CH_2-C$\underline{H}$=CH_2); 7.20-7.47 (20H, *m*, Ph-H). ^{13}C-NMR (150 MHz, $CDCl_3$) δ: 64.2 (1C, C-6); 70.1 (1C, $\underline{C}H_2$-CH=CH_2); 71.7 (1C, C-4); 74.18 (1C, C-2); 74.26 (1C, C-5); 74.8 (1C, Ph$\underline{C}H_2$); 84.0 (1C, C-3); 86.95 (1C, $\underline{C}_q(Ph)_3$); 101.7 (1C, C-1); 118.05 (1C, CH_2-CH=$\underline{C}H_2$); 127.0-128.7 (20C, Ph-C); 133.8 (1C, CH_2-$\underline{C}$H=CH_2); 138.61 (1C, Ph-C_q(Bn)); 143.7 (3C, Ph-C_q(Tr)).

6.5 Synthesis of allyl 3-*O*-benzyl-2,4-di-*O*-*tert*-butyldimetylsilyl-6-*O*-trityl- D-glucopyranoside (6)

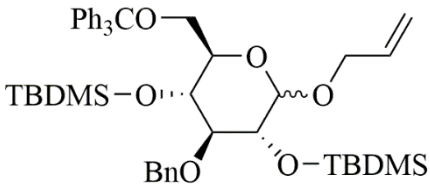

tert-Butyldimethylsilyl triflate (0.38 mL, 1.664 mmol, 3.5 eq.) was added dropwise at 0 °C to a stirred solution of allyl 3-*O*-benzyl-6-*O*-trityl-D-glucopyranoside (**5**) (0.2628 g, 0.475 mmol) and 2,6-lutidine (0.25 mL, 2.1 40 mmol, 4.5 eq.) in dry DCM (8 mL). The reaction mixture was stirred at 0 °C for 5 h in N_2 atmosphere. The mixture was diluted with DCM (10 mL) and water (10 mL), where the aqueous layer was extracted with DCM (2 x 10 mL). The combined organic extracts were washed with brine (3 x 10 mL), dried over $MgSO_4$ and evaporated under reduced pressure to give an orange oil (0.3008 g, 90%). Purification of the crude by flash column (SiO_2, 2.0 x 21 cm, Et_2O:*n*-pentane = 1:25) afforded a fluffy white solid (0.1987 g, 59%), which was a mixture of a silylated by-product and anomers of **6** (α:β = 71:29). Preparative HPLC (100% ACN) was used to isolate **6a** and **6b** in quant amounts at t_R = 9.7-10.7 and 12.8-13.7, respectively. t_R (analytical HPLC, method B) = 54.15 min (by-product); 55.96 min (**6a**); 57.95 min (**6b**). IR (cm^{-1}): 3061 (w), 2926 (m), 1253 (m), 1071 (s), 836 (s), 680 (s). HRMS (ESI) *m/z*: $[M+Na]^+$ Calcd. for $C_{47}H_{64}O_6Si_2Na$ 803.4139; Found 803.4139.

6.5.1 NMR of *α*-anomer

^{1}H-NMR (600 MHz, $CDCl_3$) δ: -0.44 (3H, *s*, Si(Me)$_2$tBu); -0.26 (3H, *s*, Si(Me)$_2$tBu); -0.06 (3H, *s*, Si(Me)$_2$tBu); 0.08 (3H, *s*, Si(Me)$_2$tBu); 0.57 (9H, *s*, Si(Me)$_2$tBu); 0.85 (9H, *s*, Si(Me)$_2$tBu); 3.05 (1H, *t*, *J* = 9.2, H-6); 3.27 (1H, *t*, *J* = 9.2, H-4); 3.36 (1H, *dd*, *J* = 3.3, 9.2, H-6); 3.66 (1H, *t*, *J* = 9.1, H-3); 3.77 (1H, *dd*, *J* = 3.7, 9.2, H-2); 4.01 (1H, *m*, *J* = 3.3, 9.2, H-5); 4.24 (1H, *dd(b)*, *J* = 2.1, 6.8, 12.8, CH$_2$-CH=CH$_2$); 4.51 (1H, *dd(b)*, *J* = 2.1, 5.4, 12.7, CH$_2$-CH=CH$_2$); 4.66 (1H, *d*, *J* = 12.1, PhCH$_2$); 4.88 (1H, *d*, *J* = 3.7, H-1); 5.02 (1H, *d*, *J* = 12.1, PhCH$_2$); 5.28 (1H, *d(b)*, *J* = 2.1, 10.4, CH$_2$-CH=CH$_2$); 5.44 (1H, *d(b)*, *J* = 2.1, 17.3, CH$_2$-CH=CH$_2$); 6.09 (1H, *dddd*, *J* = 5.4, 6.6, 10.4, 17.3, CH$_2$-CH=CH$_2$); 7.18 (1H, *m*, *J* = 8.6, *p*-Ph-H(Bn)); 7.21 (3H, *m*, *J* = 7.4, *p*-Ph-H(Tr)); 7.25-7.29 (10H, *m*, Ph-H); 7.49-7.49 (6H, *m*, Ph-H). ^{13}C-NMR (150 MHz, $CDCl_3$) δ: -4.9, -4.6, -4.5, -3.9 (4C, Si(Me)$_2$tBu); 17.7, 18.0 (2C, Si(Me)$_2$tBu-C$_q$); 25.75, 25.80 (6C, Si(Me)$_2$tBu); 64.7 (1C, C-6); 68.1 (1C, CH$_2$-CH=CH$_2$); 71.8 (1C, C-5); 71.9 (1C, C-4); 74.3 (1C, C-2); 74.8 (1C, PhCH$_2$); 82.6 (1C, C-3); 86.5 (1C, C$_q$(Ph)$_3$); 97.3 (1C, C-1); 118.0 (1C, CH$_2$-CH=CH$_2$); 126.3, 126.5, 126.9, 127.8, 128.8 (20C, Ph-C); 134.3 (1C, CH$_2$-CH=CH$_2$); 139.3 (1C, Ph-C$_q$(Bn)); 144.2 (3C, Ph-C$_q$(Tr)).

6.5.2 NMR of *β*-anomer

^{1}H-NMR (600 MHz, $CDCl_3$) δ: -0.46 (3H, *s*, Si(Me)$_2$tBu); -0.29 (3H, *s*, Si(Me)$_2$tBu); -0.07 (3H, *s*, Si(Me)$_2$tBu); 0.11 (3H, *s*, Si(Me)$_2$tBu); 0.56 (9H, *s*, Si(Me)$_2$tBu); 0.82 (9H, *s*, Si(Me)$_2$tBu); 3.18 (1H, *dd*, *J* = 8.8, 9.6, H-6); 3.29 (1H, *dd*, *J* = 1.9, 9.6, H-6); 3.32 (1H, *t*, *J* = 8.7, H-3); 3.37 (1H, *t*, *J* = 8.8, H-4); 3.57 (1H, *td*, *J* = 1.9, 8.8, H-5); 3.60 (1H, *dd*, *J* = 7.4, 8.8, H-2); 4.27 (1H, *dd(b)*, *J* = 2.2, 6.5, 12.3, CH_2-CH=CH_2); 4.42 (1H, *d*, *J* = 7.4, H-1); 4.54 (1H, *dd(b)*, *J* = 2.2, 5.4, 12.3, CH_2-CH=CH_2); 4.73 (1H, *d*, *J* = 12.2, PhCH_2); 4.94 (1H, *d*, *J* = 12.2, PhCH_2); 5.24 (1H, *d(b)*, *J* = 2.1, 10.4, CH_2-CH=CH_2); 5.38 (1H, *d(b)*, *J* = 2.1, 17.4, CH_2-CH=CH_2); 6.06 (1H, *dddd*, *J* = 5.4, 6.5, 10.4, 17.4, CH_2-CH=CH_2); 7.18 (1H, *m*, *J* = 8.6, *p*-Ph-H(Bn)); 7.21 (3H, *m*, *J* = 7.3, *p*-Ph-H(Tr)); 7.25-7.29 (10H, *m*, Ph-H); 7.47-7.49 (6H, *m*, Ph-H). ^{13}C-NMR (150 MHz, $CDCl_3$) δ: -4.8, -4.4, -3.9 (4C, Si(Me)$_2$tBu); 17.6, 18.1 (2C, Si(Me)$_2$tBu-C_q); 25.7, 26.0 (6C, Si(Me)$_2$tBu); 64.5 (1C, C-6); 70.1 (1C, CH_2-CH=CH_2); 71.8 (1C, C-4); 74.9 (1C, PhCH_2); 75.7 (1C, C-2); 76.4 (1C, C-5); 86.3 (1C, $C_q(Ph)_3$); 86.5 (1C, C-3); 102.3 (1C, C-1); 117.8 (1C, CH_2-CH=CH_2); 126.0, 126.4, 126.9, 127.75, 127.79, 128.8 (20C, Ph-C); 134.3 (1C, CH_2-CH=CH_2); 139.1 (1C, Ph-C_q(Bn)); 144.2 (3C, Ph-C_q(Tr)).

6.6 Synthesis of allyl 3-*O*-benzyl-4,6-*O*-di-*tert*-butylsilylene-*α*- and *β*-D-glucopyranoside (7a, 7b)

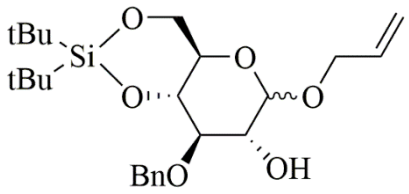

Di-*tert*-butylsilyl bis-triflate (1.26 mL, 3.867 mmol, 1.5 eq.) was added dropwise at 0 °C to a stirred solution of allyl 3-*O*-benzyl-D-glucopyranoside (**4**) (0.7966 g, 2.566 mmol) and 2,6-lutidine (1.34 mL, 11.568 mmol, 4.5 eq.) in dry DCM (32 mL). After being stirred at 0 °C for 5 h in N_2 atmosphere, the mixture was diluted with DCM (40 mL) and water (40 mL), where the aqueous layer was extracted with DCM (2 x 40 mL). The combined organic extracts were washed with brine (3 x 40 mL), dried over $MgSO_4$ and evaporated under reduced pressure to give a yellow oil (1.95 g). Purification of the crude by flash column (SiO_2, 3.0 x 25 cm, Et_2O:*n*-pentane = 1:5) allowed separation of anomers, affording **7b** (0.1624 g, 14%) as a white solid, and **7a** (0.4869 g, 43%) as a colourless oil. A fraction of anomeric mix of **7** (0.0705 g, 6%) was also collected, for a total yield of 63%. mp (**7b**) 79-83 °C. R_f (Et_2O:*n*-pentane = 1:5) = 0.26-0.48. t_R (analytical HPLC, method B) = 39.00 min (**7b**); 39.20 min (**7a**).

6.6.1 Spectoscopic data of *α*-anomer

IR (cm^{-1}): 3450 (b), 3031 (w), 2961 (m), 1035 (s), 825 (s), 651 (s). HRMI (ESI) *m/z*: $[M+Na]^+$ Calcd. for $C_{24}H_{38}O_6SiNa$ 473.2335; Found 473.2332. ^{1}H-NMR (600 MHz, $CDCl_3$) *δ*: 1.02 (9H, *s*, Si(tBu)$_2$); 1.08 (9H, *s*, Si(tBu)$_2$); 2.33 (1H, *s*(*b*), OH); 3.64 (1H, *m*, *J* = 3.4, 9.0, H-2); 3.65 (1H, *m*, *J* = 8.6, H-3); 3.80 (1H, *td*, *J* = 4.6, 9.8, H-5); 3.87 (1H, *t*, *J* = 10.0, H-6); 3.89 (1H, *t*, *J* = 9.1, H-4); 4.07 (1H, *m*, *J* = 2.1, 6.2, 12.9, C$\underline{H}_2$-CH=CH_2); 4.09 (1H, *dd*, *J* = 4.7, 10.0, H-6); 4.21 (1H, *dd(b)*, *J* = 1.9, 5.3, 12.9, C$\underline{H}_2$-CH=CH_2); 4.80 (1H, *d*, *J* = 11.5, PhC$\underline{H}_2$); 4.90 (1H, *d*, *J* = 3.4, H-1); 5.06 (1H, *d*, *J* = 11.5, PhC$\underline{H}_2$); 5.23 (1H, *d(b)*, *J* = 2.1, 10.4, CH_2-CH=C$\underline{H}_2$); 5.32 (1H, *d(b)*, *J* = 2.1, 17.1, CH_2-CH=C$\underline{H}_2$); 5.93 (1H, *dddd*, *J* = 5.3, 6.2, 10.4, 17.1, CH_2-C$\underline{H}$=CH_2); 7.28 (1H, *t(b)*, *J* = 2.6, 7.3, *p*-Ph-H); 7.34 (2H, *t(b)*, *J* = 7.5, *m*-Ph-H); 7.41 (2H, *d(b)*, *J* = 2.6, 8.3, *o*-Ph-H). ^{13}C-NMR (150 MHz, $CDCl_3$) *δ*: 22.0, 22.7 (2C, Si(tBu-C_q)$_2$); 27.0, 27.5 (6C, Si(tBu)$_2$); 66.7 (2C, C-5, C-6); 68.6 (1C, $\underline{C}H_2$-CH=CH_2); 71.7 (1C, C-2); 75.1 (1C, Ph$\underline{C}H_2$); 78.3 (1C, C-4); 81.9 (1C, C-3); 97.6 (1C, C-1); 118.0 (1C, CH_2-CH=$\underline{C}H_2$); 117.7 (1C, *p*-Ph-C); 128.0 (2C, *o*-Ph-C); 128.4 (2C, *m*-Ph-C); 133.6 (1C, CH_2-$\underline{C}$H=CH_2); 138.9 (1C, Ph-C_q).

6.6.2 Spectroscopic data of *β*-anomer

IR (cm^{-1}): 3466 (b), 3029 (w), 2929 (m), 1252 (m), 1073 (s), 831 (s), 730 (m). HRMI (ASAP) *m/z*: $[M]^+$ Calcd. for $C_{24}H_{38}O_6Si$ 450.2438; Found 450.2432. ^{1}H-NMR (600 MHz, $CDCl_3$) *δ*: 1.02 (9H, *s*, Si(tBu)$_2$); 1.08 (9H, *s*, Si(tBu)$_2$); 2.36 (1H, *d*, *J* = 2.0, OH); 3.41 (1H, *td*, *J* = 5.0, 9.8, H-5); 3.43 (1H, *t*, *J* = 8.9, H-3); 3.49 (1H, *m*, *J* = 7.7, 9.2, H-2); 3.94 (1H, *t*, *J* = 10.2, H-6); 3.95 (1H, *t*, *J* = 9.1, H-4); 4.12 (1H, *dd(b)*, *J* = 2.2, 6.3, 12.7, C$\underline{H}_2$-CH=CH_2); 4.17 (1H, *dd*, *J* = 5.0, 10.2, H-6); 4.34 (1H, *dd(b)*, *J* = 2.2, 5.3, 12.7, C$\underline{H}_2$-CH=CH_2); 4.40 (1H, *d*, *J* = 7.7, H-1); 4.81 (1H, *d*, *J* = 11.6, PhC$\underline{H}_2$); 5.05 (1H, *d*, *J* = 11.6, PhC$\underline{H}_2$); 5.22 (1H, *d(b)*, *J* = 2.2, 10.4, CH_2-CH=C$\underline{H}_2$); 5.32 (1H, *d(b)*, *J* = 2.2, 17.2, CH_2-CH=C$\underline{H}_2$); 5.92 (1H, *dddd*, *J* = 5.3, 6.3, 10.5, 17.2, CH_2-C$\underline{H}$=CH_2); 7.29 (1H, *t(b)*, *J* = 2.5, 7.3, *p*-Ph-H); 7.35 (2H, *t(b)*, *J* = 7.4, *m*-Ph-H); 7.41 (2H, *d(b)*, *J* = 2.5, 8.3, *o*-Ph-H). ^{13}C-NMR (150 MHz, $CDCl_3$) *δ*: 22.0, 22.7 (2C, Si(tBu-C_q)$_2$); 27.1, 27.4 (6C, Si(tBu)$_2$); 66.4 (1C, C-6); 70.3 (1C, $\underline{C}H_2$-CH=CH_2); 70.7 (1C, C-5); 73.5 (1C, C-2); 74.9 (1C, Ph$\underline{C}H_2$); 77.8 (1C, C-4); 83.5 (1C, C-3); 102.0 (1C, C-1); 118.1 (1C, CH_2-CH=$\underline{C}H_2$); 127.8 (1C, *p*-Ph-C); 128.0 (2C, *o*-Ph-C); 128.5 (2C, *m*-Ph-C); 133.6 (1C, CH_2-$\underline{C}$H=CH_2); 138.7 (1C, Ph-C_q).

6.7 Synthesis of allyl 3-*O*-benzyl-4,6-*O*-di-*tert*-butylsilylene-2-*O*-*tert*-butyldimethylsilyl-*α*- and *β*-D-glucopyranoside (8a, 8b)

6.7.1 Synthesis of *α*-anomer

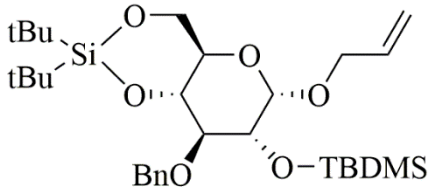

tert-Butyldimethylsilyl triflate (0.155 mL, 0.675 mmol, 1.5 eq.) was added dropwise at 0 °C to a stirred solution of anomerically pure allyl 3-*O*-benzyl-4,6-*O*-di-*tert*-butylsilylene-*α*-D-glucopyranoside (**7a**) (0.1851 g, 0.411 mmol) and 2,6-lutidine (0.105 mL, 0.906 mmol, 2 eq.) in dry DCM (6 mL). After being stirred at 0 °C for 5 h in N_2 atmosphere, the mixture was diluted with DCM (10 mL) and water (10 mL), where the aqueous layer was extracted with DCM (2 x 10 mL). The combined organic extracts were washed with brine (3 x 10 mL), dried over $MgSO_4$ and evaporated under reduced pressure to give a colourless oil (0.2318 g). Purification of the crude by flash column (SiO_2, 2.5 x 20 cm, Et_2O:*n*-pentane = 1:25) afforded **8a** as a colourless oil (0.1819 g, 78%). R_f (SiO_2, Et_2O:*n*-pentane = 1:25) = 0.38. t_R (analytical HPLC, method B) = 51.64 min. IR (cm^{-1}): 3031 (w), 2931 (m), 1252 (m), 1046 (s), 827 (s), 652 (s). HRMS (ESI) *m/z*: $[M+Na]^+$ Calcd. for $C_{30}H_{52}O_6Si_2Na$ 587.3200; Found 587.3204. ^{1}H-NMR (600 MHz, $CDCl_3$) *δ*: 0.047 (3H, *s*, Si(Me)$_2$tBu); 0.054 (3H, *s*, Si(Me)$_2$tBu); 0.91 (9H, *s*, Si(Me)$_2$tBu); 0.99 (9H, *s*, Si(tBu)$_2$); 1.06 (9H, *s*, Si(tBu)$_2$); 3.65 (1H, *dd*, *J* = 3.8, 9.2, H-2); 3.71 (1H, *m*, *J* = 9.2, H-3); 3.83-3.86 (3H, *m*, H-4, H-5, H-6); 4.05 (1H, *dd(b)*, *J* = 2.2, 6.7, 12.9, CH_2-CH=CH_2); 4.08-4.10 (1H, *m*, H-6); 4.20 (1H, *dd(b)*, *J* = 2.2, 5.4, 12.9, CH_2-CH=CH_2); 4.73 (1H, *d*, *J* = 3.8, H-1); 4.76 (1H, *d*, *J* = 10.9, PhCH_2); 4.96 (1H, *d*, *J* = 10.9, PhCH_2); 5.23 (1H, *d(b)*, *J* = 2.1, 10.4, CH_2-CH=CH_2); 5.33 (1H, *d(b)*, *J* = 2.0, 17.3, CH_2-CH=CH_2); 5.94 (1H, *dddd*, *J* = 5.4, 6.7, 10.4, 17.3, CH_2-CH=CH_2); 7.25 (1H, *m*, *J* = 2.4, 7.3, *p*-Ph-H); 7.31 (2H, *t(b)*, *J* = 7.5, *m*-Ph-H); 7.40 (2H, *d(b)*, *J* = 2.6, 8.2, *o*-Ph-H). ^{13}C-NMR (150 MHz, $CDCl_3$) *δ*: -4.8, -4.5 (2C, Si(Me)$_2$tBu); 18.1 (1C, Si(Me)$_2$tBu-C_q); 20.0, 22.7 (2C, Si(tBu-C_q)$_2$); 25.8 (3C, Si(Me)$_2$tBu); 27.1, 27.5 (6C, Si(tBu)$_2$); 66.4 (1C, C-5); 66.9 (1C, C-6); 68.7 (1C, CH_2-CH=CH_2); 72.8 (1C, C-2); 75.7 (1C, PhCH_2); 78.6 (1C, C-4); 82.1 (1C, C-3); 98.3 (1C, C-1); 118.3 (1C, CH_2-CH=CH_2); 127.3 (1C, *p*-Ph-C); 128.08, 128.11 (4C, Ph-C); 133.9 (1C, CH_2-CH=CH_2); 139.2 (1C, Ph-C_q).

6.7.2 Synthesis of *β*-anomer

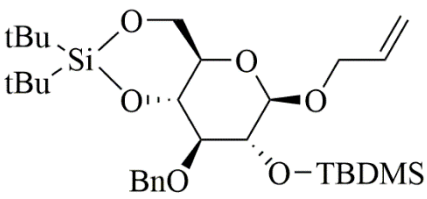

tert-Butyldimethylsilyl triflate (0.125 mL, 0.544 mmol, 1.5 eq.) was added dropwise at 0 ºC to a solution of anomerically pure allyl 3-*O*-benzyl-4,6-*O*-di-*tert*-butylsilylene-*β*-D-glucopyranoside (**7b**) (0.1624 g, 0.360 mmol) and 2,6-lutidine (0.085 mL, 0.734 mmol, 2 eq.) in dry DCM (4.5 mL). After being stirred at 0 ºC for 5 h in N_2 atmosphere, the mixture was diluted with DCM (10 mL) and water (10 mL), where the aqueous layer was extracted with DCM (2 x 10 mL). The combined organic extracts were washed with brine (3 x 10 mL), dried over $MgSO_4$ and evaporated under reduced pressure to give a white solid (0.2707 g). Purification of the crude by flash column (SiO_2, 2.5 x 19 cm, Et_2O:*n*-pentane = 1:25) afforded **8b** as white solid (0.1963 g, 96%). mp. 72-76 ºC. R_f (SiO_2, Et_2O:*n*-pentane = 1:25) = 0.38. t_R (analytical HPLC, method B) = 52.85 min. IR (cm^{-1}): 3032 (w), 2932 (m), 1250 (m), 1072 (s), 826 (s), 652 (s). HRMS (ESI) *m/z*: $[M+Na]^+$ Calcd. for $C_{30}H_{52}O_6Si_2Na$ 587.3200; Found 587.3204. ^{1}H-NMR (600 MHz, $CDCl_3$) *δ*: 0.04 (3H, *s*, Si(Me)$_2$tBu); 0.06 (3H, *s*, Si(Me)$_2$tBu); 0.89 (9H, *s*, Si(Me)$_2$tBu); 1.00 (9H, *s*, Si(tBu)$_2$); 1.05 (9H, *s*, Si(tBu)$_2$); 3.40 (1H, *m*, *J* = 5.2, 9.7, H-5); 3.41 (1H, *t*, *J* = 9.0, H-3); 3.46 (1H, *dd*, *J* = 7.2, 9.3, H-2); 3.91 (1H, *t*, *J* = 9.1, H-4); 3.92 (1H, *t*, *J* = 10.2, H-6); 4.06 (1H, *ddt*, *J* = 2.2, 6.3, 12.3, CH$_2$-CH=CH$_2$); 4.16 (1H, *dd*, *J* = 5.2, 10.2, H-6); 4.32 (1H, *ddt*, *J* = 2.1, 5.4, 12.4, CH$_2$-CH=CH$_2$); 4.33 (1H, *d*, *J* = 7.3, H-1); 4.75 (1H, *d*, *J* = 10.6, PhCH$_2$); 5.00 (1H, *d*, *J* = 10.6, PhCH$_2$); 5.18 (1H, *d(m)*, *J* = 2.1, 10.4, CH$_2$-CH=CH$_2$); 5.28 (1H, *dq*, *J* = 2.1, 17.3, CH$_2$-CH=CH$_2$); 5.92 (1H, *dddd*, *J* = 5.5, 6.3, 10.4, 17.3, CH$_2$-CH=CH$_2$); 7.26 (1H, *m*, *J* = 2.4, 7.3, *p*-Ph-H); 7.31 (2H, *m*, *J* = 7.3, *m*-Ph-H); 7.41 (1H, *m*, *J* = 2.4, 8.4, *o*-Ph-H). ^{13}C-NMR (150 MHz, $CDCl_3$) *δ*: -4.4, -4.3 (2C, Si(Me)$_2$tBu); 18.2 (1C, Si(Me)$_2$tBu-C$_q$); 19.9, 22.7 (2C, Si(tBu-C$_q$)$_2$); 25.9 (3C, Si(Me)$_2$tBu); 27.1, 27.4 (6C, Si(tBu)$_2$); 66.4 (1C, C-6); 70.3 (1C, C-5); 70.7 (1C, CH$_2$-CH=CH$_2$); 74.4 (1C, C-2); 75.6 (1C, PhCH$_2$); 78.1 (1C, C-4); 85.2 (1C, C-3); 103.1 (1C, C-1); 117.8 (1C, CH$_2$-CH=CH$_2$); 127.5 (1C, *p*-Ph-C); 128.2 (2C, *m*-Ph-C); 128.3 (2C, *o*-Ph-C); 133.8 (1C, CH$_2$-CH=CH$_2$); 138.8 (1C, Ph-C$_q$).

6.8 Synthesis of allyl 3-*O*-benzyl-2,4,6-tri-*O*-*tert*-butyldimethylsilyl-*α*- and *β*-D-glucopyranoside (9)

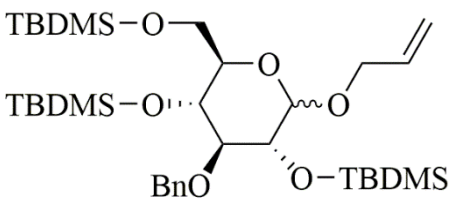

tert-Butyldimethylsilyl triflate (2.65 mL, 11.528 mmol, 4.5 eq.) was added dropwise at 0 °C to a solution of allyl 3-*O*-benzyl-D-glucopyranoside (**4**) (0.7952 g, 2.562 mmol) and 2,6-lutidine (1.95 mL, 16.652 mmol, 6.5 eq.). The reaction mixture was stirred at 0 °C for 5 h in N_2 atmosphere, then rt for the remainder of 24 h in N_2 atmosphere. The mixture was diluted with DCM (40 mL) and water (40 mL), where the aqueous layer was extracted with DCM (2 x 40 mL). The combined organic extracts were washed with brine (3 x 40 mL), dried over $MgSO_4$ and evaporated under reduced pressure to give a brown oil (1.7109 g). Preliminary purification was done on a short column (SiO_2, 4.3 x 7 cm) with *n*-pentane (ca 250 mL). Flushing with DCM and evaporating under reduced pressure gave a brown oil (1.5878 g). Purification of the crude by flash column (SiO_2, 3.0 x 20 cm, Et_2O:*n*-pentane = 1:25) afforded **9** as a colourless oil (1.2492 g, 76%), which was a mixture of anomers (*α*:*β* = 73:27). R_f (SiO_2, Et_2O:*n*-pentane = 1:25) = 0.60-0.77. t_R (analytical HPLC, method B) = 57.82-58.12 min (**9a**), 60.23-60.63 min (**9b**). IR (cm^{-1}): 3029 (w), 2953 (m), 1251 (m), 1073 (s), 831 (s), 695 (m). HRMS (ESI) *m/z*: $[M+Na]^+$ Calcd. for $C_{34}H_{64}O_6Si_3Na$ 675.3908; Found 675.3918.

6.8.1 NMR of *α*-anomer

^{1}H-NMR (600 MHz, $CDCl_3$) *δ*: -0.11 (3H, *s*, Si(Me)$_2$tBu); -0.07 (3H, *s*, Si(Me)$_2$tBu); 0.037-0.051 (6H, *m*, Si(Me)$_2$tBu); 0.061-0.067 (6H, *m*, Si(Me)$_2$tBu); 0.82-0.83 (9H, *m*, Si(Me)$_2$tBu); 0.834 (9H, *s*, Si(Me)$_2$tBu); 0.904 (9H, *s*, Si(Me)$_2$tBu); 3.50 (1H, *m*, *J* = 9.0, H-4); 3.61 (1H, *ddd*, *J* = 2.3, 6.2, 9.3, H-5); 3.66 (1H, *t*, *J* = 8.9, H-3); 3.68 (1H, *m*, *J* = 6.2, 11.1, H-6); 3.70 (1H, *m*, *J* = 3.4, 9.2, H-2); 3.855 (1H, *dd*, *J* = 2.3, 11.2, H-6); 4.00 (1H, *dd(b)*, *J* = 2.2, 6.5, 12.8, CH_2-CH=CH_2); 4.22 (1H, *dd(b)*, *J* = 2.2, 5.5, 12.8, CH_2-CH=CH_2); 4.68 (1H, *d*, *J* = 12.2, PhCH_2); 4.752 (1H, *d*, *J* = 3.5, H-1); 5.07 (1H, *d*, *J* = 12.2, PhCH_2); 5.21 (1H, *d(b)*, *J* = 2.3, 10.4, CH_2-CH=CH_2); 5.33 (1H, *d(b)*, *J* = 2.2, 17.2, CH_2-CH=CH_2); 5.96 (1H, *m*, *J* = 5.5, 7.5, 10.3, 17.2, CH_2-CH=CH_2); 7.20 (1H, *t(b)*, *p*-Ph-H); 7.26-7.32 (4H, *m*, Ph-H). ^{13}C-NMR (150 MHz, $CDCl_3$) *δ*: -5.31, -5.30, [-4.72]-[-4.54], -3.92 (6C, Si(Me)$_2$tBu); 18.00, 18.07, 18.41 (3C, Si(Me)$_2$tBu-C_q); 25.77, 25.89-25.97 (9C, Si(Me)$_2$tBu); 62.9 (1C, C-6); 68.1 (1C, CH_2-CH=CH_2); 70.9 (1C, C-4); 73.1 (1C, C-5); 74.5 (1C, C-2); 74.6 (1C, PhCH_2); 82.3 (1C, C-3);

97.6 (1C, C-1); 117.8 (1C, CH_2-CH=$\underline{C}H_2$); 126.3 (2C, Ph-C); 126.49 (1C, *p*-Ph-C); 127.8 (2C, Ph-C); 134.2 (1C, CH_2-$\underline{C}$H=CH_2); 139.4 (1C, Ph-C_q).

6.8.2 NMR of *β*-anomer

^{1}H-NMR (600 MHz, $CDCl_3$) *δ*: -0.14 (3H, *s*, Si($\underline{Me}$)$_2$tBu); -0.08 (3H, *s*, Si($\underline{Me}$)$_2$tBu); 0.037-0.051 (3H, *m*, Si($\underline{Me}$)$_2$tBu); 0.058 (3H, *s*, Si($\underline{Me}$)$_2$tBu); 0.070 (3H, *s*, Si($\underline{Me}$)$_2$tBu); 0.075 (3H, *s*, Si($\underline{Me}$)$_2$tBu); 0.80 (9H, *s*, Si(Me)$_2$$\underline{tBu}$); 0.82-0.83 (9H, *m*, Si(Me)$_2$$\underline{tBu}$); 0.899 (9H, *s*, Si(Me)$_2$$\underline{tBu}$); 3.24 (1H, *ddd*, *J* = 2.6, 5.7, 9.3, H-5); 3.32 (1H, *t*, *J* = 8.9, H-3); 3.53 (1H, *m*, *J* = 7.1, 9.3, H-2); 3.56 (1H, *t*, *J* = 9.0, H-4); 3.69 (1H, *m*, H-6); 3.875 (1H, *dd*, *J* = 2.6, 11.2, H-6); 4.06 (1H, *dd(b)*, *J* = 2.2, 6.7, 12.2, C$\underline{H}_2$-CH=CH_2); 4.27 (1H, *d*, *J* = 7.4, H-1); 4.33 (1H, *dd(b)*, *J* = 2.2, 5.4, 12.2, C$\underline{H}_2$-CH=CH_2); 4.747 (1H, *m*, *J* = 12.2, PhC$\underline{H}_2$); 4.99 (1H, *d*, *J* = 12.2, PhC$\underline{H}_2$); 5.17 (1H, *d(b)*, *J* = 2.1, 10.4, CH_2-CH=C$\underline{H}_2$); 5.26 (1H, *d(b)*, *J* = 2.1, 17.2, CH_2-CH=C$\underline{H}_2$); 5.95 (1H, *m*, *J* = 5.5, 6.6, 10.4, 17.2, CH_2-C$\underline{H}$=CH_2); 7.20 (1H, *t(b)*, *p*-Ph-H); 7.26-7.32 (4H, *m*, Ph-H). ^{13}C-NMR (150 MHz, $CDCl_3$) *δ*: -5.32, -5.05, -4.70, -4.37, -3.94, -3.93 (6C, Si($\underline{Me}$)$_2$tBu); 18.02, 18.13, 18.41 (3C, Si(Me)$_2$tBu-C_q); 25.77, 25.89-25.97 (9C, Si(Me)$_2$$\underline{tBu}$); 62.7 (1C, C-6); 70.0 (1C, $\underline{C}H_2$-CH=CH_2); 70.8 (1C, C-4); 74.8 (1C, Ph$\underline{C}H_2$); 75.7 (1C, C-2); 77.3 (1C, C-5); 86.3 (1C, C-3); 102.1 (1C, C-1); 117.6 (1C, CH_2-CH=$\underline{C}H_2$); 126.0 (2C, Ph-C); 126.47 (1C, *p*-Ph-C); 127.8 (2C, Ph-C); 134.3 (1C, CH_2-$\underline{C}$H=CH_2); 139.1 (1C, Ph-C_q).

Bibliography

1. Bukhari, S. M.; Feuerherm, A. J.; Boulfrad, F.; Zlatkovic, B.; Johansen, B.; Simić, N., *J. Serb. Chem. Soc.* **2014,** *79* (7), 12.

2. Bukhari, S. M.; Jullumstrø, F. A.; Tunset, H. M.; Isaksen, S. M.; Sæther, M.; Thvedt, T. H. K.; Gonzalez, S. V.; Schmid, R.; Brunsvik, A.; Fuglseth, E.; Zlatković, B.; Johansen, B.; Simić, N., *J. Serb. Chem. Soc.* **2016,** *81* (1), 1-12.

3. Fukase, K.; Matsumoto, T.; Ito, N.; Yoshimura, T.; Kotani, S.; Kusumoto, S., *Bull. Chem. Soc. Jpn.* **1992,** *65* (10), 2643-2654.

4. Osborn, H. M. I.; Evans, P. G.; Gemmell, N.; Osborne, S. D., *J. Pharm. Pharmacol.* **2004,** *56* (6), 691-702.

5. Kilcoyne, M.; Joshi, L., *Cardiovasc. Hematol. Agents Med. Chem.* **2007,** *5* (3), 186-197.

6. Wong, C.-H., *Carbohydrate-based Drug Discovery*. Wiley-VCH Verlag GmbH & Co. KGaA: Weinheim, Germany, 2003; Vol. 1.

7. Levy, D. E.; Fügedi, P., *The Organic Chemistry of Sugars*. 1st ed.; CRC Press: USA, 2006.

8. Ghazarian, H.; Idoni, B.; Oppenheimer, S. B., *Acta Histochem.* **2011,** *113* (3), 236-247.

9. Lindhorst, T. K., *Essentials of Carbohydrate Chemistry and Biochemistry*. Second, Revised and Updated ed.; Wiley-VCH Verlag GmbH & Co. KGaA: Weinheim, Germany, 2007.

10. Boons, G.-J.; Hale, K. J., *Organic Synthesis with Carbohydrates*. John Wiley & Sons: 2008; Vol. 1.

11. Karabulut, S.; Leszczynski, J., *J. Mol. Model.* **2013,** *19* (9), 3637-3645.

12. Hyvönen, L.; Varo, P.; Koivistoinen, P., *J. Food Sci.* **1977,** *42* (3), 657-659.

13. Ha, S.; Gao, J.; Tidor, B.; Brady, J. W.; Karplus, M., *J. Am. Chem. Soc.* **1991,** *113* (5), 1553-1557.

14. Gilchrist, T. L., *Heterocyclic Chemistry*. 3rd ed.; Addison Wesley Longman: Essex, England, 1997.

15. Mackie, W.; Perlin, A. S., *Can. J. Chem.* **1966,** *44* (17), 2039-2049.

16. Franks, F.; Lillford, P. J.; Robinson, G., *J. Chem. Soc., Faraday Trans. 1,* **1989,** *85* (8), 2417-2426.

17. Hill, K.; von Rybinski, W.; Stoll, G., *Alkyl Polyglycosides: Technology, Properties, Applications*. 1st ed.; John Wiley & Sons: 2008.

18. Juaristi, E.; Cuevas, G., *The Anomeric Effect (New Directions in Organic & Biological Chemistry)*. 1st ed.; CRC press: 1994.

19. Lemieux, R. U.; Chü, N. J. In *Abstracts*, 133rd Meeting of the American Chemical Society San Francisco, 1958.

20. Edward, J. T., *Chem. Ind.* **1955,** *36*, 1102-1104.

21. Reuben, J., *Carbohydr. Res.* **1988,** *184*, 244-246.

22. Lopes, J. F.; Gaspar, E. M. S. M., *J. Chromatogr. A* **2008,** *1188* (1), 34-42.

23. Warrent, R. W.; Caughlan, C. N.; Hargis, J. H.; Yee, K. C.; Bentrude, W. G., *J. Org. Chem.* **1978,** *43* (22), 4266-4270.

24. McBride, W. G., *The Lancet* **1961,** *278* (7216), 1358.

25. Adams, S. S.; Bresloff, P.; Mason, C. G., *J. Pharm. Pharmacol.* **1976,** *28* (3), 256-257.

26. Reich, W. S., *Biochem. J* **1939,** *33* (6), 1000-1004.

27. Li, H.; Giles, K.; Bendiak, B.; Kaplan, K.; Siems, W. F.; Hill, H. H., *Anal. Chem.* **2012,** *84* (7), 3231-3239.

28. Chaplin, M. F., Monosaccharides. In *Carbohydrate Analysis: A Practical Approach*, Chaplin, M. F.; Kennedy, J. F., Eds. IRL Press: Oxford, Washington DC, 1986; pp 1-36.

29. Haines, A. H., Relative Reactivities of Hydroxyl Groups in Carbohydrates. In *Adv. Carbohydr. Chem. Biochem.*, Tipson, R. S.; Horton, D., Eds. Academic Press Inc.: New York, USA, 1976; Vol. 33, pp 11-109.

30. Pomin, V. H., Unravelling Glycobiology by NMR spectroscopy. In *Glycosylation*, Petrescu, S., Ed. InTech: 2012.

31. Friebolin, H., *Basic One-and Two-Dimensional NMR Spectroscopy* Fifth, Completely Revised and Updated ed.; WIley-VCH Verlag GMBH: Weinheim, Germany, 2011.

32. Matwiejuk, M.; Thiem, J., *Eur. J. Org. Chem.* **2012,** *2012* (11), 2180-2187.

33. Kurahashi, T.; Mizutani, T.; Yoshida, J.-i., *J. Chem. Soc., Perkin Trans. 1* **1999,** (4), 465-474.

34. Christofides, J. C.; Davies, D. B., *J. Chem. Soc., Perkin Trans. 2* **1987,** (1), 97-102.

35. de Belder, A. N.; Lindberg, B.; Threander, O., *Acta Chem. Scand.* **1962,** *16* (8), 2005-2009.

36. Norrman, B., *Acta Chem. Scand.* **1968,** *22* (5).

37. Lenz, R. W., *J. Am. Chem. Soc.* **1960,** *82* (1), 182-186.

38. Sugihara, J. M., Relative Reactivities of Hydroxyl Groups of Carbohydrates. In *Adv. Carbohydr. Chem.*, Hudson, C. S.; Wolfrom, M. L., Eds. Academic Press Inc.: New York, USA, 1953; Vol. 8, pp 1-44.

39. Kocienski, P. J., *Protecting Groups*. 3rd ed.; Georg Thieme Verlag: Stuttgart, Germany, 2005.

40. Hanessian, S., *Preparative Carbohydrate Chemistry*. Marcel Dekker: New York, USA, 1997.

41. Nicolaou, K. C.; Mitchell, H. J., *Angew. Chem. Int. Ed.* **2001,** *40* (9), 1576-1624.

42. Corey, E. J.; Cho, H.; Rücker, C.; Hua, D. H., *Tetrahedron Lett.* **1981,** *22* (36), 3455-3458.

43. Hanashima, S.; Mizushina, Y.; Yamazaki, T.; Ohta, K.; Takahashi, S.; Sahara, H.; Sakaguchi, K.; Sugawara, F., *Biorg. Med. Chem.* **2001,** *9* (2), 367-376.

44. Kakitsubata, Y.; Aramaki, R.; Nishioka, K.; Wakao, M.; Suda, Y., *Tetrahedron Lett.* **2016,** *57* (10), 1154-1157.

45. Lee, A.; Farrand, K. J.; Dickgreber, N.; Hayman, C. M.; Jürs, S.; Hermans, I. F.; Painter, G. F., *Carbohydr. Res.* **2006,** *341* (17), 2785-2798.

46. Fischer, H. E., *Berichte der deutschen chemischen Gesellschaft* **1893,** *26* (3), 2400-2412.

47. Guchhait, G.; Misra, A. K., *Catal. Commun.* **2011,** *14* (1), 52-57.

48. Izumi, M.; Fukase, K.; Kusumoto, S., *Biosci. Biotechnol. Biochem.* **2002,** *66* (1), 211-214.

49. Pater, R. H.; Coelho, R. A.; Mowery Jr, D. F., *J. Org. Chem.* **1973,** *38* (19), 3272-3277.

50. Capon, B.; Thacker, D., *J. Chem. Soc. B,* **1967**, 1010-1013.

51. Zhang, Y.; Wang, F., *Drug Discov. Ther.* **2015,** *9* (2), 79-87.

52. Laine, R. A., *Glycobiology* **1994,** *4* (6), 759-767.

53. Galan, M. C.; Benito-Alifonso, D.; Watt, G. M., *Org. Biomol. Chem.* **2011,** *9* (10), 3598-3610.

54. Ernst, B.; Magnani, J. L., *Nat. Rev. Drug Discov.* **2009,** *8*, 661.

55. Witczak, Z. J., *Curr. Med. Chem.* **1995,** *1* (5), 392-405.

56. Dove, A., *Nat. Biotechnol.* **2001,** *19* (10), 913.

57. Nervik, S., Selective monobenzylation of allyl 4,6-di-O-benzylidene-α-D-glucopyranoside. NTNU, Department of Chemistry, Unpublished work, 2017.

58. Ness, K. A.; Migaud, M. E., *Beilstein J. Org. Chem.* **2007,** *3*, 26.

59. Bhattacharjee, S. S.; Gorin, P. A. J., *Can. J. Chem.* **1969,** *47* (7), 1195-1206.

60. Umemura, K.; Matsuyama, H.; Kobayashi, M.; Kamigata, N., *Bull. Chem. Soc. Jpn.* **1989,** *62* (9), 3026-3028.

61. Tanaka, N.; Ogawa, I.; Yoshigase, S.; Nokami, J., *Carbohydr. Res.* **2008,** *343* (15), 2675-2679.

62. Bjørnstad, F. A. Regioselective Protection and Functionalization of C-6 in The Synthesis Towards Sulfoquinovoses. Master's thesis, NTNU, 2018.

63. Clive, D. L. J.; He, X.; Postema, M. H. D.; Mashimbye, M. J., *Tetrahedron Lett.* **1998,** *39* (24), 4231-4234.

64. Clive, D. L. J.; He, X.; Postema, M. H. D.; Mashimbye, M. J., *J. Org. Chem.* **1999,** *64* (12), 4397-4410.

65. Nelson, T. D.; Crouch, D. R., *Synthesis* **1996,** *1996* (09), 1031-1069.

66. Crouch, D. R., *Tetrahedron* **2013,** *69*, 2383-2417.

67. Crouch, D. R., *Tetrahedron* **2004,** *60* (28), 5833-5871.

68. Yu, M.; Pagenkopf, B. L., *J. Org. Chem* **2002,** *67* (13), 4553-4558.

69. Masaki, O.; Hiroshi, T.; Tohru, N., *Bull. Chem. Soc. Jpn.* **2014,** *87* (1), 113-118.

70. Chen, M.-Y.; Lu, K.-C.; Lee, A. S.-Y.; Lin, C.-C., *Tetrahedron Lett.* **2002,** *43* (15), 2777-2780.

71. Yadav, J. S.; Reddy, B. V. S., *Carbohydr. Res.* **2000,** *329* (4), 885-888.

72. Gurlaga, N., Research Project Report (Untitled Work). NTNU, Department of Chemistry, Unpublished work, 2017.

73. Fang, T. T.; Bendiak, B., *J. Am. Chem. Soc.* **2007,** *129* (31), 9721-9736.

74. Nadjari, R.; Grivet, J.-P., *J. Magn. Reson.* **1991,** *91* (2), 353-361.

75. Furniss, B. S.; Hannaford, A. J.; Smith, P. W. G.; Tatchell, A. R., *Vogel's Textbook of Practical Organic Chemistry*. 5th ed.; Longman Group: Suffolk, UK, 1989.

76. Eshelman, J. E.; Epps, J. L.; Kallmerten, J., *Tetrahedron Lett.* **1993,** *34* (5), 749-752.

77. Glen, W. L.; Myers, G. S.; Grant, G. A., *J. Chem. Soc.* **1951**, 2568-2572.

78. Pacsu, E., *Berichte der deutschen chemischen Gesellschaft* **1928,** *61* (1), 137-144.

79. Sigurdsson, S. T.; Hopkins, P. B.; Belani, J.; Ghosh, S.; Andreana, P. R., Di-t-butylsilyl Bis (trifluoromethanesulfonate). In *Encyclopedia of Reagents for Organic Synthesis*, John Wiley & Sons Ltd.: 2015; Vol. 1, pp 1-27.

80. Goto, K.; Sawa, M.; Tamai, H.; Imamura, A.; Ando, H.; Ishida, H.; Kiso, M., *Chem. Eur. J.* **2016,** *22* (24), 8323-8331.

81. Gold, H.; van Delft, P.; Meeuwenoord, N.; Codée, J. D. C.; Filippov, D. V.; Eggink, G.; Overkleeft, H. S.; van der Marel, G. A., *J. Org. Chem* **2008,** *73* (23), 9458-9460.

82. Jeffrey, G. A., *An Introduction to Hydrogen Bonding*. Oxford University Press: New York, USA, 1997; Vol. 32.

83. Smith, J. M.; Borsenberger, V.; Raftery, J.; Sutherland, J. D., *Chem. Biodivers.* **2004,** *1* (10), 1418-1451.

84. Fulmer, G. R.; Miller, A. J. M.; Sherden, N. H.; Gottlieb, H. E.; Nudelman, A.; Stoltz, B. M.; Bercaw, J. E.; Goldberg, K. I., *Organometallics* **2010,** *29* (9), 2176-2179.

85. Karplus, M., *J. Chem. Phys.* **1959,** *30* (1), 11-15.

86. Karplus, M., *J. Am. Chem. Soc.* **1963,** *85* (18), 2870-2871.

87. Silverstein, R. M.; Webster, F. X.; Kiemle, D. J.; Bryce, D. L., *Spectrometric Identification of Organic Compounds*. 8th ed.; John Wiley & Sons: New York, USA, 2014.

88. Angyal, S. J.; James, K., *Carbohydr. Res.* **1970,** *12* (1), 147-149.

89. Tamura, J.-i.; Koike, S.; Shimadate, T., *J. Carbohydr. Chem.* **1992,** *11* (4), 531-535.

90. Bertolini, M.; Glaudemans, C. P. J., *Carbohydr. Res.* **1970,** *15* (2), 263-270.

91. Angibeaud, P.; Defaye, J.; Gadelle, A.; Utille, J.-P., *Synthesis* **1985,** *1985* (12), 1123-1125.

92. Howells, R.; Mc Cown, J., *Chem. Rev.* **1977,** *77* (1), 69-92.

93. Di Bussolo, V.; Kim, Y.-J.; Gin, D. Y., *J. Am. Chem. Soc.* **1998,** *120* (51), 13515-13516.

94. Bronnimann, C. E.; Chuang, I. S.; Hawkins, B. L.; Maciel, G. E., *J. Am. Chem. Soc.* **1987,** *109* (5), 1562-1564.

95. Bronnimann, C. E.; Zeigler, R. C.; Maciel, G. E., *J. Am. Chem. Soc.* **1988,** *110* (7), 2023-2026.

96. Stang, P. J.; Hanack, M.; Subramanian, L. R., *Synthesis* **1982,** *1982* (02), 85-126.

Appendices

A Spectroscopic Data – Compound 3

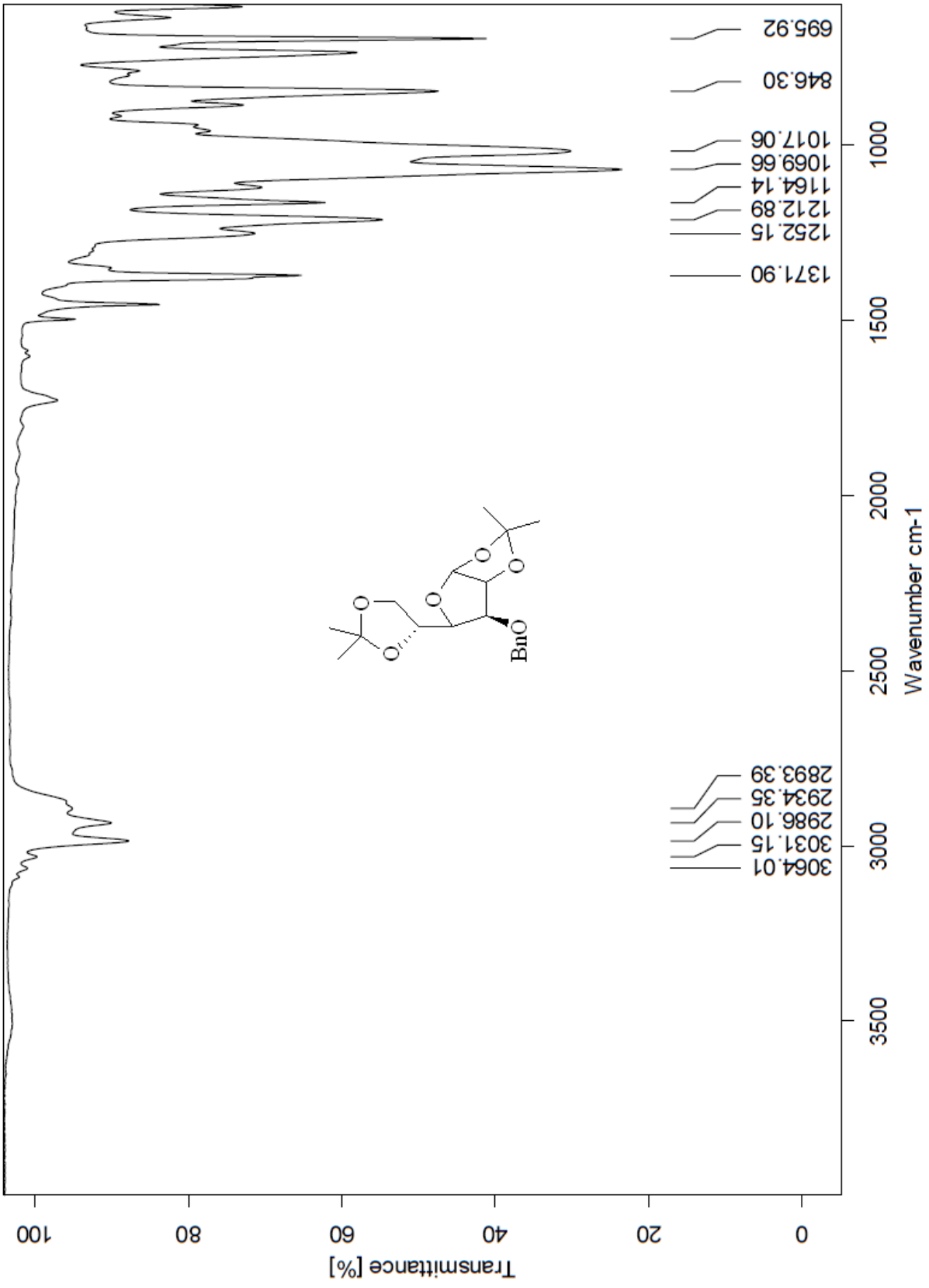

Figure A.1: IR spectrum of **3**.

Single Mass Analysis
Tolerance = 3.0 PPM / DBE: min = -1.5, max = 50.0
Element prediction: Off
Number of isotope peaks used for i-FIT = 3

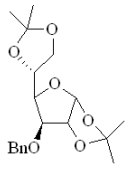

Monoisotopic Mass, Even Electron Ions
667 formula(e) evaluated with 4 results within limits (all results (up to 1000) for each mass)
Elements Used:
C: 0-500 H: 0-1000 O: 0-10 Na: 0-1 Si: 0-4 I: 0-1

2018-135 57 (1.066) AM2 (Ar,35000.0,0.00,0.00); Cm (55:57)
1: TOF MS ES+

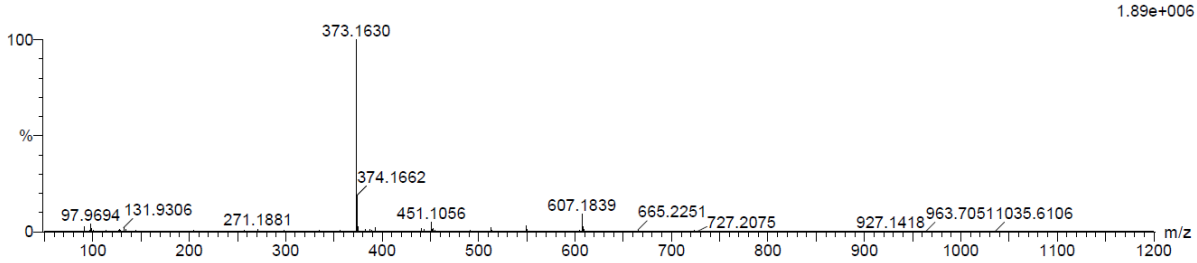

Minimum:				-1.5				
Maximum:		5000.0	3.0	50.0				
Mass	Calc. Mass	mDa	PPM	DBE	i-FIT	Norm	Conf(%)	Formula
373.1630	373.1627	0.3	0.8	6.5	1190.8	0.000	100.00	C19 H26 O6 Na
	373.1624	0.6	1.6	13.5	1205.6	14.769	0.00	C24 H25 O2 Si
	373.1631	-0.1	-0.3	5.5	1208.2	17.352	0.00	C18 H30 O3 Na Si2
	373.1635	-0.5	-1.3	4.5	1210.6	19.723	0.00	C17 H34 Na Si4

Figure A.2: HRMS spectrum of compound **3**.

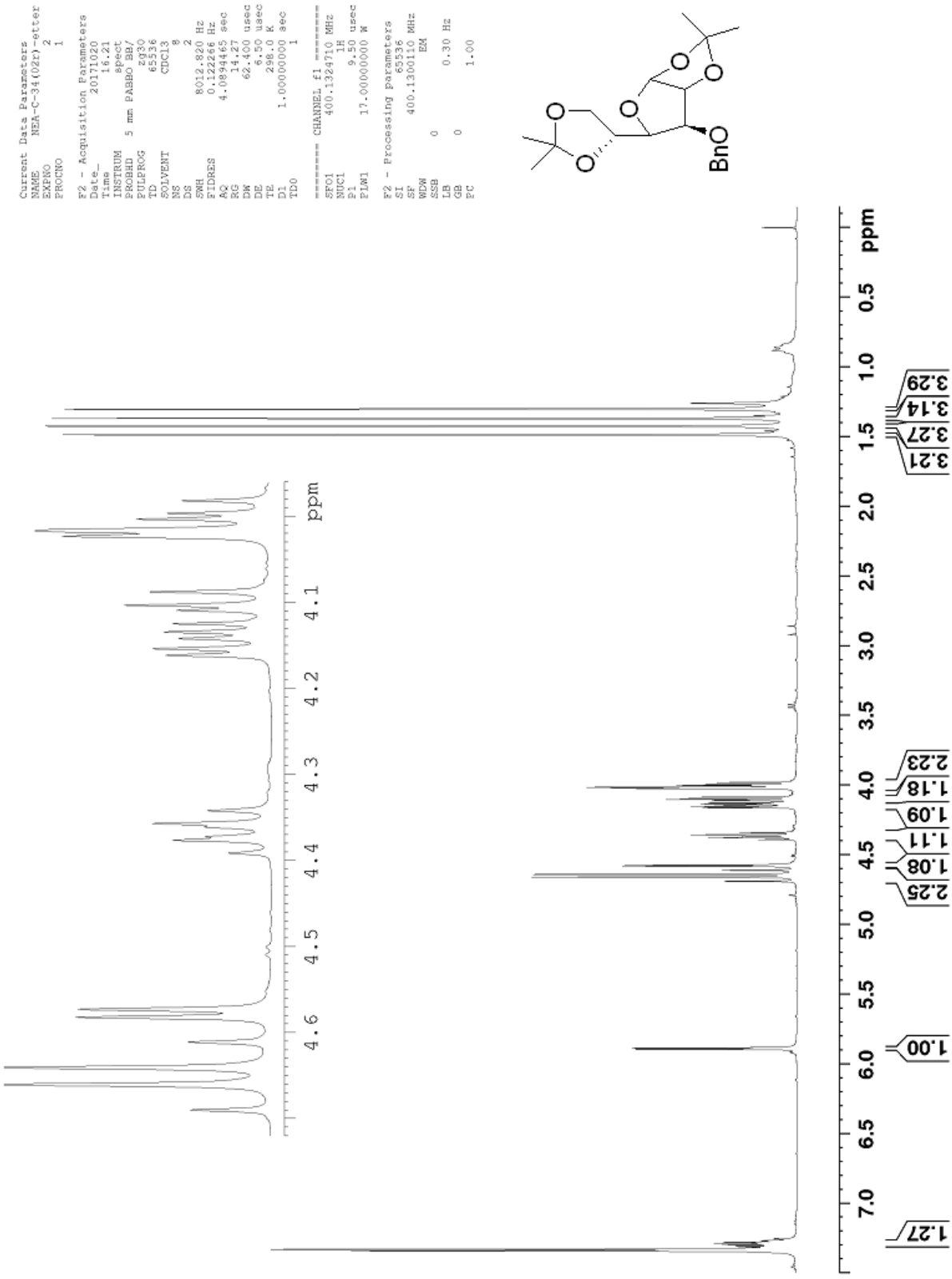

Figure A.3: ^{1}H-NMR spectrum of compound **3**.

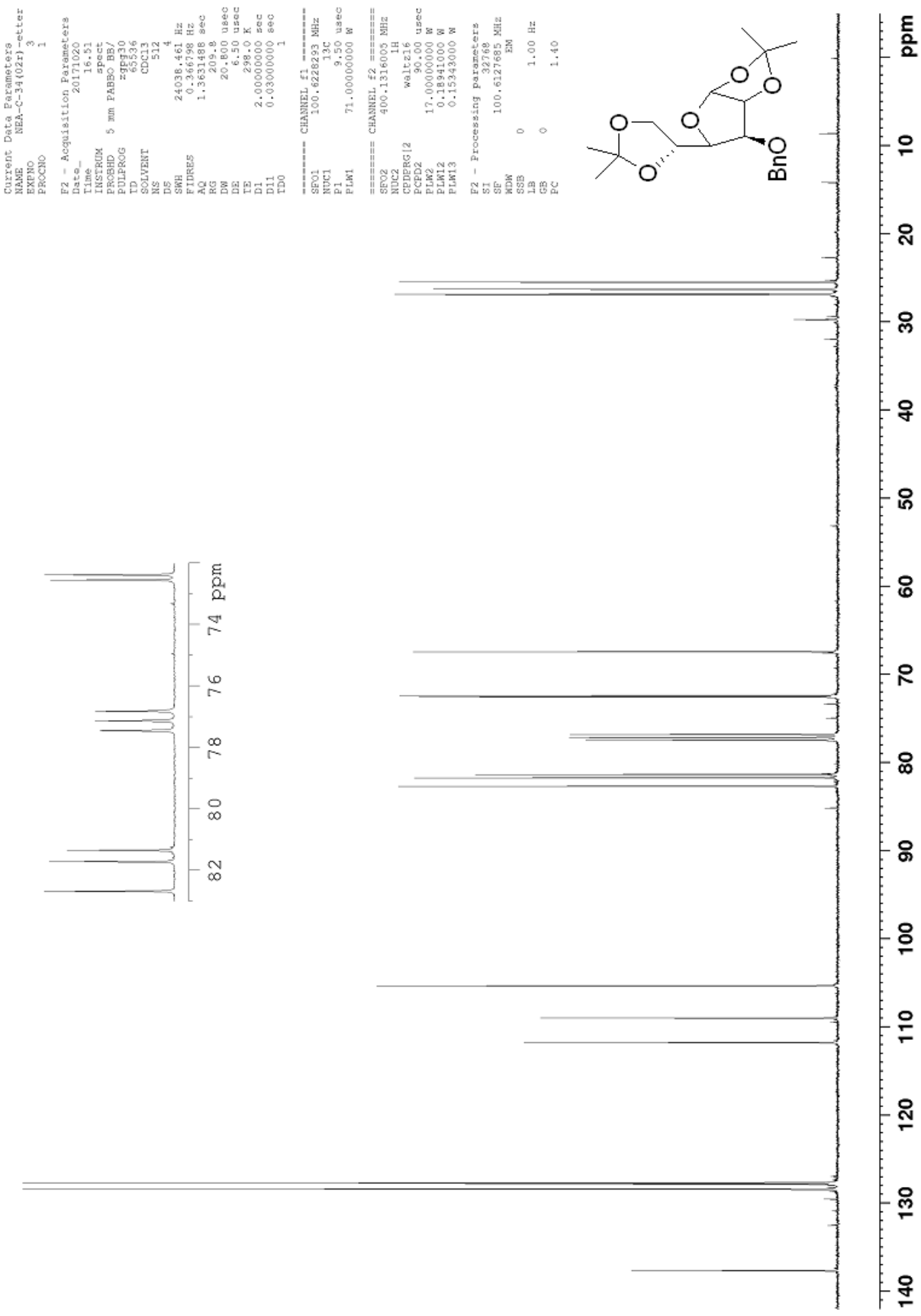

Figure A.4: ^{13}C-NMR spectrum of compound **3**.

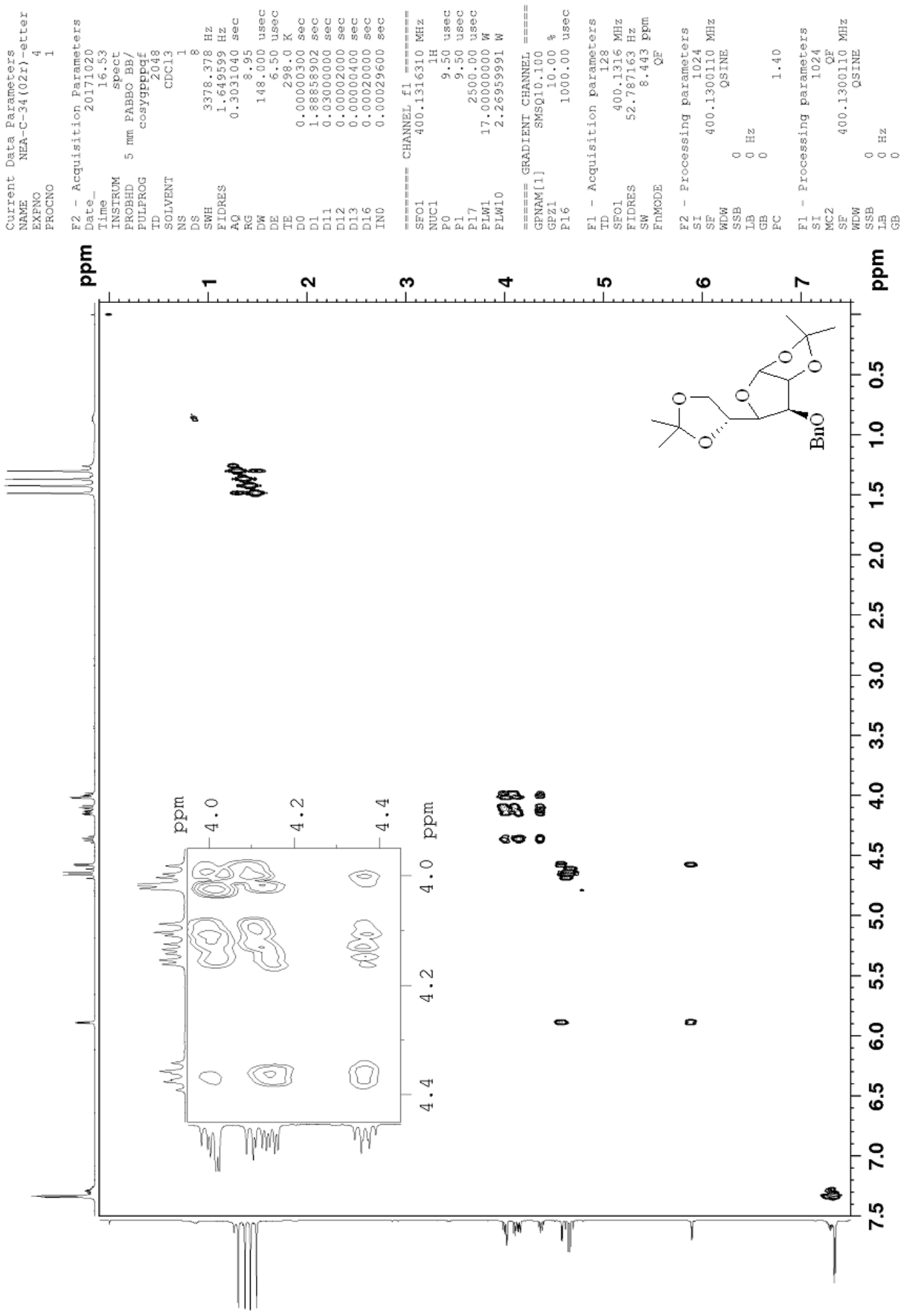

Figure A.5: H,H-COSY spectrum of compound **3**.

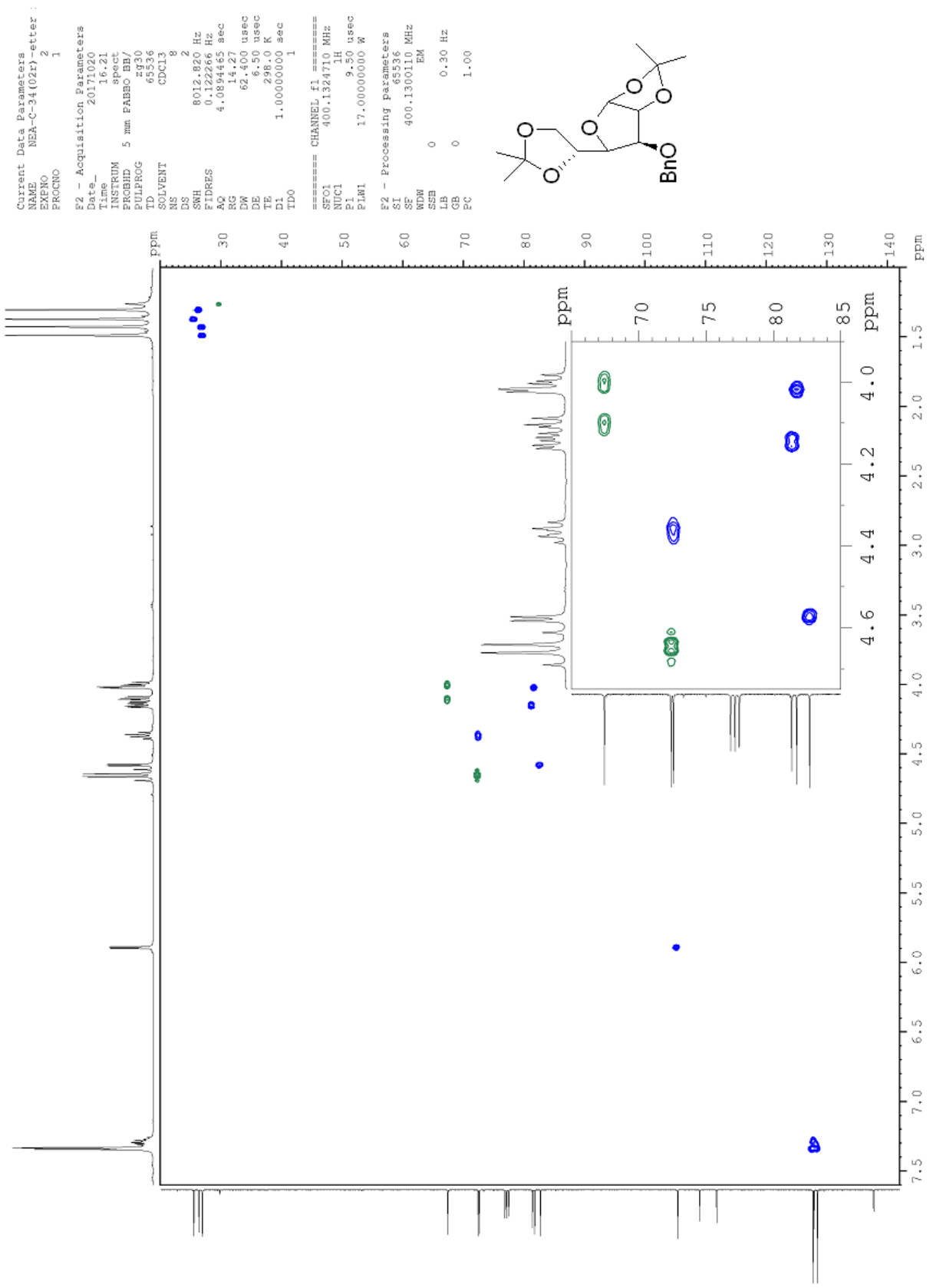

Figure A.6: HSQC spectrum of compound **3**.

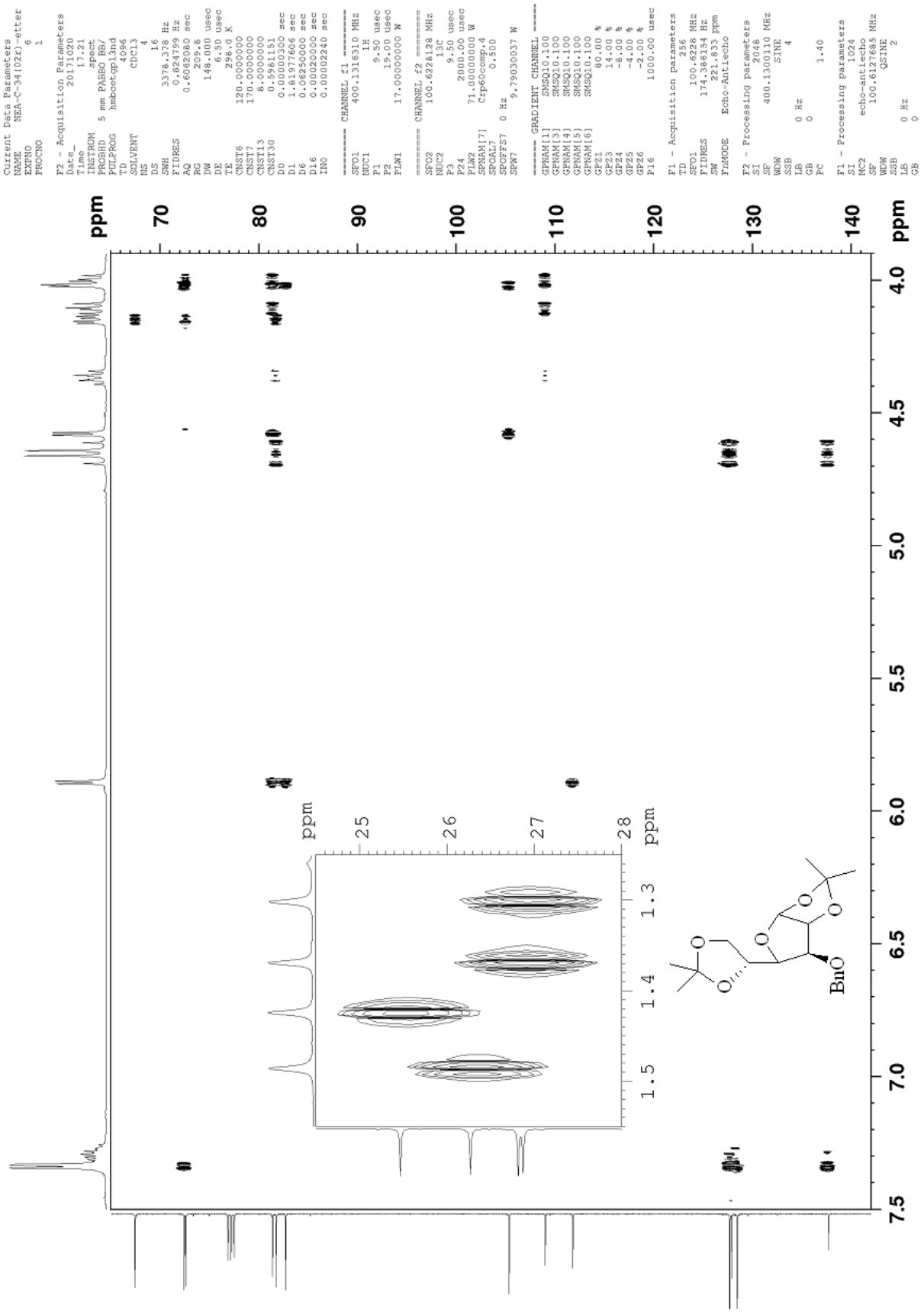

Figure A.7: HMBC spectrum of compound **3**.

B Spectroscopic Data – Compound 4

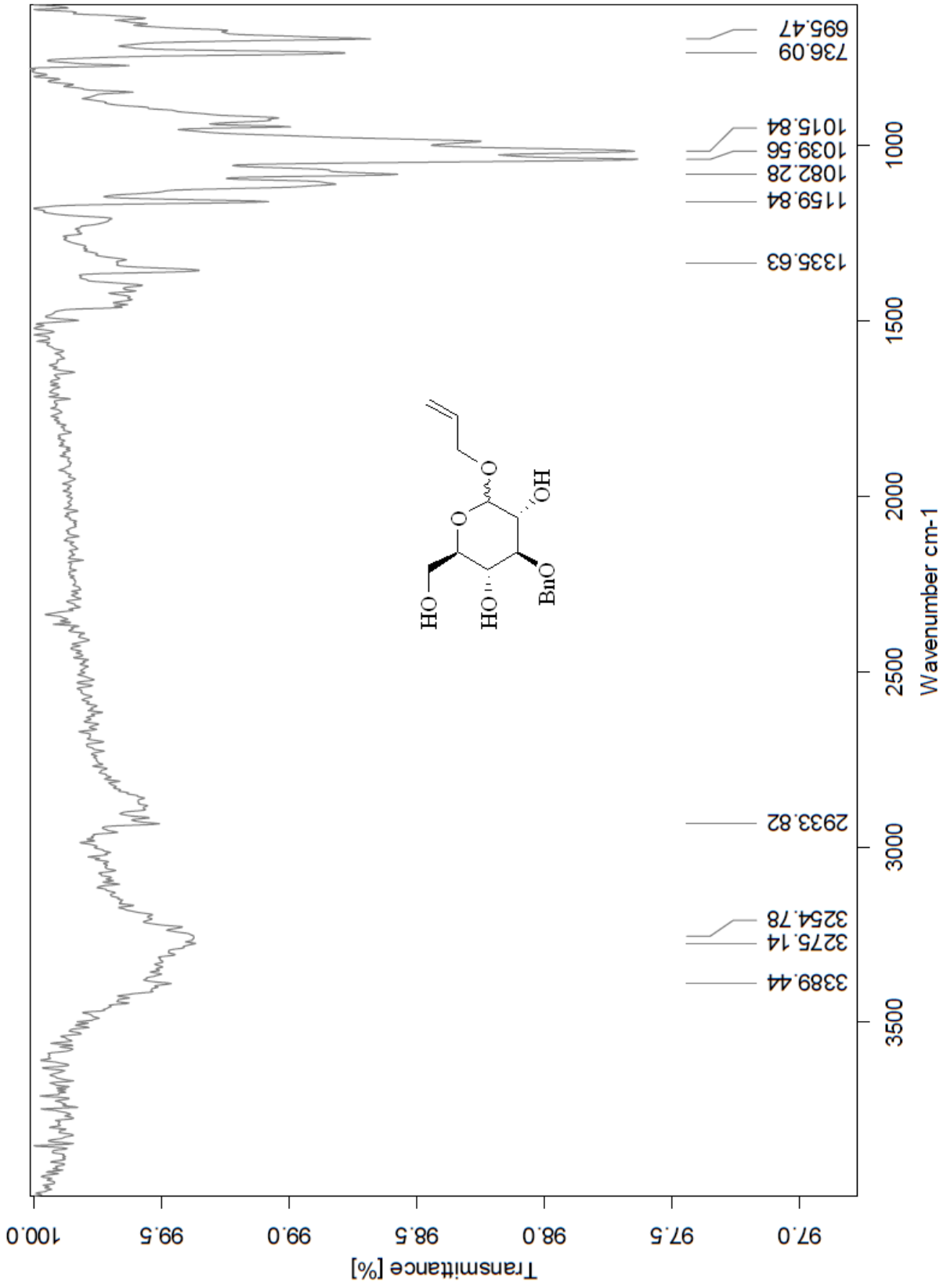

Figure B.1: IR spectrum of compound **4**, which is an anomeric mixture.

Single Mass Analysis
Tolerance = 3.0 PPM / DBE: min = -1.5, max = 50.0
Element prediction: Off
Number of isotope peaks used for i-FIT = 3

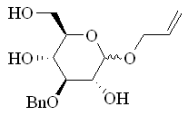

Monoisotopic Mass, Even Electron Ions
552 formula(e) evaluated with 4 results within limits (all results (up to 1000) for each mass)
Elements Used:
C: 0-500 H: 0-1000 O: 0-10 Na: 0-1 Si: 0-4 I: 0-1

2018-134 44 (0.820) AM2 (Ar,35000.0,0.00,0.00); Cm (44:46)
1: TOF MS ES+

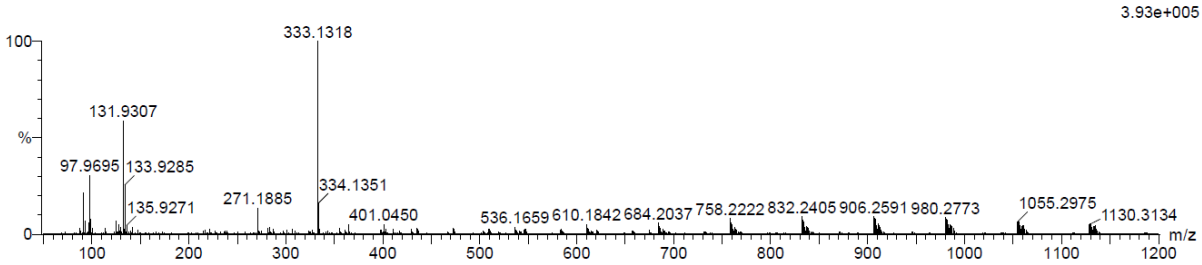

Minimum:				-1.5				
Maximum:		5000.0	3.0	50.0				
Mass	Calc. Mass	mDa	PPM	DBE	i-FIT	Norm	Conf(%)	Formula
333.1318	333.1314	0.4	1.2	5.5	1127.4	0.000	100.00	C16 H22 O6 Na
	333.1311	0.7	2.1	12.5	1144.4	17.032	0.00	C21 H21 O2 Si
	333.1318	0.0	0.0	4.5	1146.8	19.446	0.00	C15 H26 O3 Na Si2
	333.1322	-0.4	-1.2	3.5	1149.2	21.826	0.00	C14 H30 Na Si4

Figure B.2: HRMS spectrum of compound **4**, which is an anomeric mixture.

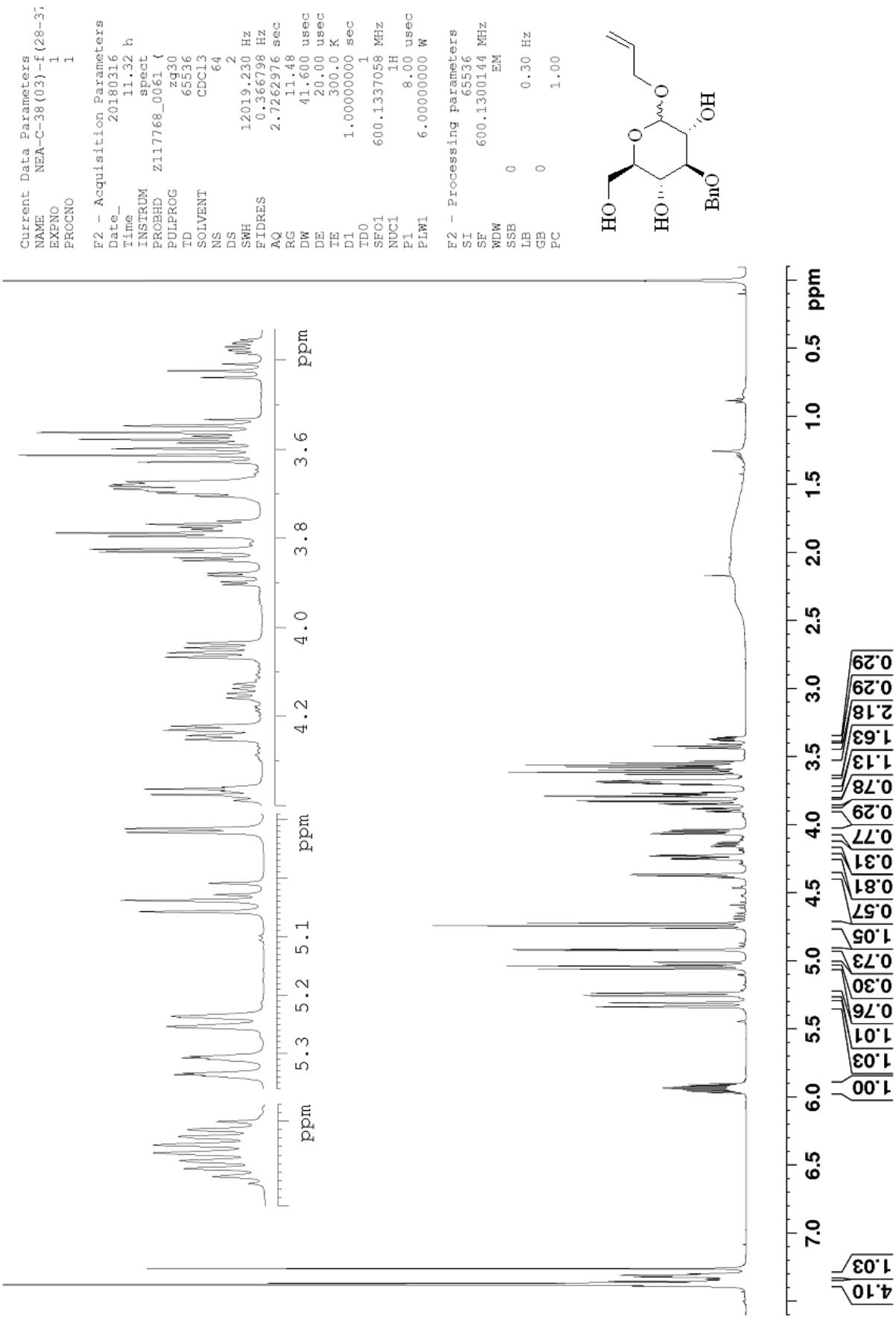

Figure B.3: ^{1}H-NMR spectrum of compound **4**, which is an anomeric mixture.

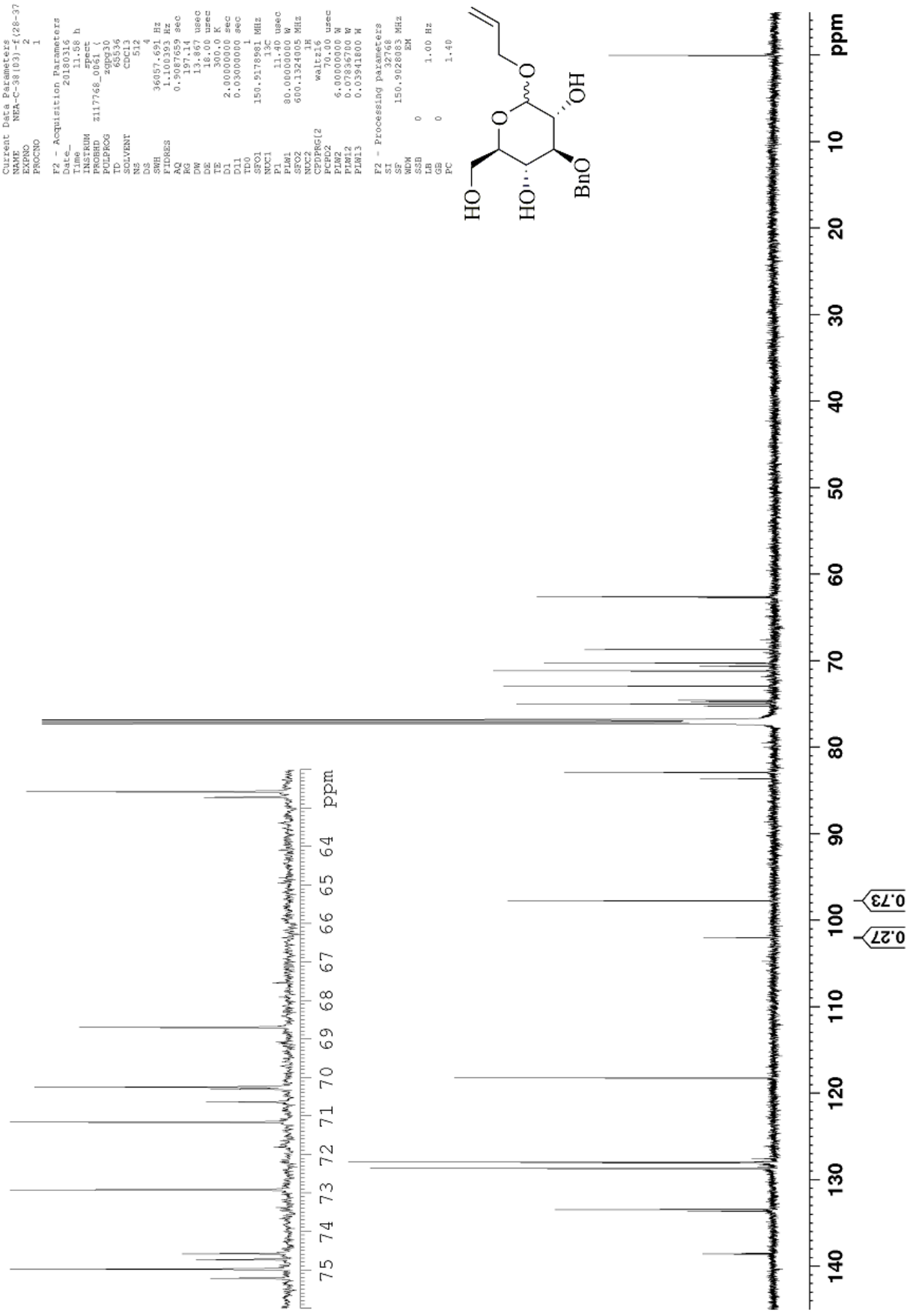

Figure B.4: ^{13}C-NMR spectrum of compound **4**, which is an anomeric mixture.

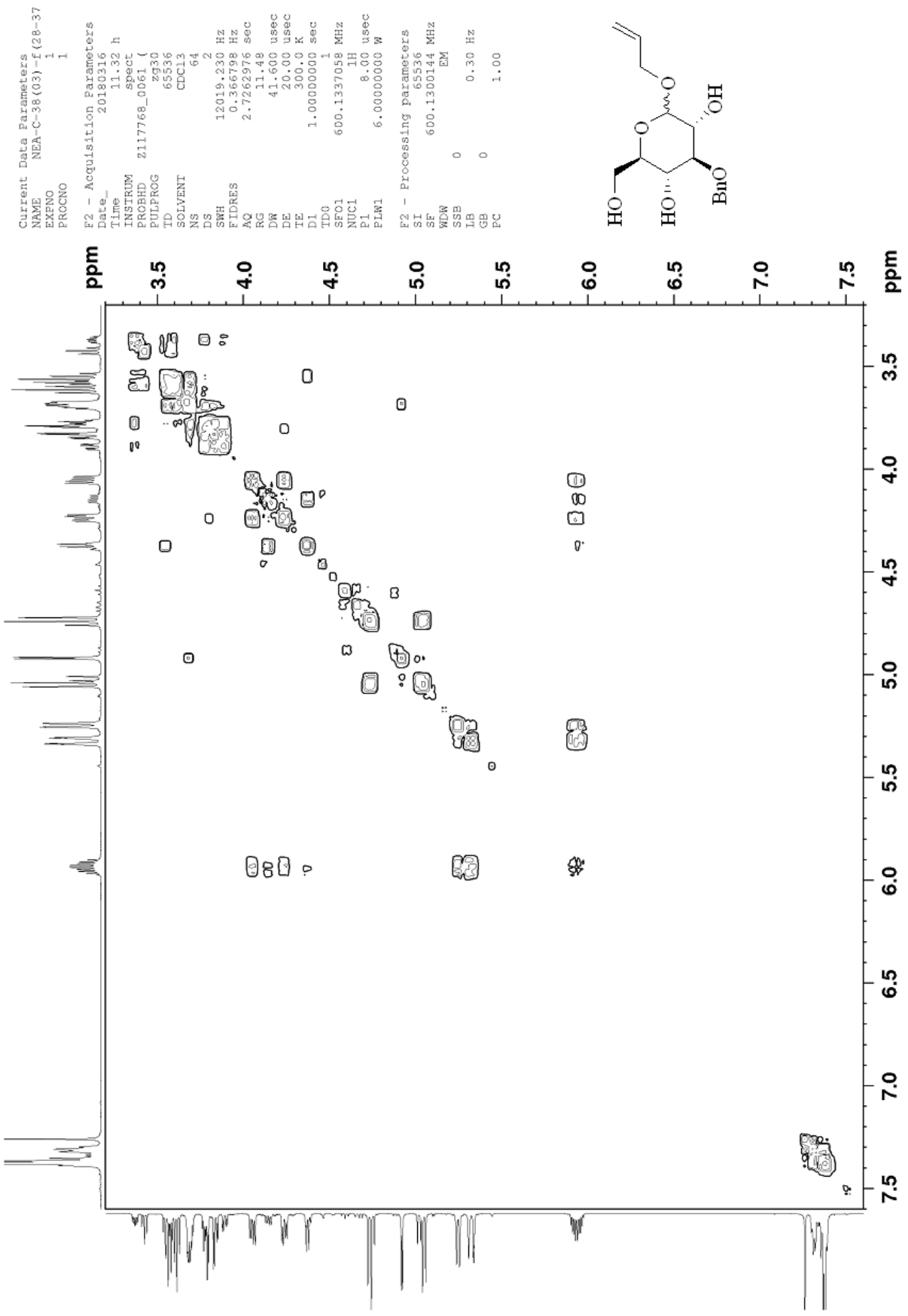

Figure B.5: H,H-COSY spectrum of compound **4**, which is an anomeric mixture.

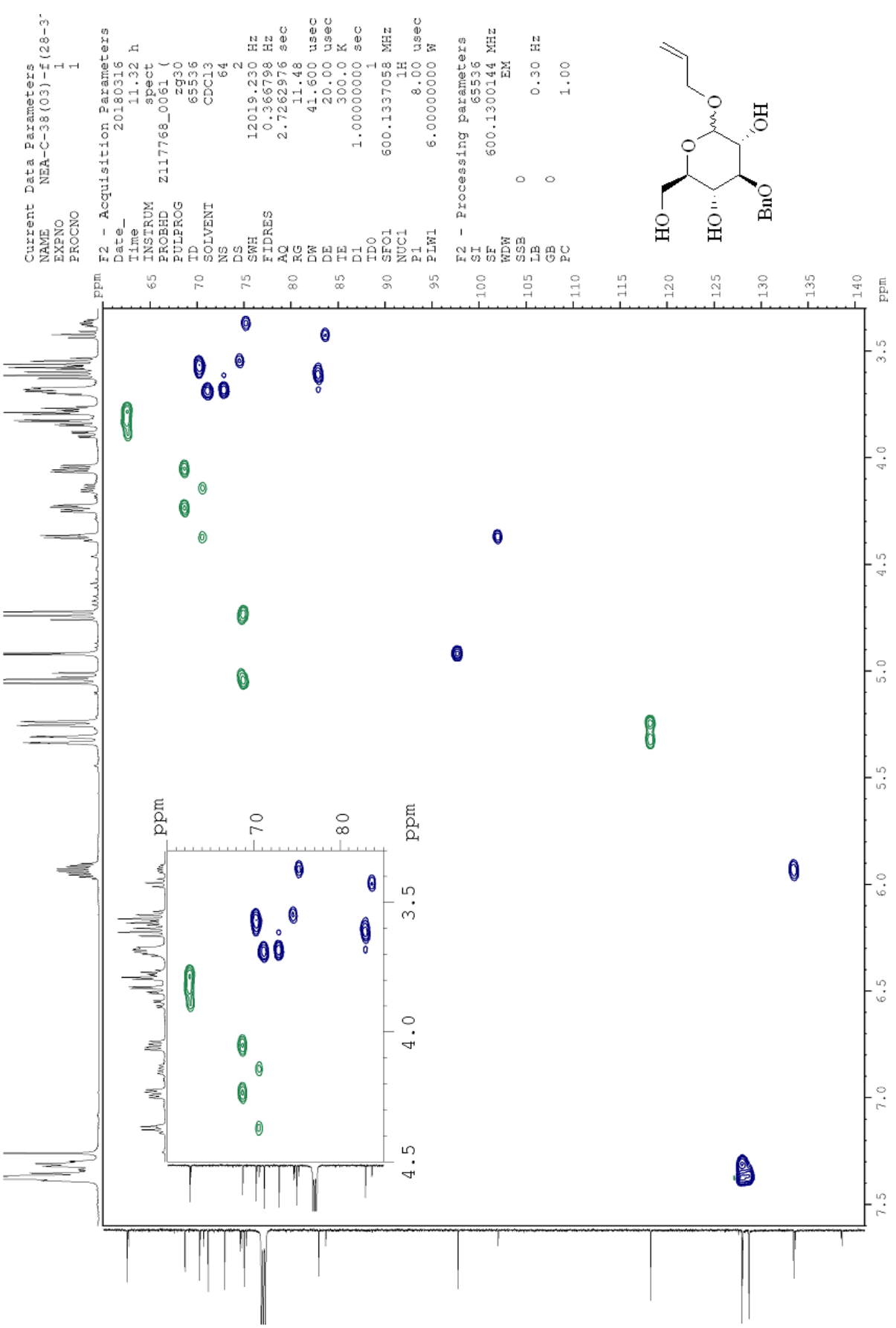

Figure B.6: HSQC spectrum of compound **4**, which is an anomeric mixture.

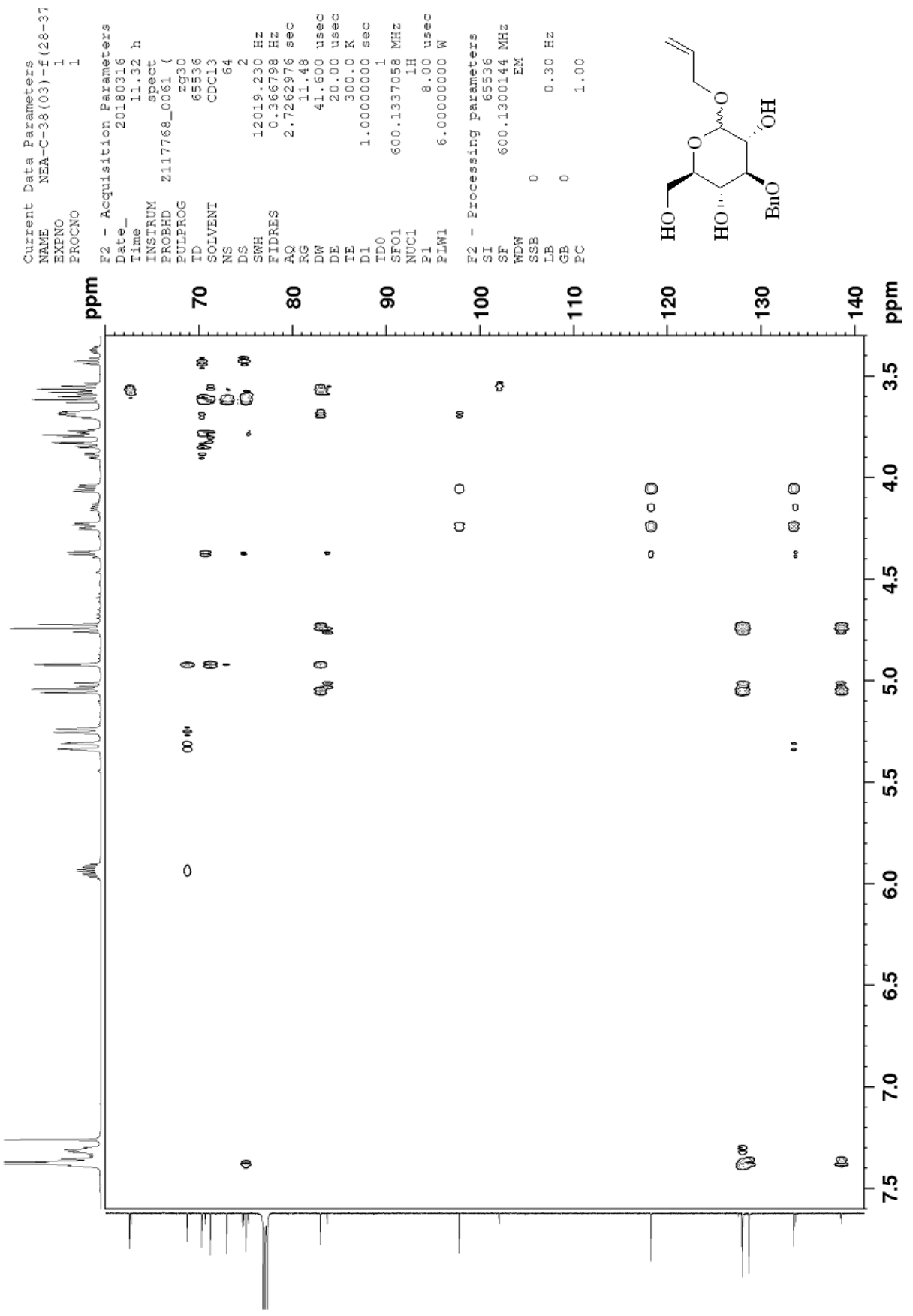

Figure B.7: HMBC spectrum of compound **4**, which is an anomeric mixture.

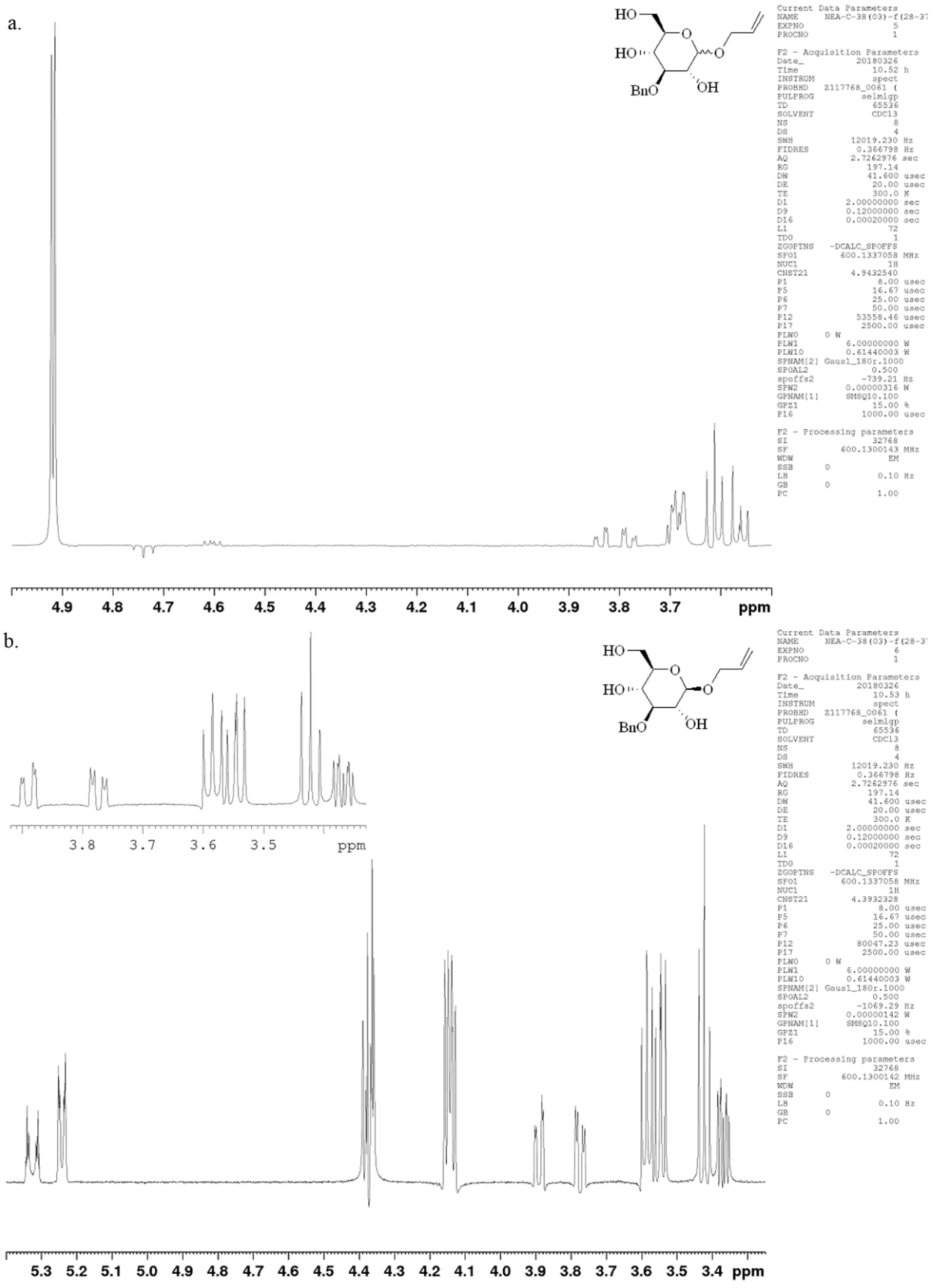

Figure B.8: 1D TOCSY spectra of compound **4**, selectively irradiating a. H_{α}-1; b. H_{β}-1.

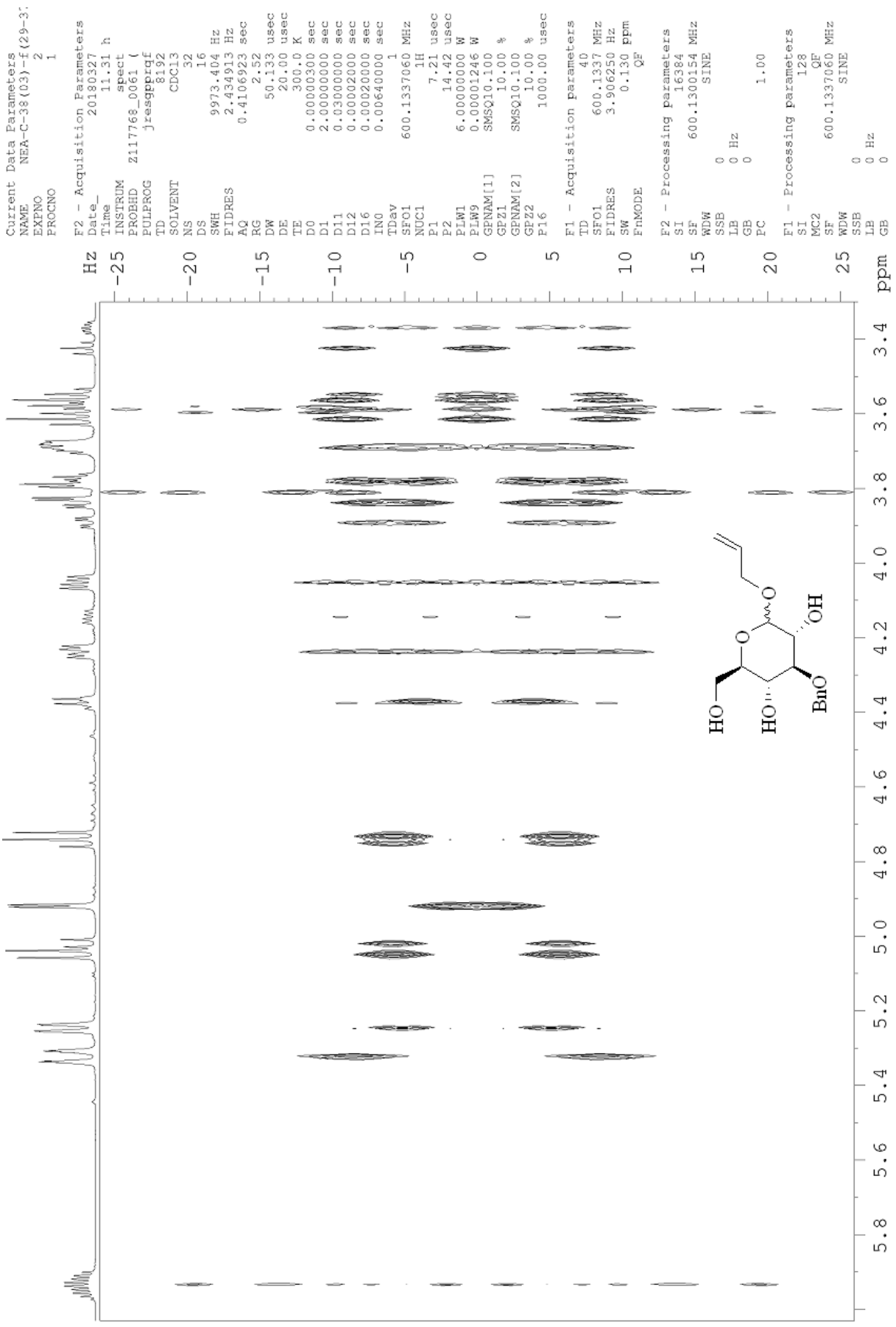

Figure B.9: JRES spectrum of compound **4**, which is an anomeric mixture.

C Spectroscopic Data – Compound 5

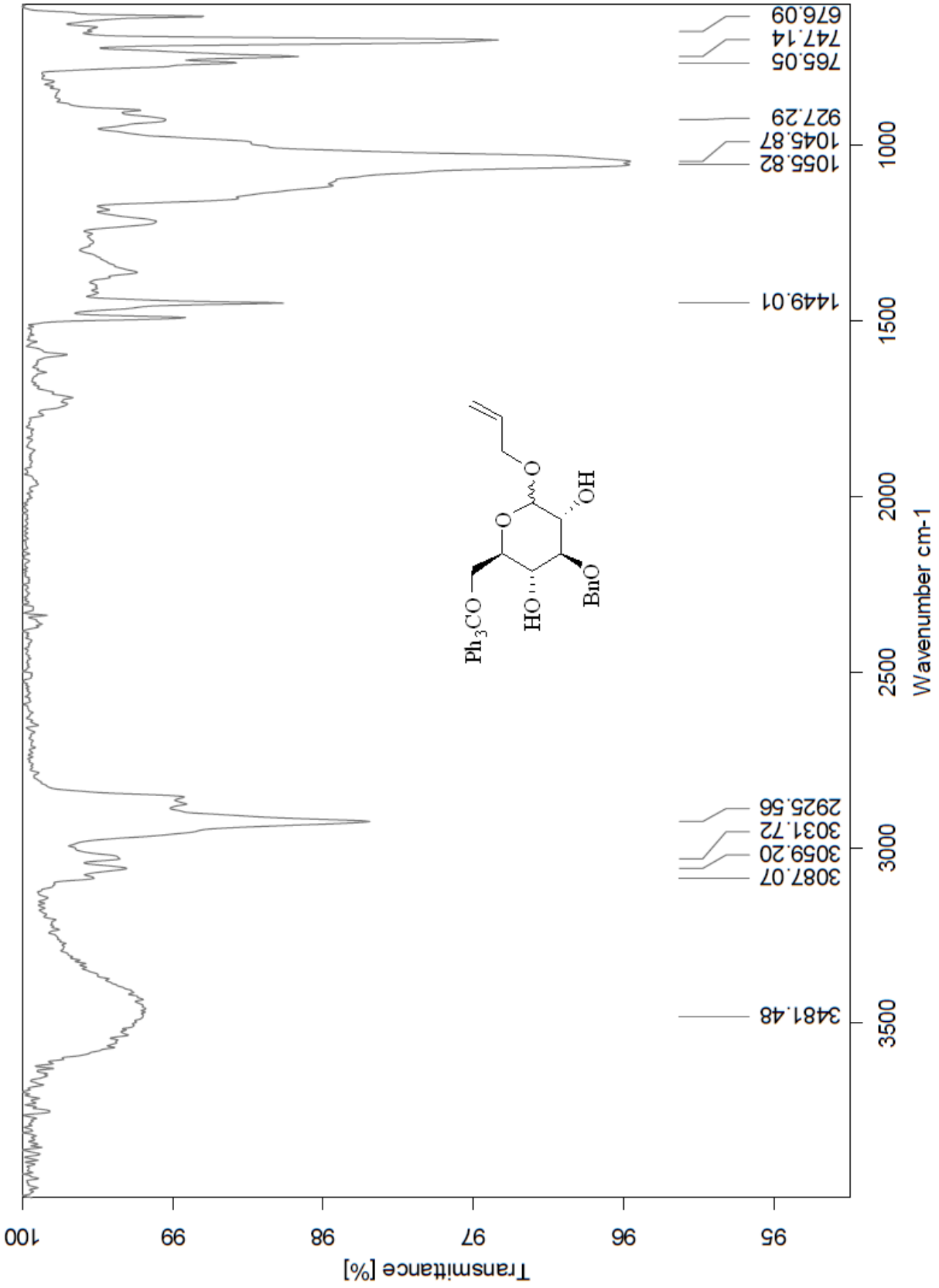

Figure C.1: IR spectrum of compound **5**, which is an anomeric mixture.

Single Mass Analysis
Tolerance = 3.0 PPM / DBE: min = -1.5, max = 50.0
Element prediction: Off
Number of isotope peaks used for i-FIT = 3

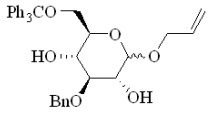

Monoisotopic Mass, Even Electron Ions
1226 formula(e) evaluated with 8 results within limits (all results (up to 1000) for each mass)
Elements Used:
C: 0-500 H: 0-1000 O: 0-10 Na: 0-1 Si: 0-4 I: 0-1

2018-133 49 (0.917) AM2 (Ar,35000.0,0.00,0.00); Cm (48:50)
1: TOF MS ES+

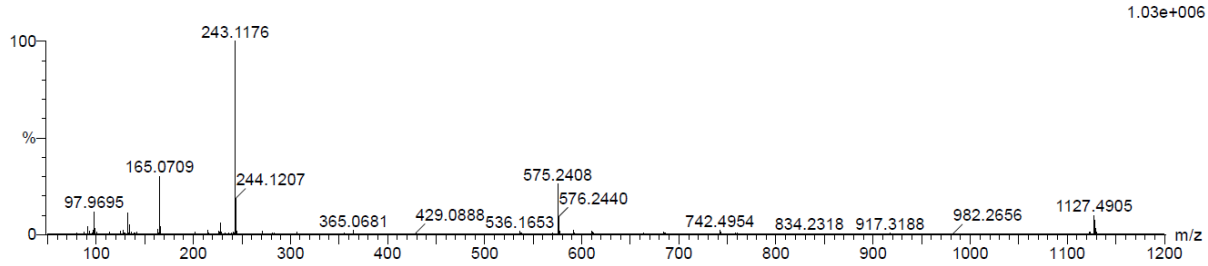

Minimum:				-1.5				
Maximum:		5000.0	3.0	50.0				
Mass	Calc. Mass	mDa	PPM	DBE	i-FIT	Norm	Conf(%)	Formula
575.2408	575.2410	-0.2	-0.3	17.5	787.5	0.001	99.87	C35 H36 O6 Na
	575.2417	-0.9	-1.6	4.5	794.8	7.217	0.07	C27 H48 O3 Si I
	575.2393	1.5	2.6	1.5	795.2	7.617	0.05	C25 H49 O3 Na Si I
	575.2406	0.2	0.3	24.5	797.7	10.196	0.00	C40 H35 O2 Si
	575.2414	-0.6	-1.0	16.5	800.6	13.072	0.00	C34 H40 O3 Na Si2
	575.2421	-1.3	-2.3	3.5	802.1	14.521	0.00	C26 H52 Si3 I
	575.2397	1.1	1.9	0.5	802.5	14.962	0.00	C24 H53 Na Si3 I
	575.2418	-1.0	-1.7	15.5	803.6	16.026	0.00	C33 H44 Na Si4

Figure C.2: HRMS spectrum of compound **5**, which is an anomeric mixture.

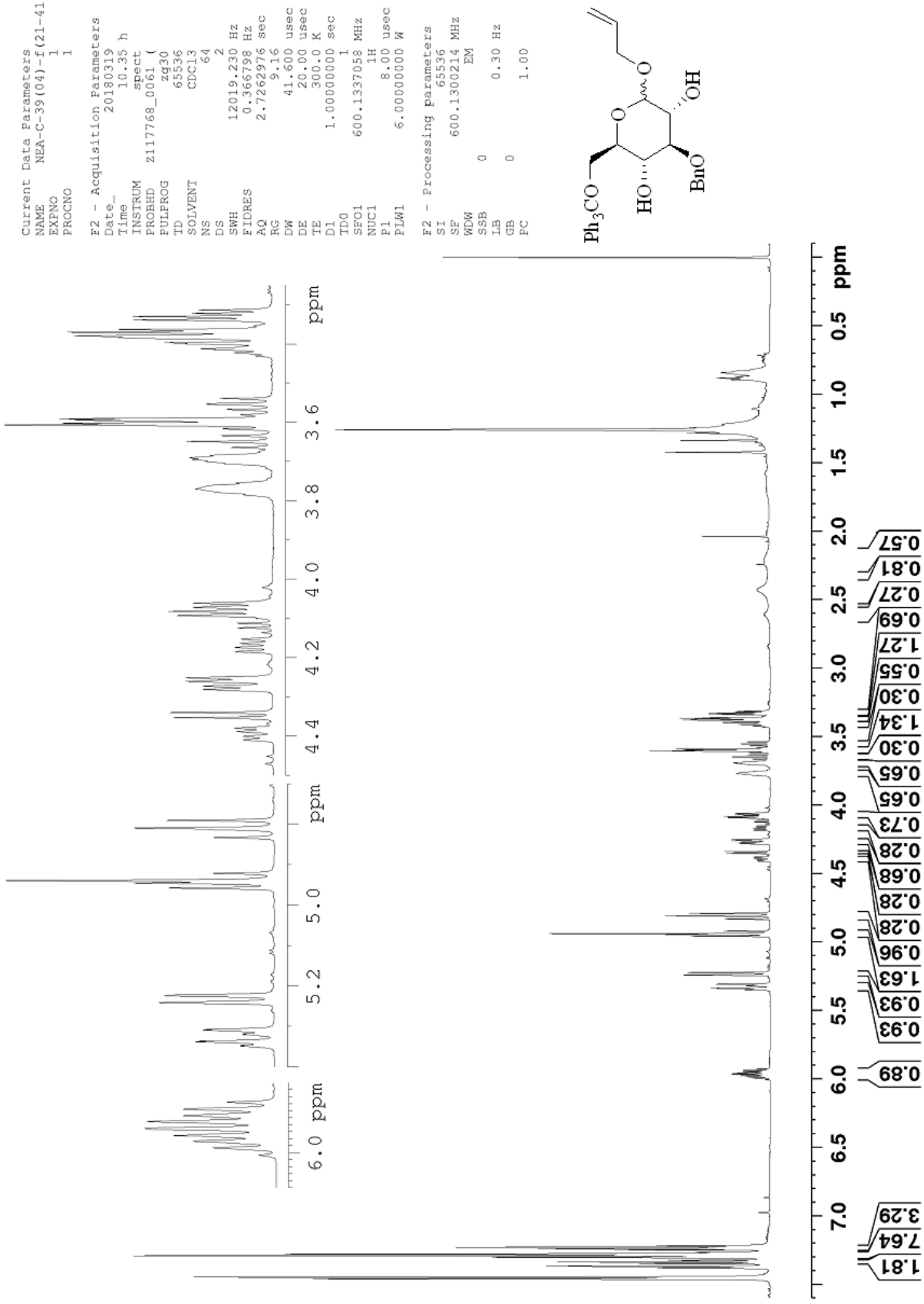

Figure C.3: ^{1}H-NMR spectrum of compound **5**, which is an anomeric mixture.

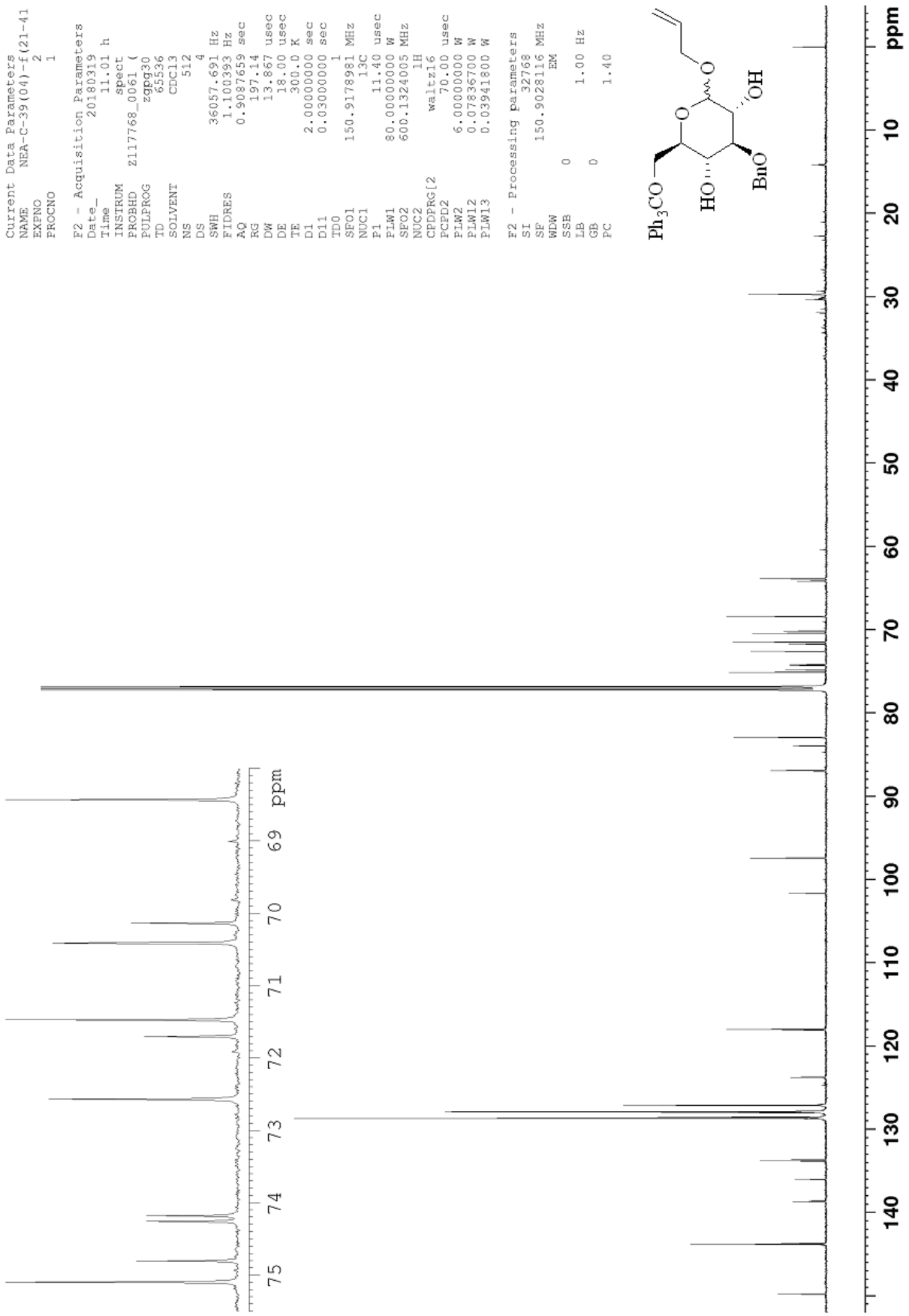

Figure C.4: ^{13}C-NMR spectrum of compound **5**, which is an anomeric mixture.

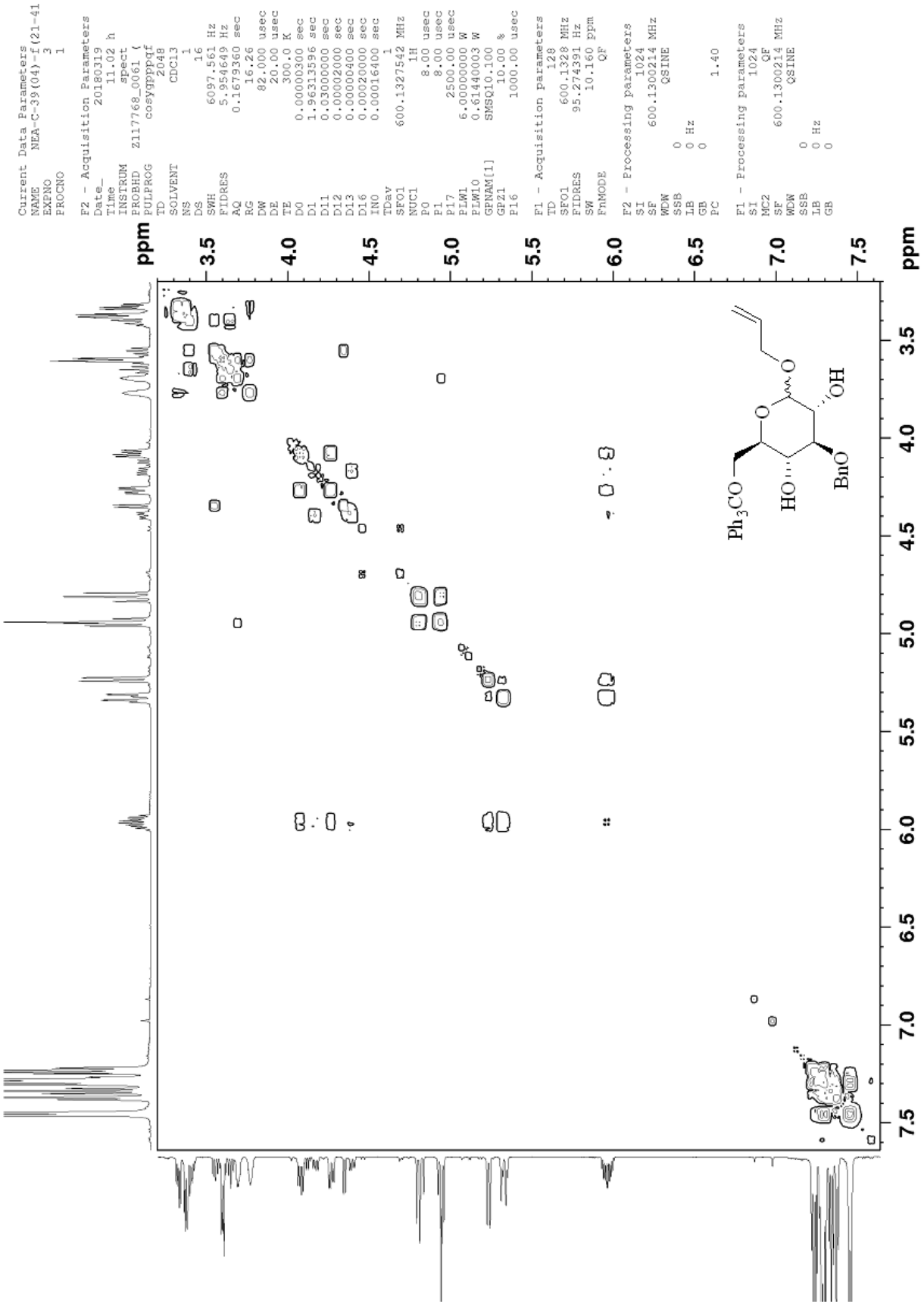

Figure C.5: H,H-COSY spectrum of compound **5**, which is an anomeric mixture.

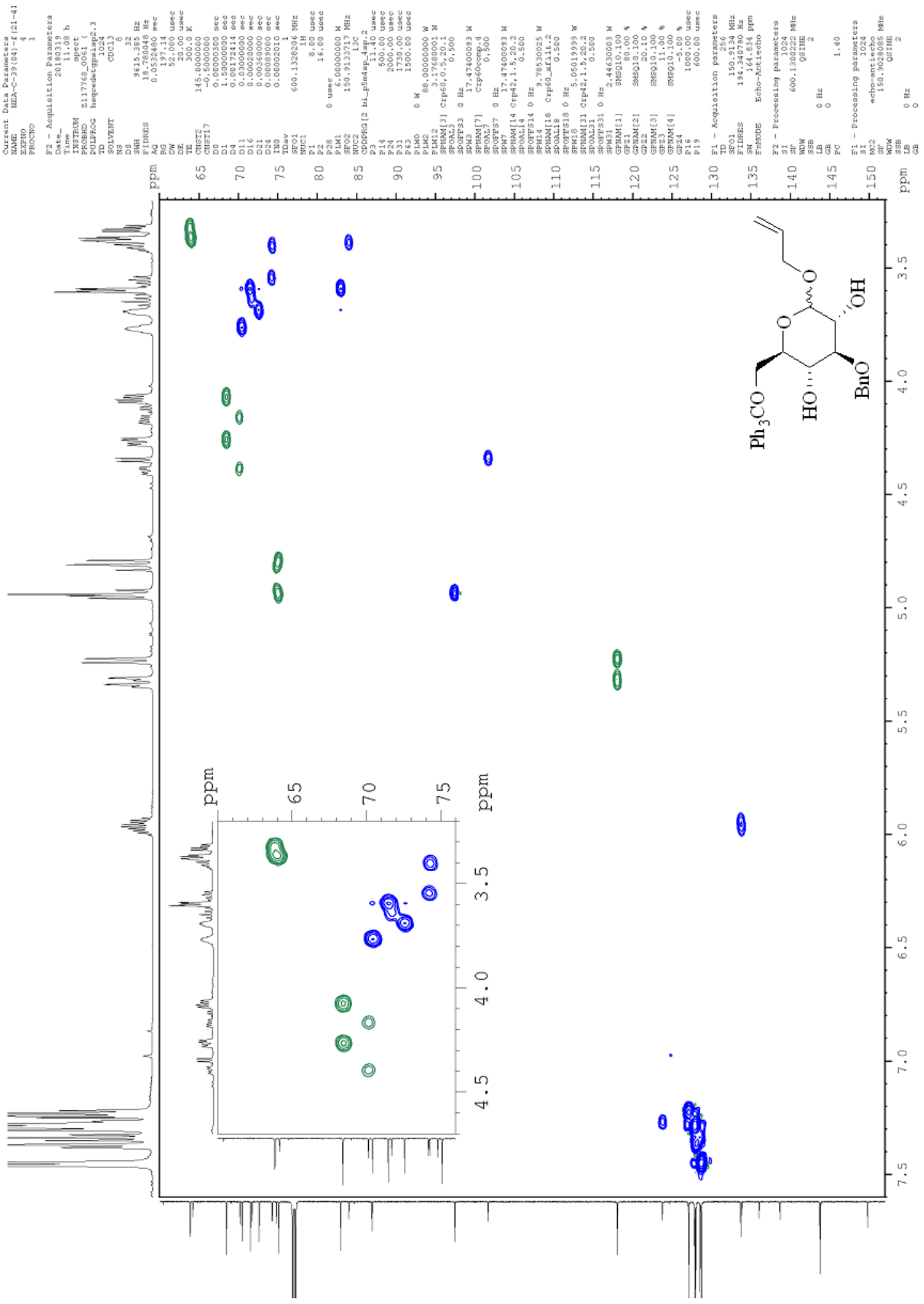

Figure C.6: HSQC spectrum of compound **5**, which is an anomeric mixture.

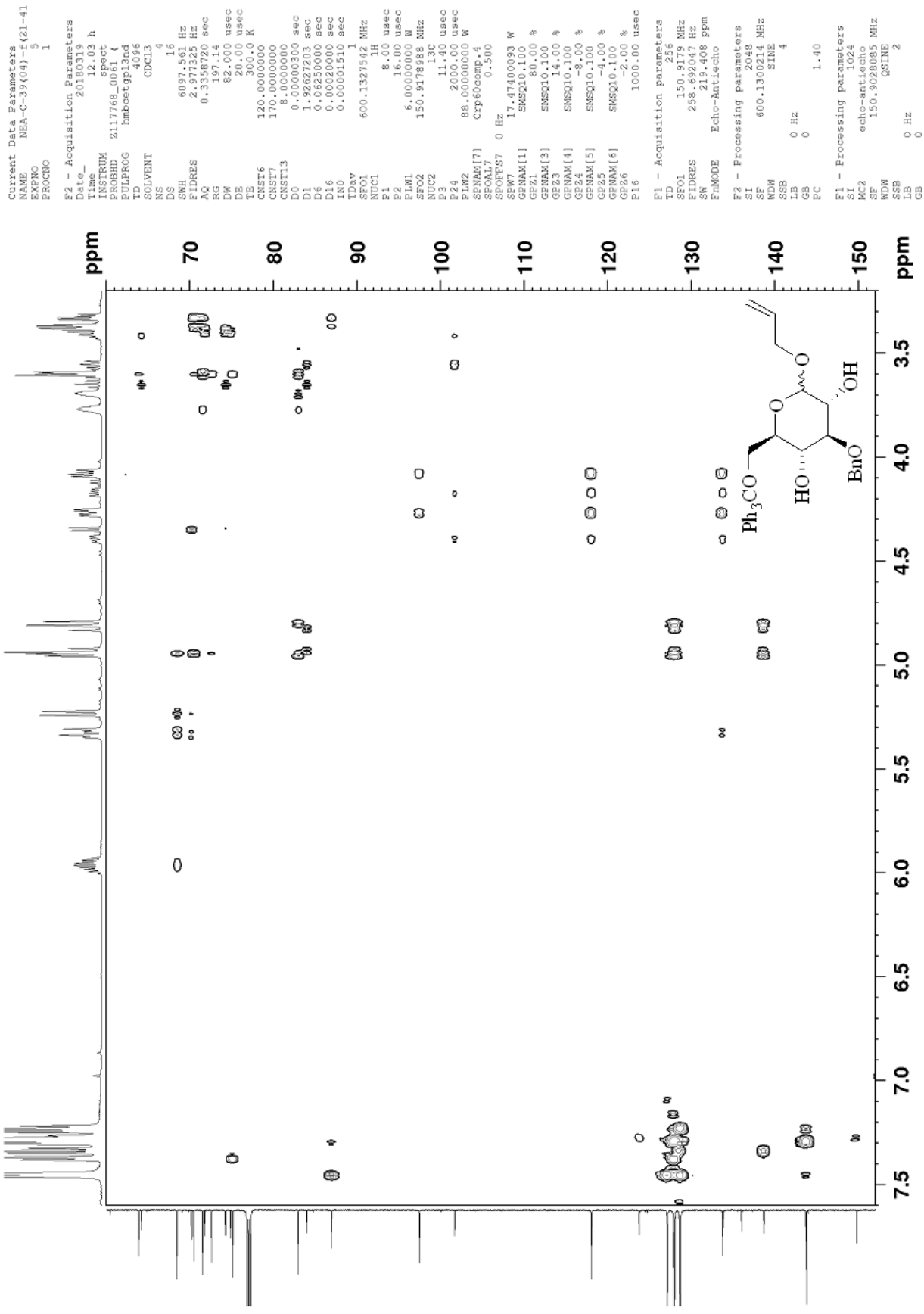

Figure C.7: HMBC spectrum of compound **5**, which is an anomeric mixture.

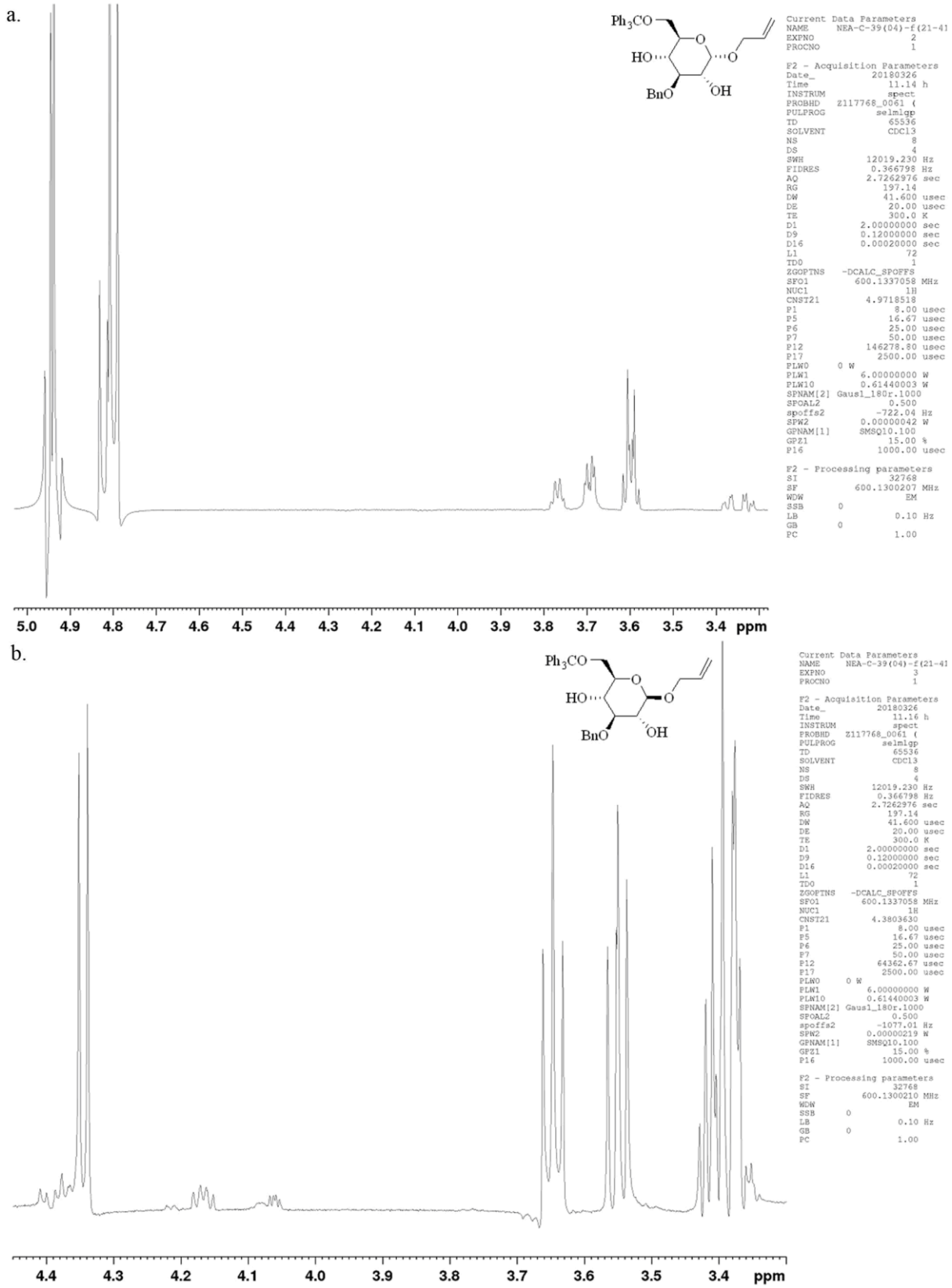

Figure C.8: 1D TOCSY spectra of compound **5**, selectively irradiating a. H_{α}-1; b. H_{β}-1.

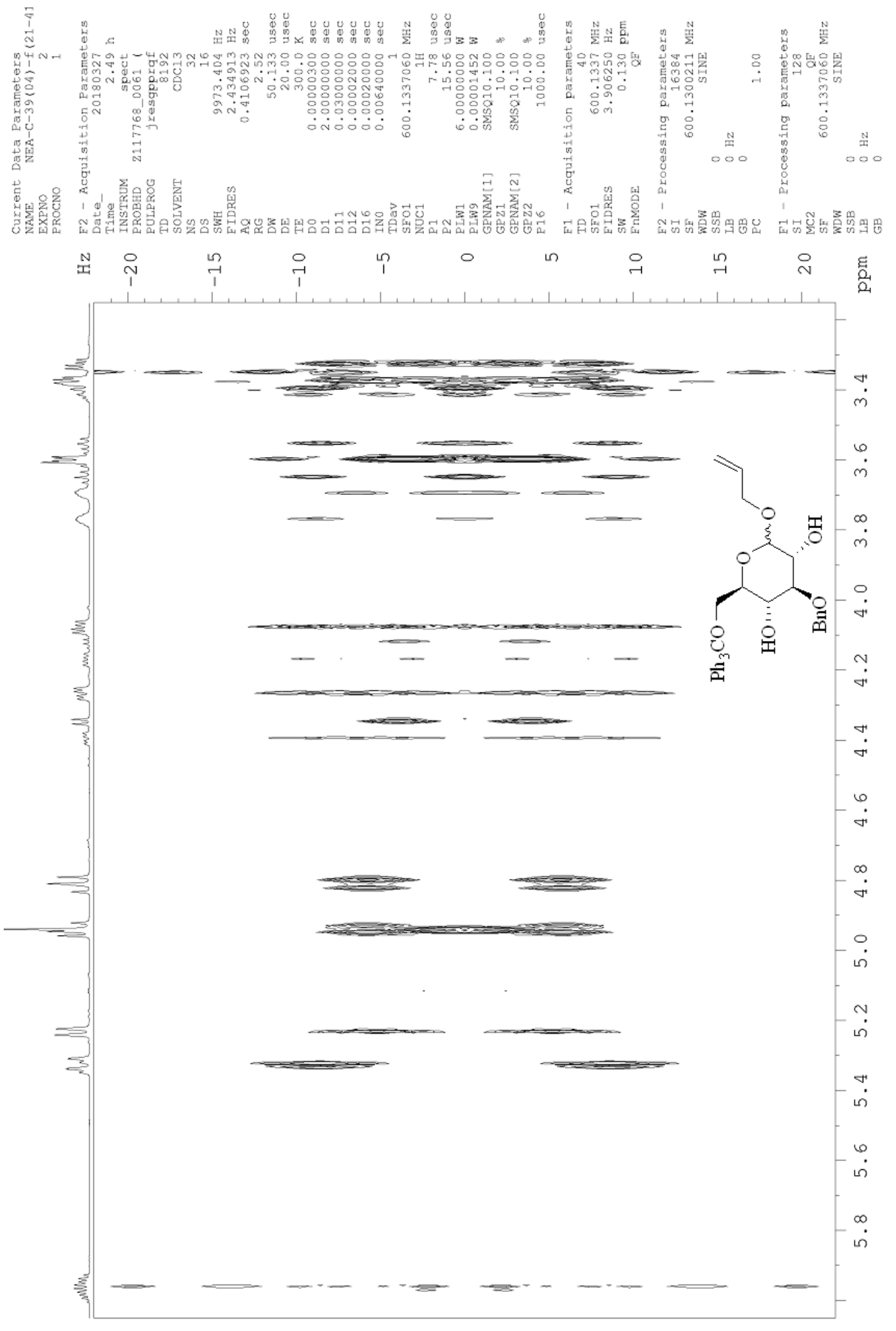

Figure C.9: JRES spectrum of compound **5**, which is an anomeric mixture.

D Spectroscopic Data – Compound 6a

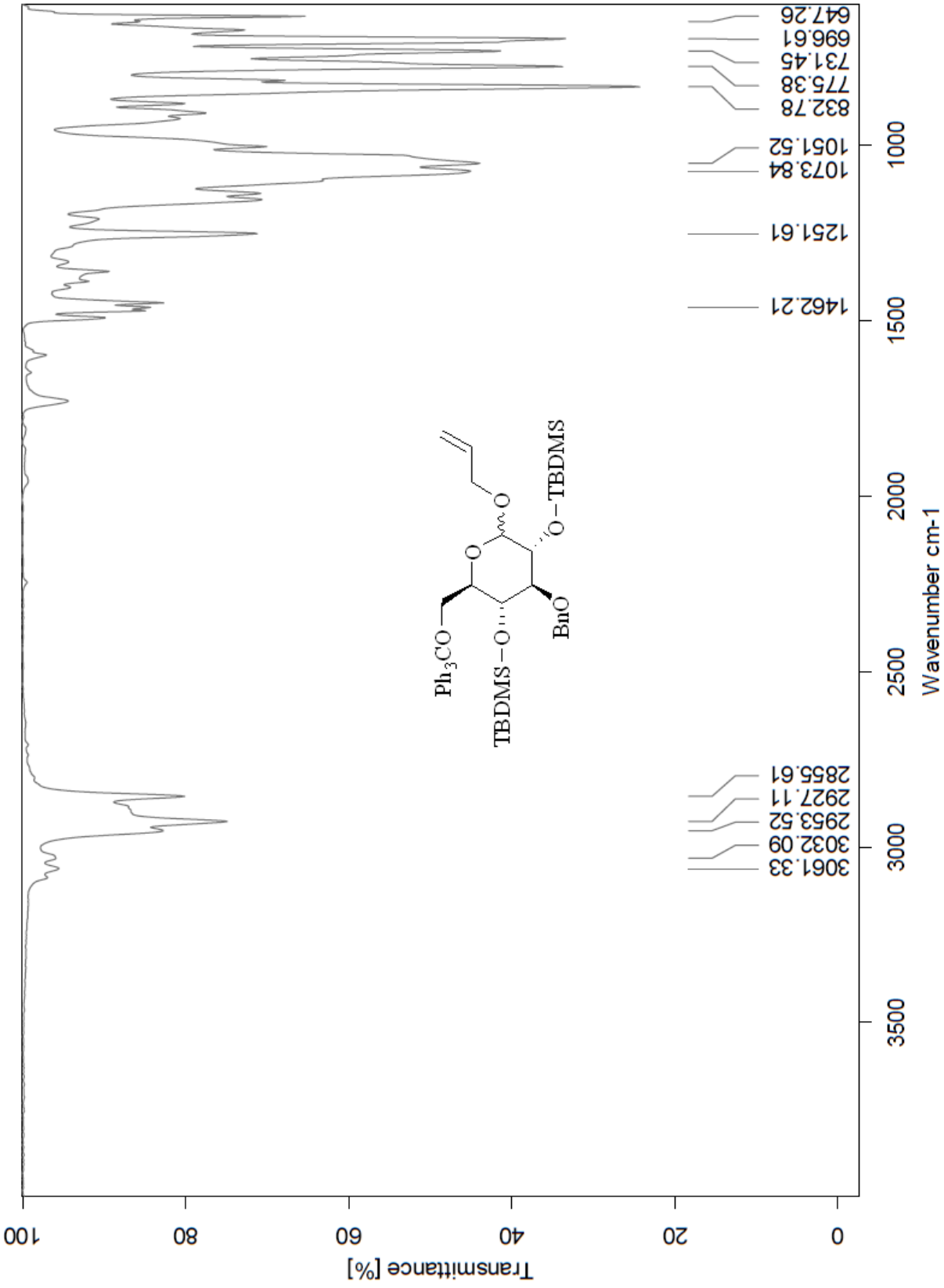

Figure D.1: IR spectrum of compound **6**, which is an anomeric mixture.

Single Mass Analysis
Tolerance = 3.0 PPM / DBE: min = -1.5, max = 50.0
Element prediction: Off
Number of isotope peaks used for i-FIT = 3

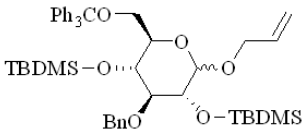

Monoisotopic Mass, Even Electron Ions
56255 formula(e) evaluated with 135 results within limits (all results (up to 1000) for each mass)
Elements Used:
C: 0-500 H: 0-1000 N: 0-100 O: 0-100 Si: 0-3 Na: 0-1

sondre 2017 19 (0.203) AM2 (Ar,35000.0,0.00,0.00); Cm (19:23)
1: TOF MS ES+

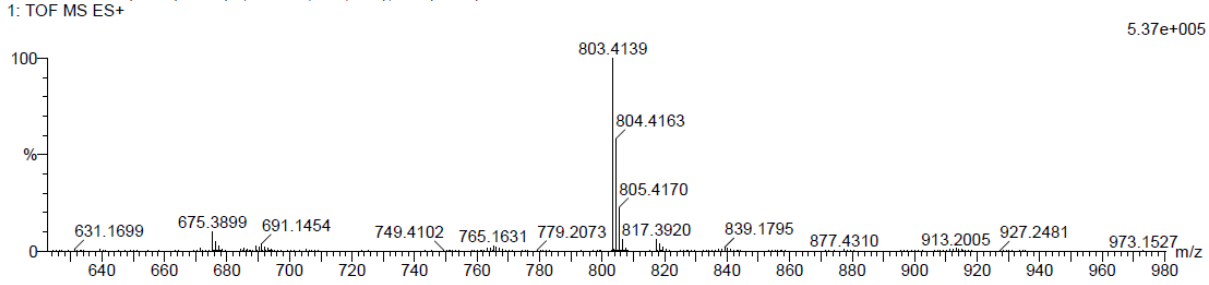

Minimum:				-1.5				
Maximum:		5.0	3.0	50.0				
Mass	Calc. Mass	mDa	PPM	DBE	i-FIT	Norm	Conf(%)	Formula
803.4139	803.4136	0.3	0.4	21.5	674.5	1.747	17.43	C45 H59 N6 O4 Si2
	803.4139	0.0	0.0	17.5	674.9	2.167	11.45	C47 H64 O6 Si2 Na
	803.4132	0.7	0.9	25.5	675.0	2.292	10.10	C53 H59 O5 Si
	803.4123	1.6	2.0	16.5	675.0	2.312	9.91	C44 H63 N2 O8 Si2
	803.4126	1.3	1.6	23.5	675.3	2.576	7.60	C44 H56 N10 Si2 Na
	803.4121	1.8	2.2	27.5	675.4	2.659	7.00	C52 H56 N4 O Si Na
	803.4158	-1.9	-2.4	15.5	676.1	3.330	3.58	C33 H56 N16 O3 Si2 Na
	803.4150	-1.1	-1.4	26.5	676.1	3.344	3.53	C46 H55 N10 Si2
	803.4137	0.2	0.2	18.5	676.3	3.609	2.71	C38 H55 N12 O6 Si
	803.4140	-0.1	-0.1	14.5	676.4	3.693	2.49	C40 H60 N6 O8 Si Na
	803.4155	-1.6	-2.0	19.5	676.4	3.697	2.48	C31 H51 N22 O Si2
	803.4144	-0.5	-0.6	10.5	676.4	3.713	2.44	C32 H60 N12 O7 Si2 Na
	803.4150	-1.1	-1.4	23.5	676.5	3.789	2.26	C39 H51 N16 O2 Si
	803.4155	-1.6	-2.0	8.5	676.9	4.148	1.58	C33 H63 N8 O11 Si2
	803.4141	-0.2	-0.2	3.5	677.0	4.319	1.33	C32 H67 N4 O15 Si2
	803.4152	-1.3	-1.6	22.5	677.1	4.336	1.31	C48 H60 N4 O2 Si2 Na
	803.4153	-1.4	-1.7	19.5	677.1	4.341	1.30	C41 H56 N10 O4 Si Na

Figure D.2: HRMS spectrum of compound **6**, which is an anomeric mixture.

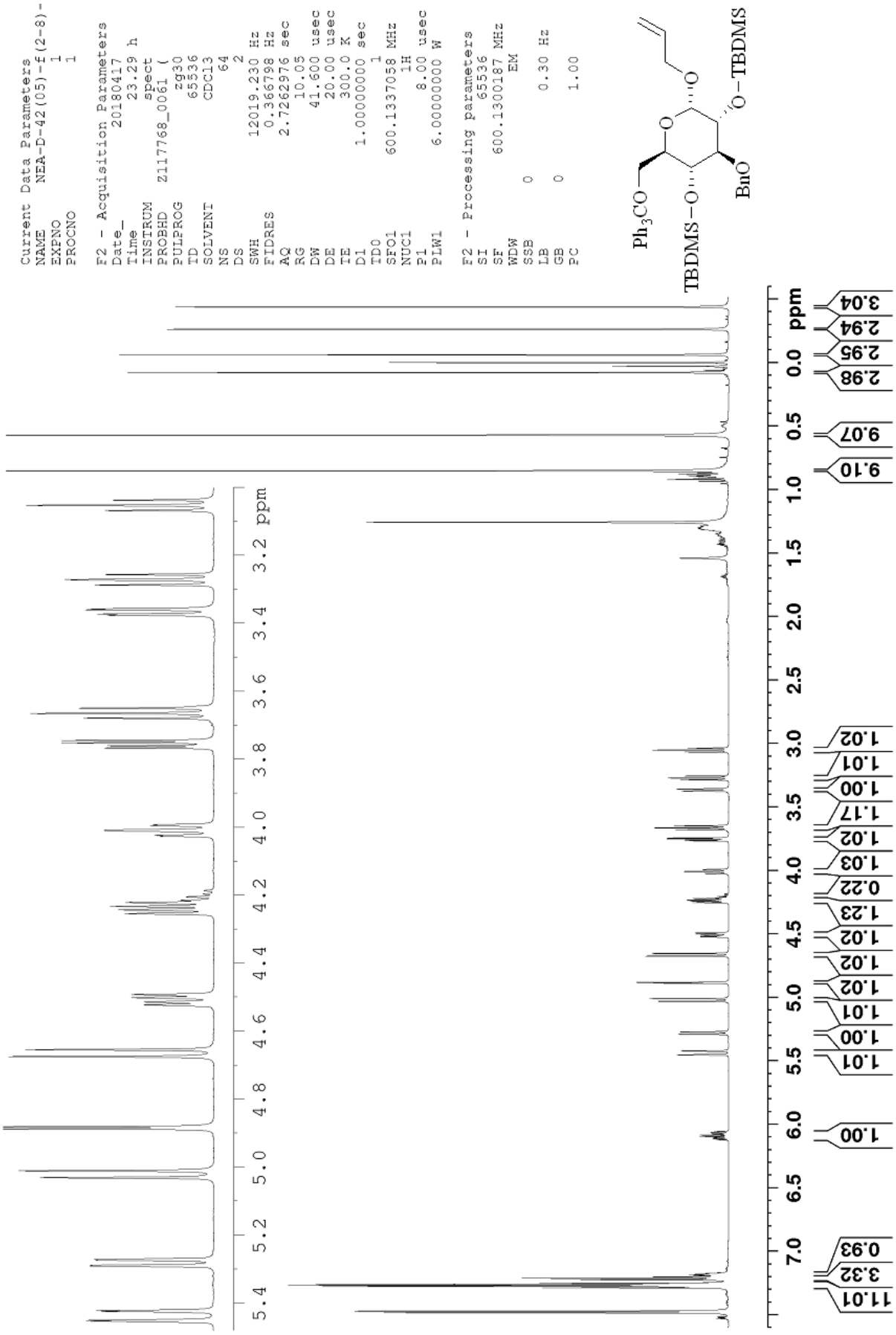

Figure D.3: ^{1}H-NMR spectrum of compound **6a**.

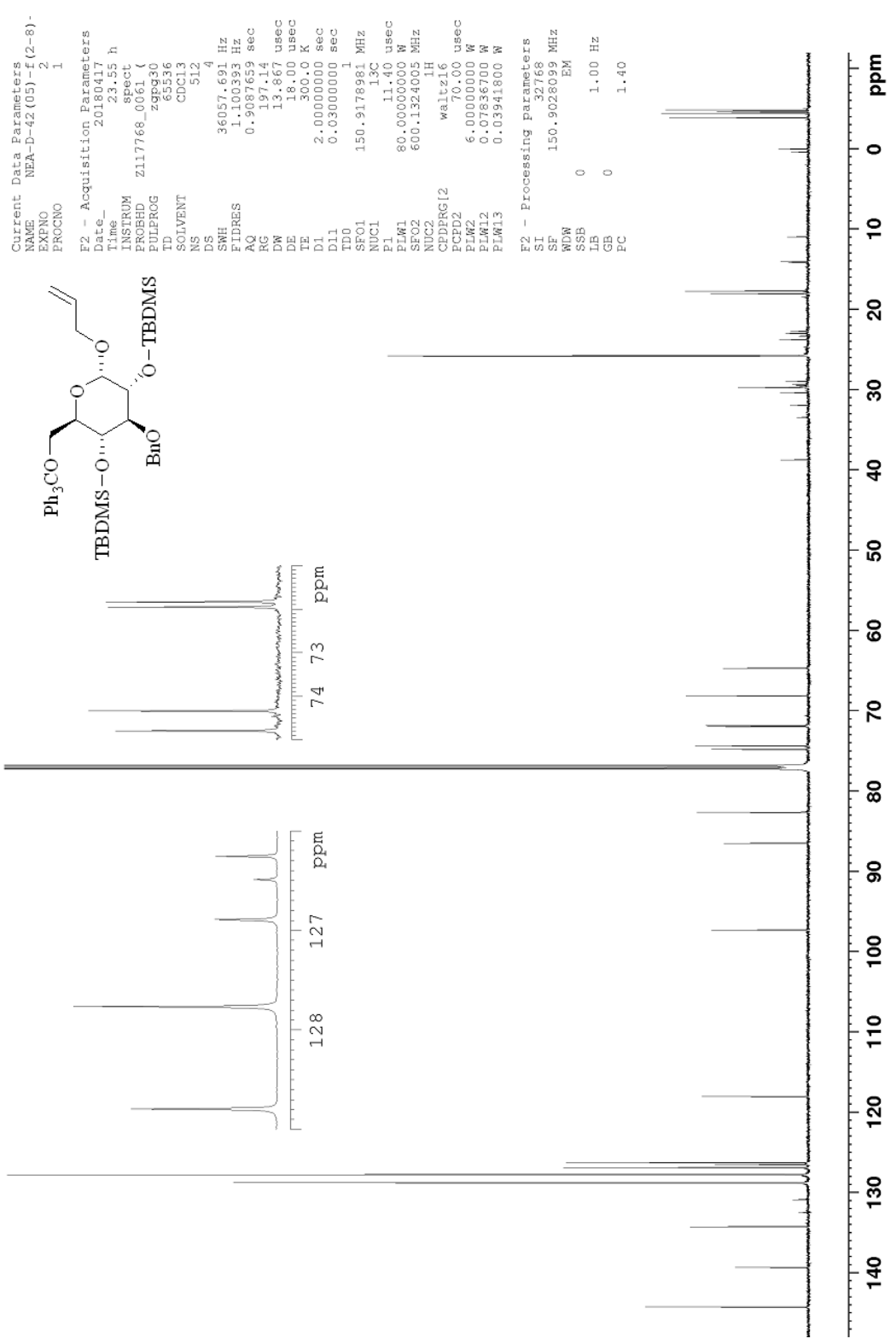

Figure D.4: ^{13}C-NMR spectrum of compound **6a**.

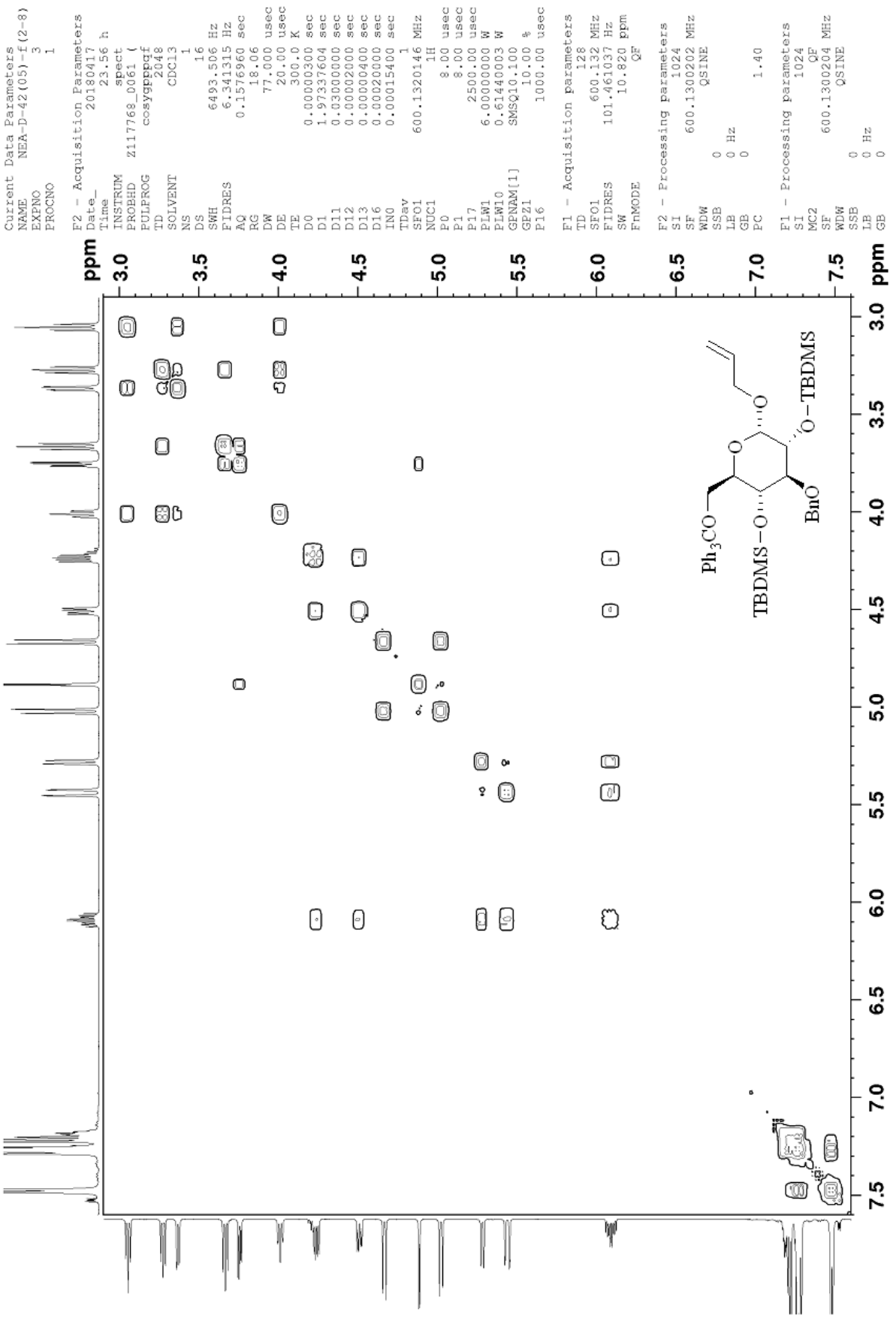

Figure D.5: H,H-COSY spectrum of compound **6a**.

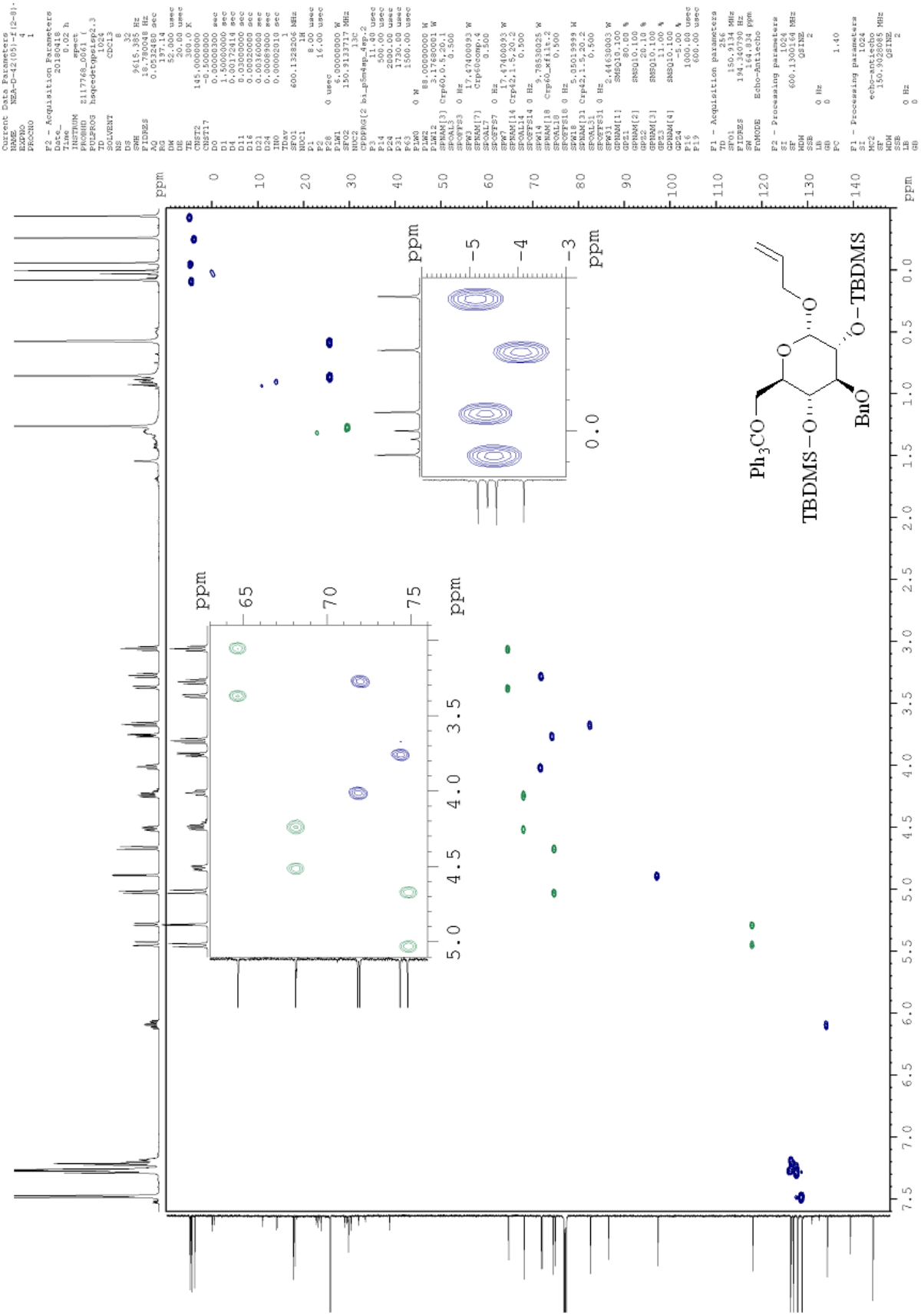

Figure D.6: HSQC spectrum of compound **6a**.

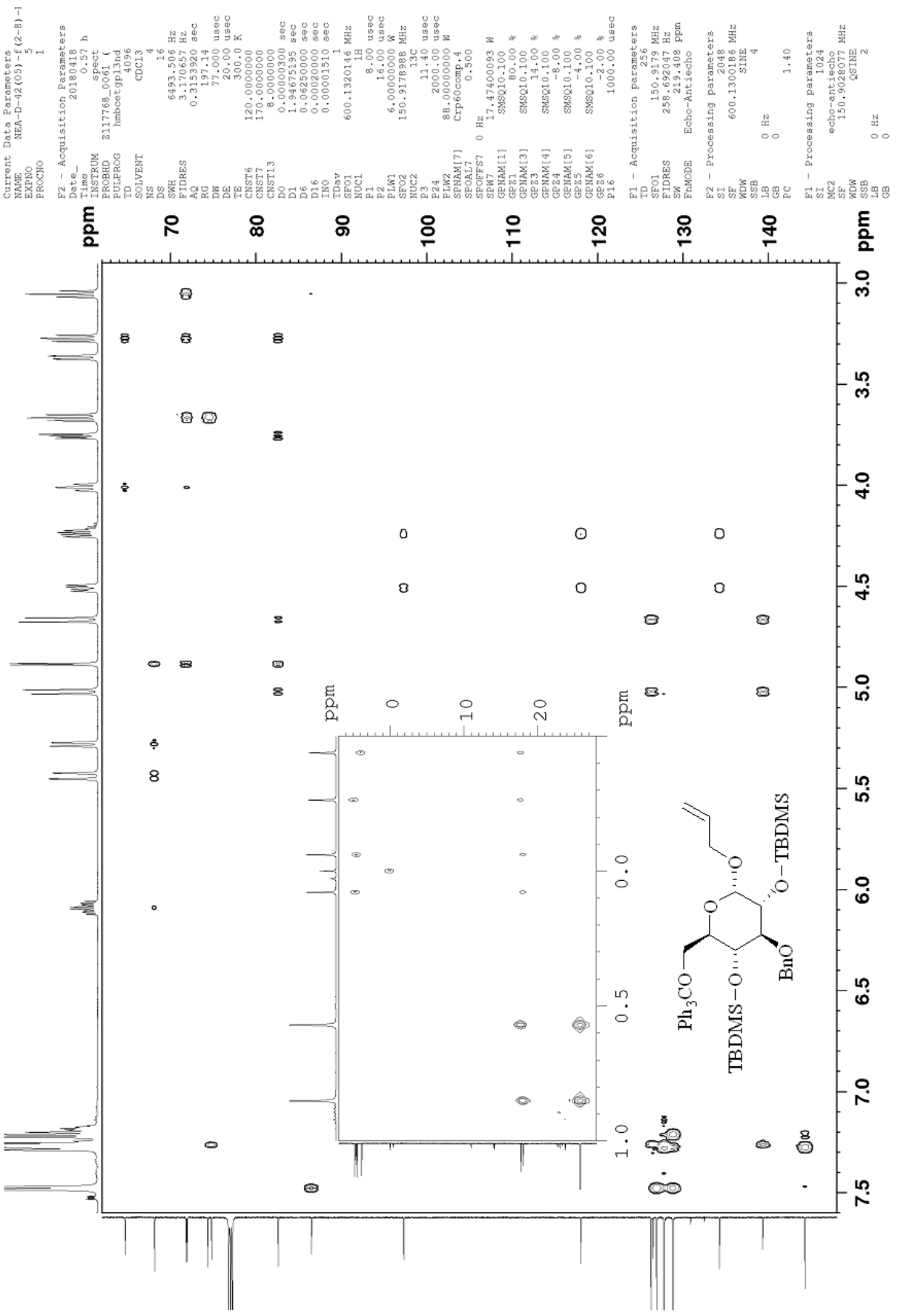

Figure D.7: HMBC spectrum of compound **6a**.

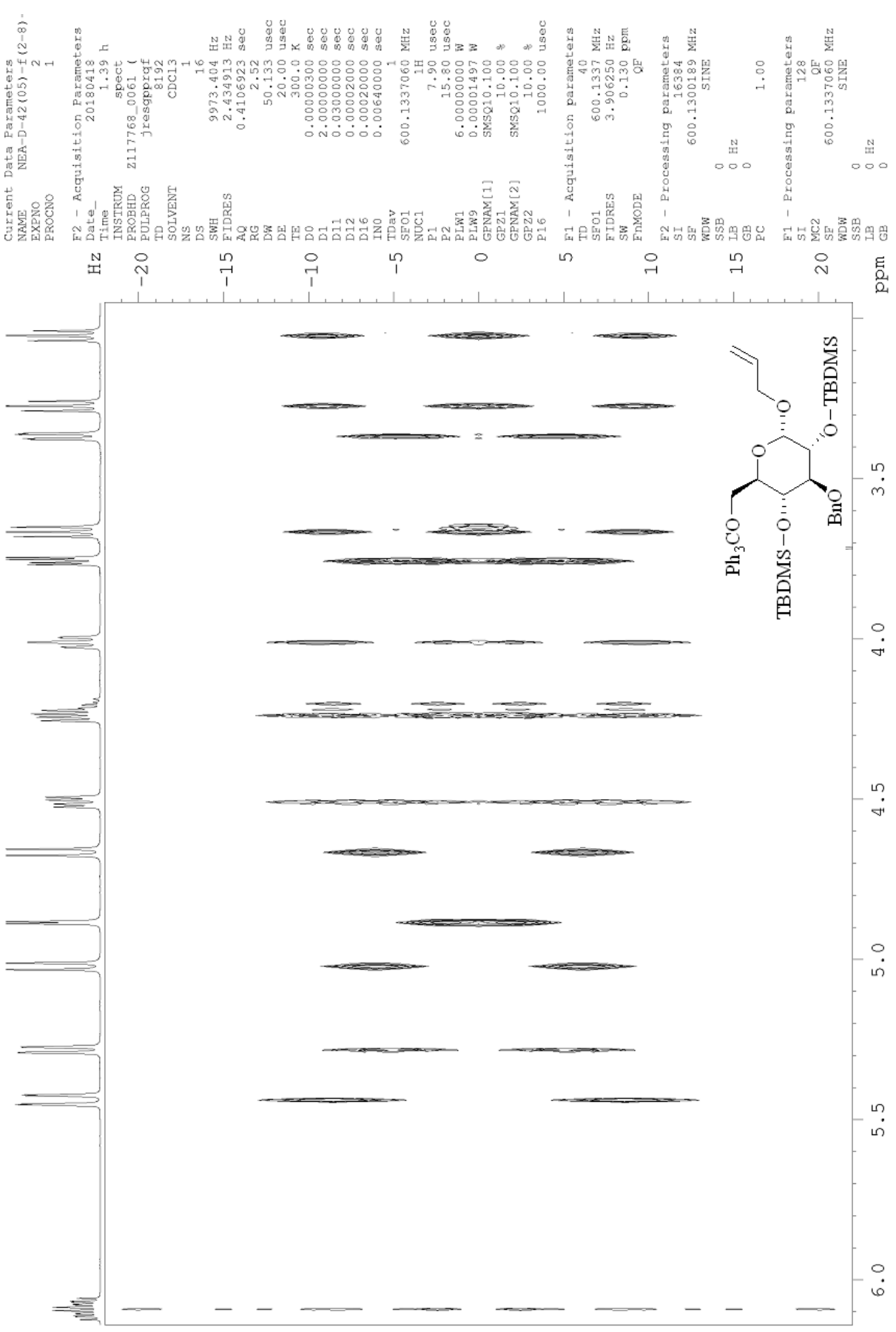

Figure D.8: JRES spectrum of compound **6a**.

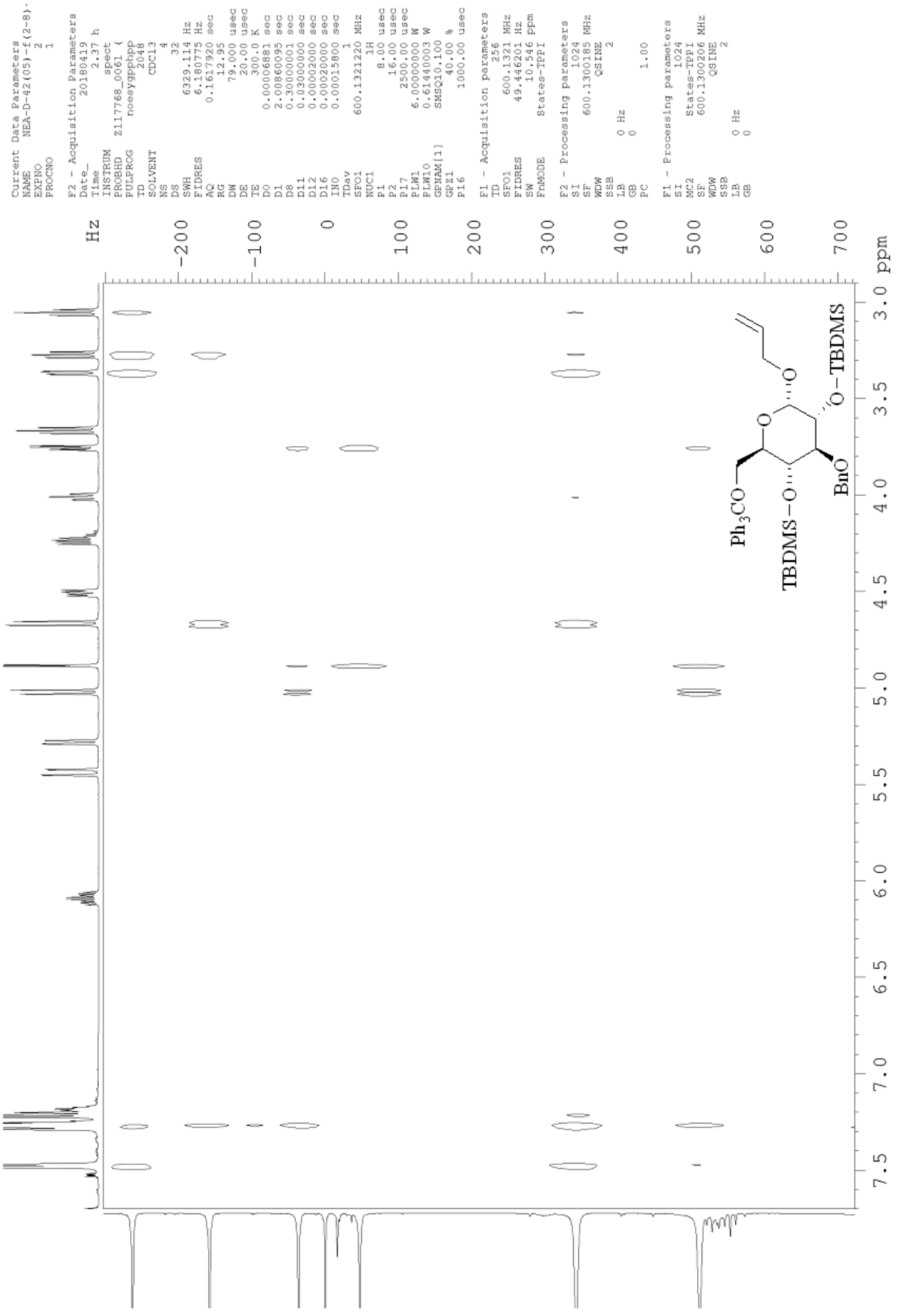

Figure D.9: NOESY spectrum of silyl alkyl protons of compound **6a**.

E Spectroscopic Data – Compound 6b

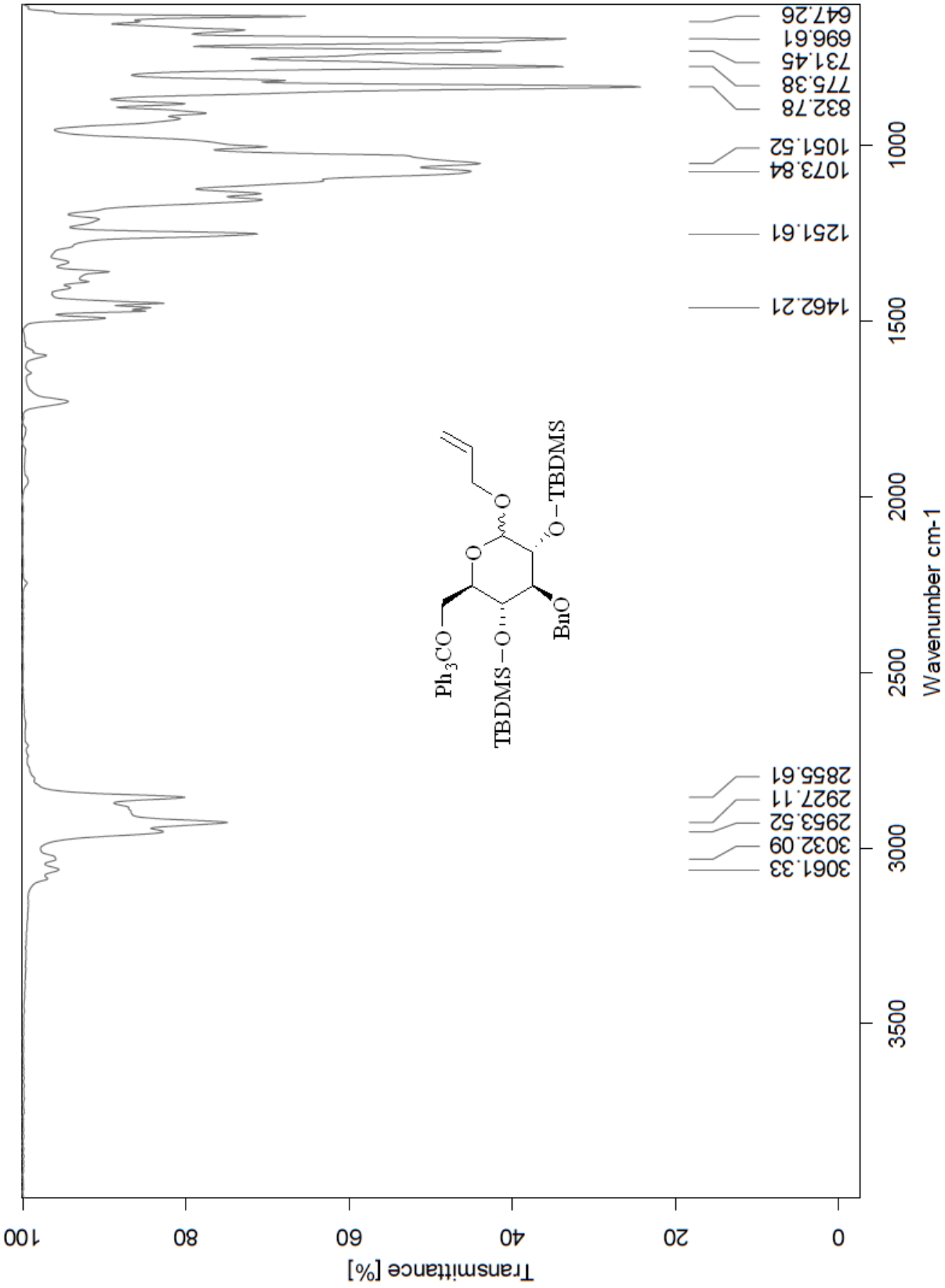

Figure E.1: IR spectrum of compound **6**, which is an anomeric mixture.

Single Mass Analysis
Tolerance = 3.0 PPM / DBE: min = -1.5, max = 50.0
Element prediction: Off
Number of isotope peaks used for i-FIT = 3

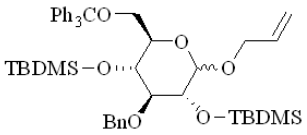

Monoisotopic Mass, Even Electron Ions
56255 formula(e) evaluated with 135 results within limits (all results (up to 1000) for each mass)
Elements Used:
C: 0-500 H: 0-1000 N: 0-100 O: 0-100 Si: 0-3 Na: 0-1

sondre 2017 19 (0.203) AM2 (Ar,35000.0,0.00,0.00); Cm (19:23)
1: TOF MS ES+

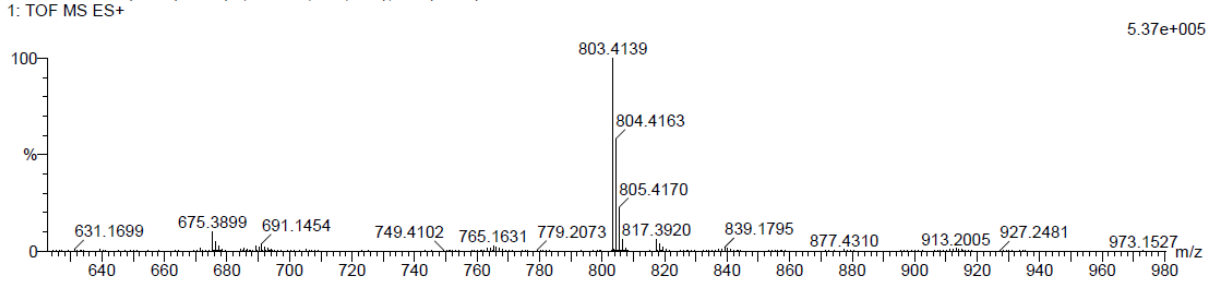

Minimum:				-1.5				
Maximum:		5.0	3.0	50.0				
Mass	Calc. Mass	mDa	PPM	DBE	i-FIT	Norm	Conf(%)	Formula
803.4139	803.4136	0.3	0.4	21.5	674.5	1.747	17.43	C45 H59 N6 O4 Si2
	803.4139	0.0	0.0	17.5	674.9	2.167	11.45	C47 H64 O6 Si2 Na
	803.4132	0.7	0.9	25.5	675.0	2.292	10.10	C53 H59 O5 Si
	803.4123	1.6	2.0	16.5	675.0	2.312	9.91	C44 H63 N2 O8 Si2
	803.4126	1.3	1.6	23.5	675.3	2.576	7.60	C44 H56 N10 Si2 Na
	803.4121	1.8	2.2	27.5	675.4	2.659	7.00	C52 H56 N4 O Si Na
	803.4158	-1.9	-2.4	15.5	676.1	3.330	3.58	C33 H56 N16 O3 Si2 Na
	803.4150	-1.1	-1.4	26.5	676.1	3.344	3.53	C46 H55 N10 Si2
	803.4137	0.2	0.2	18.5	676.3	3.609	2.71	C38 H55 N12 O6 Si
	803.4140	-0.1	-0.1	14.5	676.4	3.693	2.49	C40 H60 N6 O8 Si Na
	803.4155	-1.6	-2.0	19.5	676.4	3.697	2.48	C31 H51 N22 O Si2
	803.4144	-0.5	-0.6	10.5	676.4	3.713	2.44	C32 H60 N12 O7 Si2 Na
	803.4150	-1.1	-1.4	23.5	676.5	3.789	2.26	C39 H51 N16 O2 Si
	803.4155	-1.6	-2.0	8.5	676.9	4.148	1.58	C33 H63 N8 O11 Si2
	803.4141	-0.2	-0.2	3.5	677.0	4.319	1.33	C32 H67 N4 O15 Si2
	803.4152	-1.3	-1.6	22.5	677.1	4.336	1.31	C48 H60 N4 O2 Si2 Na
	803.4153	-1.4	-1.7	19.5	677.1	4.341	1.30	C41 H56 N10 O4 Si Na

Figure E.2: HRMS spectrum of compound **6**, which is an anomeric mixture.

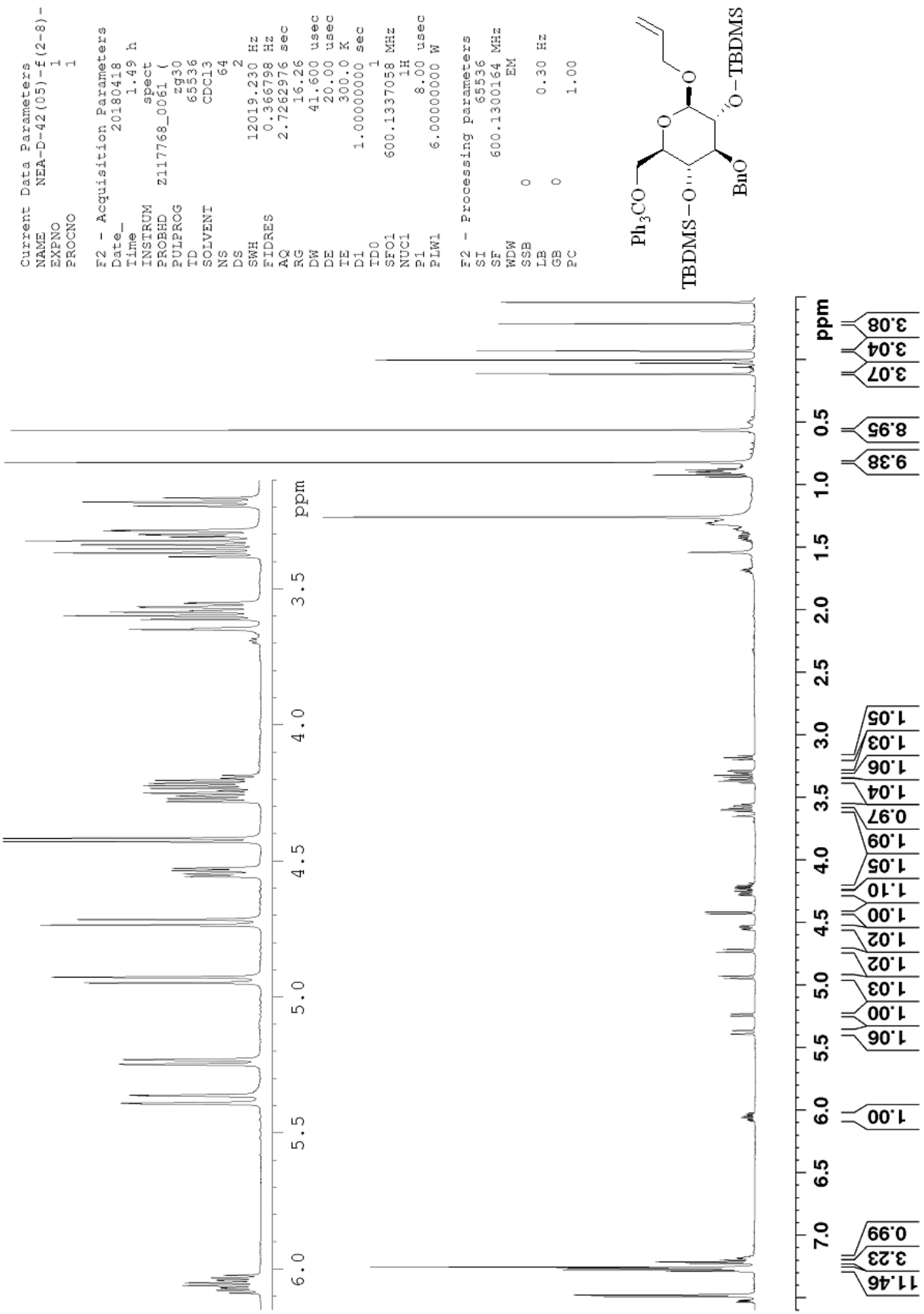

Figure E.3: ^{1}H-NMR spectrum of compound **6b**.

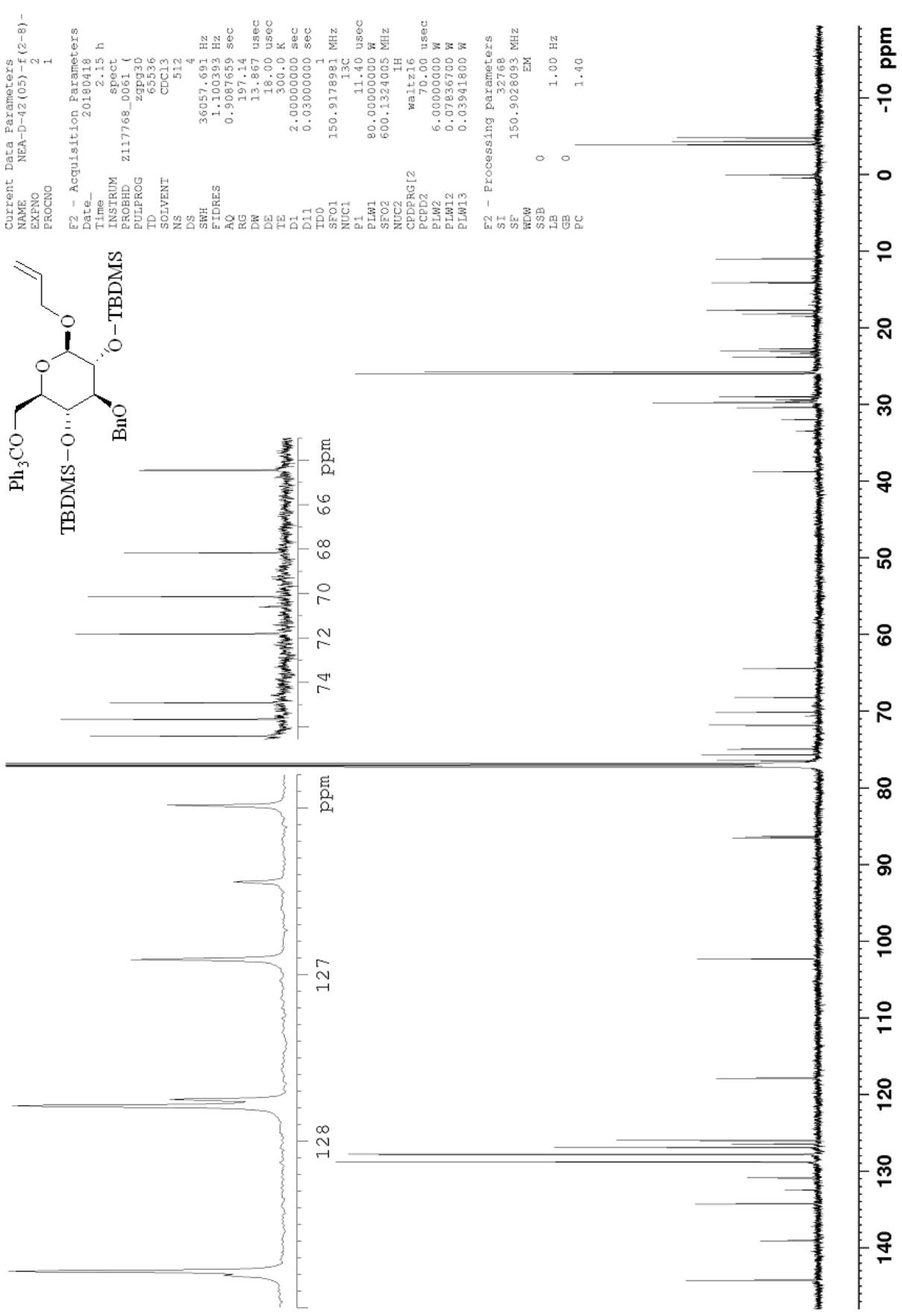

Figure E.4: ^{13}C-NMR spectrum of compound **6b**.

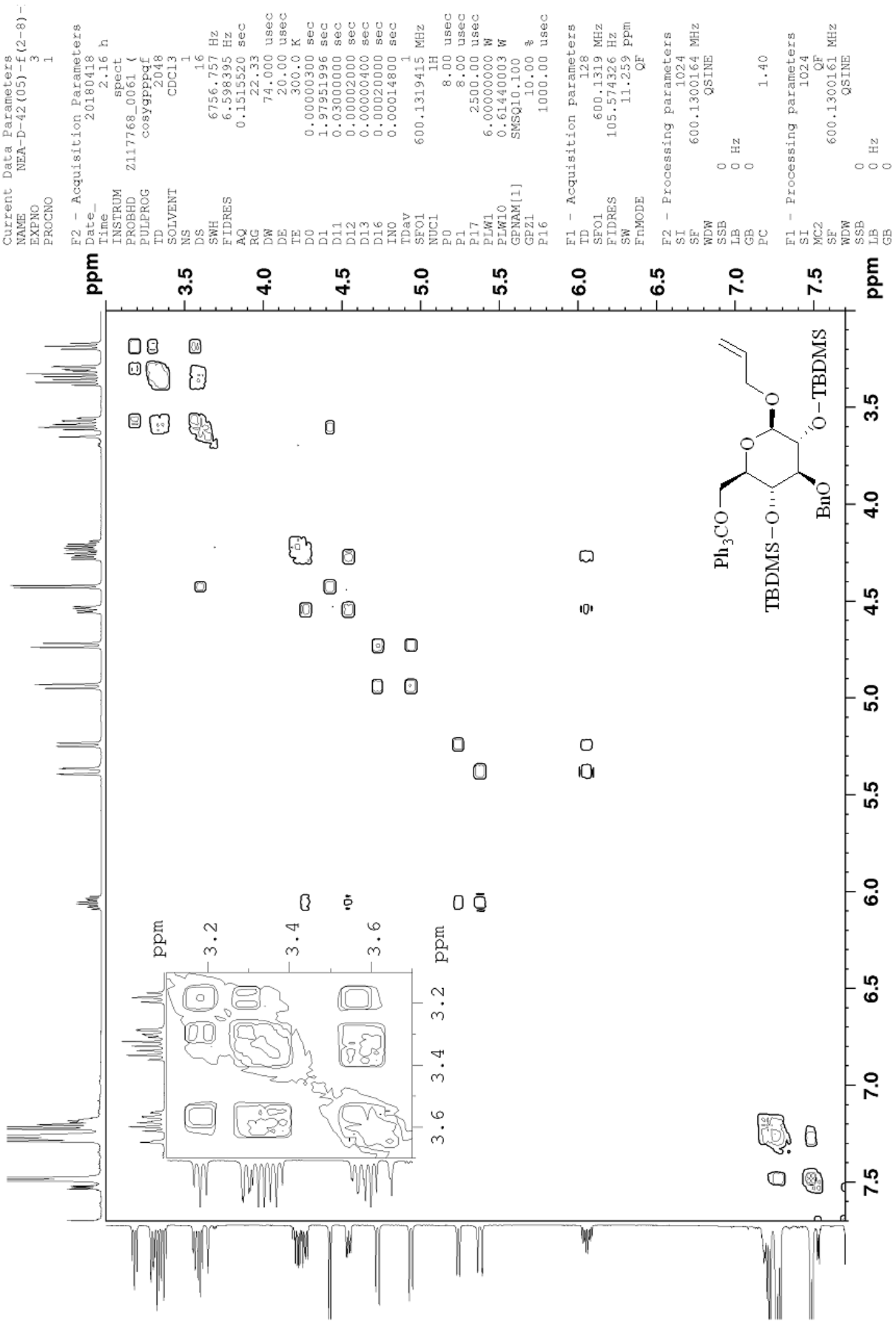

Figure E.5: H,H-COSY spectrum of compound **6b**.

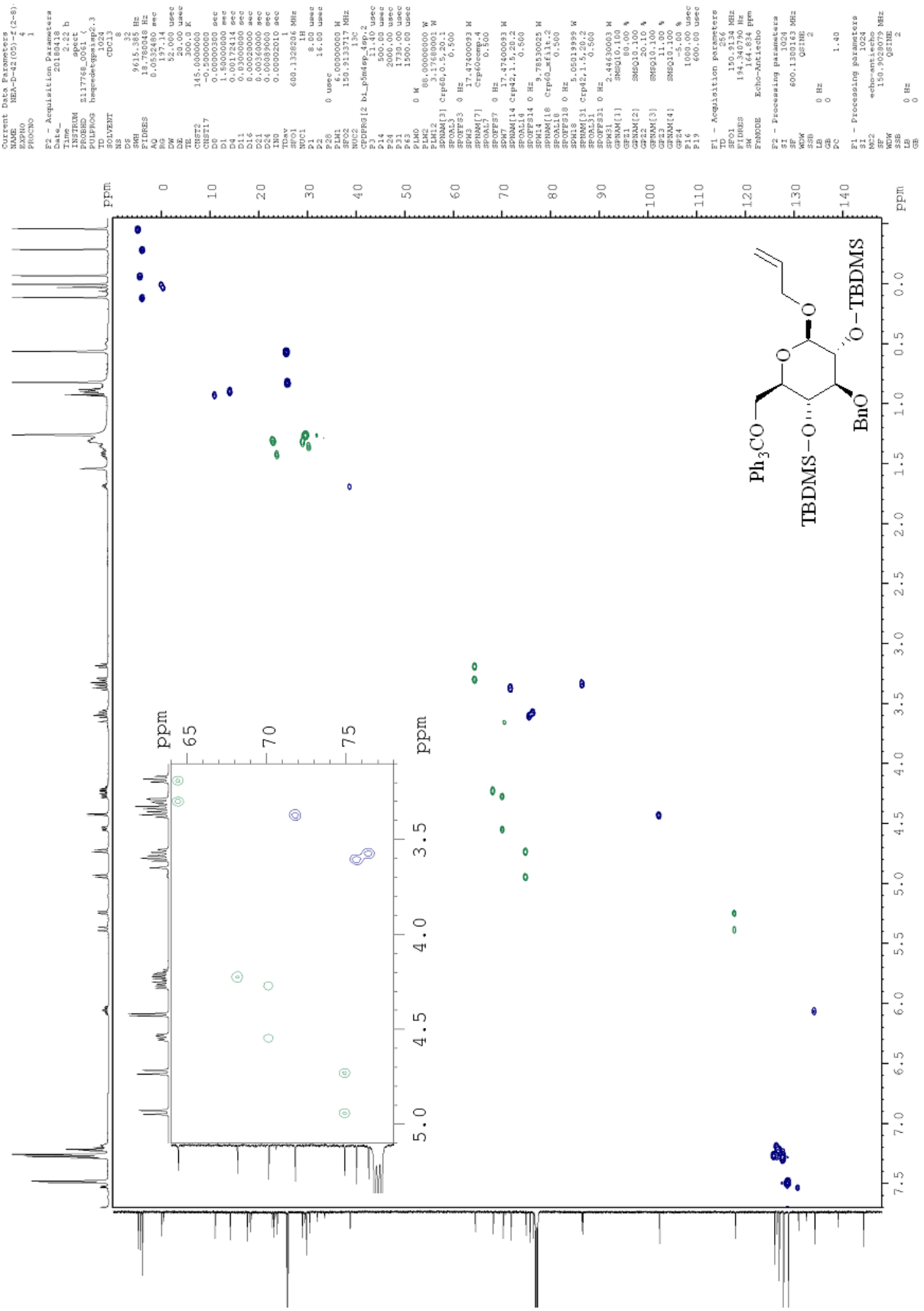

Figure E.6: HSQC spectrum of compound **6b**.

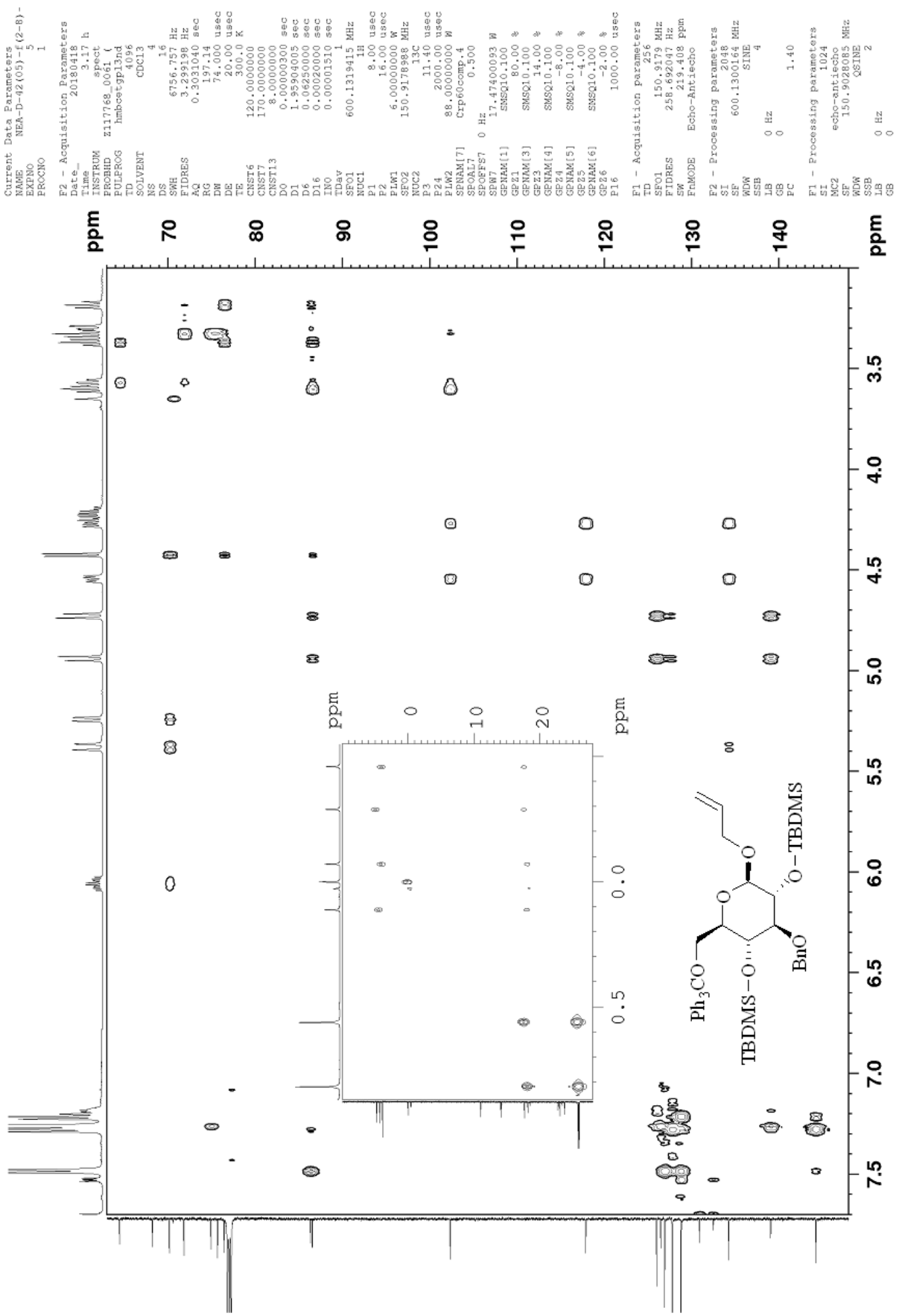

Figure E.7: HMBC spectrum of compound **6b**.

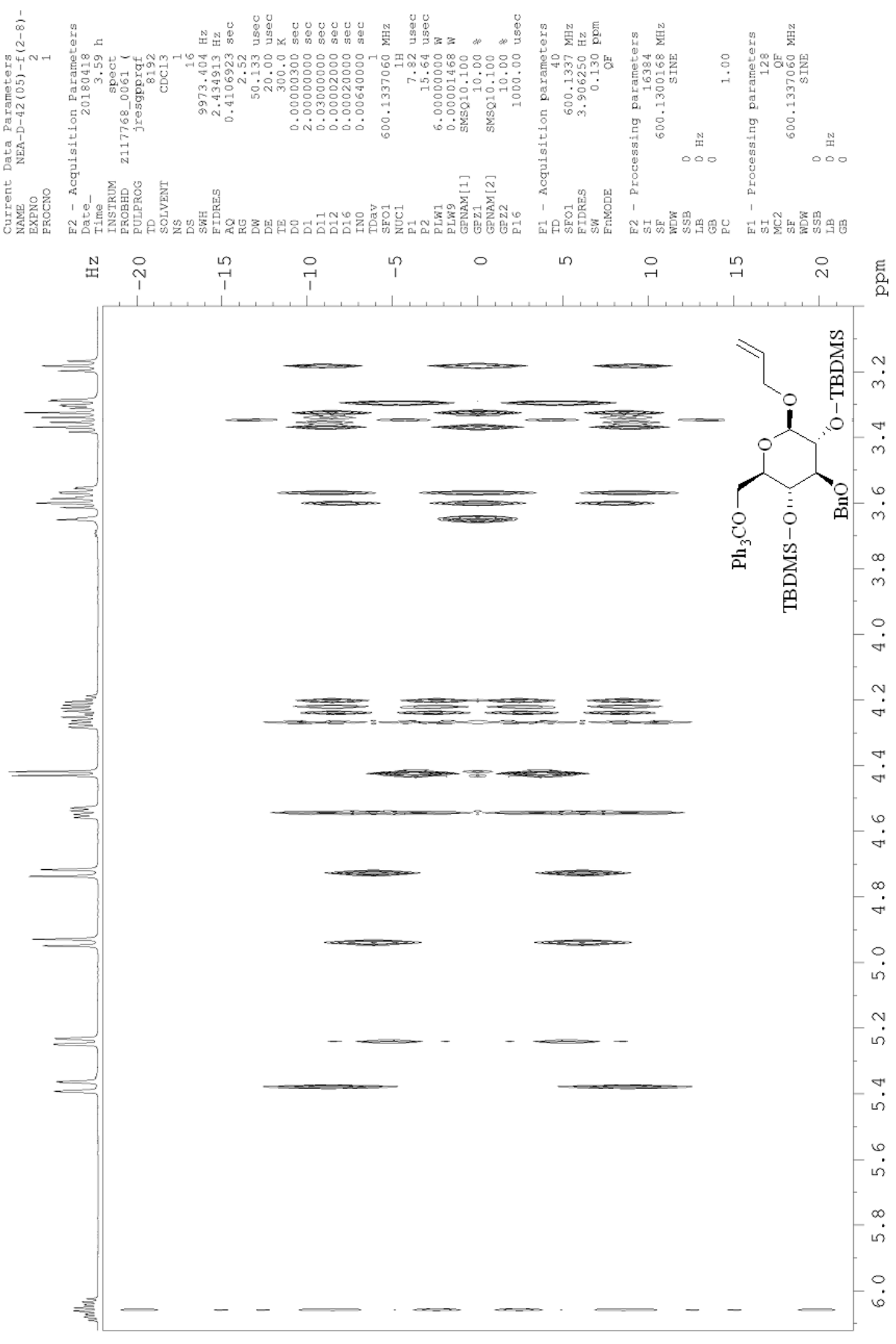

Figure E.8: JRES spectrum of compound **6b**.

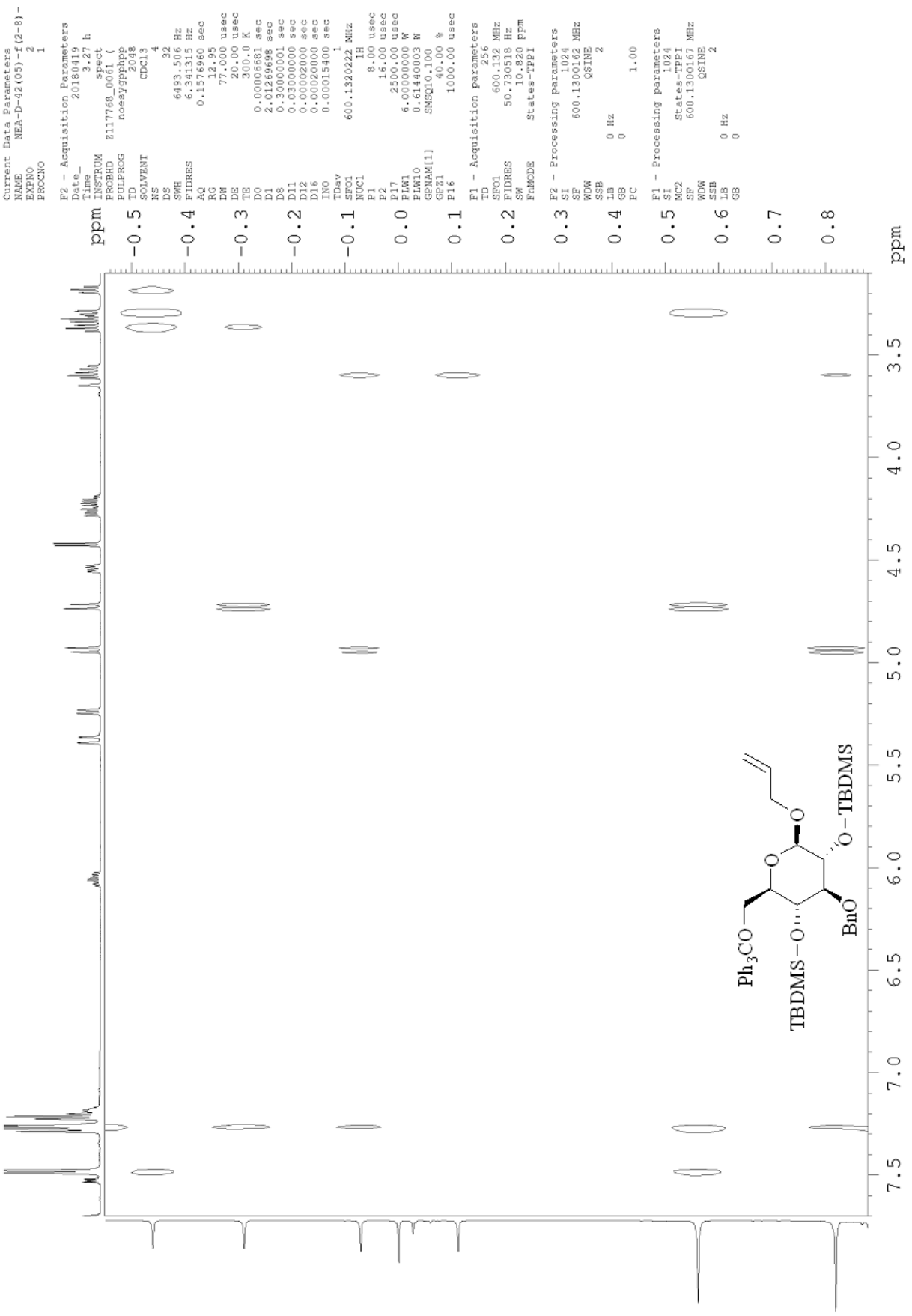

Figure E.9: NOESY spectrum of silyl alkyl protons of compound **6b**.

F Spectroscopic Data – Compound 7a

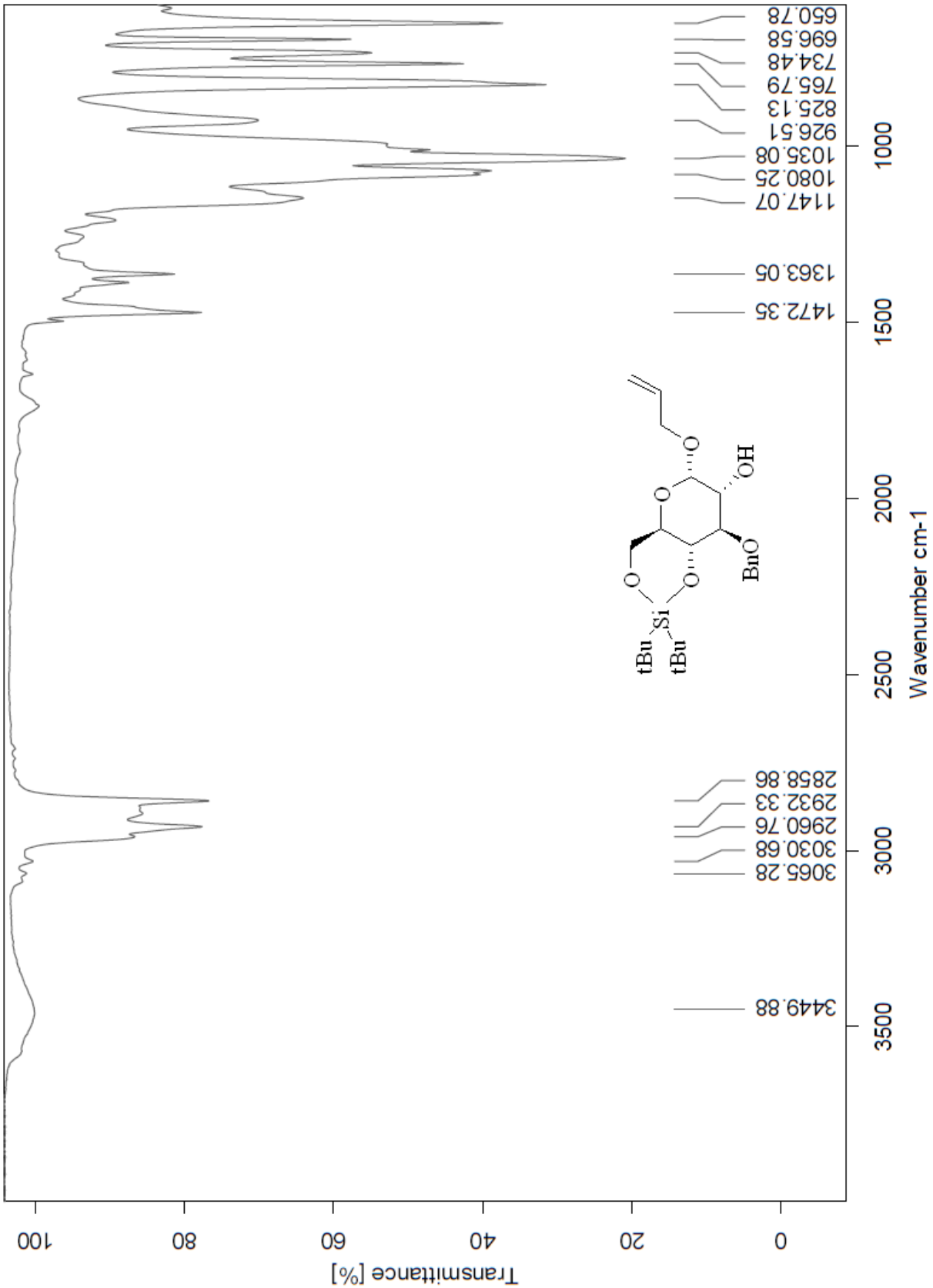

Figure F.1: IR spectrum of compound **7a**.

Single Mass Analysis
Tolerance = 3.0 PPM / DBE: min = -1.5, max = 50.0
Element prediction: Off
Number of isotope peaks used for i-FIT = 3

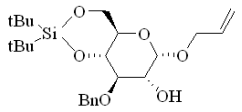

Monoisotopic Mass, Even Electron Ions
1258 formula(e) evaluated with 6 results within limits (all results (up to 1000) for each mass)
Elements Used:
C: 0-500 H: 0-1000 O: 0-10 Na: 0-1 Si: 0-4 I: 0-1

2018-136 48 (0.900) AM2 (Ar,35000.0,0.00,0.00); Cm (47:49)
1: TOF MS ES+

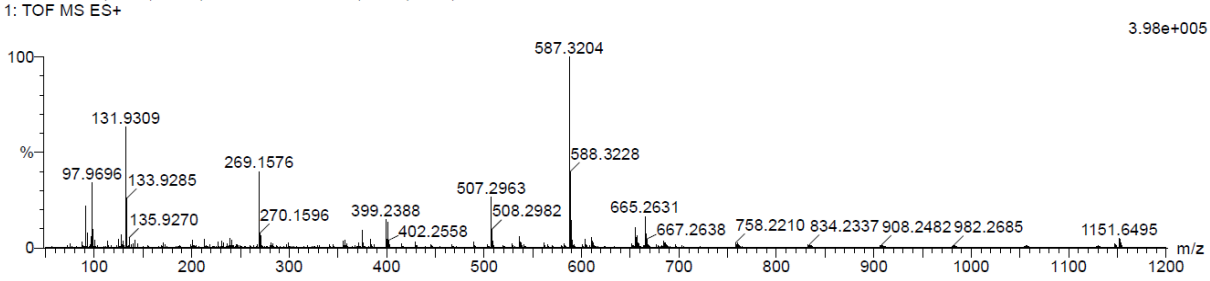

Minimum:				-1.5				
Maximum:		5000.0	3.0	50.0				
Mass	Calc. Mass	mDa	PPM	DBE	i-FIT	Norm	Conf(%)	Formula
587.3204	587.3200	0.4	0.7	6.5	793.1	0.082	92.17	C30 H52 O6 Na Si2
	587.3193	1.1	1.9	14.5	795.6	2.596	7.46	C36 H47 O5 Si
	587.3197	0.7	1.2	13.5	798.8	5.772	0.31	C35 H51 O2 Si3
	587.3204	0.0	0.0	5.5	800.5	7.545	0.05	C29 H56 O3 Na Si4
	587.3196	0.8	1.4	7.5	803.2	10.167	0.00	C31 H48 O9 Na
	587.3220	-1.6	-2.7	10.5	803.4	10.432	0.00	C33 H47 O9

Figure F.2: HRMS spectrum of compound **7a**.

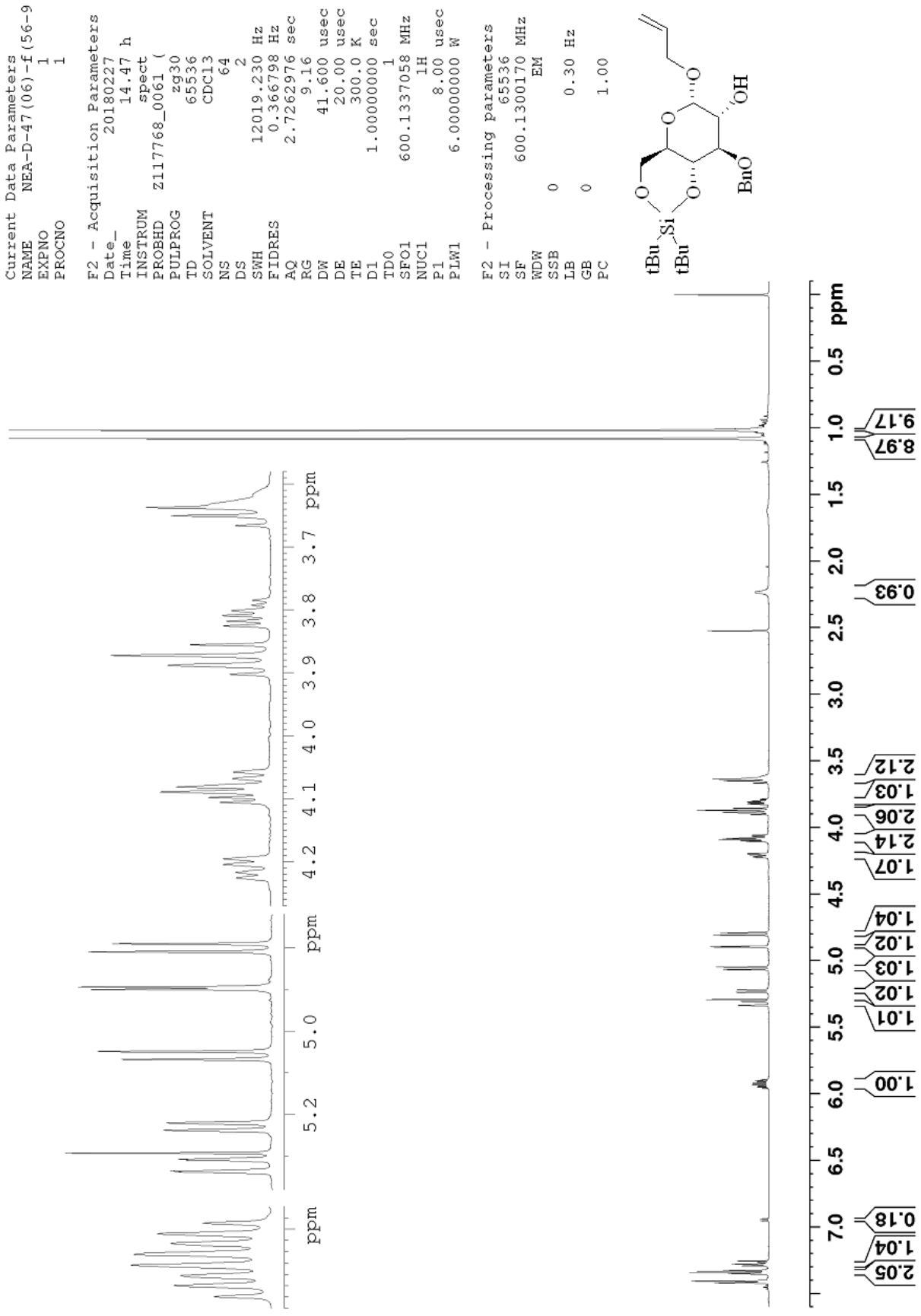

Figure F.3: ^{1}H-NMR spectrum of compound **7a**.

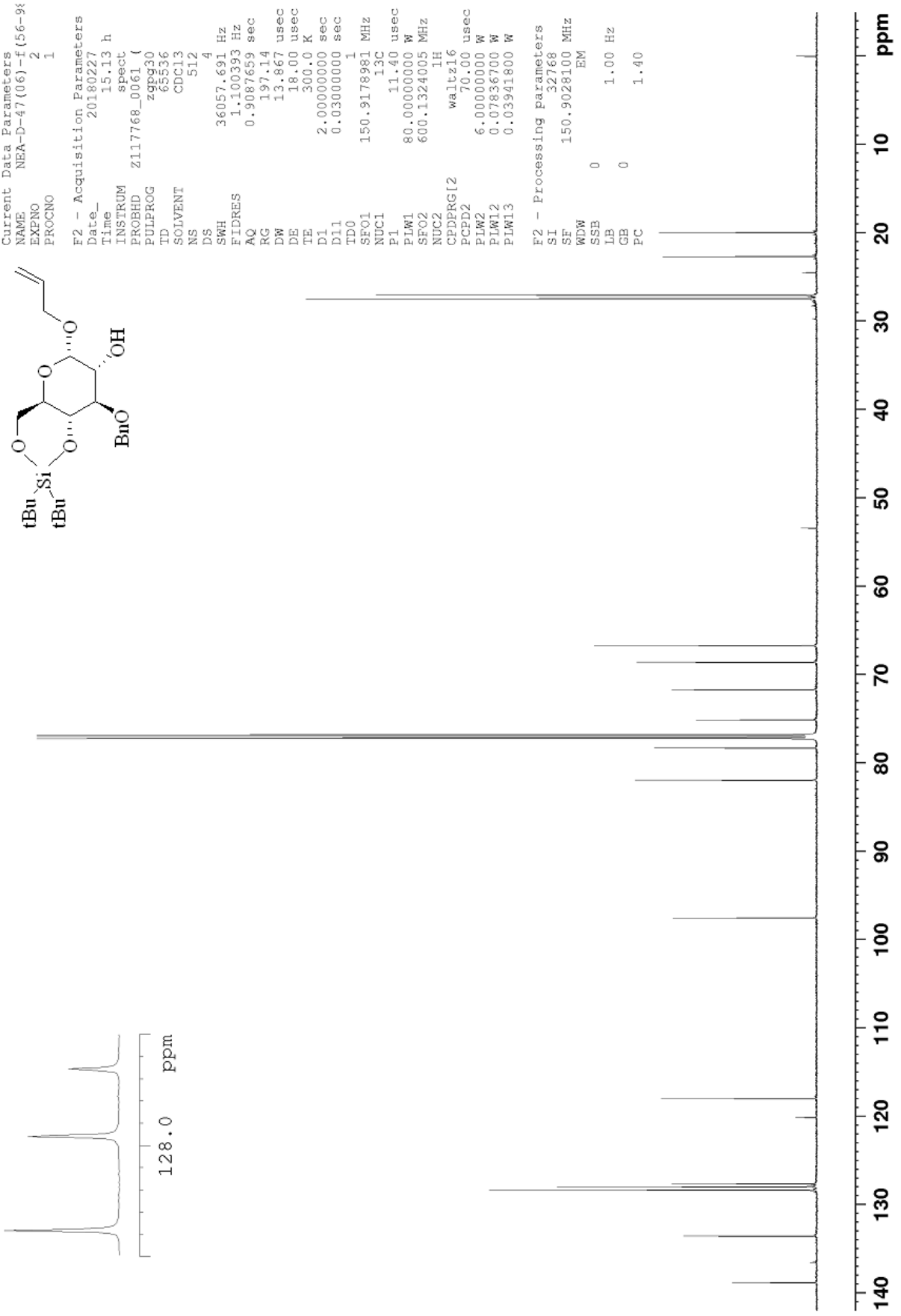

Figure F.4: ^{13}C-NMR spectrum of compound **7a**.

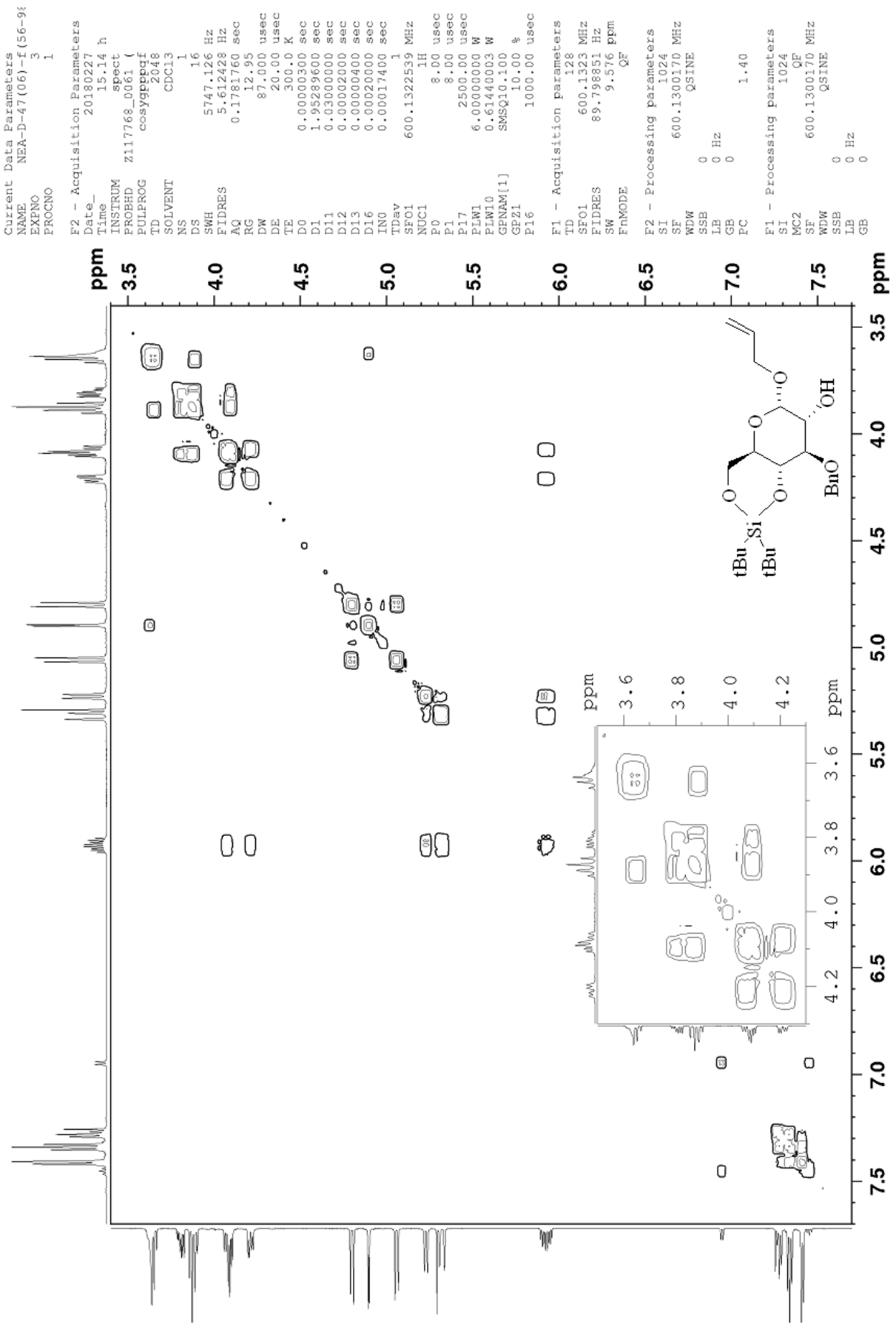

Figure F.5: H,H-COSY spectrum of compound **7a**.

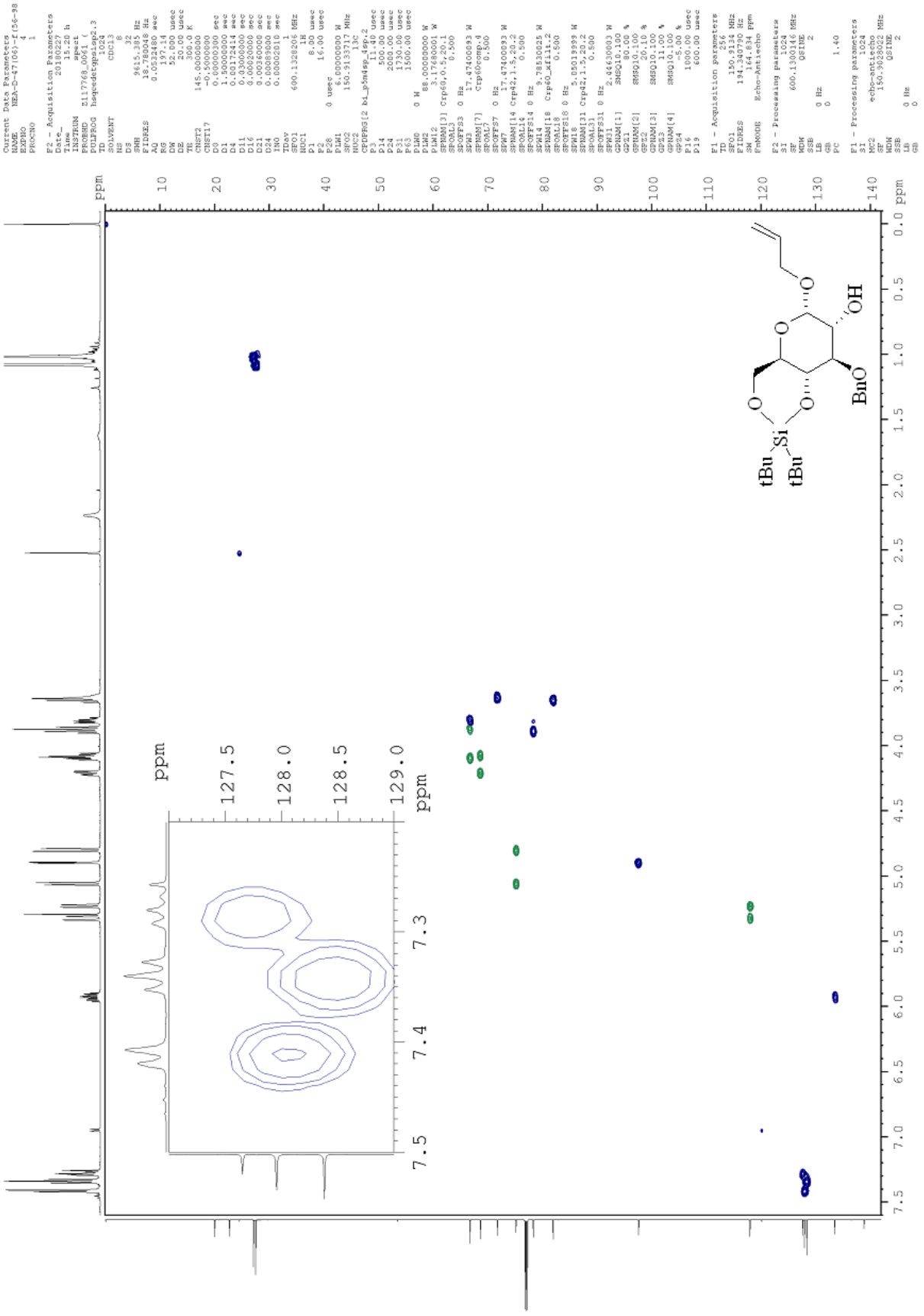

Figure F.6: HSQC spectrum of compound **7a**.

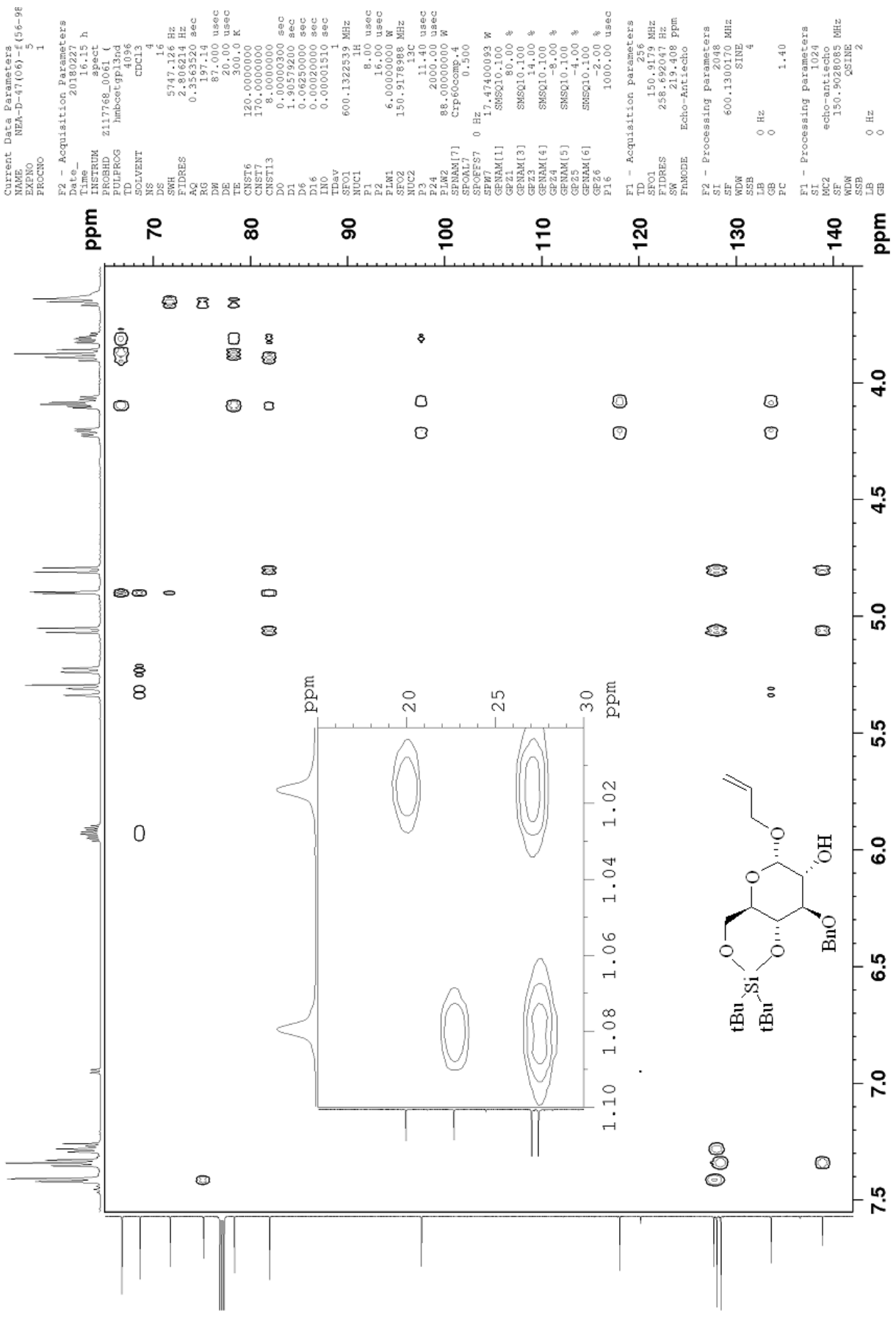

Figure F.7: HMBC spectrum of compound **7a**.

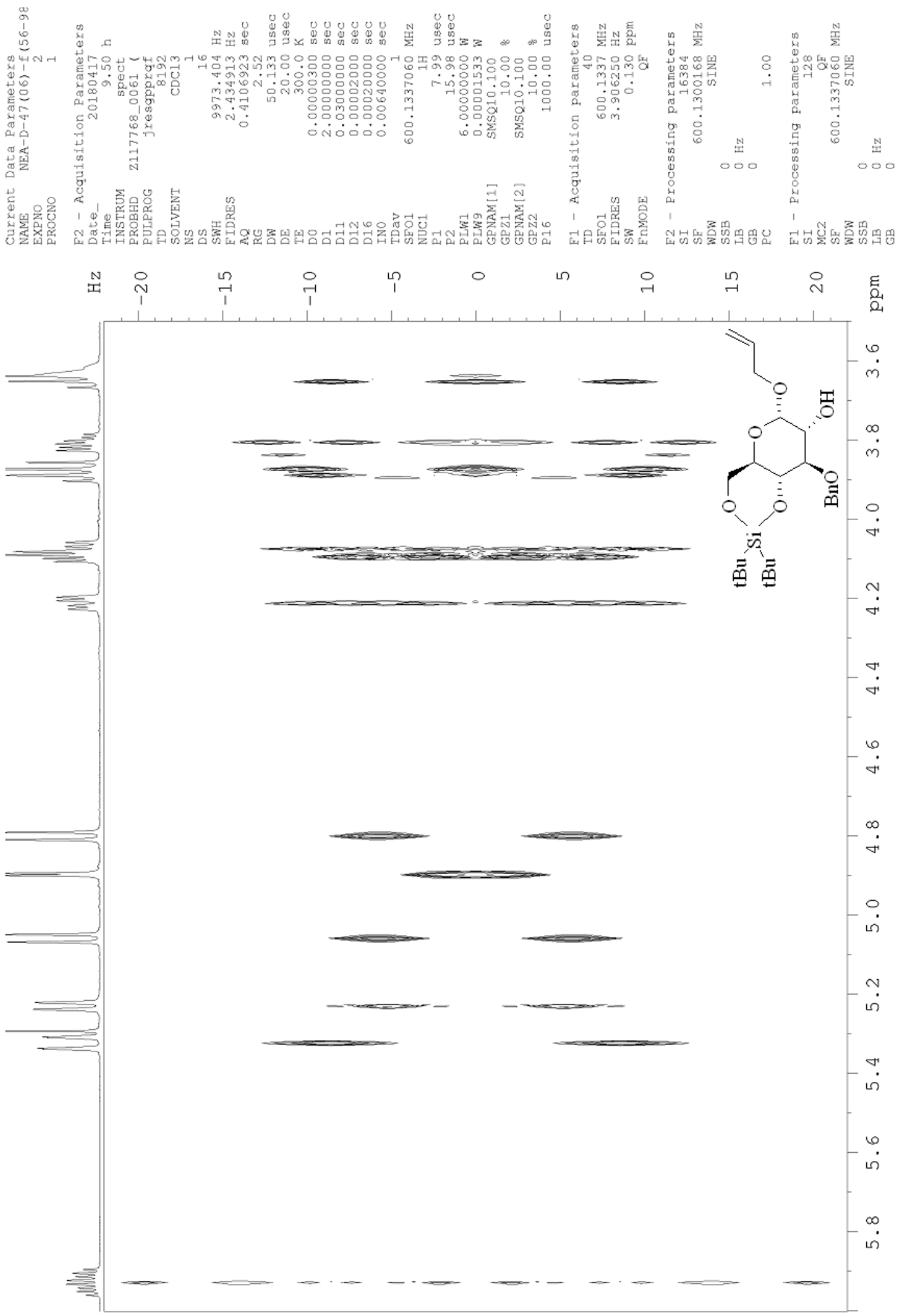

Figure F.8: JRES spectrum of compound **7a**.

G Spectroscopic Data – Compound 7b

Figure G.1: IR spectrum of compound **7b**.

Single Mass Analysis
Tolerance = 3.0 PPM / DBE: min = -1.5, max = 50.0
Element prediction: Off
Number of isotope peaks used for i-FIT = 3

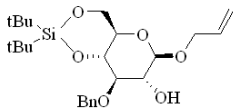

Monoisotopic Mass, Even Electron Ions
1258 formula(e) evaluated with 6 results within limits (all results (up to 1000) for each mass)
Elements Used:
C: 0-500 H: 0-1000 O: 0-10 Na: 0-1 I: 0-1 Si: 0-4

2018-132 44 (0.820) AM2 (Ar,35000.0,0.00,0.00); Cm (44:46)
1: TOF MS ES+

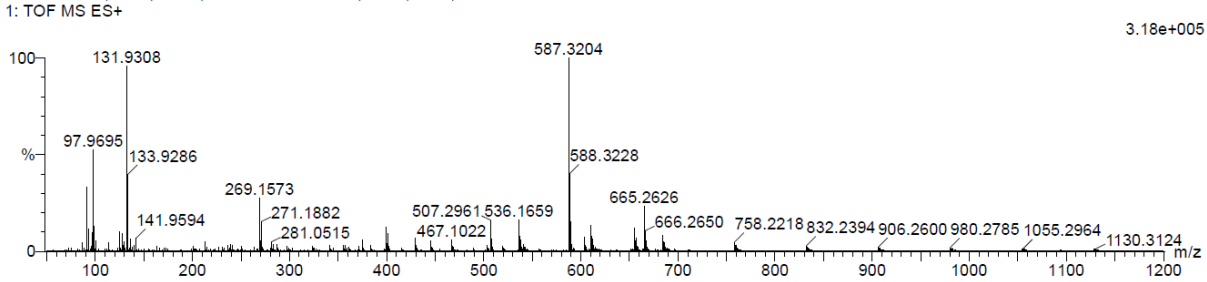

Minimum:				-1.5				
Maximum:		5000.0	3.0	50.0				
Mass	Calc. Mass	mDa	PPM	DBE	i-FIT	Norm	Conf(%)	Formula
587.3204	587.3200	0.4	0.7	6.5	787.8	0.010	98.96	C30 H52 O6 Na Si2
	587.3193	1.1	1.9	14.5	793.0	5.235	0.53	C36 H47 O5 Si
	587.3197	0.7	1.2	13.5	793.5	5.794	0.30	C35 H51 O2 Si3
	587.3204	0.0	0.0	5.5	794.0	6.217	0.20	C29 H56 O3 Na Si4
	587.3196	0.8	1.4	7.5	799.8	12.066	0.00	C31 H48 O9 Na
	587.3220	-1.6	-2.7	10.5	800.0	12.261	0.00	C33 H47 O9

Figure G.2: HRMS spectrum of compound **7b**.

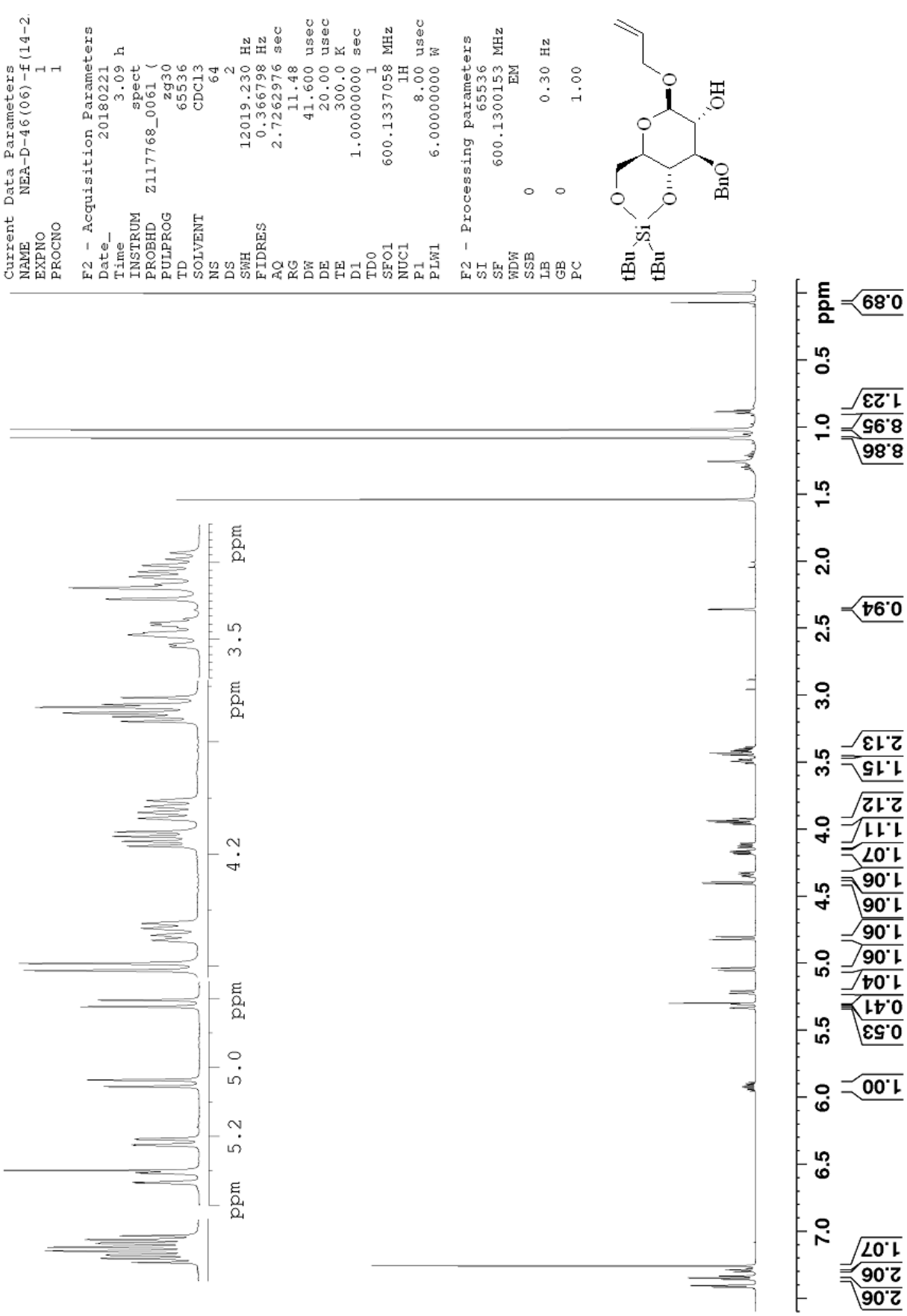

Figure G.3: ^{1}H-NMR spectrum of compound **7b**.

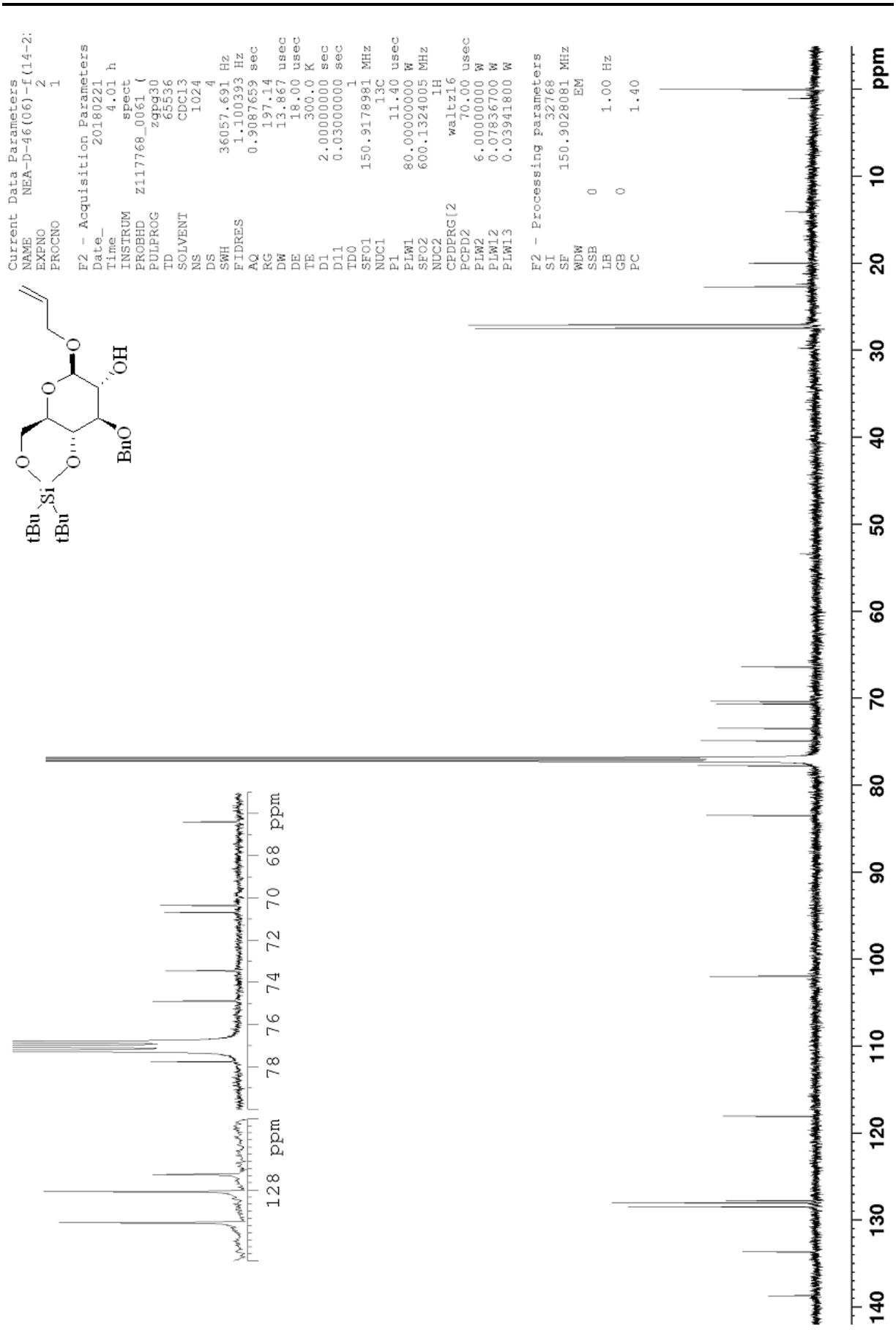

Figure G.4: ^{13}C-NMR spectrum of compound **7b**.

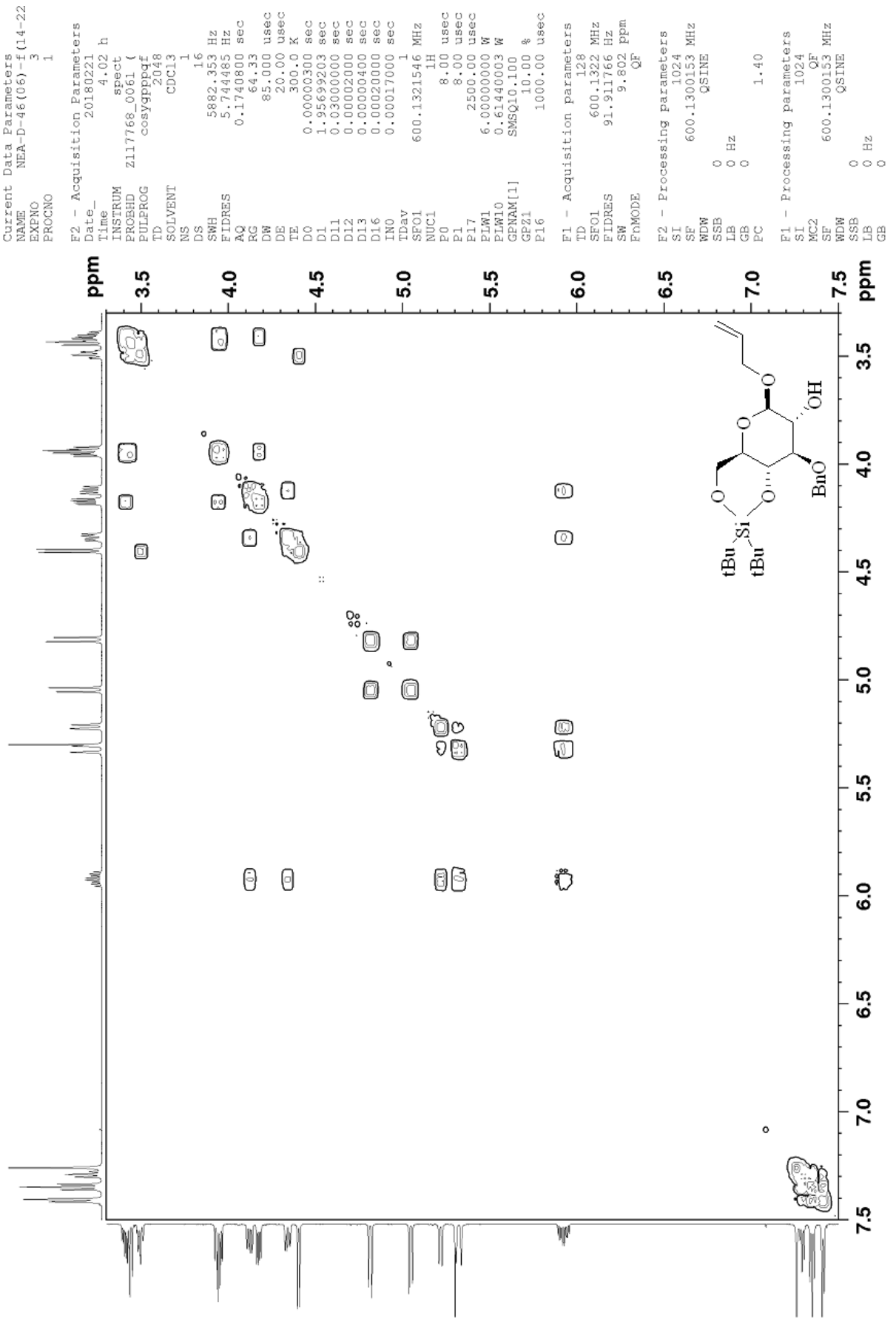

Figure G.5: H,H-COSY spectrum of compound **7b**.

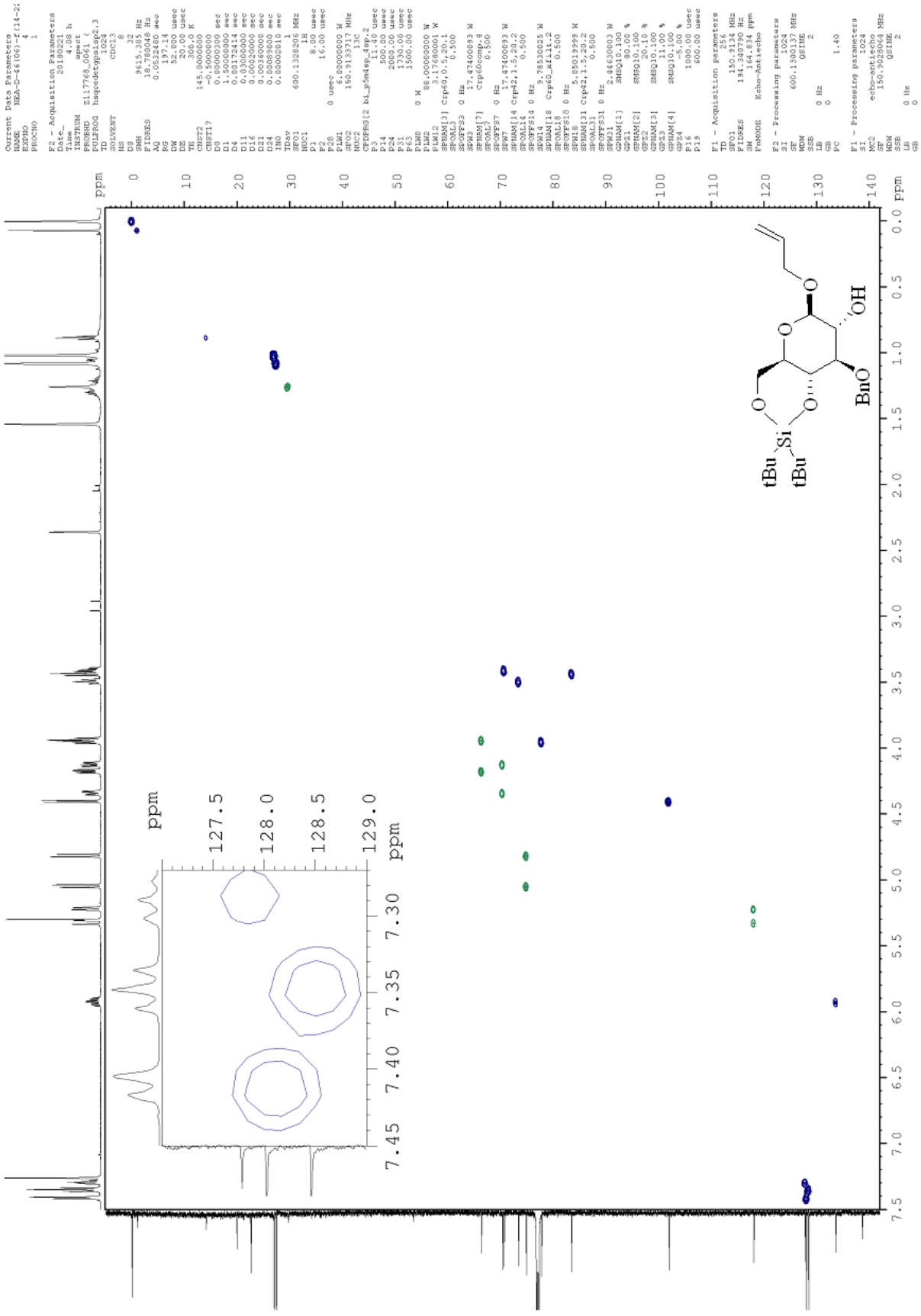

Figure G.6: HSQC spectrum of compound **7b**.

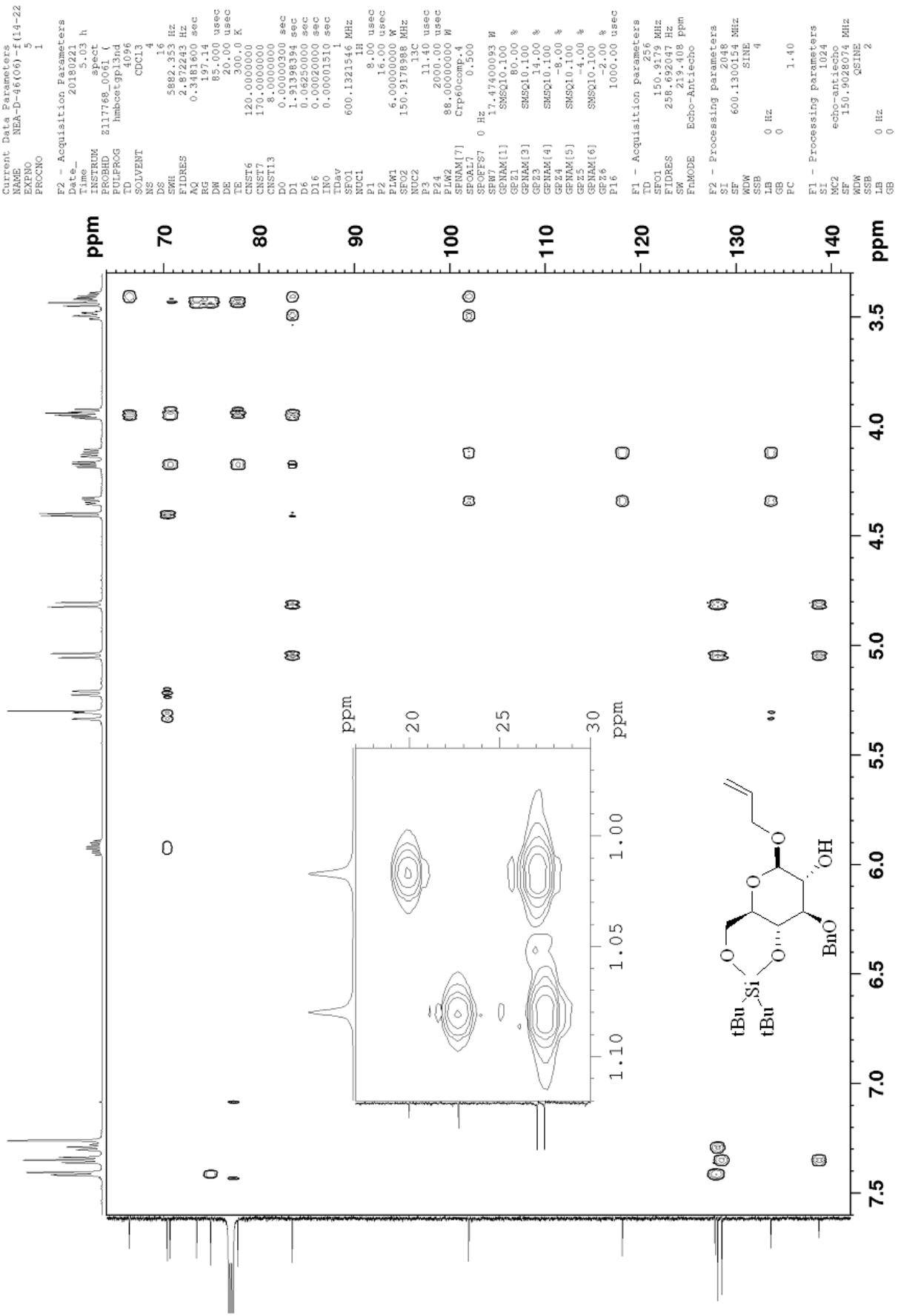

Figure G.7: HMBC spectrum of compound **7b**.

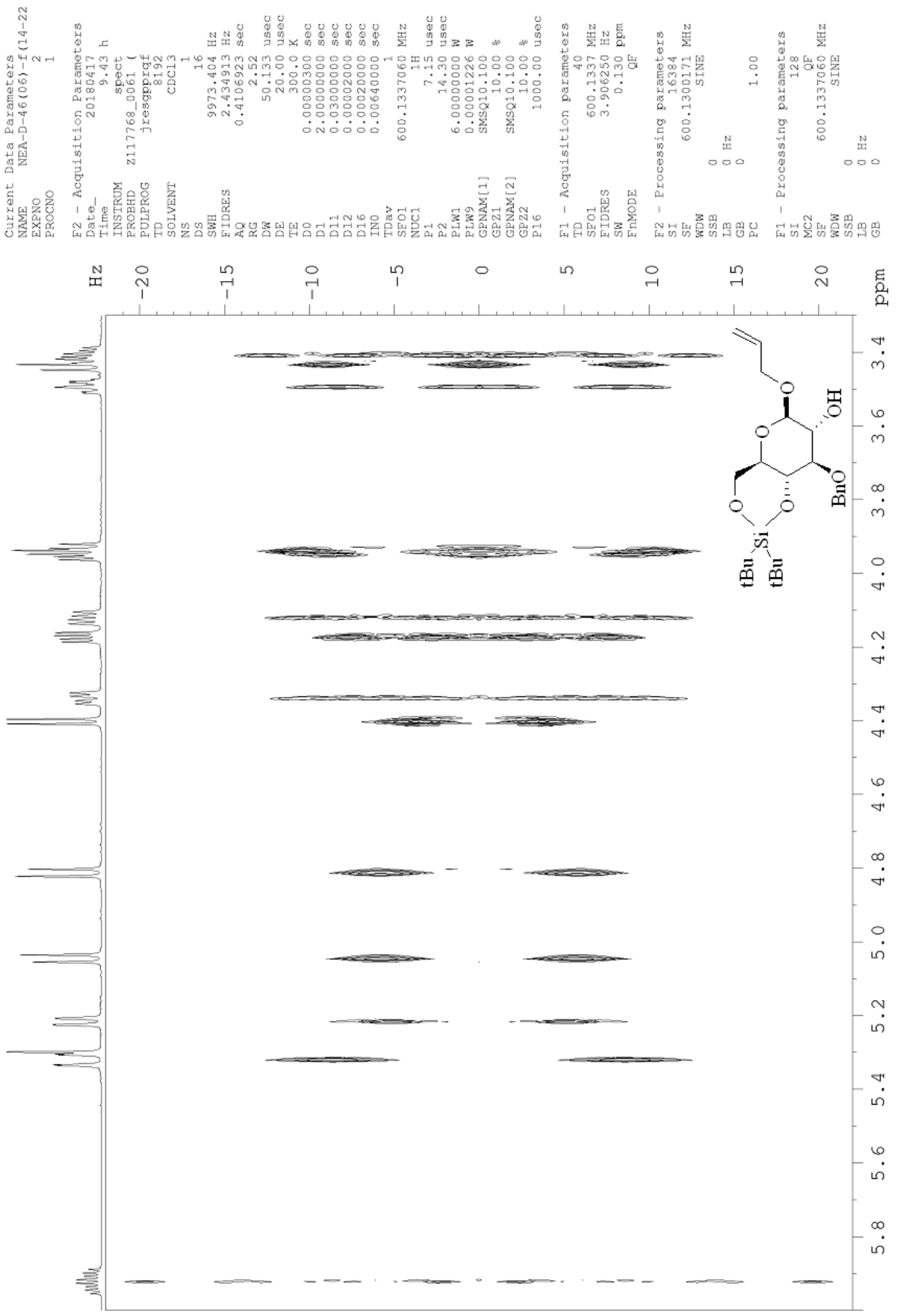

Figure G.8: JRES spectrum of compound **7b**.

H Spectroscopic Data – Compound 8a

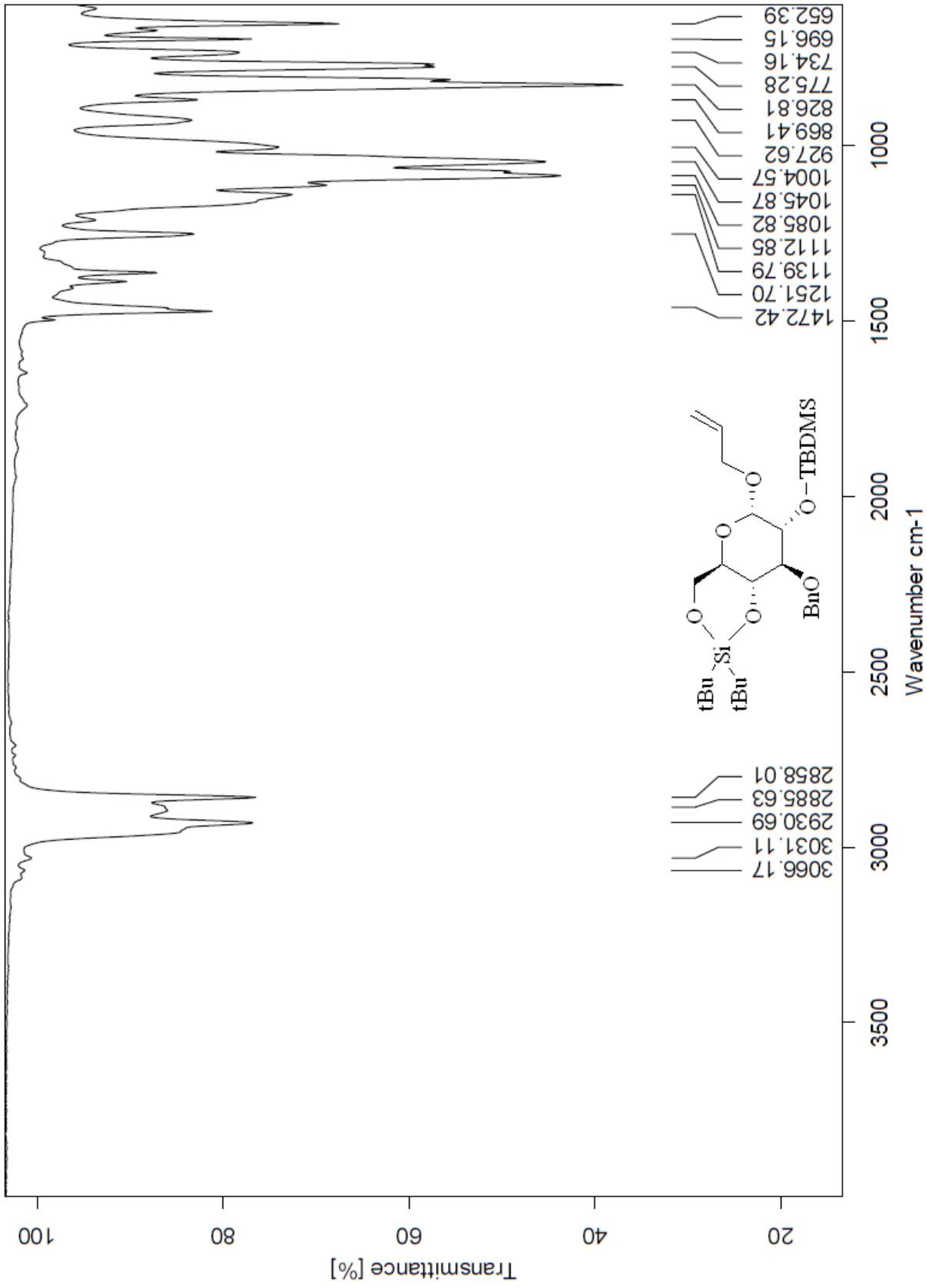

Figure H.1: IR spectrum of compound **8a**.

Single Mass Analysis
Tolerance = 3.0 PPM / DBE: min = -1.5, max = 50.0
Element prediction: Off
Number of isotope peaks used for i-FIT = 3

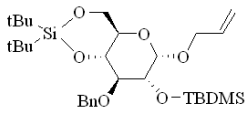

Monoisotopic Mass, Even Electron Ions
1258 formula(e) evaluated with 6 results within limits (all results (up to 1000) for each mass)
Elements Used:
C: 0-500 H: 0-1000 O: 0-10 Na: 0-1 Si: 0-4 I: 0-1

2018-136 48 (0.900) AM2 (Ar,35000.0,0.00,0.00); Cm (47:49)
1: TOF MS ES+

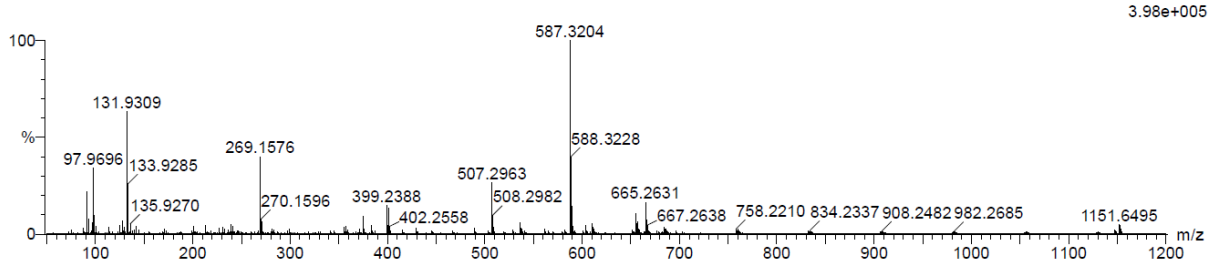

Minimum:				-1.5				
Maximum:		5000.0	3.0	50.0				
Mass	Calc. Mass	mDa	PPM	DBE	i-FIT	Norm	Conf(%)	Formula
587.3204	587.3200	0.4	0.7	6.5	793.1	0.082	92.17	C30 H52 O6 Na Si2
	587.3193	1.1	1.9	14.5	795.6	2.596	7.46	C36 H47 O5 Si
	587.3197	0.7	1.2	13.5	798.8	5.772	0.31	C35 H51 O2 Si3
	587.3204	0.0	0.0	5.5	800.5	7.545	0.05	C29 H56 O3 Na Si4
	587.3196	0.8	1.4	7.5	803.2	10.167	0.00	C31 H48 O9 Na
	587.3220	-1.6	-2.7	10.5	803.4	10.432	0.00	C33 H47 O9

Figure H.2: HRMS spectrum of compound **8a**.

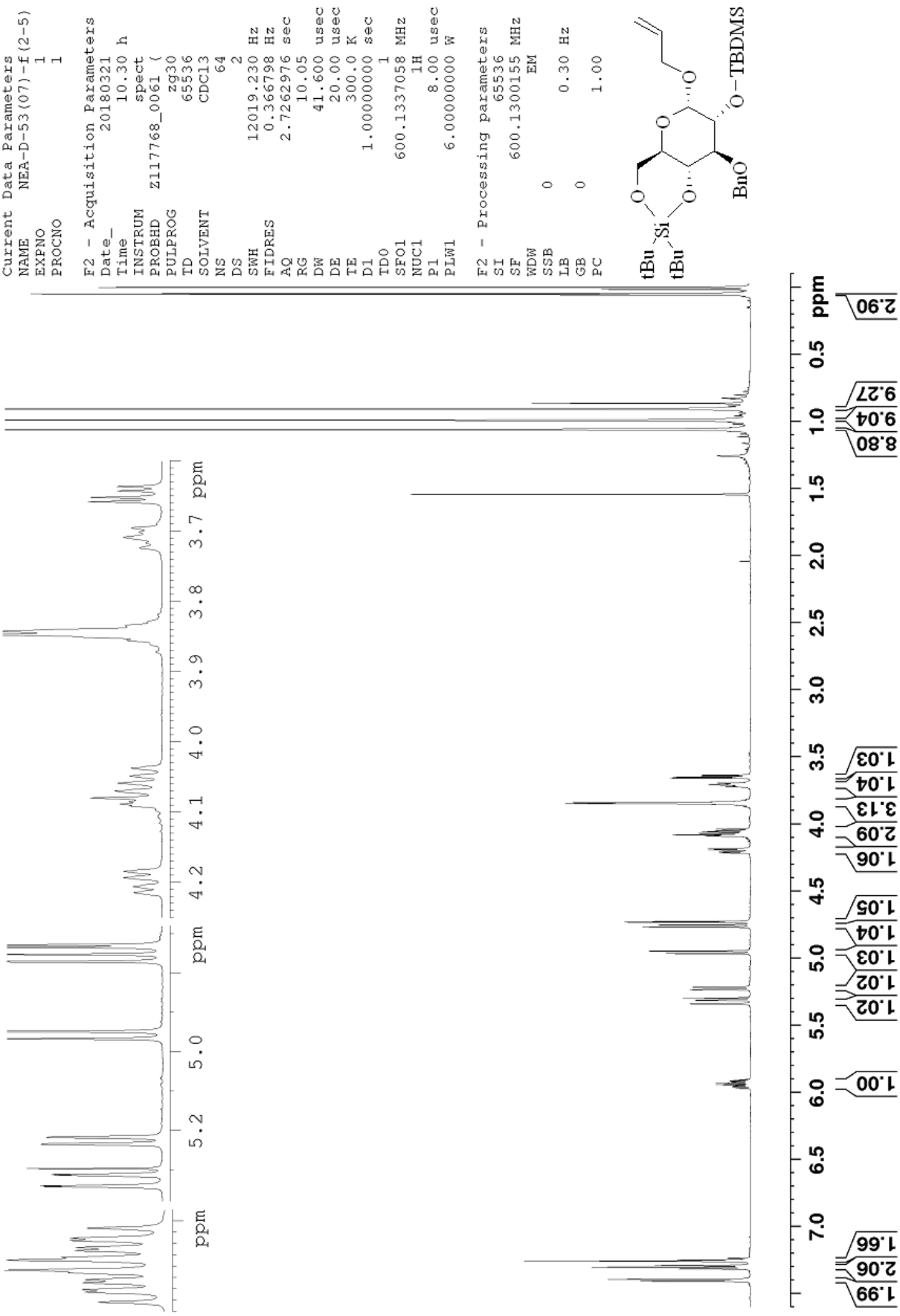

Figure H.3: ^{1}H-NMR spectrum of compound **8a**.

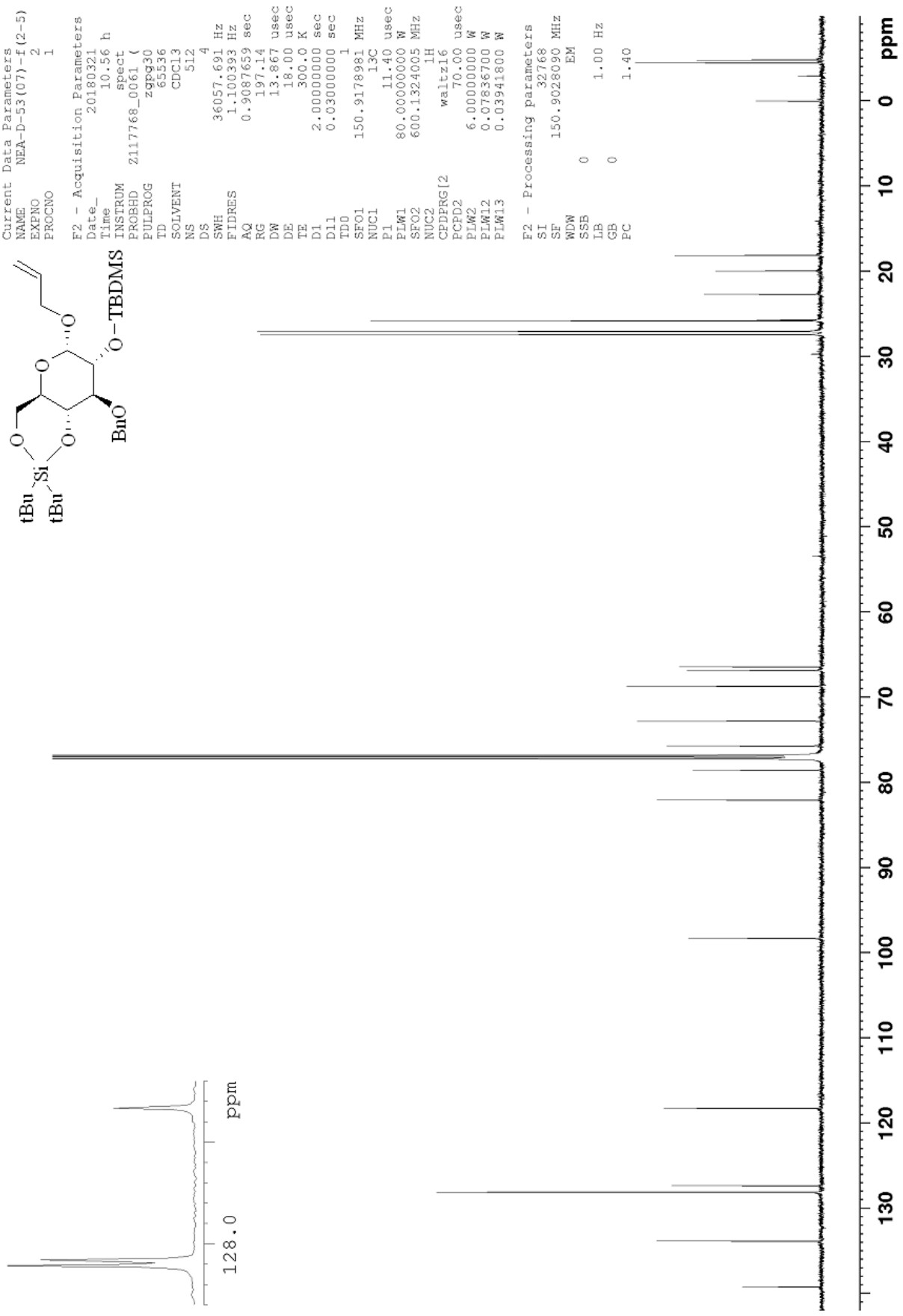

Figure H.4: ^{13}C-NMR spectrum of compound **8a**.

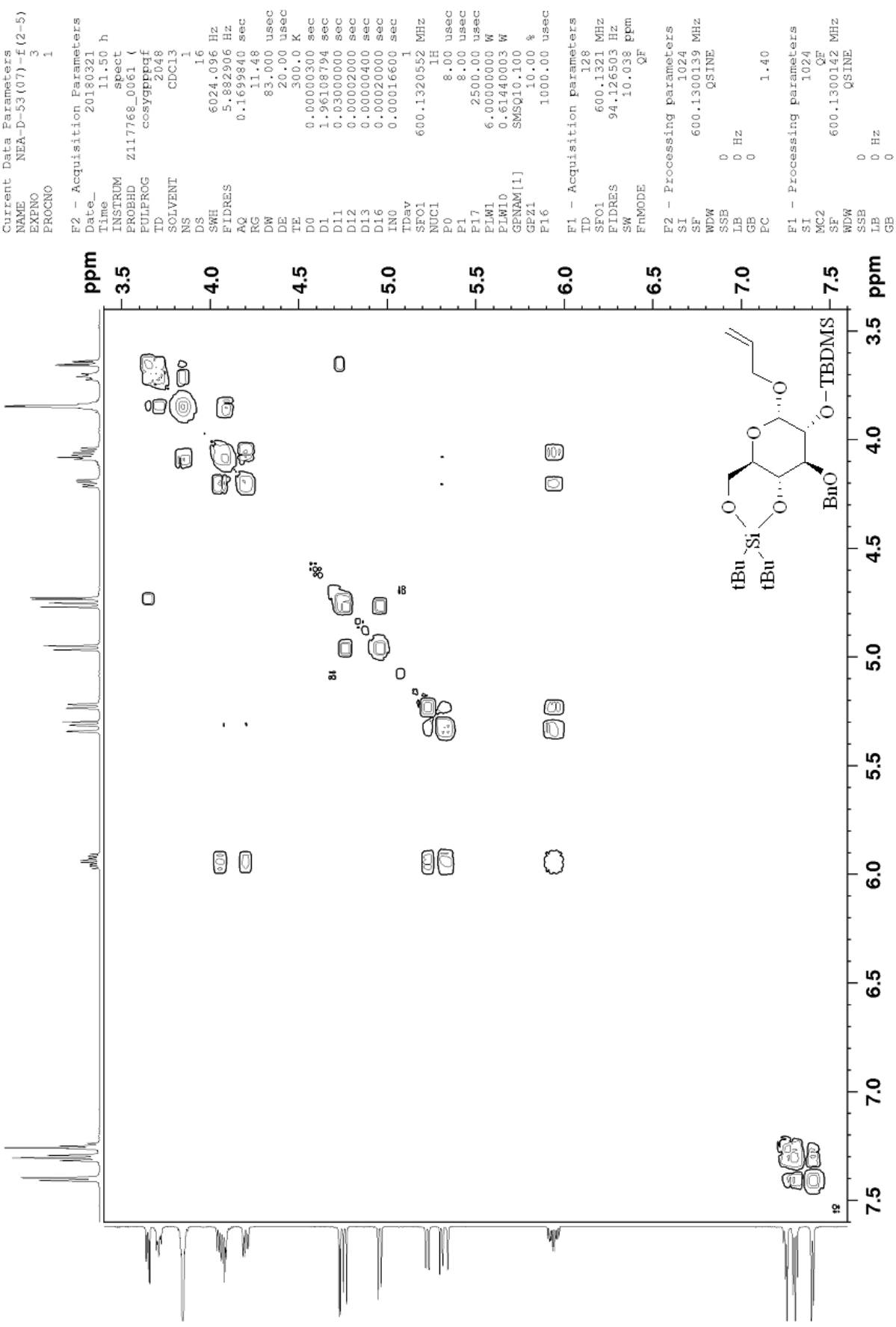

Figure H.5: H,H-COSY spectrum of compound **8a**.

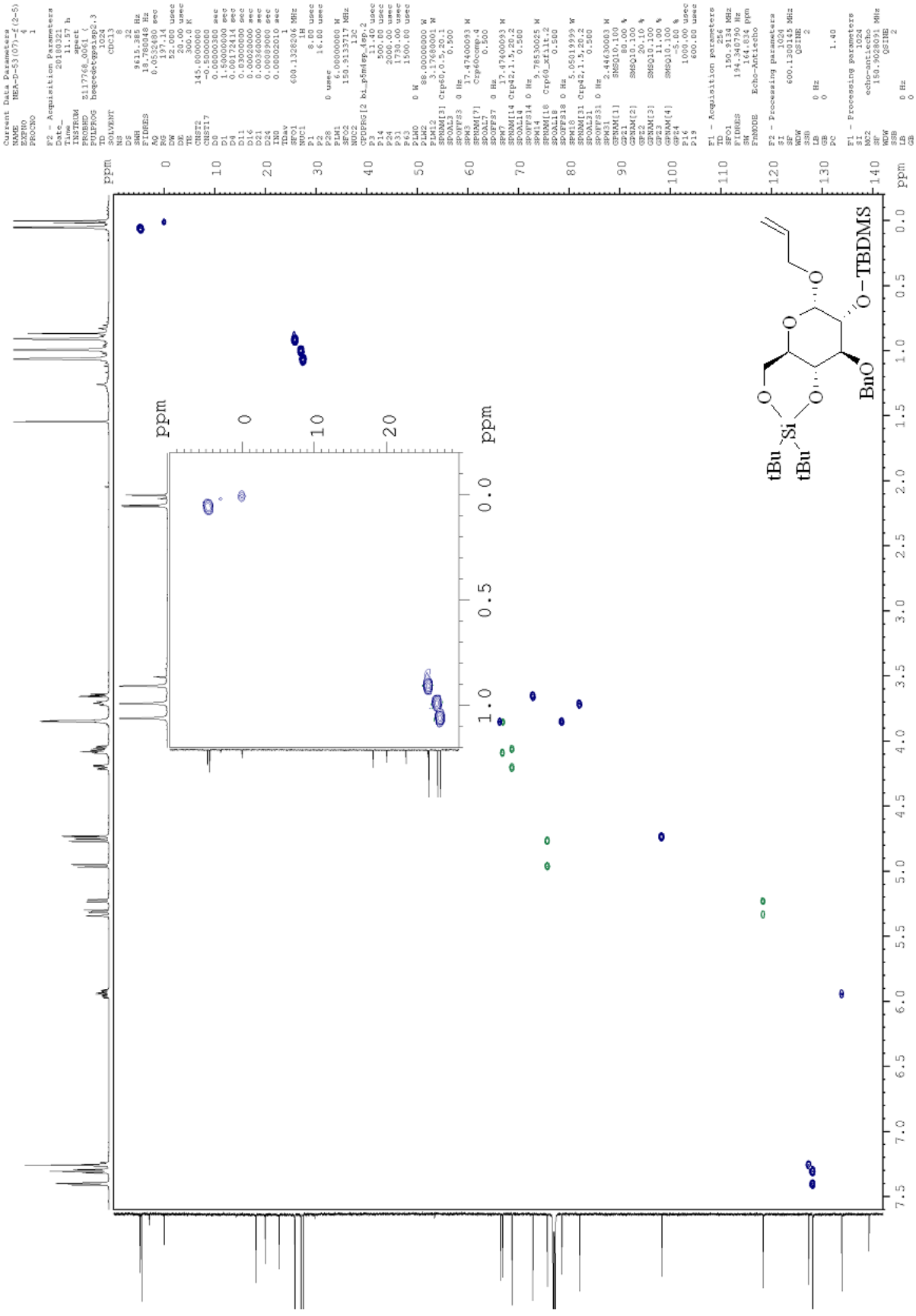

Figure H.6: HSQC spectrum of compound **8a**.

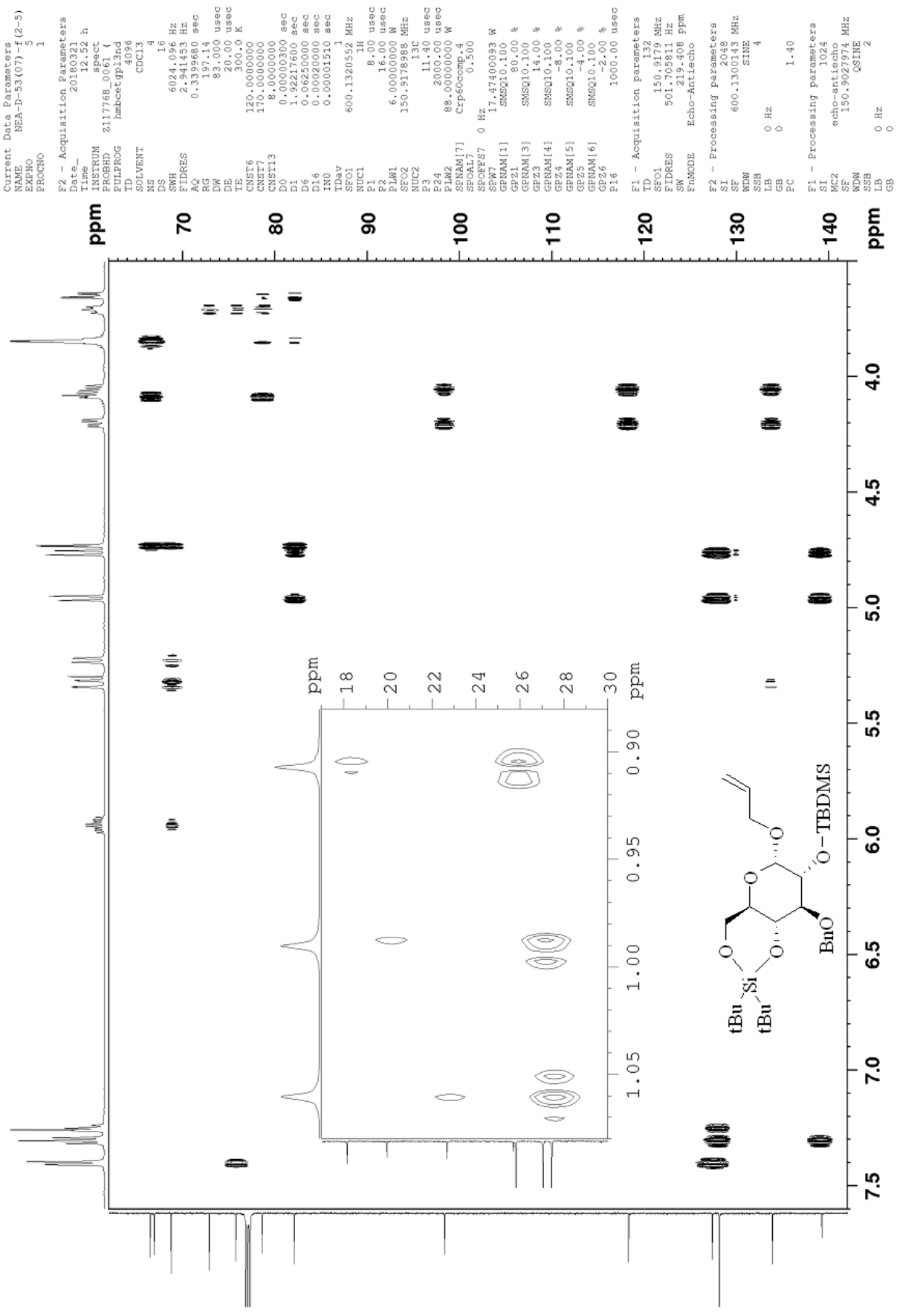

Figure H.7: HMBC spectrum of compound **8a**.

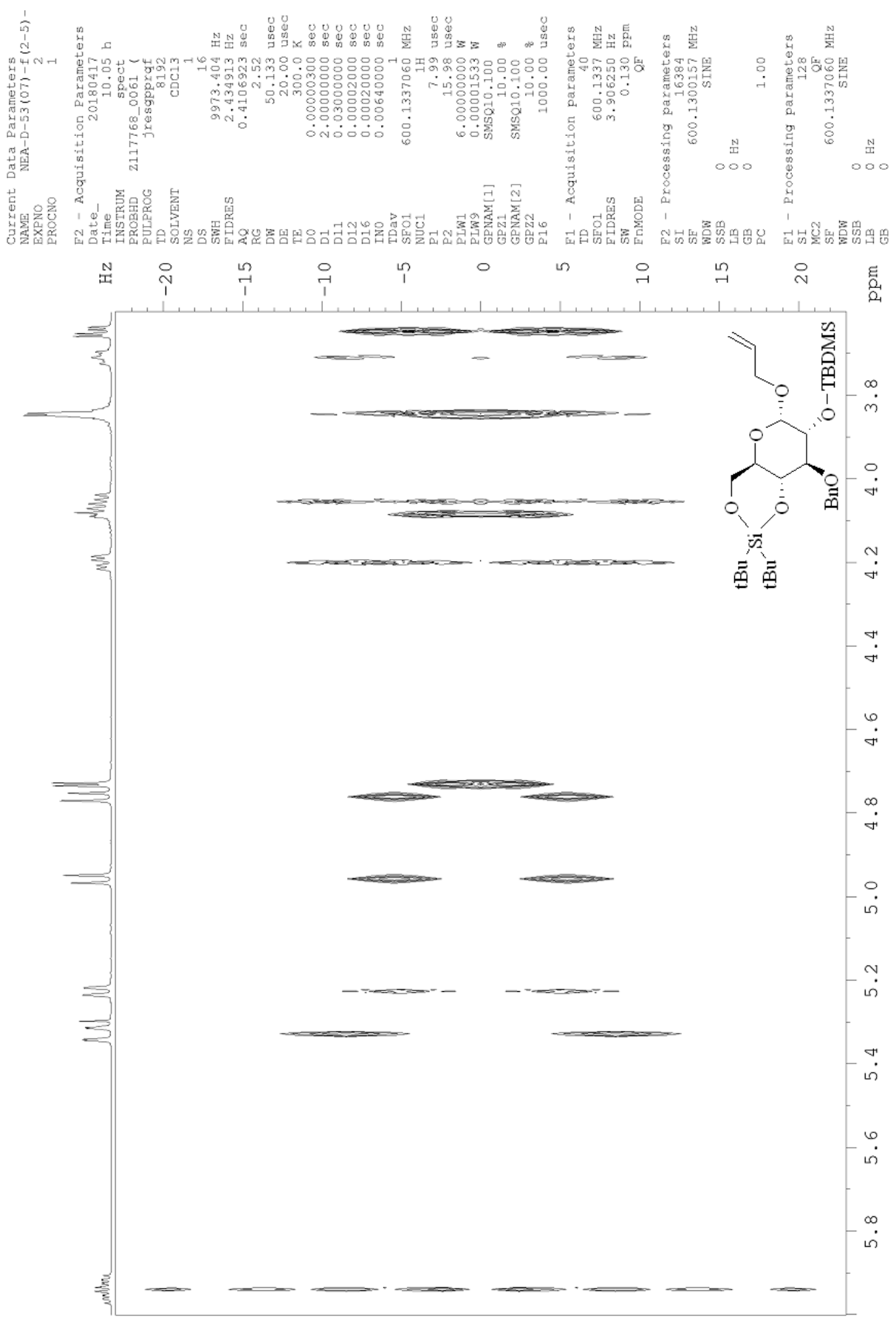

Figure H.8: JRES spectrum of compound **8a**.

I Spectroscopic Data – Compound 8b

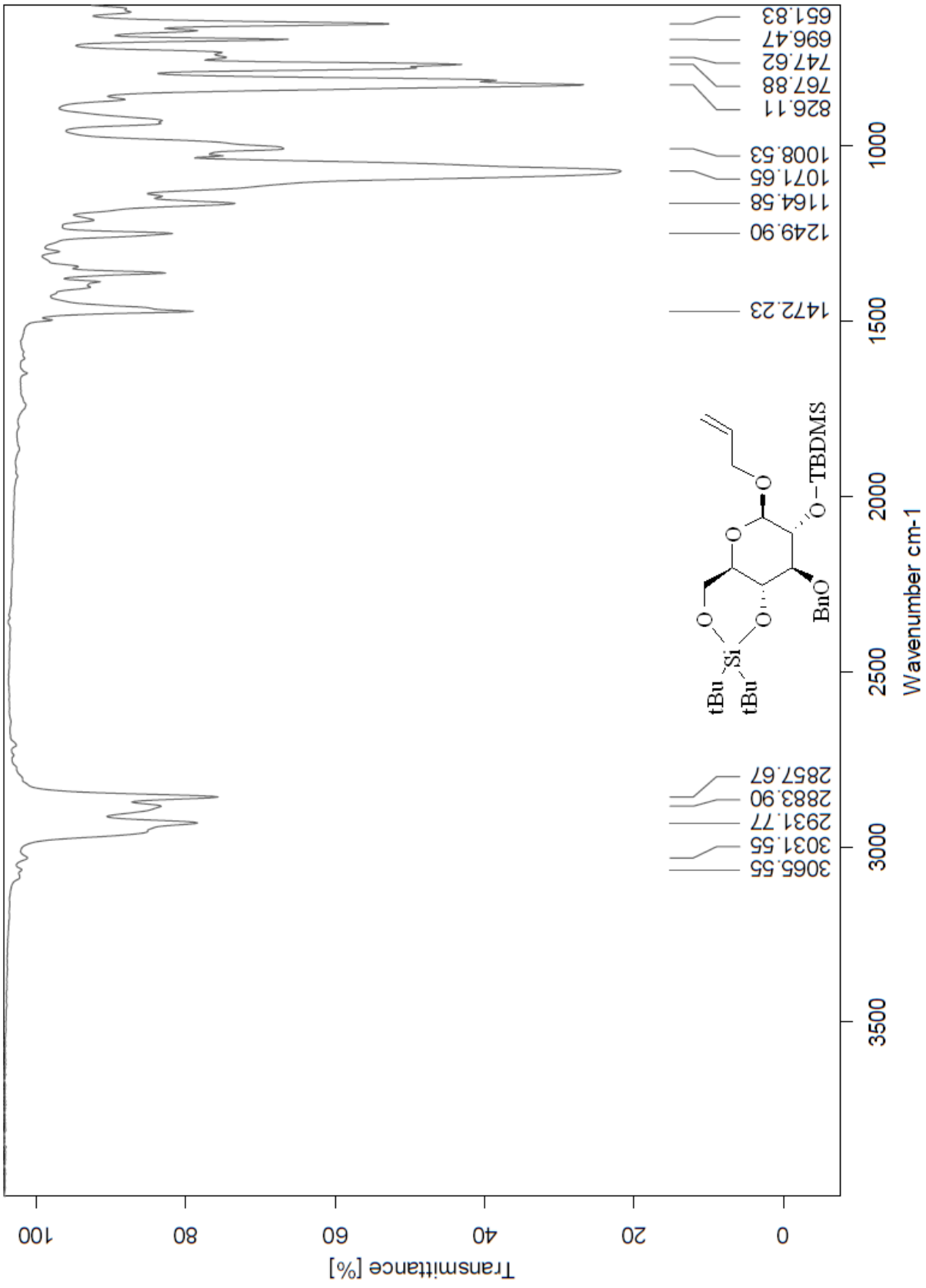

Figure I.1: IR spectrum of compound **8b**.

Single Mass Analysis
Tolerance = 3.0 PPM / DBE: min = -1.5, max = 50.0
Element prediction: Off
Number of isotope peaks used for i-FIT = 3

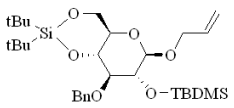

Monoisotopic Mass, Even Electron Ions
1258 formula(e) evaluated with 6 results within limits (all results (up to 1000) for each mass)
Elements Used:
C: 0-500 H: 0-1000 O: 0-10 Na: 0-1 I: 0-1 Si: 0-4

2018-132 44 (0.820) AM2 (Ar,35000.0,0.00,0.00); Cm (44:46)
1: TOF MS ES+

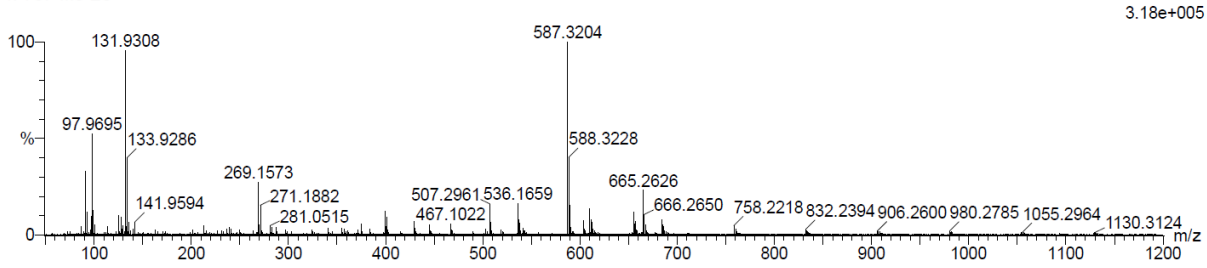

Minimum:				-1.5				
Maximum:		5000.0	3.0	50.0				
Mass	Calc. Mass	mDa	PPM	DBE	i-FIT	Norm	Conf(%)	Formula
587.3204	587.3200	0.4	0.7	6.5	787.8	0.010	98.96	C30 H52 O6 Na Si2
	587.3193	1.1	1.9	14.5	793.0	5.235	0.53	C36 H47 O5 Si
	587.3197	0.7	1.2	13.5	793.5	5.794	0.30	C35 H51 O2 Si3
	587.3204	0.0	0.0	5.5	794.0	6.217	0.20	C29 H56 O3 Na Si4
	587.3196	0.8	1.4	7.5	799.8	12.066	0.00	C31 H48 O9 Na
	587.3220	-1.6	-2.7	10.5	800.0	12.261	0.00	C33 H47 O9

Figure I.2: HRMS spectrum of compound **8b**.

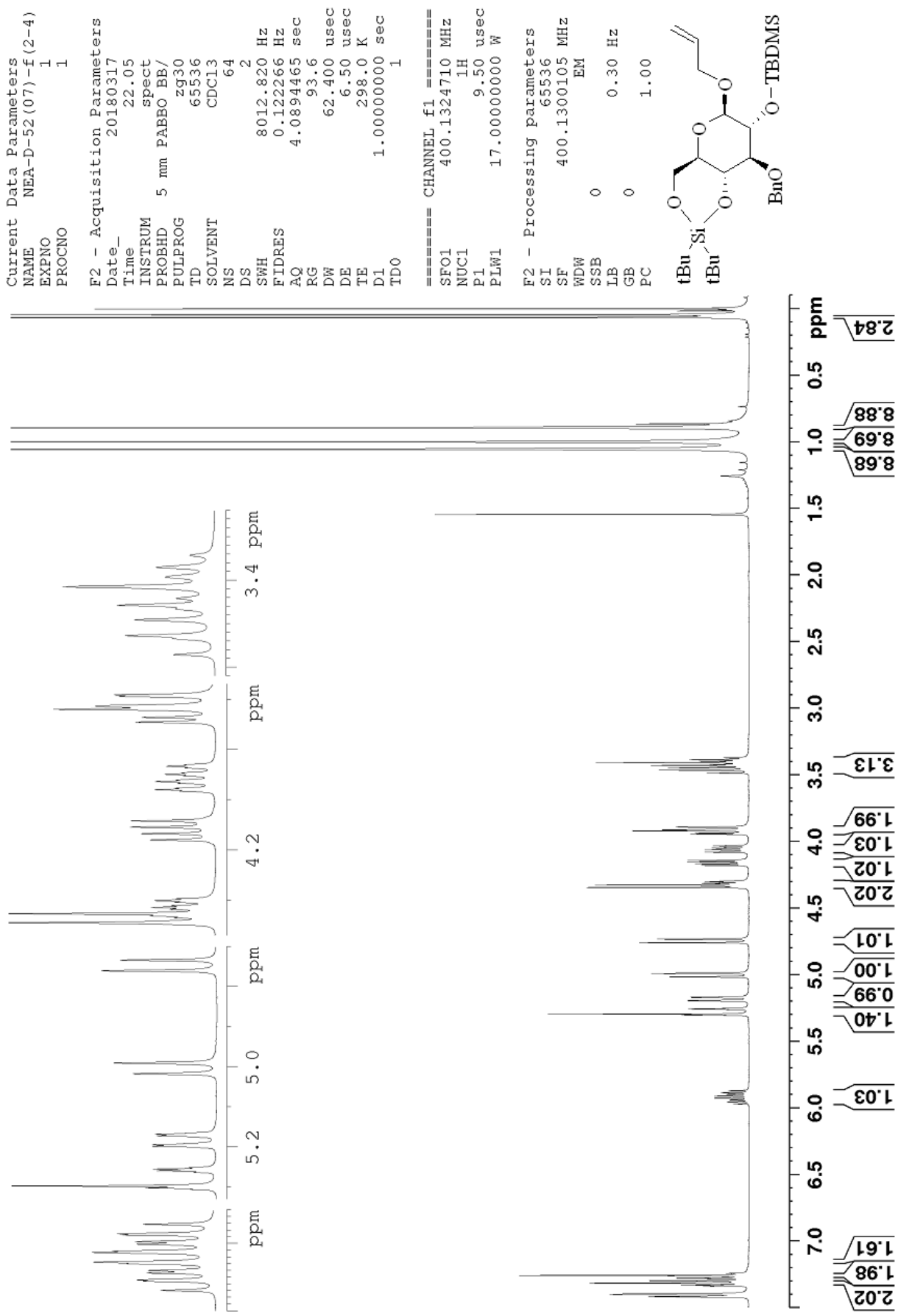

Figure I.3: ^{1}H-NMR spectrum of compound **8b**.

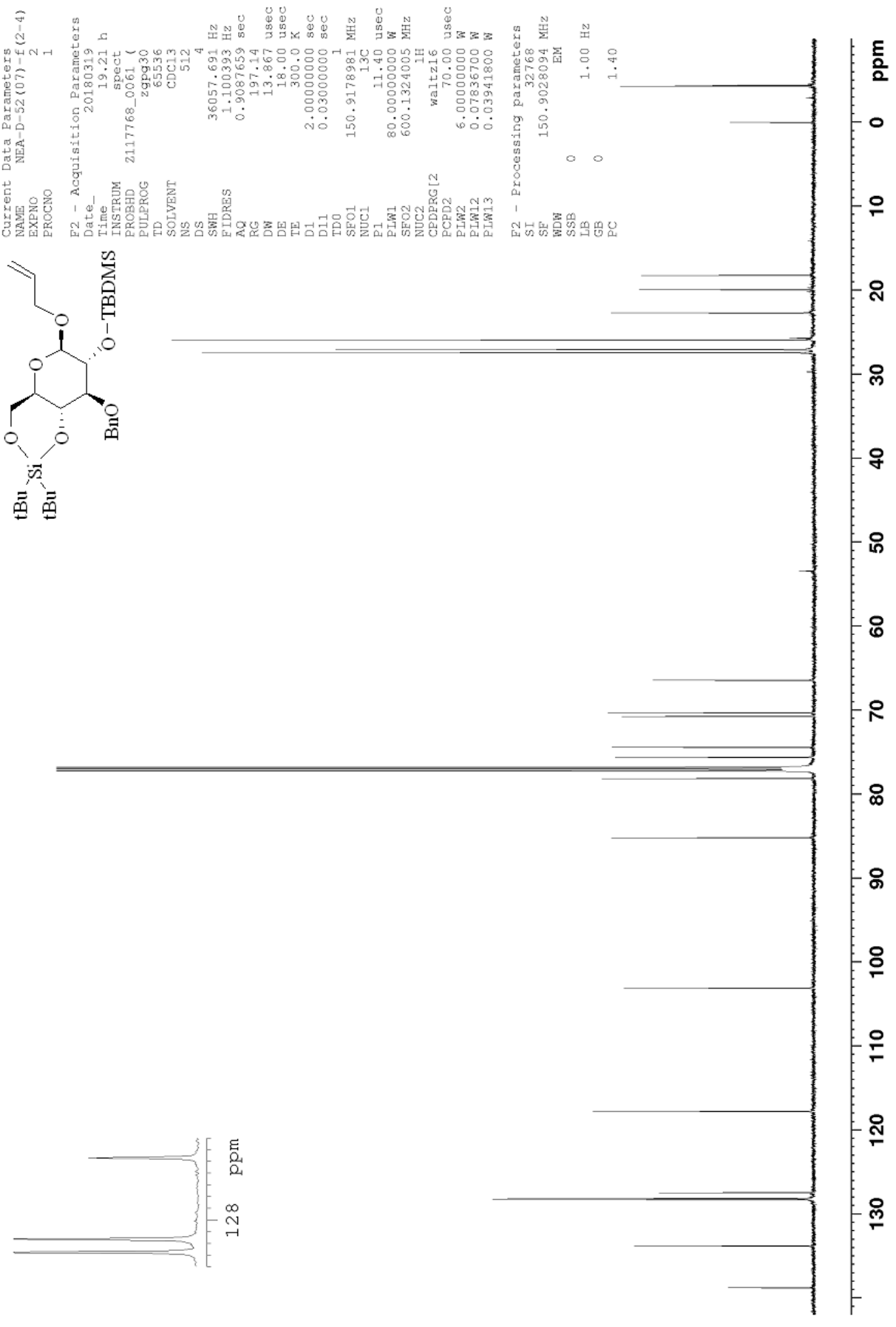

Figure I.4: ^{13}C-NMR spectrum of compound **8b**.

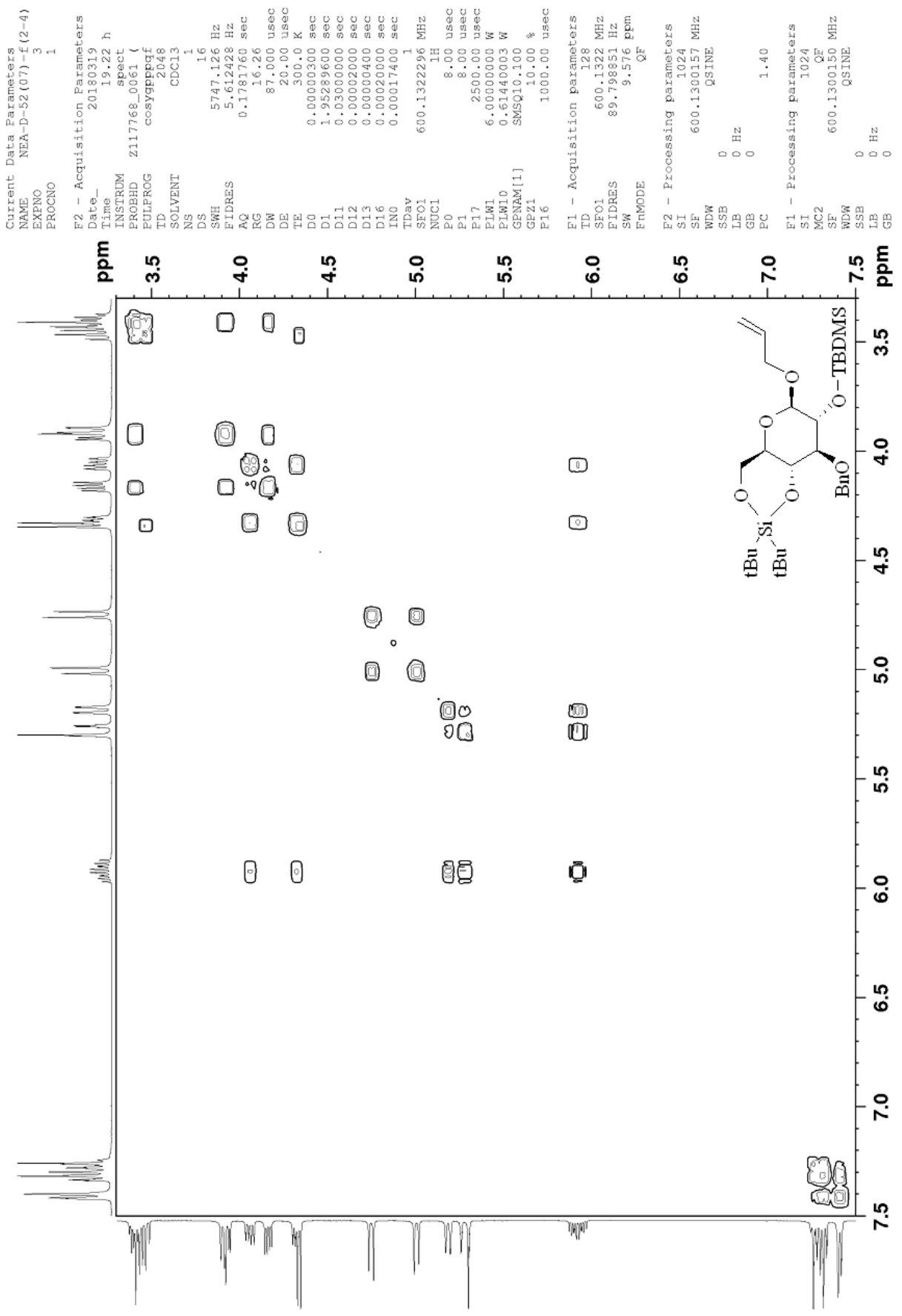

Figure I.5: H,H-COSY spectrum of compound **8b**.

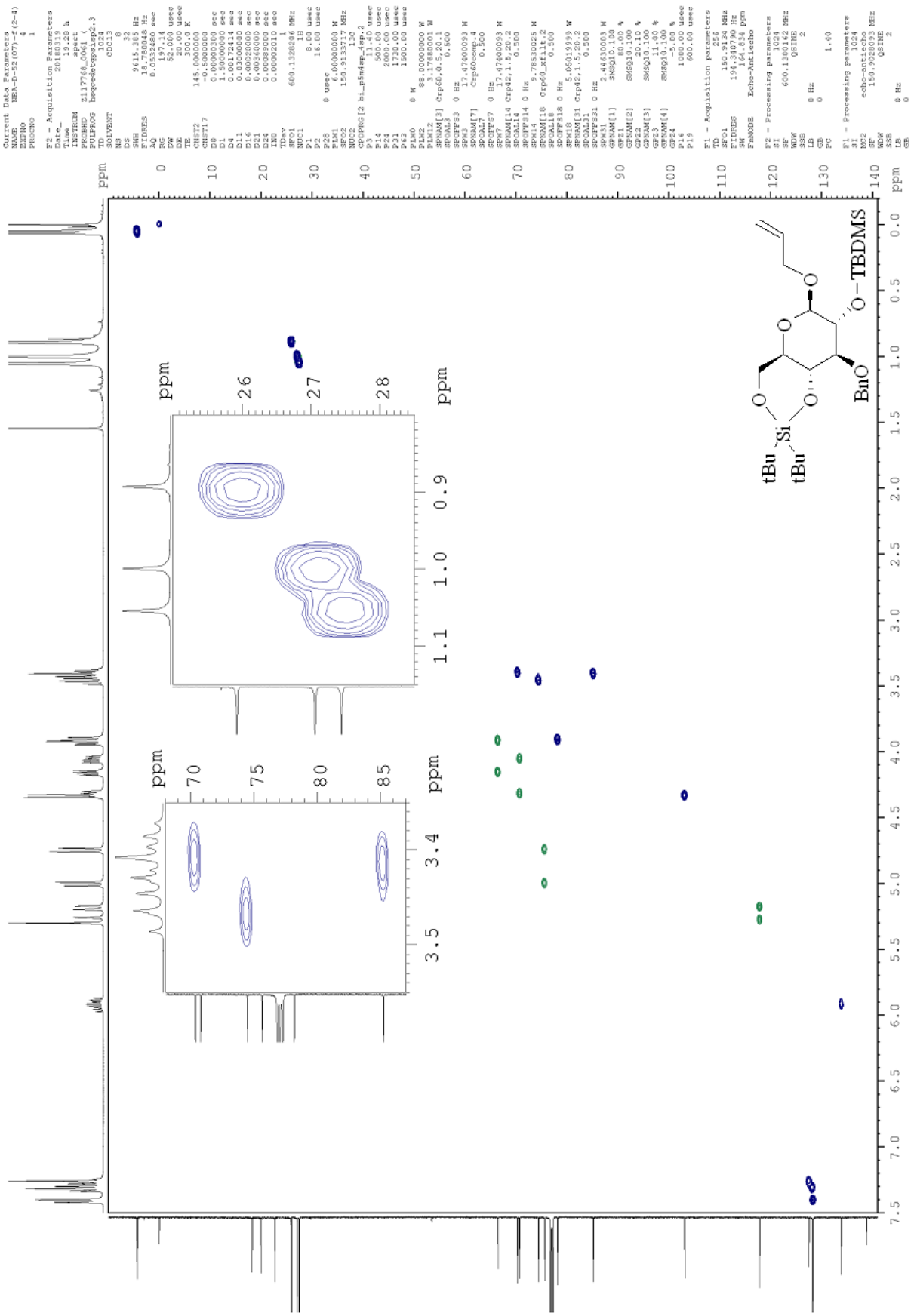

Figure I.6: HSQC spectrum of compound **8b**.

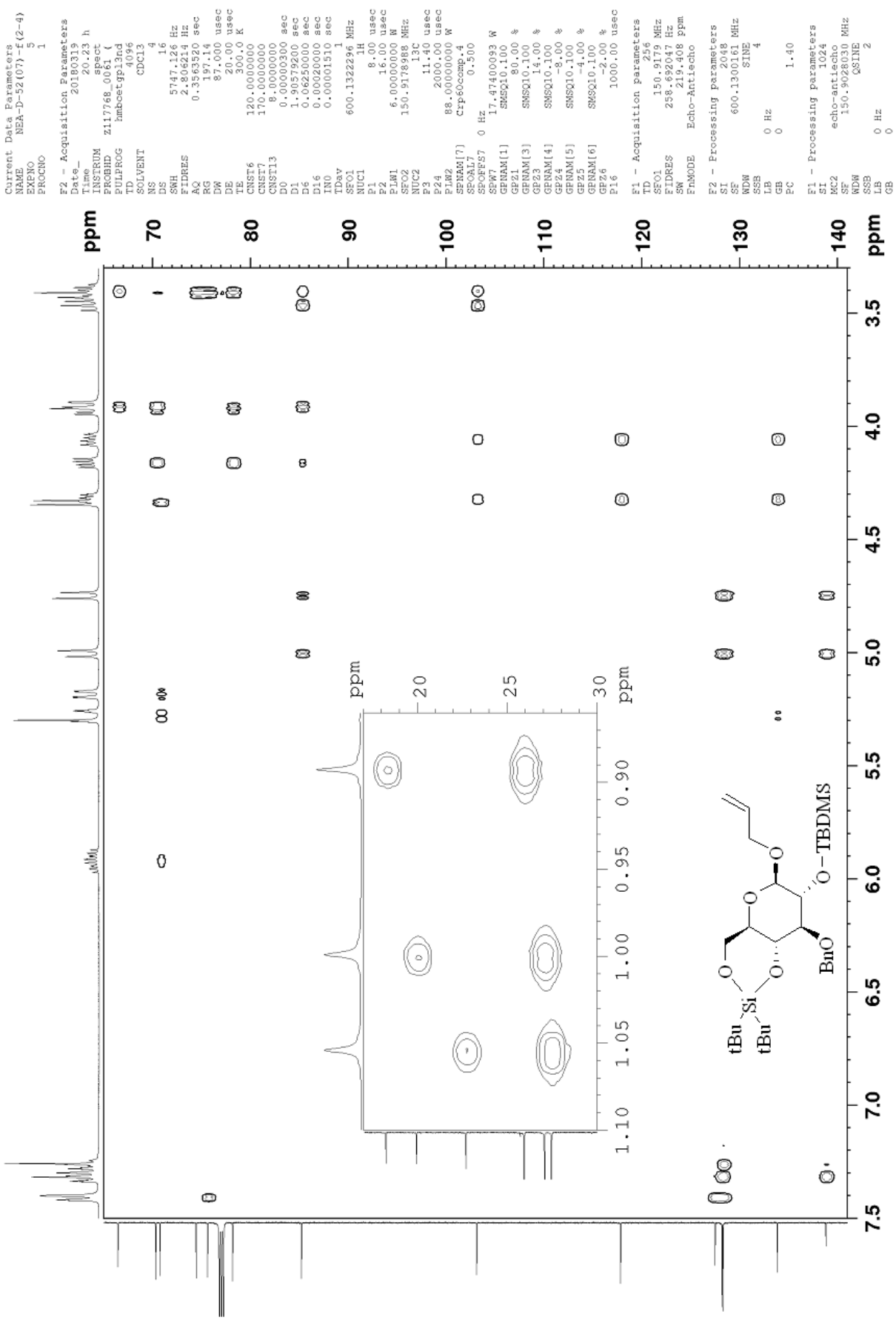

Figure I.7: HMBC spectrum of compound **8b**.

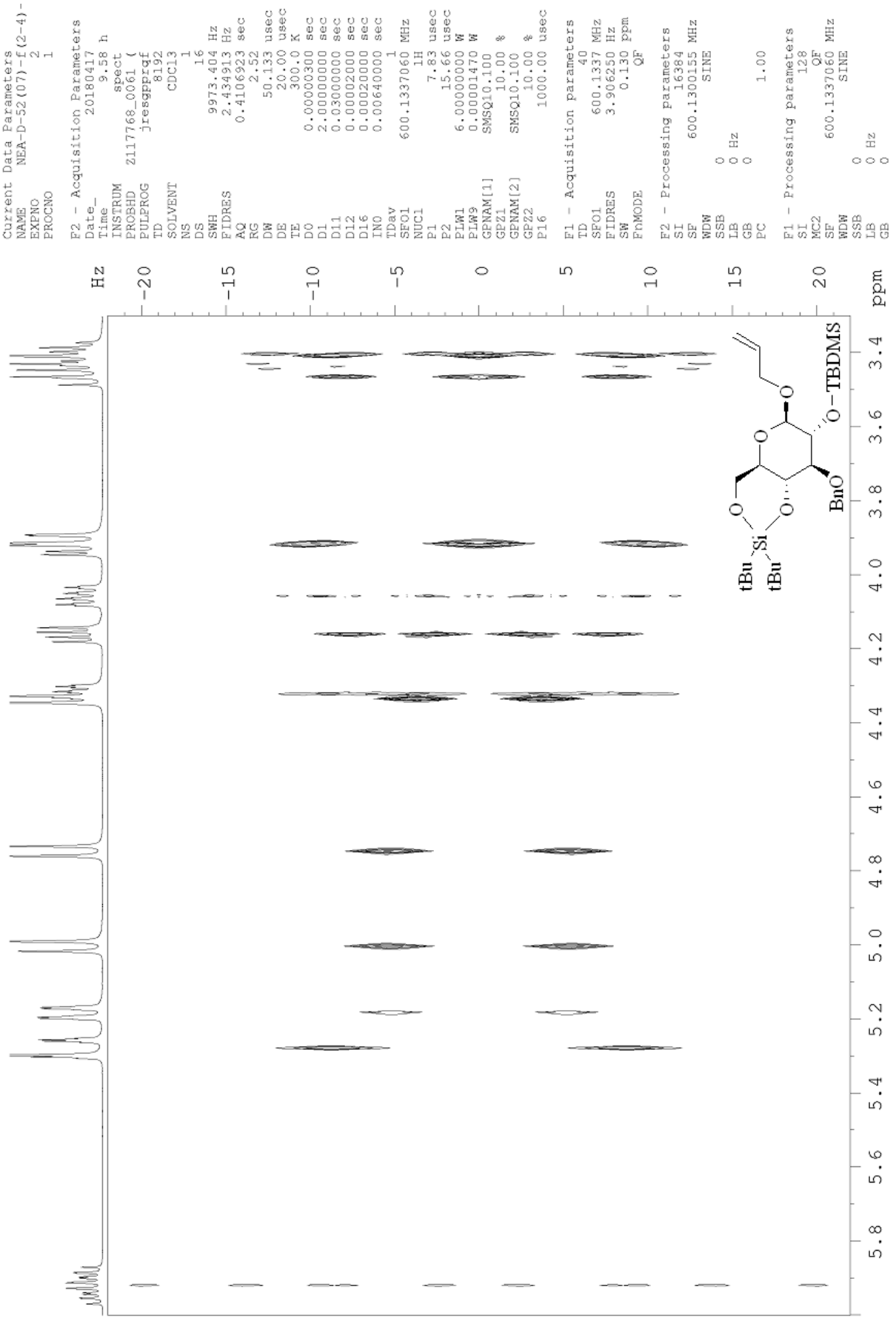

Figure I.8: JRES spectrum of compound **8b**.

J Spectroscopic Data – Compound 9

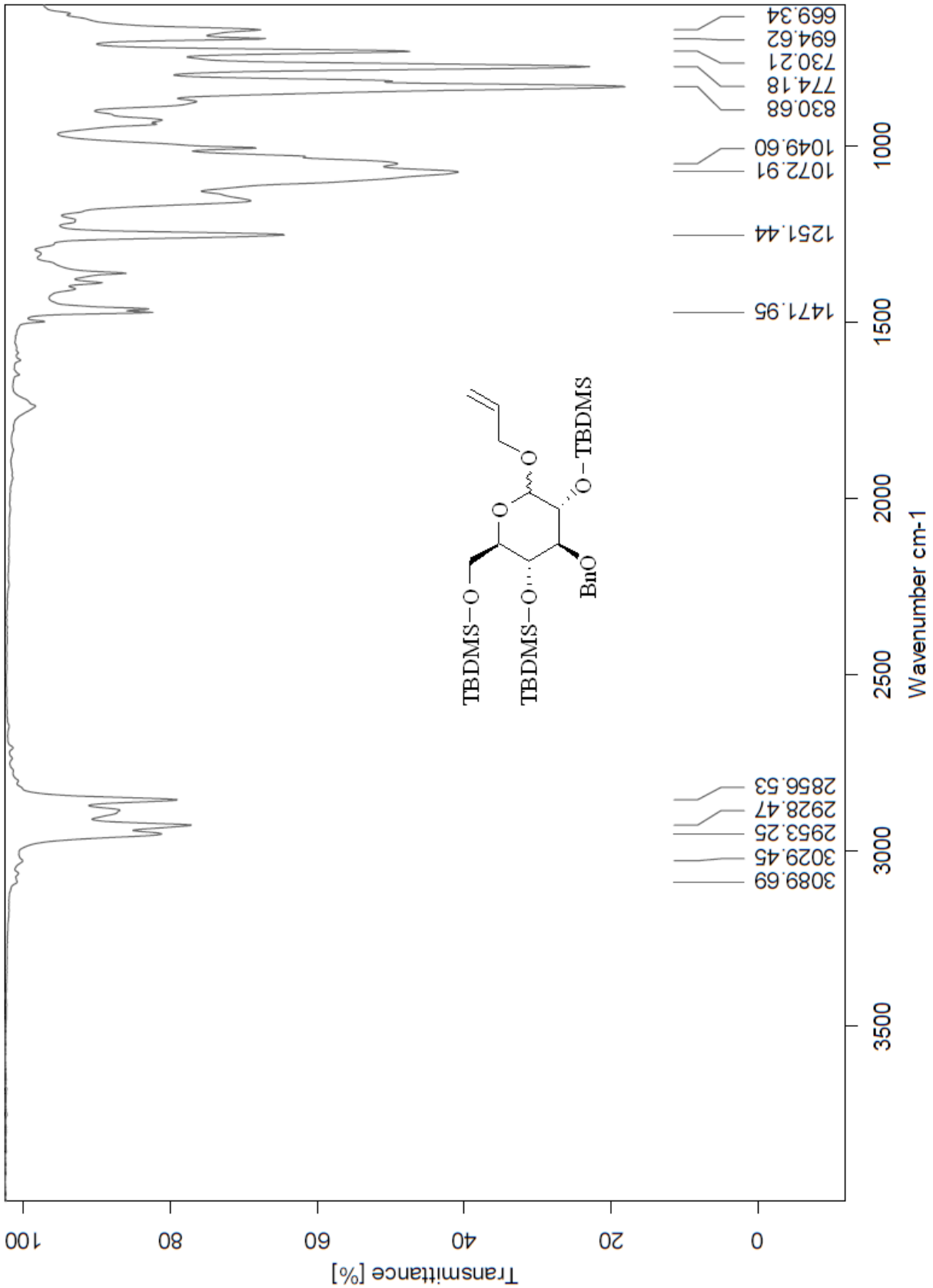

Figure J.1: IR spectrum of compound **9**, which is an anomeric mixture.

Single Mass Analysis
Tolerance = 3.0 PPM / DBE: min = -1.5, max = 50.0
Element prediction: Off
Number of isotope peaks used for i-FIT = 3

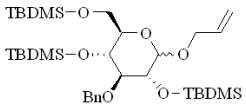

Monoisotopic Mass, Even Electron Ions
1572 formula(e) evaluated with 7 results within limits (all results (up to 1000) for each mass)
Elements Used:
C: 0-500 H: 0-1000 O: 0-100 Na: 0-1 Si: 0-3

2018-42esi 51 (0.488) AM2 (Ar,35000.0,0.00,0.00); Cm (51:52)
1: TOF MS ES+

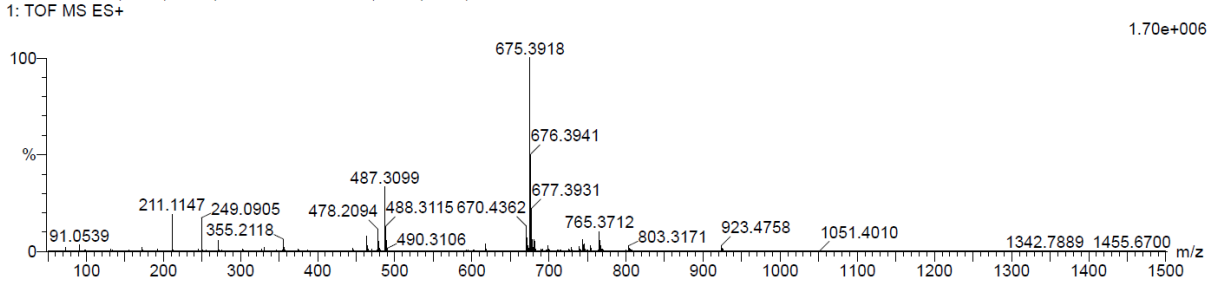

Minimum:				-1.5				
Maximum:		5.0	3.0	50.0				
Mass	Calc. Mass	mDa	PPM	DBE	i-FIT	Norm	Conf(%)	Formula
675.3918	675.3908	1.0	1.5	5.5	901.8	0.274	76.04	C34 H64 O6 Na Si3
	675.3901	1.7	2.5	13.5	903.2	1.634	19.51	C40 H59 O5 Si2
	675.3932	-1.4	-2.1	8.5	904.8	3.310	3.65	C36 H63 O6 Si3
	675.3936	-1.8	-2.7	1.5	906.5	4.959	0.70	C31 H64 O10 Na Si2
	675.3904	1.4	2.1	6.5	908.9	7.359	0.06	C35 H60 O9 Na Si
	675.3928	-1.0	-1.5	9.5	909.6	8.047	0.03	C37 H59 O9 Si
	675.3932	-1.4	-2.1	2.5	915.3	13.756	0.00	C32 H60 O13 Na

Figure J.2: HRMS spectrum of compound **9**, which is an anomeric mixture.

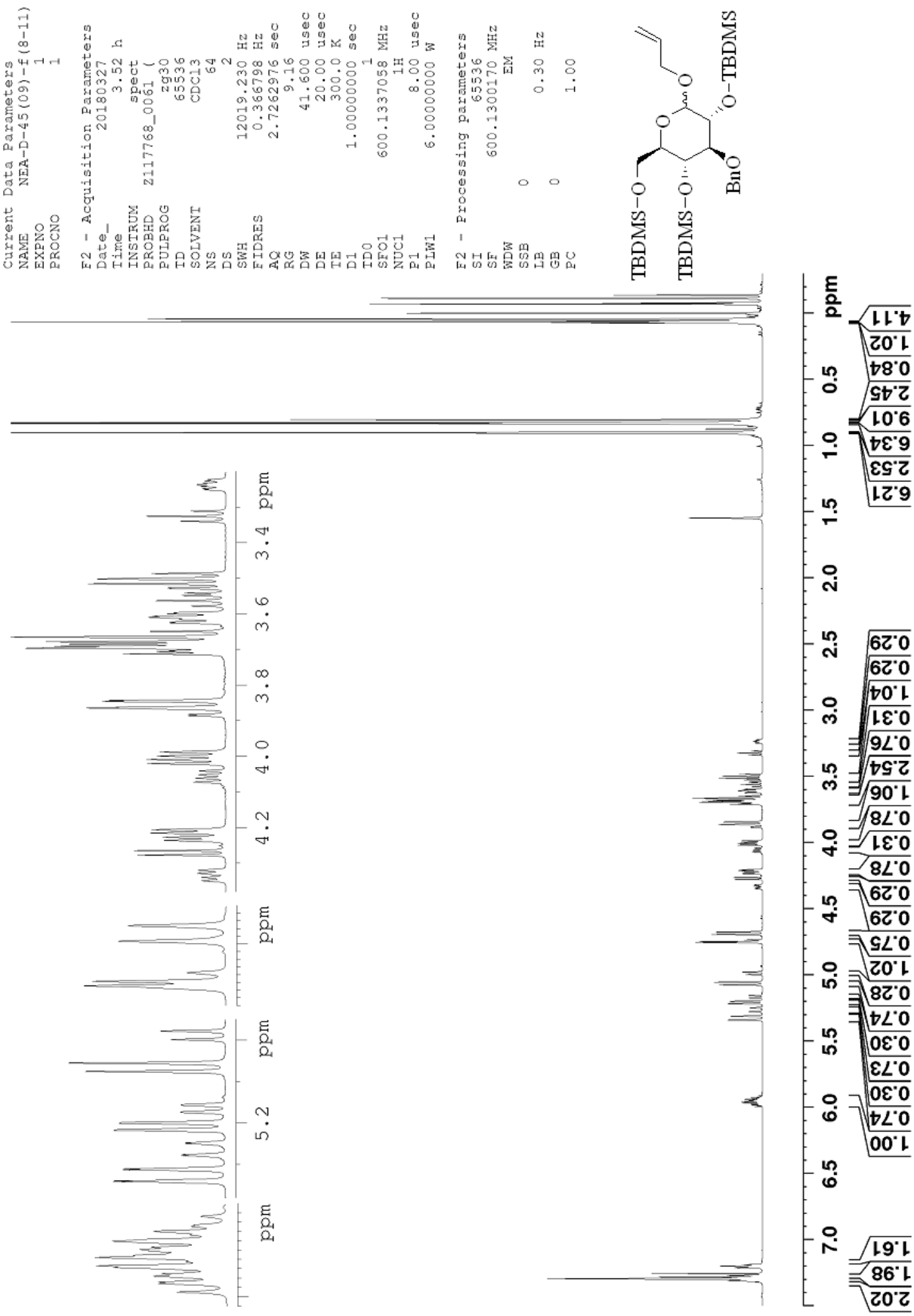

Figure J.3: ^{1}H-NMR spectrum of compound **9**, which is an anomeric mixture.

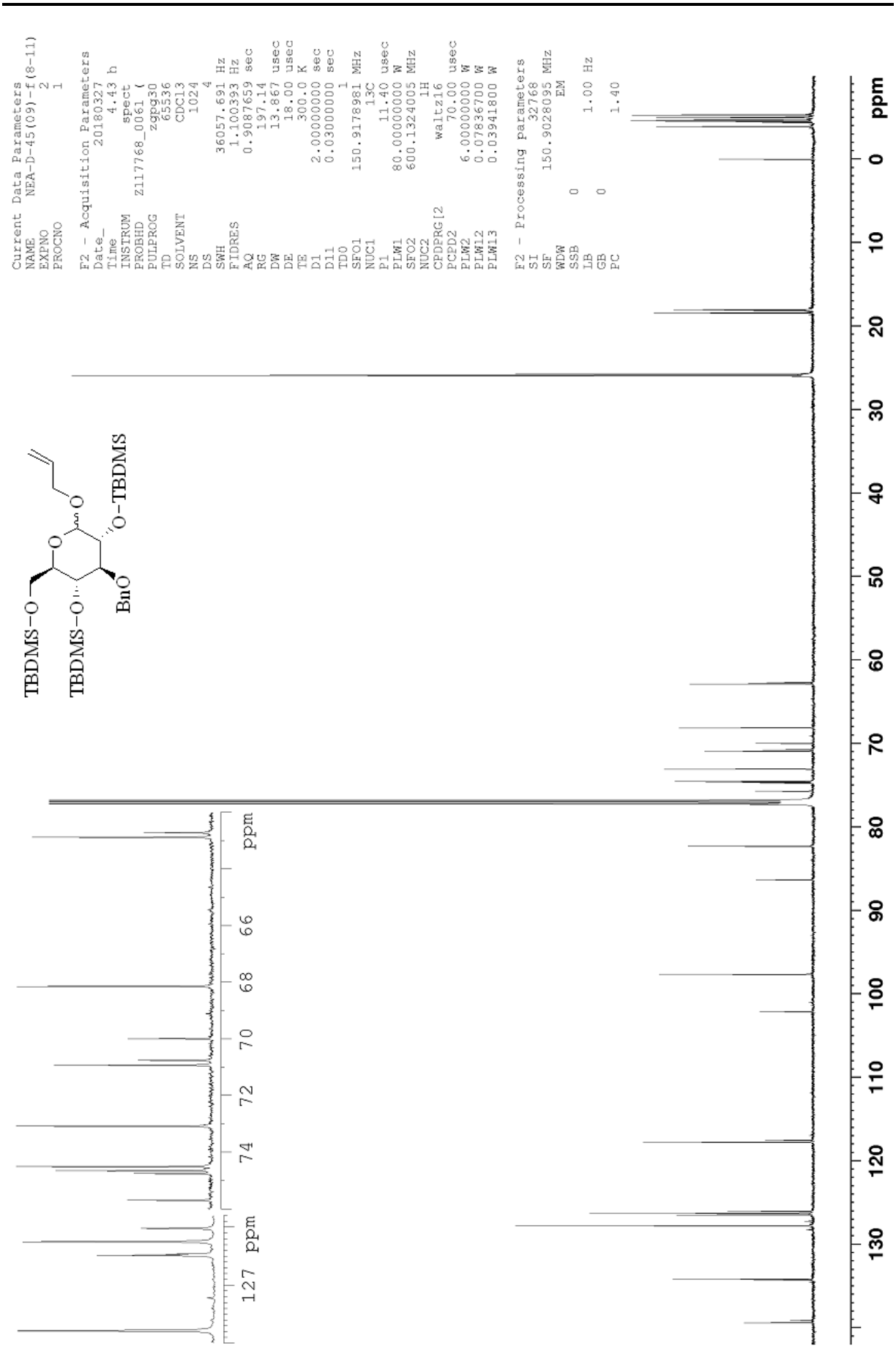

Figure J.4: ^{13}C-NMR spectrum of compound **9**, which is an anomeric mixture.

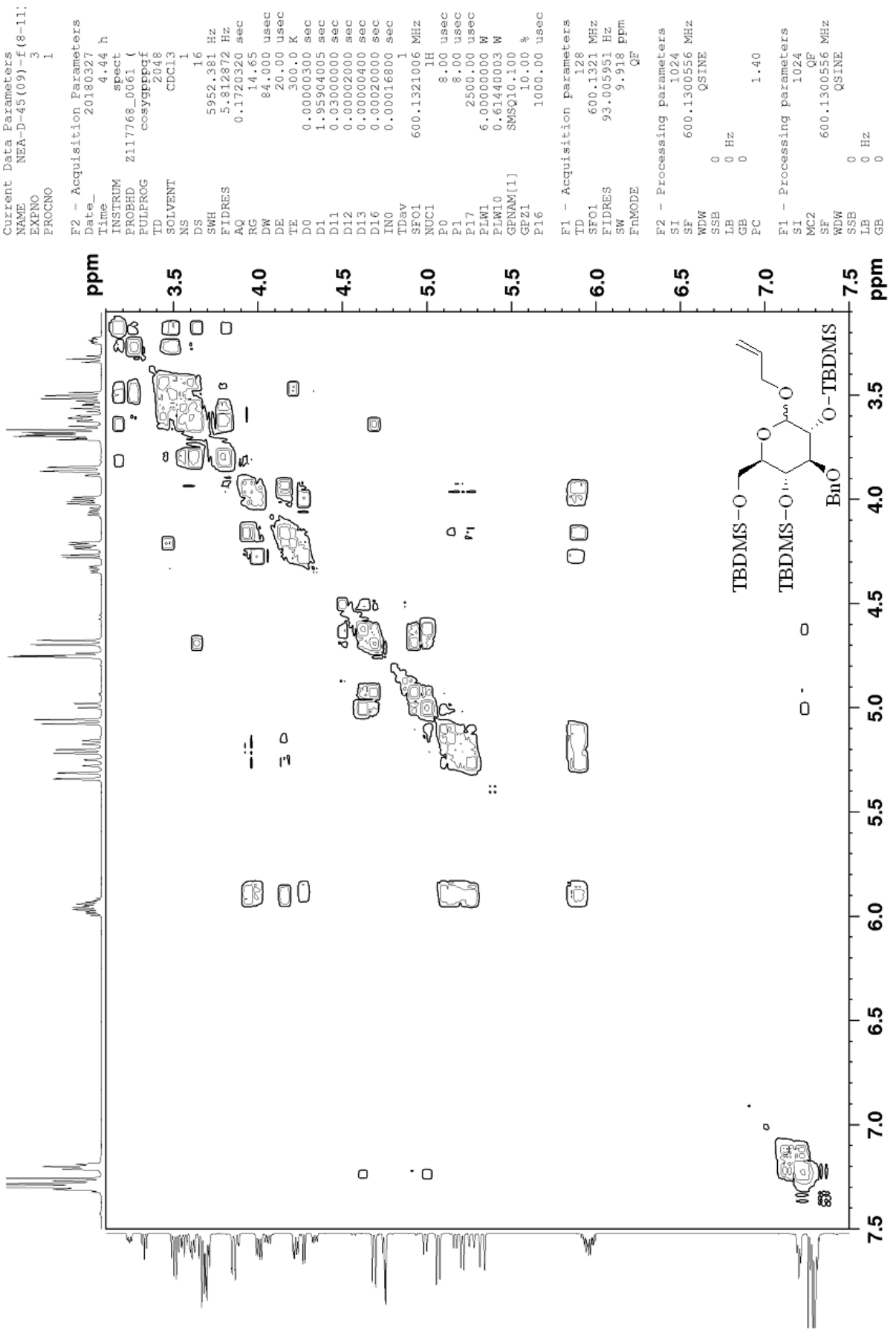

Figure J.5: H,H-COSY spectrum of compound **9**, which is an anomeric mixture.

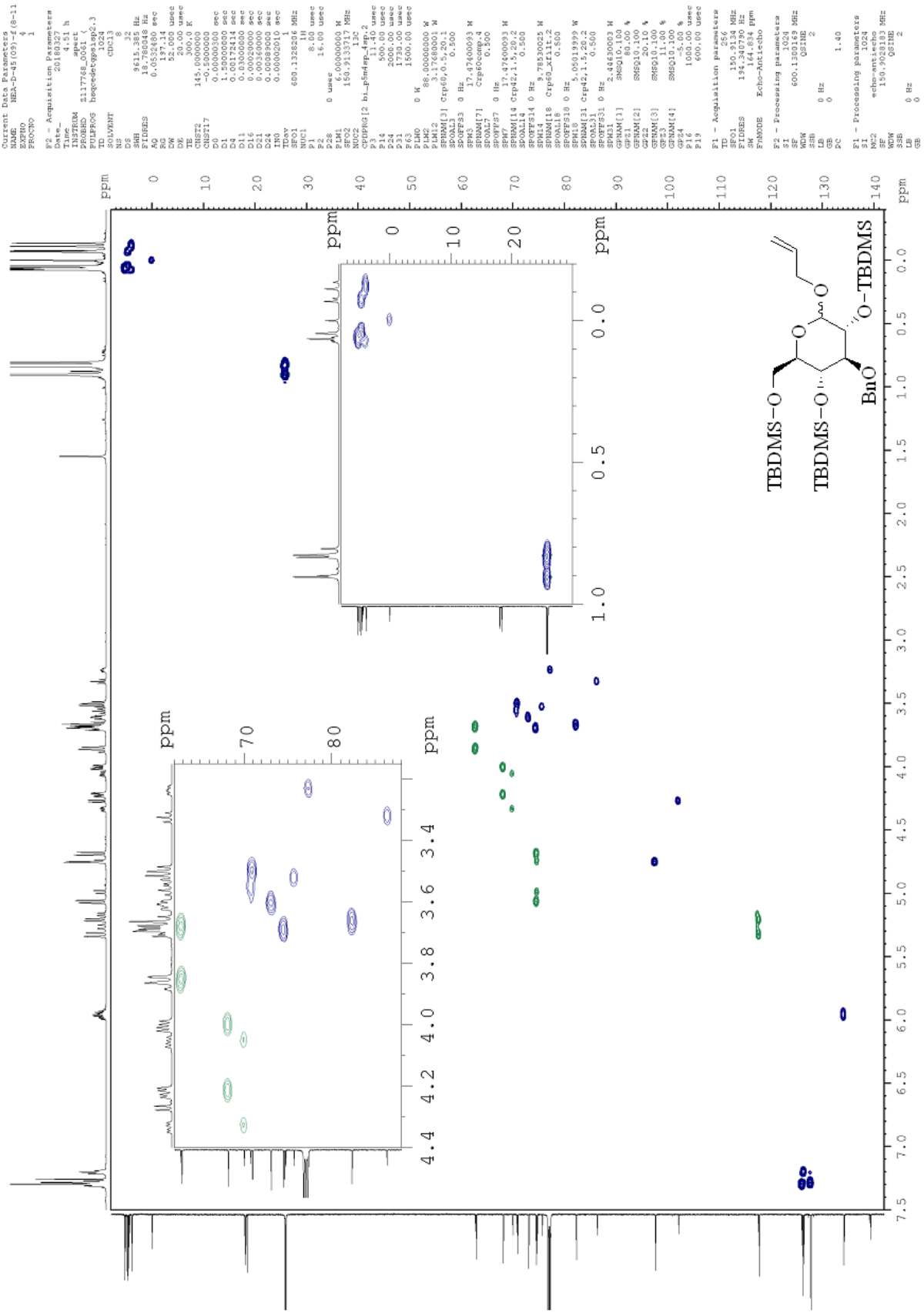

Figure J.6: HSQC spectrum of compound **9**, which is an anomeric mixture.

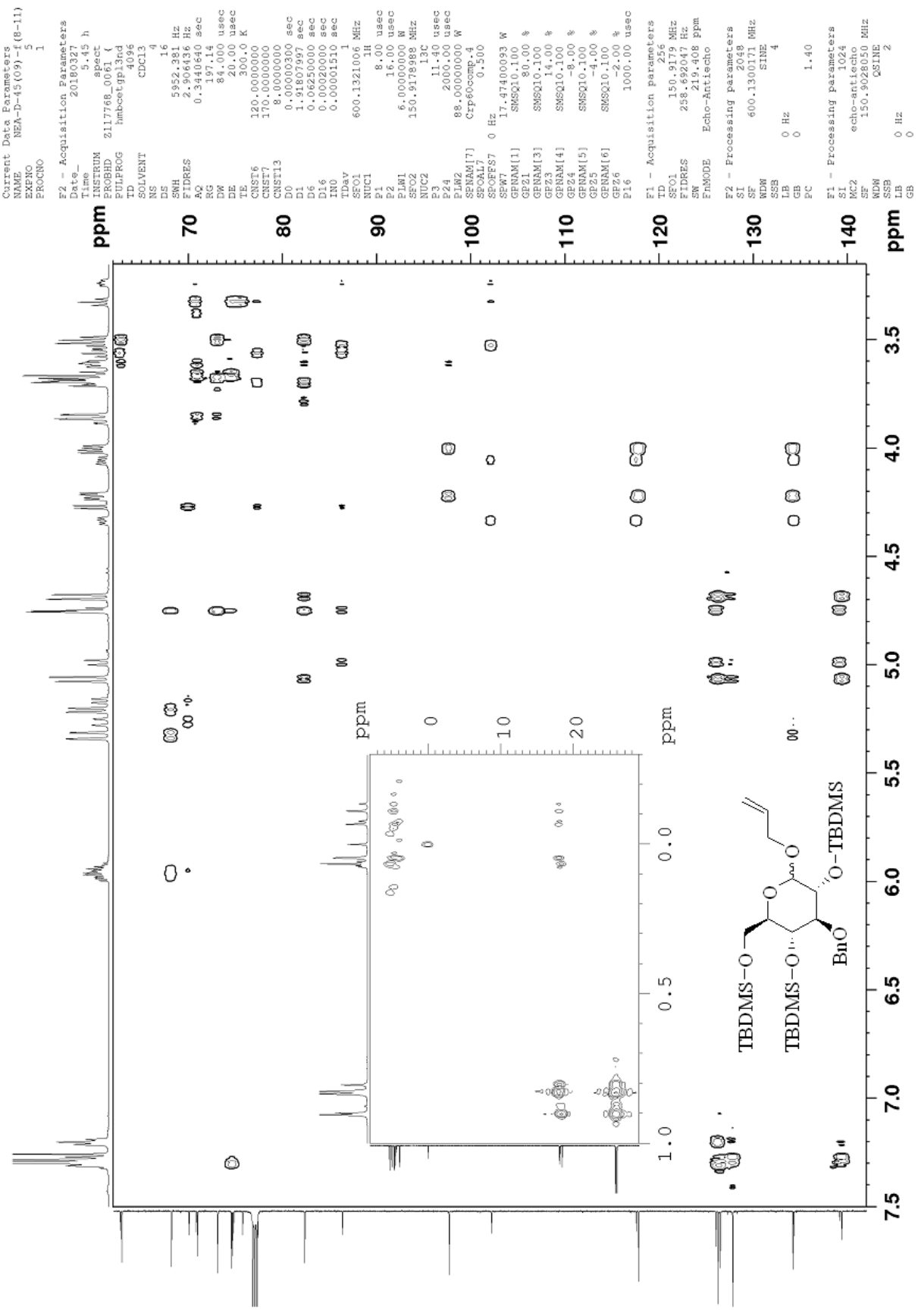

Figure J.7: HMBC spectrum of compound **9**, which is an anomeric mixture.

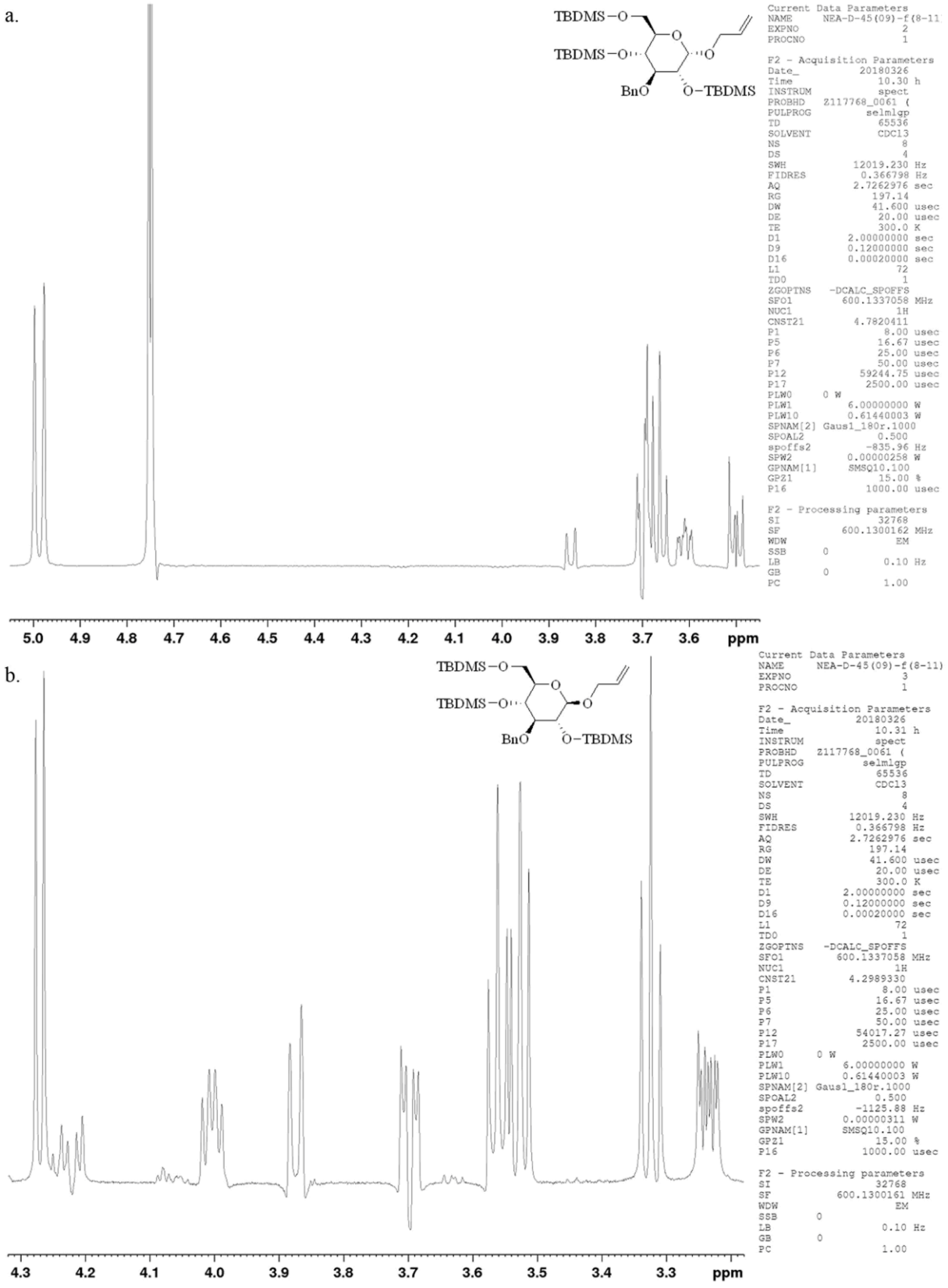

Figure J.8: 1D TOCSY spectra of compound **9**, selectively irradiating a. H_{α}-1; b. H_{β}-1.

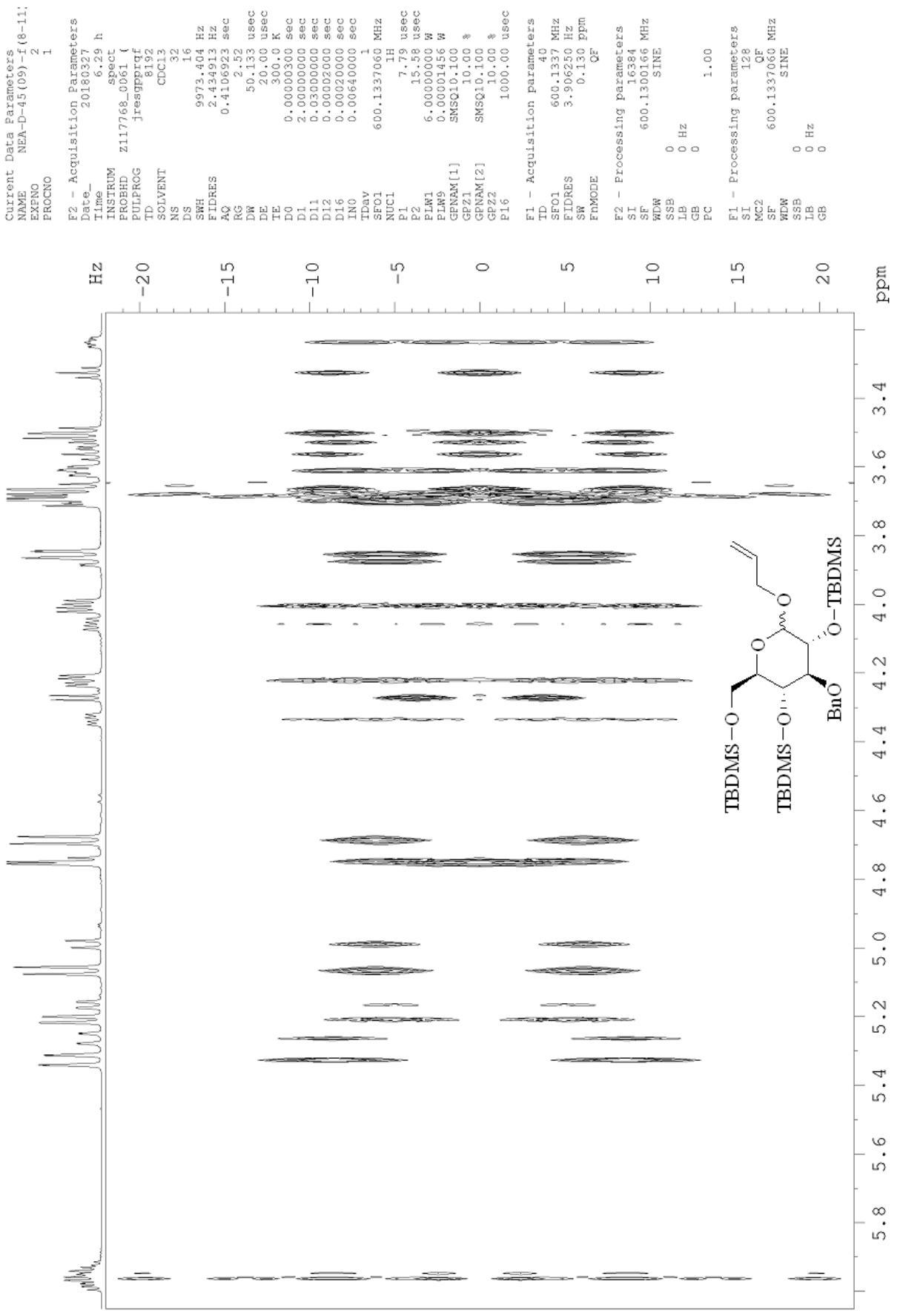

Figure J.9: JRES spectrum of compound **9**, which is an anomeric mixture.

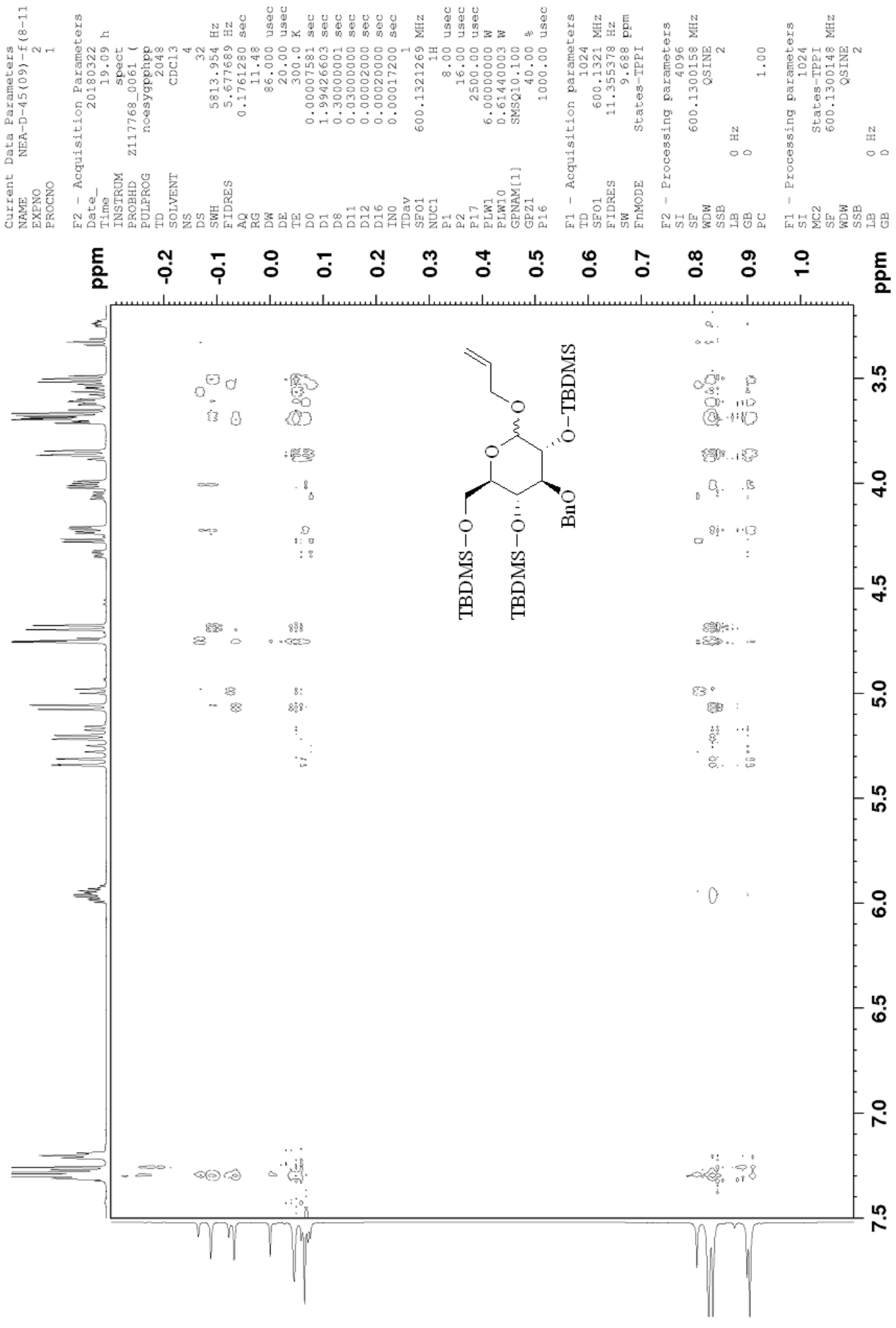

Figure J.10: NOESY spectrum silyl alkyl protons of compound **9**, which is an anomeric mixture.

K Spectroscopic Data – By-product of reaction of 5 to 6

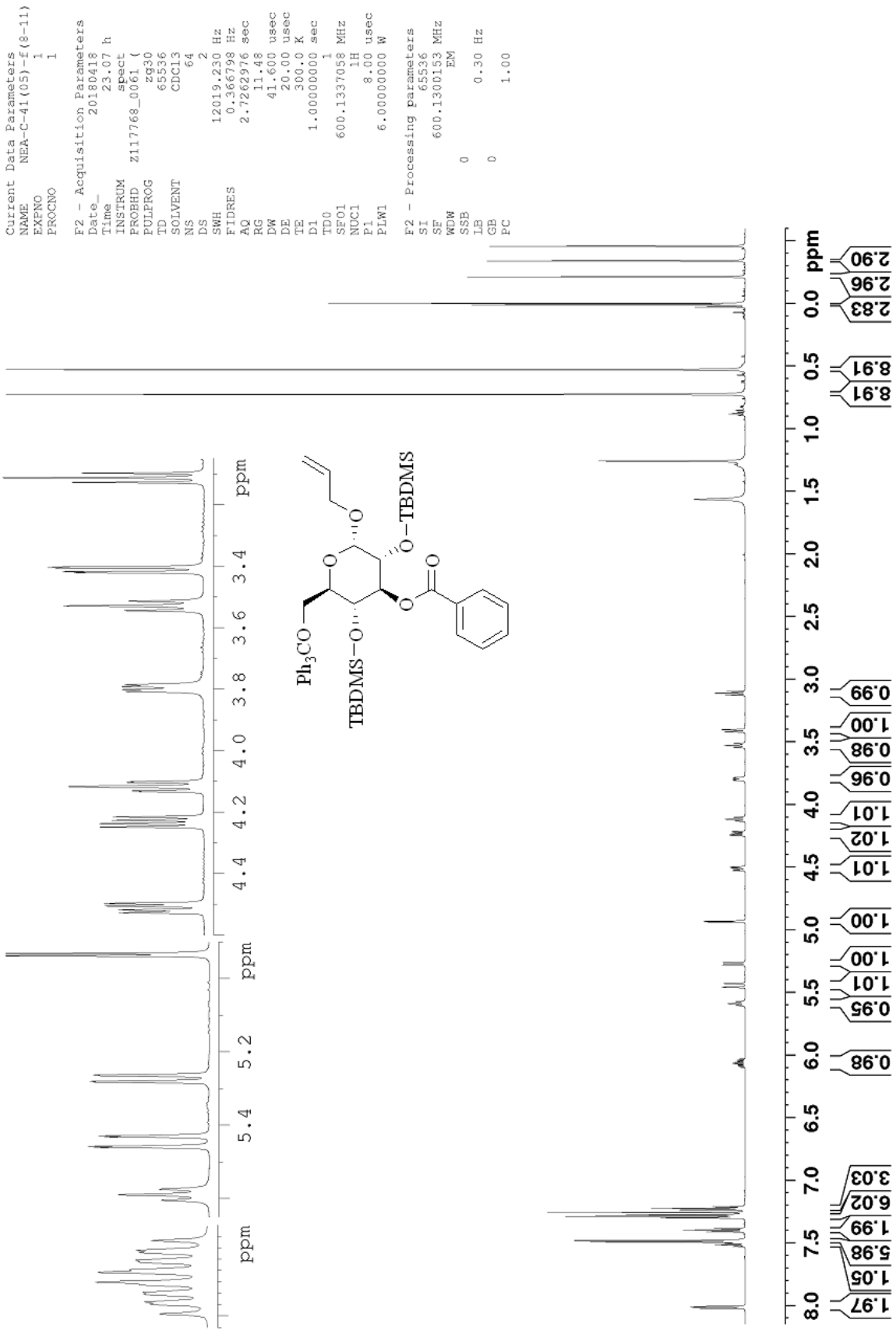

Figure K.1: [1]H-NMR spectrum of by-product isolated from reaction of **5** to **6**.

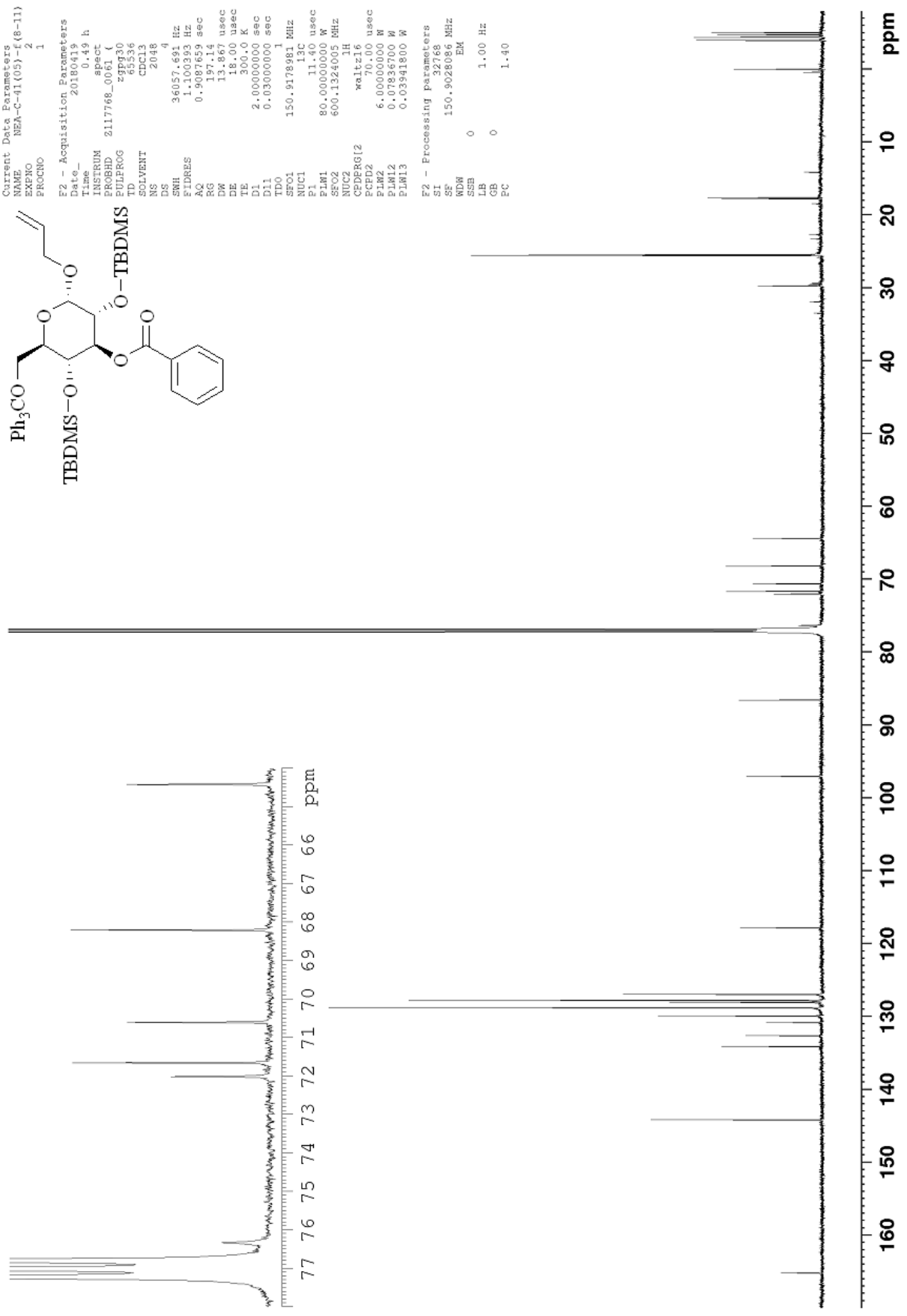

Figure K.2: ^{13}C-NMR spectrum of by-product isolated from reaction of **5** to **6**.

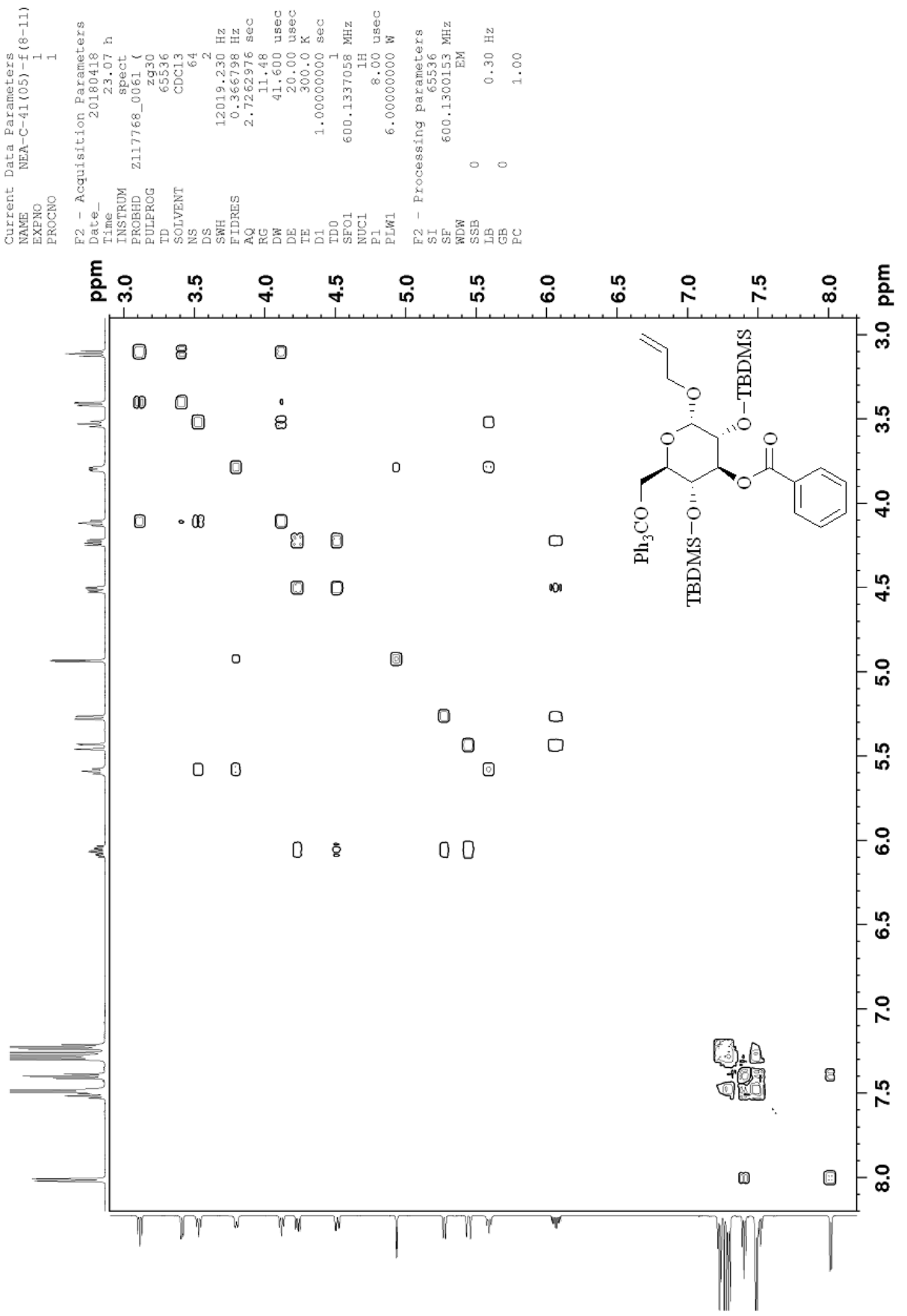

Figure K.3: H,H-COSY spectrum of by-product isolated from reaction of **5** to **6**.

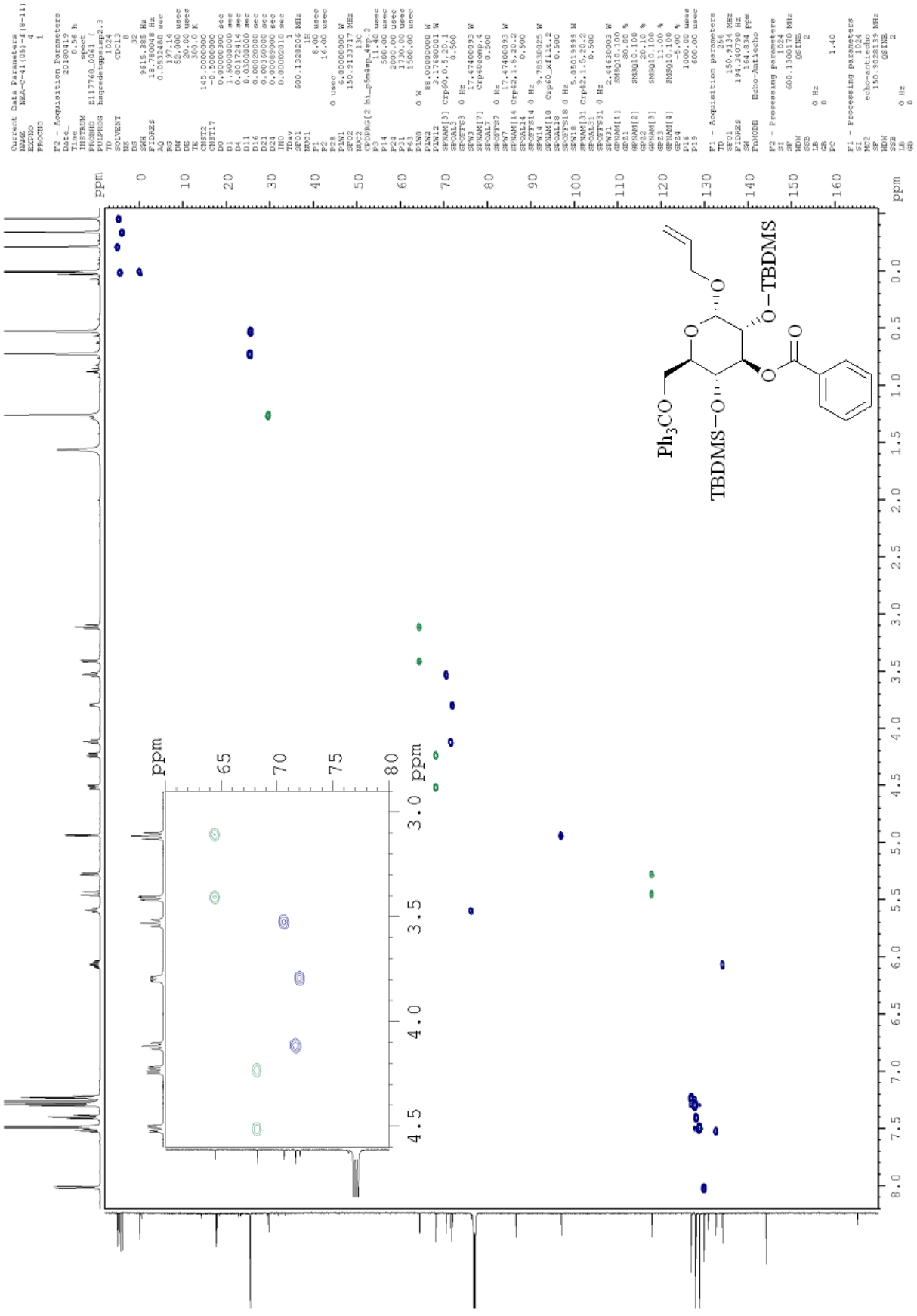

Figure K.4: HSQC spectrum of by-product isolated from reaction of **5** to **6**.

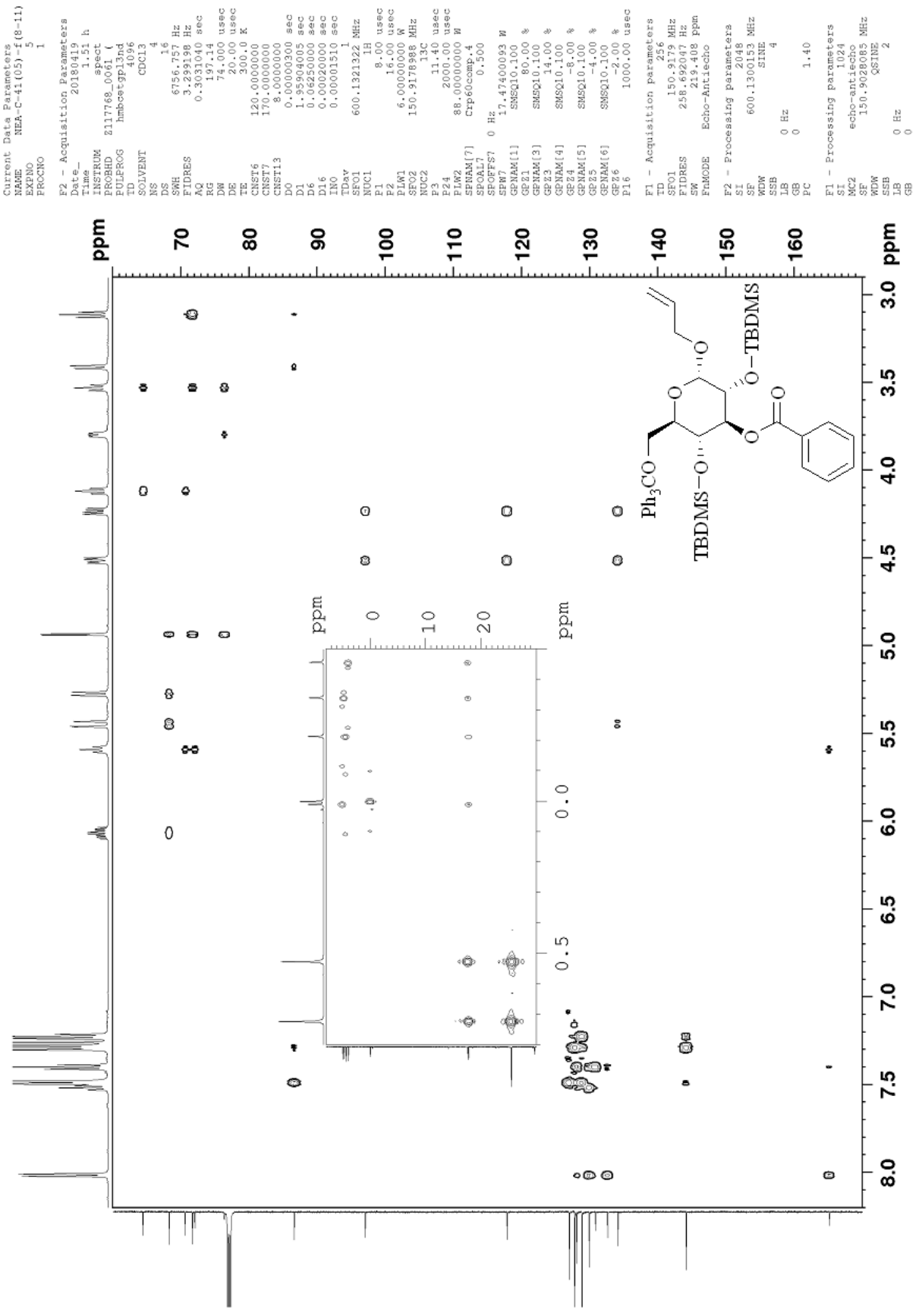

Figure K.5: HMBC spectrum of by-product isolated from reaction of **5** to **6**.

L Spectroscopic Data – By-product of reaction of 4 to 7

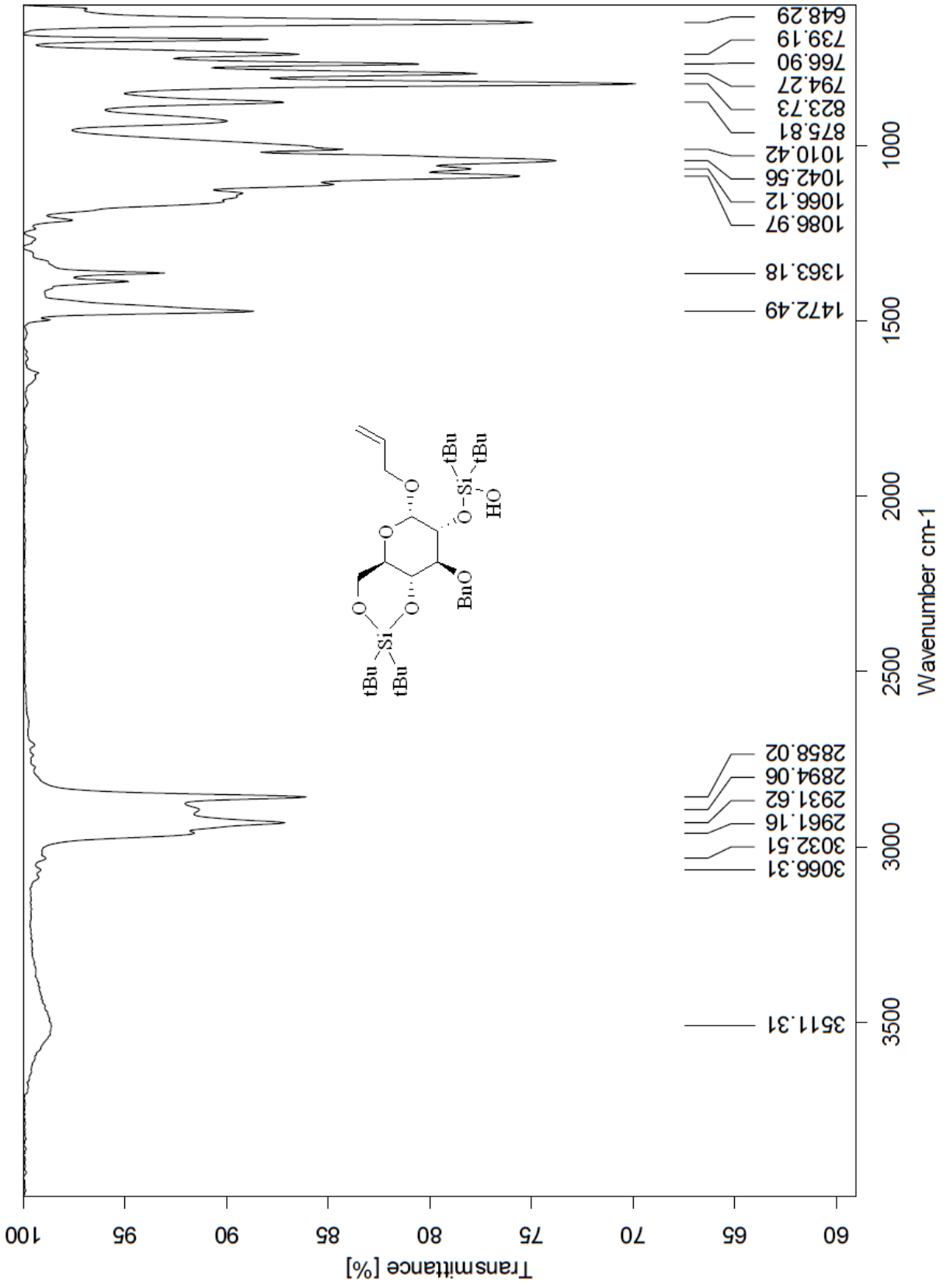

Figure L.1: IR spectrum of by-product isolated from reaction of **4** to **7**.

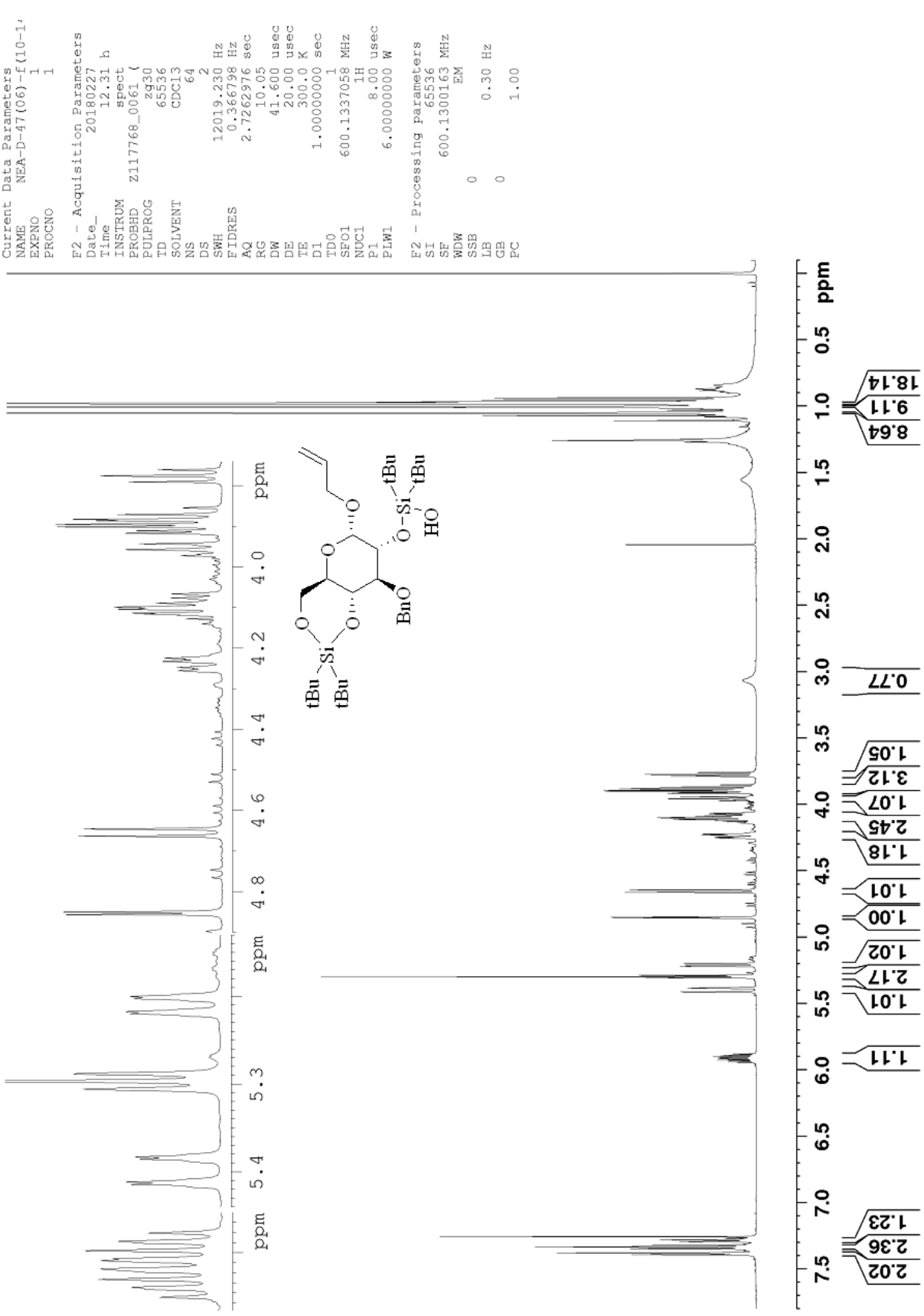

Figure L.2: [1]H-NMR spectrum of by-product isolated from reaction of **4** to **7**.

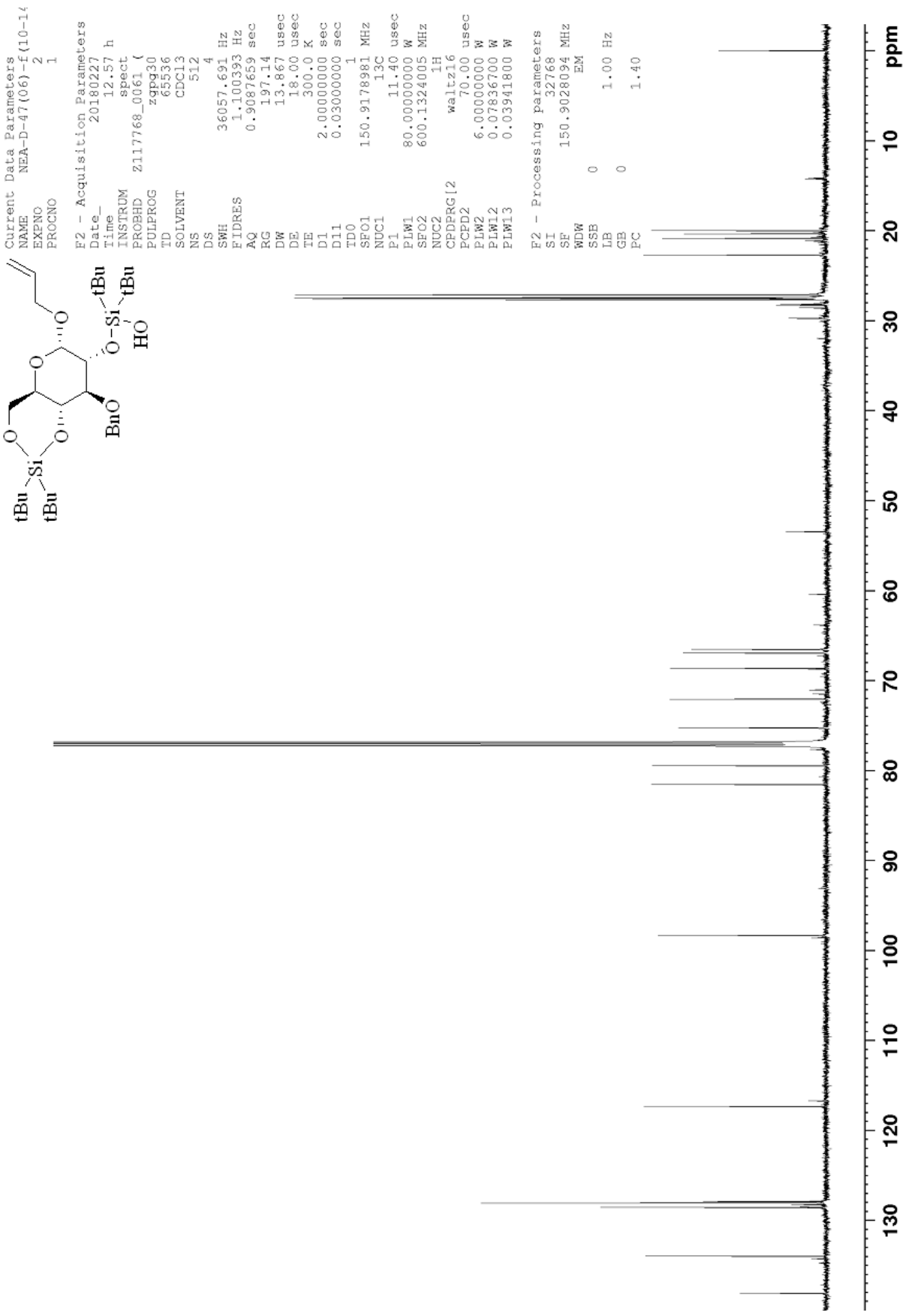

Figure L.3: ^{13}C-NMR spectrum of by-product isolated from reaction of **4** to **7**.

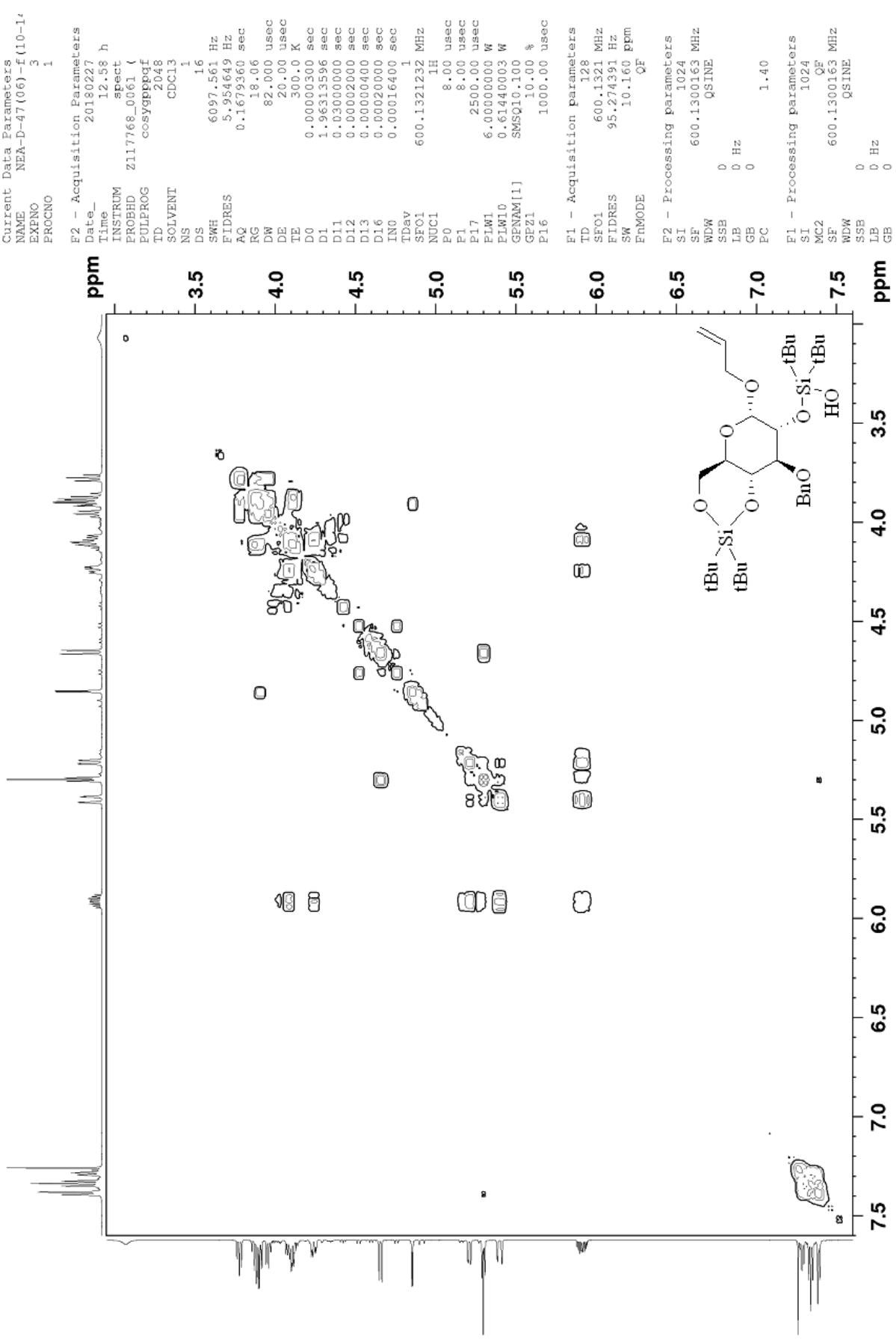

Figure L.4: H,H-COSY spectrum of by-product isolated from reaction of **4** to **7**.

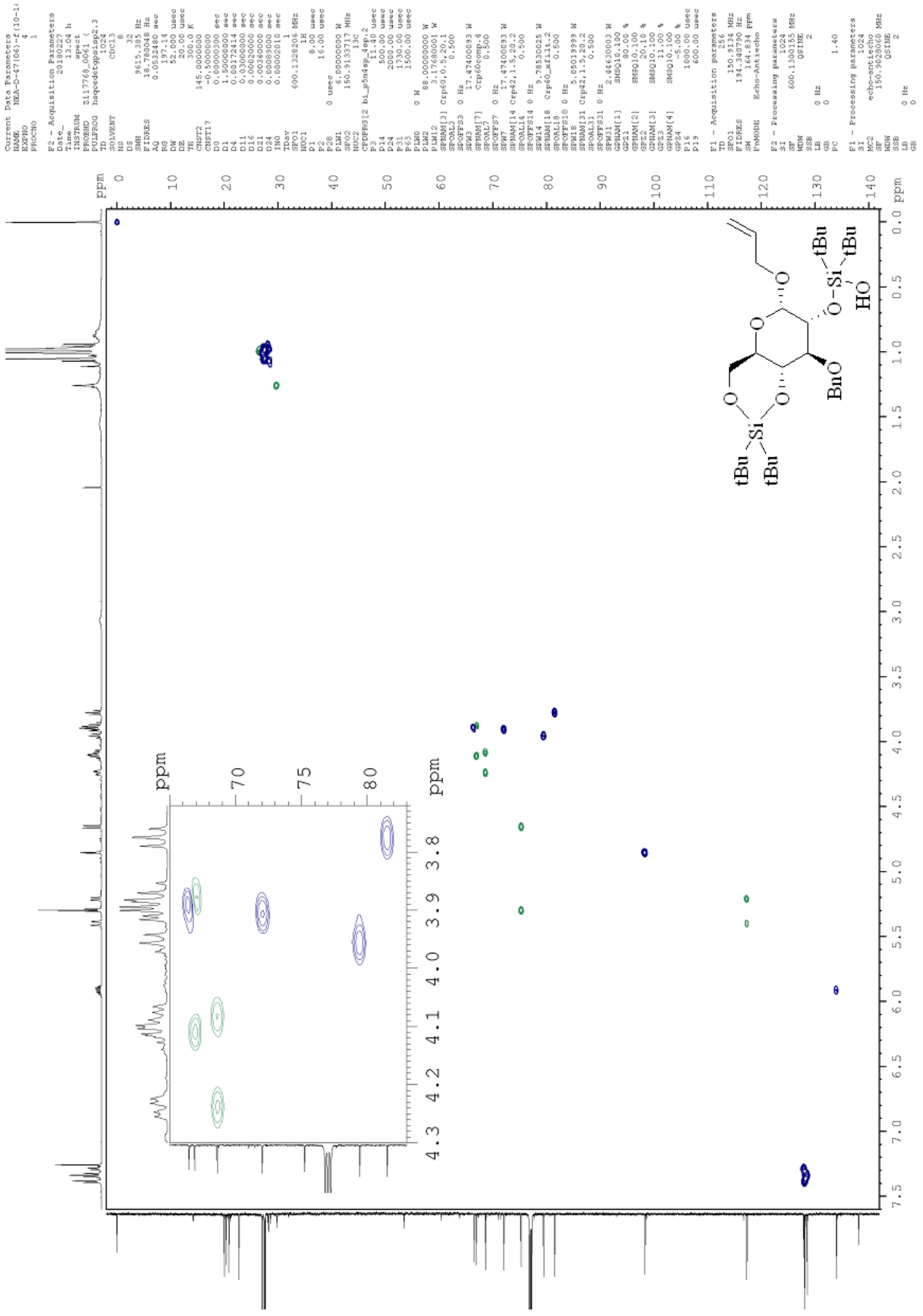

Figure L.5: HSQC spectrum of by-product isolated from reaction of **4** to **7**.

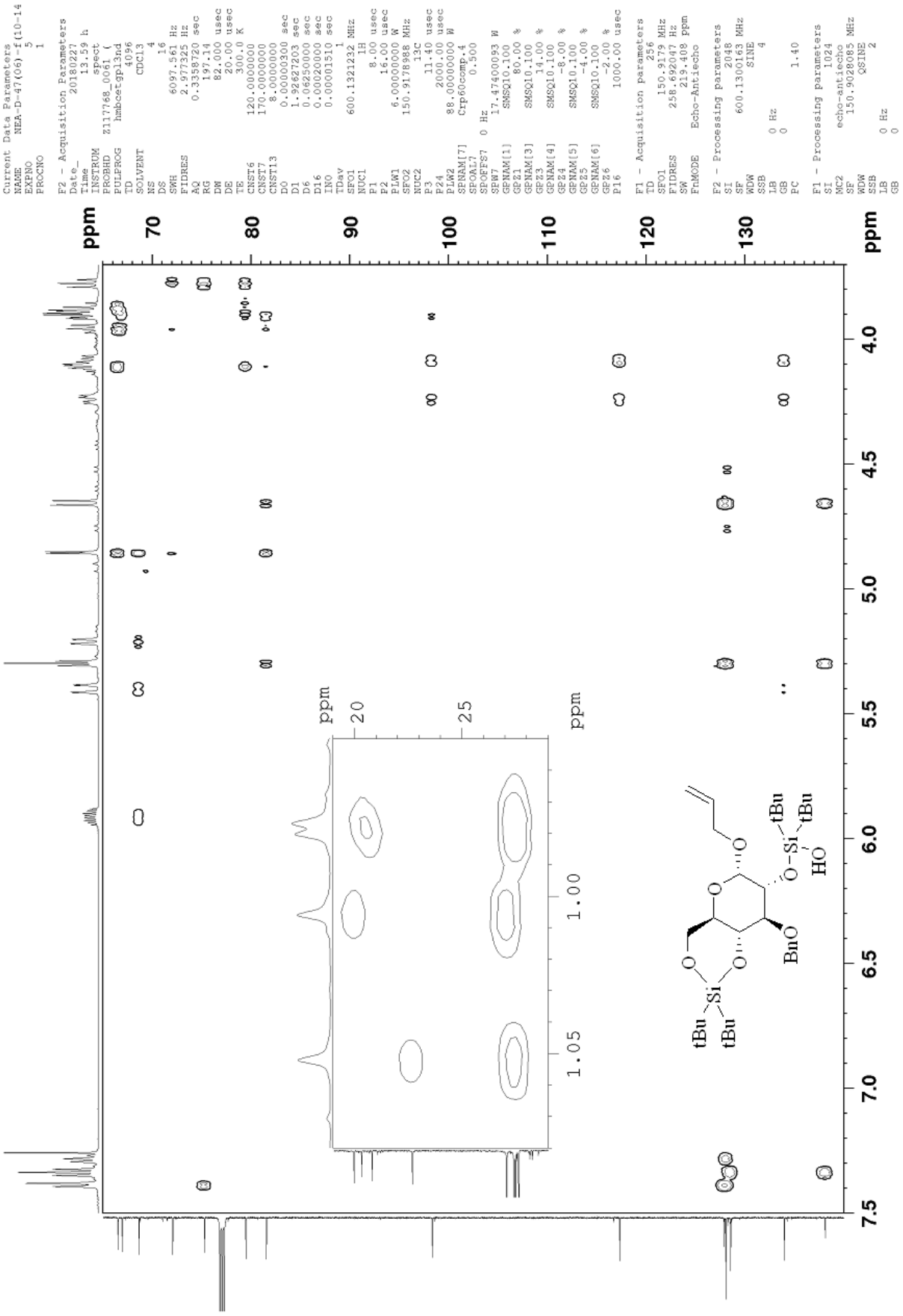

Figure L.6: HMBC spectrum of by-product isolated from reaction of **4** to **7**.